

Degradation of di (2-ethylhexyl) phthalate by marine sediment
bacteria and identification of key degraders and degradative
genes



A Dissertation Submitted in Partial Fulfillment of the Requirements
for the Degree of Doctor of Philosophy in Hazardous Substance and
Environmental Management
Inter-Department of Environmental Management
GRADUATE SCHOOL
Chulalongkorn University
Academic Year 2022
Copyright of Chulalongkorn University

การย่อยสลายไดทิวเอทิลเฮกซิลพทาเลต โดยกลุ่มแบคทีเรียจากดินตะกอนทะเลและการระบุชนิดของ
แบคทีเรียและยีนที่ทำหน้าที่หลักในการย่อยสลาย



วิทยานิพนธ์นี้เป็นส่วนหนึ่งของการศึกษาตามหลักสูตรปริญญาวิทยาศาสตรดุษฎีบัณฑิต
สาขาวิชาการจัดการสารอันตรายและสิ่งแวดล้อม สหสาขาวิชาการจัดการสิ่งแวดล้อม
บัณฑิตวิทยาลัย จุฬาลงกรณ์มหาวิทยาลัย
ปีการศึกษา 2565
ลิขสิทธิ์ของจุฬาลงกรณ์มหาวิทยาลัย

Thesis Title	Degradation of di (2-ethylhexyl) phthalate by marine sediment bacteria and identification of key degraders and degradative genes
By	Miss Ritu Ningthoujam
Field of Study	Hazardous Substance and Environmental Management
Thesis Advisor	Associate Professor Dr. ONRUTHAI PINYAKONG, Ph.D.

Accepted by the GRADUATE SCHOOL, Chulalongkorn University in Partial Fulfillment of the Requirement for the Doctor of Philosophy

..... Dean of the GRADUATE SCHOOL
 (Associate Professor Dr. YOOTTHANA CHUPPUNNARAT, Ph.D.)

DISSERTATION COMMITTEE

..... Chairman
 (Associate Professor Dr. Prinpida Sonthiphand, Ph.D.)

..... Thesis Advisor
 (Associate Professor Dr. ONRUTHAI PINYAKONG, Ph.D.)

..... Examiner
 (Associate Professor Dr. EKAWAN LUEPROMCHAI, Ph.D.)

..... Examiner
 (Associate Professor Dr. TAWAN LIMPIYAKORN, Ph.D.)

..... Examiner
 (Dr. Nattapong Tuntiwiwattanapun, Ph.D.)

..... Examiner
 (Dr. Pokchat Chutivisut, Ph.D.)

ริศู นิงจูแฉม : การย่อยสลายไดฟทอลเฮกซิลฟทาเลตโดยกลุ่มแบคทีเรียจากดินตะกอนทะเลและการระบุชนิดของแบคทีเรียและยีนที่ทำหน้าทีหลักในการย่อยสลาย. (Degradation of di (2-ethylhexyl) phthalate by marine sediment bacteria and identification of key degraders and degradative genes) อ.ที่ปรึกษาหลัก : รศ. ดร.อรุณทิพย์ ภิญญาคง

ได-2-เอทิลเฮกซิล ฟทาเลต (Di-2-ethylhexyl phthalate: DEHP) คือ สารเติมแต่งพลาสติก หรือพลาสติกไซเซอร์ประเภทฟทาเลตเอสเทอร์ (Phthalate esters: PAEs) ที่มีความเป็นพิษ ซึ่งพบการปนเปื้อนของ DEHP สูงทั้งในตะกอนทะเลและสัตว์ทะเล ปัจจุบันมีการศึกษาการย่อยสลายทางชีวภาพของ DEHP โดยแบคทีเรียที่สกัดแยกได้จากสิ่งแวดล้อมที่หลากหลาย อย่างไรก็ตาม ข้อมูลเกี่ยวกับความสามารถของแบคทีเรียจากตะกอนทะเลในการย่อยสลาย DEHP และ PAEs ชนิดต่างๆ ยังมีน้อยมาก ดังนั้นงานวิจัยนี้ ผู้วิจัยจึงคัดเลือกกลุ่มแบคทีเรียจากตะกอนทะเล พบกลุ่มแบคทีเรีย C10 มีประสิทธิภาพสูงในการย่อยสลาย PAEs สายยาว จำนวน 4 ชนิด ได้แก่ DEHP, ไดบิวทิลฟทาเลต (dibutyl phthalate: DBP), ไดเอทิล ฟทาเลต (diethyl phthalate: DEP), และไดเมทิล ฟทาเลต (dimethyl phthalate: DMP) เมื่อวิเคราะห์สายพันธุ์แบคทีเรียของกลุ่มแบคทีเรีย C10 ในระหว่างการย่อยสลาย PAEs พบว่าแบคทีเรียส่วนใหญ่เป็นสกุล *Glutamicibacter*, *Ochrobactrum*, *Pseudomonas*, *Bacillus*, *Stenotrophomonas*, และ *Methylophaga* ซึ่งสกุล *Brevibacterium*, *Ochrobactrum*, *Achromobacter*, *Bacillus*, *Sporosarcina*, และ *Microbacterium* มีจำนวนเพิ่มขึ้นในระหว่างการย่อยสลายสารเมแทบอลิซึมของ DEHP ได้แก่ มอนอเอทิลเฮกซิลฟทาเลต 2-เอทิลเฮกซานอล กรดฟทาเลทิก และกรดโปรโตคาเทอจิก การวิเคราะห์เครือข่ายของปฏิสัมพันธ์ในกลุ่มแบคทีเรีย C10 สามารถทำนายได้ว่า *Bacillus*, *Stenotrophomonas* และ *Microbacterium* เป็นสกุลหลักที่มีบทบาทสำคัญในการย่อยสลาย PAEs ซึ่งสอดคล้องกับการทดสอบการย่อยสลาย PAEs โดยแบคทีเรียสายพันธุ์เดี่ยว จำนวนทั้งหมด 21 สายพันธุ์ ที่ถูกคัดเลือกอย่างจำเพาะจากกลุ่มแบคทีเรีย C10 ซึ่งพบว่า *Microbacterium* sp. OR21, *Stenotrophomonas acidaminiphila* OR13, *Microbacterium* sp. OR16, *Sporosarcina* sp. OR19, และ *Cytobacillus firmus* OR20 มีประสิทธิภาพในการย่อยสลาย DEHP ความเข้มข้น 100 มิลลิกรัมต่อลิตร สูงที่สุดที่ 84.5, 83.7, 59.1, 43.4, และ 40.6 เปอร์เซ็นต์ ตามลำดับ ภายในระยะเวลา 8 วัน การศึกษานี้รายงานประสิทธิภาพการย่อยสลายทางชีวภาพของ DEHP โดย *S. acidaminiphila*, *Sporosarcina* sp., และ *Cytobacillus firmus* เป็นครั้งแรก นอกจากนี้ยังพบการเจริญของแบคทีเรียหลายสายพันธุ์ในสกุล *Bacillus*, *Microbacterium*, *Stenotrophomonas*, และ *Sporosarcina* เมื่อใช้สารเมแทบอลิซึมของ DEHP เป็นแหล่งคาร์บอน จากผลการศึกษาประสิทธิภาพการย่อยสลาย DEHP การใช้สารเมแทบอลิซึม และการทำนายปฏิสัมพันธ์ ส่งผลให้ *Microbacterium* sp. OR21, *Microbacterium* sp. OR16, และ *Sporosarcina* sp. OR05 ถูกคัดเลือกสำหรับสร้างเป็นกลุ่มแบคทีเรีย A02 ซึ่งพบว่ามีความสามารถในการย่อยสลาย PAEs ได้หลายชนิด และมีประสิทธิภาพสูงกว่าสายพันธุ์เดี่ยว อันเนื่องมาจากปฏิสัมพันธ์ในการทำงานเสริมกันของแบคทีเรียในกลุ่ม รวมถึงกลุ่มแบคทีเรีย A02 ยังสามารถย่อยสลายสารเมแทบอลิซึมของ DEHP ได้ด้วย เมื่อเติมกลุ่มแบคทีเรีย A02 ในตะกอนเดิมจากฟาร์มกุ้งที่ถูกจำลองให้ปนเปื้อนด้วย DEHP พบว่า A02 ร่วมกับจุลินทรีย์ท้องถิ่น สามารถเพิ่มประสิทธิภาพของการย่อยสลาย DEHP ได้เป็น 80 เปอร์เซ็นต์ ภายในระยะเวลา 26 วัน เมื่อวิเคราะห์จีโนมของแบคทีเรียทั้ง 3 สายพันธุ์ใน A02 พบยีนที่เกี่ยวข้องกับการย่อยสลายฟทาเลต ซึ่งการวิเคราะห์จีโนมและประสิทธิภาพการย่อยสลาย ถูกใช้เป็นข้อมูลสำหรับทำนายวิถีการย่อยสลาย PAEs โดยกลุ่มแบคทีเรีย A02 ดังนั้นการศึกษานี้จึงเผยให้เห็นข้อมูลที่ยังไม่ก่อกอมีผู้ทราบมาก่อนเกี่ยวกับศักยภาพในการย่อยสลาย PAEs ของแบคทีเรียที่สกัดแยกได้จากตะกอนในทะเล รวมถึงแสดงให้เห็นถึงแนวทางอย่างง่ายในการทำนายและคัดแยกสายพันธุ์เดี่ยวที่มีประสิทธิภาพในการย่อยสลายสารมลพิษ อย่างไรก็ตาม กลุ่มแบคทีเรียนี้ยังคงจำเป็นต้องถูกพัฒนาต่อไป เพื่อเพิ่มศักยภาพของการย่อยสลาย DEHP และ PAEs สำหรับนำไปประยุกต์ใช้ในสิ่งแวดล้อมทางทะเลต่อไปในอนาคต

สาขาวิชา การจัดการสารอันตรายและสิ่งแวดล้อม
ปีการศึกษา 2565

ลายมือชื่อ นิสิต
ลายมือชื่อ อ.ที่ปรึกษาหลัก

6187832020 : MAJOR HAZARDOUS SUBSTANCE AND ENVIRONMENTAL
MANAGEMENT

KEYWORD: phthalate ester, bacterial consortium, marine sediment, microcosm, network
analysis, genome analysis

Ritu Ningthoujam : Degradation of di (2-ethylhexyl) phthalate by marine sediment
bacteria and identification of key degraders and degradative genes. Advisor: Assoc. Prof.
Dr. ONRUTHAI PINYAKONG, Ph.D.

Di (2-ethylhexyl) phthalate (DEHP) is a toxic phthalate ester (PAE) plasticizer that is predominantly detected in marine sediment and biota. DEHP degradation by bacteria from several environments has been studied, but very little is known about marine sediment bacteria that can degrade DEHP and other PAEs. Therefore, in this study, we enriched a bacterial consortium C10 that can degrade four PAEs of varying alkyl chain lengths (DEHP, dibutyl phthalate, diethyl phthalate, and dimethyl phthalate; separately and as a mixture) from marine sediment. The major bacterial genera in C10 during the degradation of the PAEs were *Glutamicibacter*, *Ochrobactrum*, *Pseudomonas*, *Bacillus*, *Stenotrophomonas*, and *Methylophaga*. Meanwhile, *Brevibacterium*, *Ochrobactrum*, *Achromobacter*, *Bacillus*, *Sporosarcina*, and *Microbacterium* populations were enhanced by DEHP intermediates (monoethylhexyl phthalate, 2-ethylhexanol, phthalic acid, and protocatechuic acid). Through network analyses, it was predicted that *Bacillus*, *Stenotrophomonas*, and *Microbacterium* were the key phthalate-degraders in C10. Twenty-one isolates were obtained from C10 through selective isolation and the best DEHP-degraders were *Microbacterium* sp. OR21, *Stenotrophomonas acidaminiphila* OR13, *Microbacterium* sp. OR16, *Sporosarcina* sp. OR19, and *Cytobacillus firmus* OR20 (84.5, 83.7, 59.1, 43.4, and 40.6% degradation of 100 mg/L DEHP in 8 d), thus lending support to the prediction of key degraders. This is the first report of DEHP degradation by *S. acidaminiphila*, *Sporosarcina* sp., and *Cytobacillus firmus*. Furthermore, several isolates of *Bacillus*, *Microbacterium*, *Stenotrophomonas*, and *Sporosarcina* could utilize DEHP intermediates as sole carbon source. Isolates *Microbacterium* sp. OR21, *Microbacterium* sp. OR16, and *Sporosarcina* sp. OR05 were selected based on DEHP degradation efficiency, ability to utilize DEHP intermediates, and predicted interactions. A defined consortium of these three isolates (A02) could degrade multiple PAEs more efficiently than the individual strains, which could be attributable to synergistic interactions among the bacterial strains in A02. Furthermore, Consortium A02 could degrade DEHP intermediates (monoethylhexyl phthalate, phthalic acid, and protocatechuic acid). Bioaugmentation with A02 could enhance DEHP degradation (80% in 26 d) by indigenous microbes in microcosms of saline sediment from a shrimp farm. Genomic analyses of the three strains revealed the presence of several phthalate-degradation genes. Based on this information and experimental degradation results, the pathway of PAE degradation by Consortium A02 was predicted. Thus, this study reveals as yet unknown insights into the PAE-degrading potential of marine sediment bacteria and demonstrates a simple approach for the prediction and isolation of key pollutant-degraders from complex bacterial communities. Furthermore, a defined consortium with potential applicability for DEHP/PAE degradation in saline environments was developed.

Field of Study:	Hazardous Substance and Environmental Management	Student's Signature
Academic Year:	2022	Advisor's Signature

ACKNOWLEDGEMENTS

I owe immense gratitude to a great number of people who have helped shape this project to its successful completion. First and foremost, I am thankful to my advisor Associate Professor Dr. Onruthai Pinyakong. This project would not have been possible without Dr. Pinyakong's support, guidance, and encouragement. In addition to providing valuable feedback at every stage of this project, Dr. Pinyakong showed me great compassion and understanding through the many challenges of this project. I am also thankful to Dr. Pinyakong for allowing me access to laboratory facilities, equipment, and other resources during the course of their project. I also owe gratitude to the Southeast Asian Fisheries Development Center (SEAFDEC), Assistant Professor Dr. Penjai Sompongchaiyakul, and Dr. Sujaree Bureekul for providing the marine sediment used in this study.

This project has greatly benefitted from the valuable comments and suggestions of my Ph.D. dissertation committee. I give my heartfelt thanks to Associate Professor Dr. Prinpida Sonthiphand (Chairperson and External committee member), Associate Professor Dr. Ekawan Luepromchai, Associate Professor Dr. Tawan Limpiyakorn, Dr. Nattapong Tuntiwattanapun, and Dr. Pokchat Chutivisut for their time and contribution to this project.

This research was funded by the Thailand Science Research and Innovation Fund Chulalongkorn University (CU_FRB65_dis (4)_092_23_22) and the 90th Anniversary of Chulalongkorn University Scholarship under the Ratchadapisek Somphot Endowment Fund. I would like to acknowledge the Graduate School, Chulalongkorn University and the International Program for Hazardous Substance and Environmental Management (IP-HSM) for providing the 100th Anniversary Chulalongkorn University Fund for Doctoral Scholarship.

Throughout my Ph.D. project, I have had the honor to work alongside and learn from an outstanding group of past and present lab mates. I would like to thank Dr. Chatsuda Sakdapetsiri, Dr. Kallayanee Naloka, Dr. Natthariga Laothamteep, Miss Chanokporn Muangchinda, Miss Parichaya Tiralerdpanich, Mr. Adisan Rungsahiranrut, Miss Theodora Mega Putri, Miss Naphatsakorn Woratecha, Miss Chavisa Jeerasantikul, and Mr. Jirakit Jaroornunganan.

On a personal note, I would like to express my deepest appreciation to my family and friends for being the strongest support system through the ups and downs of my Ph.D. journey. I am forever indebted to my parents, Basant and Limanaro, who instilled in me the value of hard work, integrity, and perseverance through the inspiring lives they lead. They are the beacon of all my achievements. I am grateful to my sister, Ribica, for the humor and light she has brought to the most difficult challenges. I also owe immense gratitude to Avnish Mistry for his unconditional support.

Ritu Ningthoujam

TABLE OF CONTENTS

	Page
ABSTRACT (THAI)	iii
ABSTRACT (ENGLISH).....	iv
ACKNOWLEDGEMENTS	v
TABLE OF CONTENTS.....	vi
List of Tables	xi
List of Figures	xiii
CHAPTER 1	17
INTRODUCTION	17
1.1 Statement of problem.....	17
1.2 Research hypotheses	23
1.3 Research objectives	23
1.4 Scope of the study.....	23
1.5 Experimental setup	26
CHAPTER 2	27
LITERATURE REVIEW	27
2.1 Phthalate esters: types, uses, and properties	27
2.2 Phthalate esters in the marine ecosystem.....	29
2.3 Toxicity of phthalate esters.....	34
2.4 Phthalate ester degradation processes.....	36
2.4.1 Abiotic processes for phthalate ester degradation.....	36
2.4.2 Biodegradation of phthalate esters	37
2.4.2.1 Biodegradation of phthalate esters by fungi and algae.....	37
2.4.2.2 Biodegradation of phthalate esters by bacteria.....	37
2.5 Biodegradation of phthalate esters in soil and sediment	45
2.5.1 Biodegradation of phthalate esters by indigenous soil/sediment bacteria.....	45

2.5.2 Biodegradation of phthalate esters via bioaugmentation with exogenous bacteria	47
2.6 Mechanism of bacteria-mediated phthalate ester degradation.....	50
2.6.1 Pathway of bacteria-mediated phthalate ester degradation	50
2.6.2 Enzymes and genes involved in bacteria-mediated phthalate ester biodegradation	51
2.7 Microbial co-occurrence networks	59
CHAPTER 3	63
MATERIALS AND METHODS.....	63
3.1 Chemicals and materials	63
3.2 Experimental procedure.....	66
3.3 Phase I.....	67
3.3.1 Enrichment of bacterial consortia from marine sediment with DEHP as a carbon source.....	67
3.3.2 Preparation of inoculum for enriched bacterial consortia	67
3.3.3 Preliminary investigation of the DEHP-degrading capabilities of the nine enriched consortia.....	68
3.3.4 Degradation of other phthalate esters by the enriched consortia and growth on DEHP intermediates.....	70
3.3.5 Taxonomic classification of the bacterial communities in the enriched consortia and sediment samples	71
3.3.6 16S rRNA gene amplicon sequencing.....	72
3.3.7 Kinetics of DEHP degradation by C10	72
3.3.8 Bacterial co-occurrence patterns and prediction of bacterial community function.....	73
3.4 Phase II	74
3.4.1 Selective isolation of bacterial strains in C10 and identification of isolated bacterial stains	74
3.4.2 Preparation of inoculum for single bacterial strains.....	74
3.4.3 Characterization of the bacterial isolates from C10	75
3.5 Phase III.....	76

3.5.1 Creation of defined bacterial consortia and screening their PAE degradation activities.....	76
3.5.2 Whole genome sequencing.....	77
3.5.3 Degradation of DEHP intermediates.....	77
3.5.4. Sediment microcosm study.....	78
3.5.4.1 Microcosm setup.....	78
3.5.4.2 Quantification of DEHP concentrations and bacterial numbers ..	79
3.5.4.3 Studying the bacterial community in sediment microcosms during DEHP degradation.....	81
CHAPTER 4.....	82
RESULTS AND DISCUSSION.....	82
4.1 Phase I.....	82
4.1.1 Enrichment of bacterial consortia from marine sediment with DEHP as a carbon source.....	82
4.1.2 Preliminary investigation of the DEHP-degrading capabilities of the nine enriched consortia.....	82
4.1.3 Degradation of other phthalate esters by C10, C22, and C33.....	85
4.1.4 Taxonomic classification of the bacterial communities in the enriched consortia and sediment samples.....	94
4.1.4.1 Bacterial communities in the marine sediment and corresponding enriched consortia.....	94
4.1.4.2 Bacterial communities of C10, C22, and C33 during degradation of the PAE mixture.....	99
4.1.4.3 Bacterial communities of C10 during degradation of different PAEs and growth on DEHP intermediates.....	109
4.1.5 Changes in the predicted metabolic potential of the bacterial communities of C10 induced by PAEs and DEHP intermediates.....	114
4.1.6 Co-occurrence patterns of C10 at the genus level and prediction of key degraders.....	118
4.2 Phase 2.....	123
4.2.1 Selective isolation of bacterial strains in C10 and identification of isolated bacterial stains.....	123

4.2.2	Characterization of the bacterial isolates from C10	125
4.2.2.1	DEHP degradation activities of the isolates from C10.....	125
4.2.2.2	Growth of the isolates from C10 on DEHP intermediates as sole source of carbon.....	133
4.2.2.3	Oil displacement activities of the isolates from C10.....	138
4.2.3	Selection of isolates for defined consortia creation.....	138
4.3	Phase III	140
4.3.1	Phthalate ester degradation efficiencies of defined bacterial consortia .	140
4.3.1.1	Comparison of the PAE degradation efficiencies of enriched consortium C10 and defined consortia created using bacterial isolates of C10	148
4.3.2	Degradation of DEHP intermediates	149
4.3.3	Genome sequencing and functional annotation.....	151
4.3.3.1	Detection of genes encoding potential phthalate degradation enzymes	158
4.3.3.2	Predicted pathway of DEHP biodegradation by Consortium A02 based on genomic analysis	190
4.3.3.3	Predicted roles of OR05, OR16, and OR21 in DEHP degradation by Consortium A02	195
4.3.4	Sediment microcosm study	198
CHAPTER 5	204
CONCLUSIONS AND RECOMMENDATIONS	204
5.1	Conclusions.....	204
5.2	Recommendations.....	209
5.3	Research benefits	214
REFERENCES	215
APPENDIX	233
Appendix A:	Media composition.....	233
Appendix B:	Standard curves	234
Appendix C:	Marine sediment properties.....	244
Appendix D:	Phase I Results	245

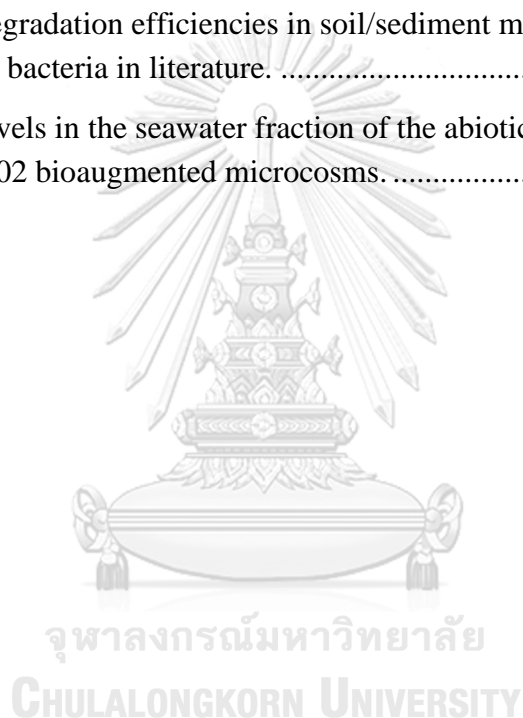
Appendix E: Phase II Results	264
Appendix F: Phase III Results	279
VITA.....	306



List of Tables

	Page
Table 1 Properties and uses of commonly used phthalate esters (adapted from Boll et al (2020), Baloyi et al (2021), and Cousins et al (2003)).	27
Table 2 Phthalate ester levels in the marine ecosystem.	32
Table 3 Bacterial strains reported for phthalate ester degradation.	40
Table 4 Genes/enzymes with reported role in phthalate ester degradation.	57
Table 5 Sampling locations of the nine marine sediment samples used for enrichment.	64
Table 6 Kinetic equations of the degradation of different initial DEHP concentrations by C10.	91
Table 7 Alpha diversity indices (Shannon index, Faith's phylogenetic diversity, and observed OTUs) of the bacterial communities of the nine marine sediment samples and corresponding enriched consortia.	94
Table 8 Taxonomic classification of the bacterial community of C10 on Day 4 of degradation of the PAE mixture based on long-read 16S rRNA gene amplicon sequencing.	102
Table 9 Alpha diversity indices (Shannon index, Faith's phylogenetic diversity, and observed OTUs) of C10, C22, and C33 bacterial communities in the presence of different substrates.	107
Table 10 Co-occurrence network parameters of C10 at the genus level observed in the presence of DEHP, DBP, DEP, and DMP (separately and as a mixture) and MEHP, 2-ethylhexanol, phthalic acid, and protocatechuic acid).	121
Table 11 Node parameters of the co-occurrence network of C10 at the genus level in the presence of DEHP, DBP, DEP, and DMP (separately and as a mixture) and MEHP, 2-ethylhexanol, phthalic acid, and protocatechuic acid.	121
Table 12 Taxonomic identification of the bacterial isolates from C10.	124
Table 13 Overview of the DEHP degradation activities, growth characteristics and oil displacement abilities of the isolates from C10.	129
Table 14 Genomic and annotation features of OR05, OR16, and OR21.	151
Table 15 Functional annotation of the CDS in the genomes of OR05, OR16, and OR21.	162

Table 16 Hits for phthalate ester-degradative genes reported in literature in the genomes of <i>Microbacterium</i> sp. OR16 and <i>Microbacterium</i> sp. OR21 via local BLAST searches.	177
Table 17 Genes in OR05, OR16, and OR21 mapped to the benzoate degradation via hydroxylation pathway.....	186
Table 18 Enzymes used for the prediction of the PAE degradation pathway of Consortium A02.....	196
Table 19 Physical and chemical properties of sediment used in the microcosm study.	198
Table 20 DEHP degradation efficiencies in soil/sediment microcosms by augmentation with bacteria in literature.	200
Table 21 DEHP levels in the seawater fraction of the abiotic control, natural attenuation, and A02 bioaugmented microcosms.	203



List of Figures

	Page
Figure 1 Generalized pathway for the biodegradation of phthalate esters under aerobic conditions adapted from literature.	51
Figure 2 Map showing the sampling sites (in the Gulf of Thailand) of the marine sediment samples used in this study.	65
Figure 3 Schematics of bacterial inoculum preparation.	68
Figure 4 Schematics of residual DEHP extraction from the degradation medium.	69
Figure 5 Set-up of the sediment microcosm study.....	79
Figure 6 DEHP (100 mg/L) degradation efficiencies of the nine enriched bacterial consortia on days 4 and 6. Different letters indicate significantly different ($p < 0.05$) average percent DEHP degradation values.	83
Figure 7 Viable cell counts of the nine enriched bacterial consortia on days 4 and 6 of DEHP degradation and in the biological control.	84
Figure 8 a) Percent degradation of DMP, DEP, and DBP (100 mg/L each) by C10, C22, and C33 on Day 4; (b) Viable cell counts of C10, C22, and C33 on Day 0 and Day 4 of degradation of DMP, DEP, and DBP. Different letters indicate statistically different average percent degradation and log CFU/mL values.	86
Figure 9 PAE concentration remaining during degradation of a mixture of DEHP, DBP, DEP, and DMP (100 mg/L each; total concentration: 400 mg/L) by C10 (a); C22 (b); C33 (c); and in the abiotic control (d); and viable cells counts (log CFU/mL) of C10, C22, and C33 during degradation of the PAE mixture (e).	89
Figure 10 Degradation of different concentrations of DEHP (50 – 800 mg/L) by C10.	91
Figure 11 Viable cell numbers of C10 cultured with MEHP, 2-ethylhexanol (2-EHA), phthalic acid (PA), and protocatechuic acid (PCA) as the sole source of carbon. BC refers to the biological control wherein C10 was cultured without the addition of any carbon source.	93
Figure 12 Principal coordinate analysis plot of beta diversity based on weighted UniFrac distances between the bacterial communities of the nine marine sediment samples and corresponding enriched consortia.....	95
Figure 13 Bacterial communities of the nine marine sediment samples at the class level.....	96

Figure 14 Bacterial communities of the enriched bacterial consortia at the class level.	97
Figure 15 Bacterial communities of the enriched bacterial consortia at the genus level.	98
Figure 16 Bacterial communities of C10 on days 2, 4, and 6 of the degradation of a mixture of DEHP, DBP, DEP, and DMP at the class level (a) and the genus level (b).	101
Figure 17 Bacterial communities of C22 on days 2, 4, 6, and 8 of the degradation of a mixture of DEHP, DBP, DEP, and DMP at the class level (a) and the genus level (b).	104
Figure 18 Bacterial communities of C33 on days 2, 4, 6, and 8 of the degradation of a mixture of DEHP, DBP, DEP, and DMP at the class level (a) and the genus level (b).	106
Figure 19 Principal coordinate analysis plot of beta diversity based on a weighted UniFrac of the bacterial communities of C10 (circle), C22 (diamond), and C33 (star) in the presence of different substrates. D2M, D4M, D6M, and D8M indicate bacterial communities on days 2, 4, 6, and 8 of the degradation of a mixture of DEHP, DBP, DEP, and DMP.....	108
Figure 20 Bacterial communities of C10 on Day 4 of DEHP, DBP, DEP, and DMP degradation at the class level (a) and the genus level (b).	110
Figure 21 Bacterial communities of C10 on Day 4 of growth on MEHP, 2-ethylhexanol (2-EHA), phthalic acid (PA), and protocatechuic acid (PCA) at the class level (a) and the genus level (b).....	112
Figure 22 Level 3 KEGG functions under Global and overview maps assigned to the bacterial communities of C10 during degradation of DEHP, DBP, DEP, and DMP, on days 2, 4, and 6 of the degradation of the PAE mixture (D2M, D4M, and D6M, respectively), and cultured with MEHP, 2-ethylhexanol (2-EHA), phthalic acid (PA), and protocatechuic acid (PCA) as sole source of carbon.....	116
Figure 23 Top nineteen KEGG level pathways (excluding Global and overview maps) assigned to the bacterial communities of C10 during degradation of DEHP, DBP, DEP, and DMP, on days 2, 4, and 6 of the degradation of the PAE mixture (D2M, D4M, and D6M, respectively), and cultured with MEHP, 2-ethylhexanol (2-EHA), phthalic acid (PA), and protocatechuic acid (PCA) as sole source of carbon.	117
Figure 24 Level 3 KEGG functions under Xenobiotics degradation and metabolism assigned to the bacterial communities of C10 during degradation of DEHP, DBP, DEP, and DMP, on days 2, 4, and 6 of the degradation of the PAE mixture (D2M,	

D4M, and D6M, respectively), and cultured with MEHP, 2-ethylhexanol (2-EHA), phthalic acid (PA), and protocatechuic acid (PCA) as sole source of carbon.	118
Figure 25 Predicted co-occurrence patterns of C10 bacterial community members at the genus level: (a) overall network in the presence of DEHP intermediates and PAEs, (b) subnetwork in the presence of DEHP intermediates, and (c) subnetwork in the presence of DEHP, DBP, DEP, and DMP (separately and as a mixture).....	120
Figure 26 Percent DEHP (100 mg/L) degradation by the twenty-one isolates from C10 on Day 8. The different letters significantly different ($p < 0.05$) percent DEHP degradation values.	127
Figure 27 Viable cell counts of the bacterial isolates from C10 on Day 0 and Day 8 of DEHP degradation.	128
Figure 28 Growth of the bacterial isolates from C10 on 100 mg/L DEHP, MEHP, monobutyl phthalate (MBP), phthalic acid (PA), and protocatechuic acid (PCA) and 100 and 200 mg/L 2-ethylhexanol (EHA-100 and EHA-200) as the sole carbon source. Different letters indicate significantly different ($p < 0.05$) log CFU/mL (Day 5-Day 0) values.	137
Figure 29 Degradation efficiencies of 100 mg/L of DMP, DEP, DBP, and DEHP (separately) on Day 4. The different letters indicate significantly different ($p < 0.05$) percent degradation values for each PAE type.	142
Figure 30 DEHP (100 mg/L) degradation efficiencies of OR21, OR05 +OR21, Consortium A01, and Consortium A02 on days 2, 4, 6, and 8. Different letters indicate significantly different ($p < 0.05$) percent degradation values.	143
Figure 31 Remaining PAE concentrations during degradation of a mixture of DEHP, DBP, DEP, and DMP (100 mg/L each) by Consortium A01 (a), Consortium A02 (b), OR05 + OR21 (c), and OR21 (d). The different letters indicate significantly different ($p < 0.05$) DEHP concentrations in the different treatments (a-d) at each sampling point.	145
Figure 32 Viable cell counts of Consortium A01, Consortium A02, and OR05 + OR21 during degradation of the PAE mixture (Mix PAE) and DEHP.....	147
Figure 33 Percent degradation of MEHP on Day 8 by OR05, OR16, OR21, OR05+OR16, OR05+OR21, and Consortium A02. Different letters indicate significantly ($p < 0.05$) different values.....	150
Figure 34 Percent degradation of phthalic acid (a) and protocatechuic acid (b) on Day 4 by OR05, OR16, OR21, OR05+OR16, OR05+OR21, and Consortium A02. Different letters indicate significantly ($p < 0.05$) different values.....	151

Figure 35 Circular map of <i>Sporosarcina</i> sp. OR05 based on genome sequencing and annotation. The inner to outer circles represent GC skew, GC content, CDS on the reverse strand, CDS on the forward strand, and contigs.....	152
Figure 36 Circular map of <i>Microbacterium</i> sp. OR16 based on genome sequencing and annotation. The inner to outer circles represent GC skew, GC content, CDS on the reverse strand, CDS on the forward strand, and contigs.....	154
Figure 37 Circular map of <i>Microbacterium</i> sp. OR21 based on genome sequencing and annotation. The inner to outer circles represent GC skew, GC content, CDS on the reverse strand, CDS on the forward strand, and contigs.....	155
Figure 38 KEGG pathways mapped to genes in the genomes of OR05, OR16, and OR21 (a) and sub-division of the Xenobiotics biodegradation and metabolism pathway (b) assigned to genes in OR05, OR16, and OR21.....	156
Figure 39 Stress response (a) and membrane transport (b) KEGG pathways assigned to genes in the genomes of OR05, OR16, and OR21.	157
Figure 40 PAE degradation pathway predicted based on genomic analysis on OR05, OR16, and OR21. The dashed lines represent degradation steps for which enzymes are unknown or have not been detected in the genomes of OR05, OR16, and OR21. The numbers within the boxes represent the potential degradation enzymes detected in the genomes of OR05, OR16, and OR21 (Table 18).....	194
Figure 41 Remaining DEHP concentration (a) and percent DEHP degradation (b) in sediment of abiotic control, natural attenuation, and A02 bioaugmented microcosms. Different letters indicate significantly different ($p < 0.05$) percent DEHP degradation.	202
Figure 42 Overview of research results.	207

CHAPTER 1

INTRODUCTION

1.1 Statement of problem

Phthalate esters or phthalic acid esters (PAEs) are non-halogenated esters of phthalic acid and can be divided into two main types based on the length of their carbon side chains: low-molecular-weight PAEs and high-molecular-weight PAEs (Hidalgo-Serrano et al 2022). These chemicals are primarily used as plasticizers to enhance the flexibility and durability of plastic products (Sun et al 2015, Zhu et al 2018, Zhu et al 2019a). PAEs are also present in cosmetics, pharmaceuticals, pesticides, propellants, and insecticides (Zhu et al 2018). Owing to their excellent plasticizing efficiency and low production cost (Xu et al 2017), PAEs are the most widely used plasticizers, accounting for about 65% of the global plasticizer market (Wright et al 2020), while di (2-ethylhexyl) phthalate (DEHP) is the most abundantly produced and widely used PAE (Hu et al 2020, Kastner et al 2012, Xu et al 2017, Zhao et al 2018a, Zhu et al 2018). Plasticizers make up approximately 40% to 60% of the total weight of plasticized products (Sun et al 2015, Zhu et al 2019b).

PAEs are not covalently bound to polymers chains and, therefore, readily leach from plasticized products into the environment (Kastner et al 2012, Magdouli et al 2013, Xu et al 2017, Zhao et al 2018a, Zhu et al 2018, Zhu et al 2019b). Thus, PAEs have emerged as ubiquitous environmental pollutants, with DEHP reported to be the predominant PAE in several environments, particularly in marine sediments (Kim et al 2020, Paluselli & Kim 2020, Xu et al 2017, Zhu et al 2019b). Widespread environmental occurrence of PAEs increases the risk of human exposure through inhalation, ingestion, and dermal contact (Chang et al 2021b). In fact, PAE

metabolites have been detected in human urine, feces, and blood samples (Wang & Qian 2021). This is a serious concern because some PAEs are reported to be endocrine disruptors, carcinogenic, and mutagenic (Yuan et al 2010, Zhu et al 2019a). Therefore, the U.S. Environmental Protection Agency (EPA) and the European Union have classified DEHP, diethyl phthalate (DEP), dimethyl phthalate (DMP), and dibutyl phthalate (DBP) as priority pollutants (Yuan et al 2010). Furthermore, many PAEs have been banned or restricted in food handling and storage products, childcare items, and toys in countries like the US, China, Australia, and Japan (Chang et al 2021a, Wang & Qian 2021).

Current methods for PAE remediation include abiotic processes, such as photolysis (Wang et al 2019a), and biotic processes such as degradation by microbes including bacteria (Das et al 2021) and phytoremediation (Xiaoyan et al 2015). Nevertheless, PAE degradation via natural processes, such as hydrolysis and photolysis, is typically slow (Lu et al 2009, Xu et al 2008, Zhu et al 2018). The hydrolysis and photolysis half-lives of DEHP in water are 2000 and 0.12-1.5 yr, respectively (Net et al 2015). Bacterial degradation is widely reported to be an effective approach for PAE remediation (Lu et al 2009, Xu et al 2008, Yuan et al 2010, Zhu et al 2018, Zhu et al 2019a). However, toxic intermediates, such as monoethylhexyl phthalate (MEHP), 2-ethylhexanol, and phthalic acid, may accumulate (Zhu et al 2018). The biodegradation of PAEs requires the participation of diverse enzymes such as esterases, dioxygenases, and decarboxylases, and dehydrogenases (Das et al 2021), all of which may not be produced by a single bacterial species. Breakdown of DEHP by indigenous soil bacteria led to the accumulation of MEHP and 2-ethylhexanol (Kastner et al 2012, Zhu et al 2018). Furthermore, some PAE-

degrading bacteria cannot utilize all the intermediates formed during PAE degradation (Zhao et al 2018a, Zhao et al 2021). Many of the negative health effects associated with DEHP are reportedly attributable to MEHP and 2-ethylhexanol (Gao & Wen 2016, Paluselli et al 2019) and both metabolites are persistent in the environment (Lv et al 2018). Phthalic acid is also reported to be toxic to some bacterial strains (Wright et al 2020). Therefore, there is a need to identify efficient degraders of DEHP and its toxic intermediates such as MEHP, 2-ethylhexanol, and phthalic acid.

Several bacterial strains that can degrade DEHP effectively in aqueous media have been isolated, but the few studies that have investigated their performance in remediation of DEHP-contaminated soil or sediment have observed markedly reduced degradation (Wang et al 2019b, Zhao et al 2018a). A solution could be the use of bacterial consortia, which has been rarely studied for PAE degradation (Bai et al 2020, Li et al 2018). A bacterial consortium refers to an association of two or more bacterial strains, that exist as a community and act together, usually to their mutual benefit (Festa et al 2017). Almost all microorganisms exist in consortia in nature (Rapp et al 2020) and the population density of desired bacteria, such as bacteria with DEHP degradation activity, in these natural consortia can be enriched (referred to as an enriched consortium) by creating favorable growth conditions (Madhuri et al 2019). A defined bacterial consortium, on the other hand, is an artificially constructed co-culture of two or more bacterial strains. The metabolic powers of multiple bacterial strains can be harnessed in such a consortium and, hence, can potentially exceed the metabolic capacity of single bacterial strains during degradation of environmental pollutants (Qian et al 2020).

PAE contamination in the marine environment is becoming a serious concern (Hidalgo-Serrano et al 2022). Owing to their hydrophobicity and high octanol-water partition coefficient, PAEs in the marine environment tend to adsorb to the sediment fraction, and consequently PAEs are frequently reported in marine sediment (Hu et al 2020). Furthermore, the widespread accumulation of PAEs and their metabolites (Hidalgo-Serrano et al 2022) indicate that the indigenous microbial community may not harbor enough degraders of PAEs and their intermediates. Despite this, knowledge about key PAE-degraders in marine sediment is severely lacking. Little information is available about the marine bacterial groups stimulated by DEHP and the contribution of different bacterial strains to breakdown of PAEs and corresponding metabolites in marine sediment. High-throughput 16S rRNA gene amplicon sequencing can be used to monitor bacterial communities, in terms of members and their abundance, during degradation of different environmental pollutants (Bai et al 2020, Muangchinda et al 2018). The functional potential of bacterial communities can be inferred from the partial 16S rRNA gene sequences obtained using tools such as PICRUSt (Douglas et al 2020) and Tax4Fun (Wemheuer et al 2020). Although these tools cannot be used as a replacement for metagenome-based functional analysis, they can be used to gain initial insights into how bacterial community functions change or adapt in response to environmental pollutants. Similarly, patterns of bacterial co-occurrence predicted through statistical network analyses are considered to be well representative of bacterial community interactions (Ishimoto et al 2021). In recent years, many researchers have investigated microbial co-occurrence patterns in soil (Ishimoto et al 2021, Wang et al 2021d) and sediment (Yan et al 2019, Zhang et al 2022) contaminated with various pollutants. Co-

occurrence patterns could reveal potentially important bacterial members in a community such as hub taxa and key connectors and useful insights into bacterial taxa that have major influences on community structure and function (Banerjee et al 2018, Ishimoto et al 2021). Such an approach could also be used to identify cooperators that enhance biodegradation of environmental pollutants (Wang et al 2021d) and guide the creation of defined consortia of bacteria with the potential for synergistic interactions for the effective biodegradation of environmental pollutants.

A handful of researchers have analyzed the whole genome sequences of PAE-degraders, such as *Bacillus subtilis* (Xu et al 2021), *Pseudarthrobacter defluvii* (Chen et al 2021), and *Rhodococcus* sp. LW-XY12 (Song et al 2022) and predicted genes coding for degradative enzymes. Knowledge about genes involved in the degradation of PAEs is required to understand the mechanism of bacterial PAE degradation, which will assist in achieving effective bioremediation. Genome sequencing and annotation can reveal the genetic basis of biodegradation, adaptability of bacterial strains to different environmental conditions, and potential metabolic pathways for degradation (An et al 2020, Xu et al 2021). This will pave the way towards a better understanding of the mechanism of phthalate degradation by individual bacterial isolates and bacterial consortia, thus facilitating the development of effective bioremediation solutions.

Aquaculture production is growing rapidly and consequently, the quality of the aquaculture environment, which in turn influences the quality of aquaculture products intended for human consumption, has been receiving increasing scrutiny in recent years (Zhang et al 2021). The extensive use of plastic cages, fishing nets and

lines, polyvinylchloride pipes, and other tools used in aquaculture practices are known to release toxic contaminants into the surrounding environment (Bringer et al 2021, Rios-Fuster et al 2022). Cheng, et al. observed that DEHP was the predominant PAE in water and sediment samples of fish aquaculture ponds in Pearl River Delta, China (Cheng et al 2019). DMP, DEP, DEHP, and DBP were also detected in materials collected from an aquaculture oyster farm in South-West France (Bringer et al 2021). Hence, it would be useful to develop biodegradation solutions that could be applied to treat PAE-contamination in aquaculture sediment.

Therefore, this study aims to enrich bacterial consortia that can degrade several PAEs (DEHP, DBP, DMP, and DEP) from marine sediment and predict key degraders based on the bacterial community dynamics of and co-occurrence patterns in the enriched consortia during PAE degradation. The next objective is to selectively isolate the predicted key degraders and investigate their abilities to utilize DEHP and its metabolites as sole carbon source. Based on this information, strains with diverse metabolic capabilities will be selected to create a defined bacterial consortium. The genes involved in DEHP degradation will be predicted via genomic analyses. Finally, the degradation performance of the defined consortium in DEHP-spiked sediment microcosms will be evaluated. The ultimate goals of this study are to gain insights about which bacterial members may play key roles in PAE degradation in the marine environment and to obtain a bacterial consortium with the potential for effective bioremediation of PAE-contaminated sediment.

1.2 Research hypotheses

1. Marine sediment will contain bacteria that can degrade DEHP and/or its metabolites such as mono-ethylhexyl phthalate, 2-ethylhexanol, and phthalic acid.
2. A defined bacterial consortium of key degraders isolated from a DEHP-enriched consortium will be able to degrade DEHP and its metabolites.
3. DEHP biodegradation in sediment microcosms bioaugmented with the defined bacterial consortium will be higher than DEHP biodegradation by natural attenuation.

1.3 Research objectives

1. Obtain enriched bacterial consortia that can utilize DEHP as a source of carbon from marine sediments.
2. Investigate the DEHP degradation activity of enriched consortia and identify key bacterial members involved.
3. Isolate and characterize the bacterial strains comprising the enriched bacterial consortia and determine their DEHP degradation activities.
4. Create defined consortia using combinations of the isolated bacterial strains and investigate their DEHP degradation activities.
5. Explore the DEHP degradation performance and impacts of defined bacterial consortia in sediment microcosms.

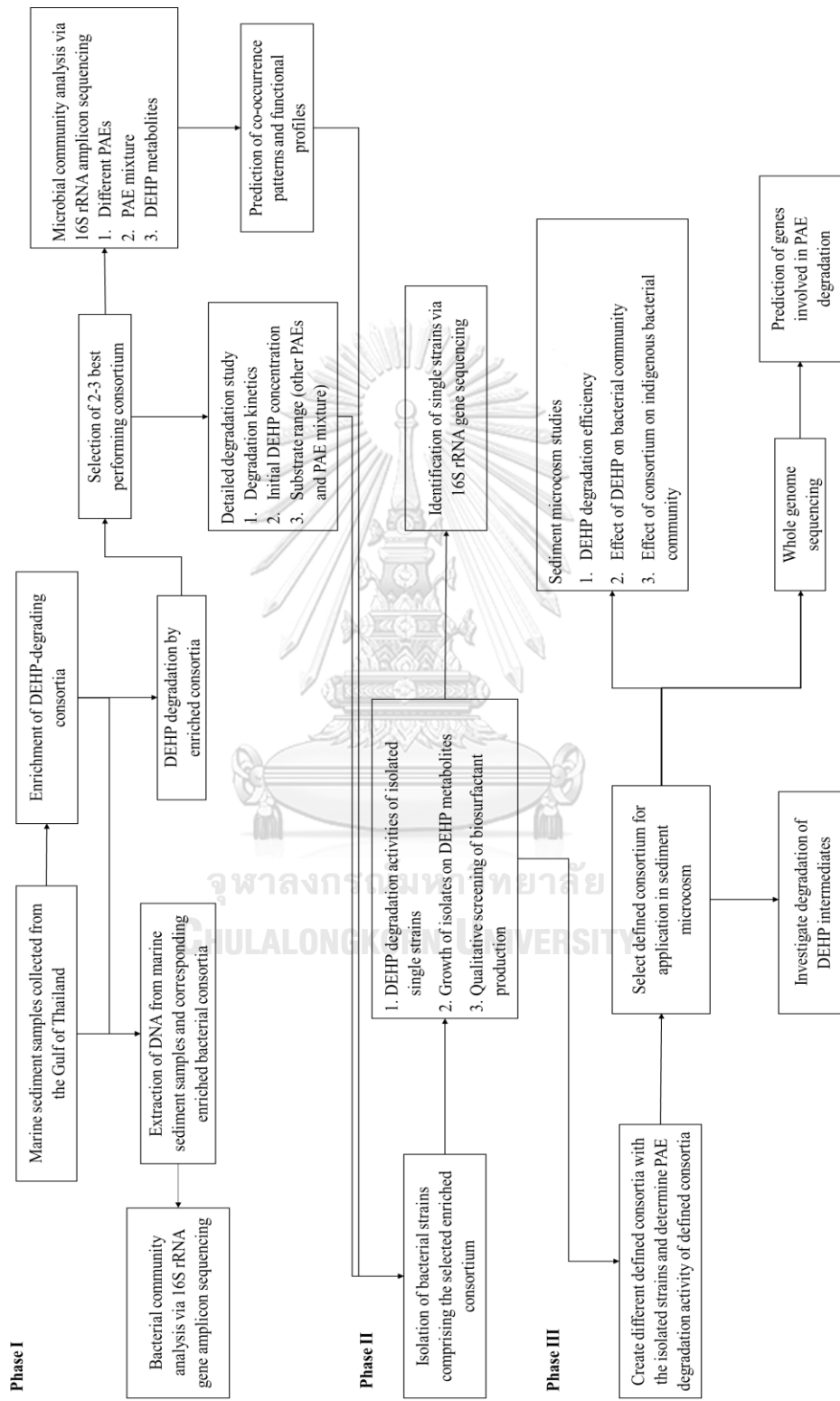
1.4 Scope of the study

1. Marine sediment samples collected from the Gulf of Thailand were used for enrichment of DEHP-degrading bacterial consortia.

2. A bacterial consortium C10 (or MSCU 1093) enriched from marine sediment from the same region and deposited in Culture Collection, Chulalongkorn University, was also used in this study.
3. DNA extracted from sediment and enriched consortia was submitted to Omics Sciences & Bioinformatics Center, Chulalongkorn University for 16S rRNA gene amplicon sequencing.
4. Bacterial co-occurrence patterns and functional profiles were predicted using R-based tools Compositionality Corrected by REnormalizaion and Permutation (CCREPE) and Tax4Fun2, respectively.
5. Nutrient seawater supplemented with the target phthalate ester (DEHP, DBP, DEP or DMP) was used as degradation medium.
6. Residual phthalate ester was extracted using dichloromethane and quantified using a Gas Chromatograph equipped with a flame ionization detector (GC-FID).
7. Bacterial growth was monitored via plate count method (on 0.25X Zobell Marine Agar, ZMA) and optical density at 600 nm was measured using a UV-visible spectrophotometer.
8. Enriched consortium with the best DEHP degradation activity was selected for further studies.
9. Bacterial strains in the selected enriched consortium were isolated on nutrient seawater agar (with 50 mg/L DEHP), 0.25X ZMA, and other selective agar media, which were designed based on the bacterial community information obtained via 16S rRNA gene amplicon sequencing.
10. The isolates were identified via 16S rRNA gene sequencing.

11. Bacterial isolates were screened on the basis of their DEHP degradation activities, growth characteristics on DEHP metabolites (MEHP, 2-ethylhexanol, phthalic acid, and protocatechuic acid), and biosurfactant productivity.
12. The selected isolates were used to create different defined consortia after confirming the absence of any antagonistic interactions using the cross-streak method.
13. The degradation activities of the defined consortia for DEHP, DBP, DEP, and DMP (separately and as a mixture) were screened and the best performing consortium was selected for further studies.
14. The genes involved in DEHP degradation by the selected defined consortium were predicted via genome sequencing and analysis.
15. Degradation of the DEHP metabolites (MEHP, 2-ethylhexanol, phthalic acid, and protocatechuic acid) by the selected defined consortium and its component bacterial strains were examined.
16. The DEHP degradation performance of the selected defined were studied in sediment microcosms.

1.5 Experimental setup



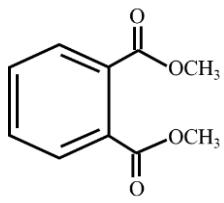
CHAPTER 2

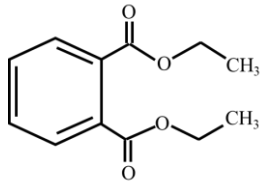
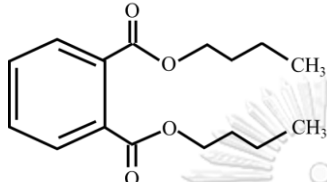
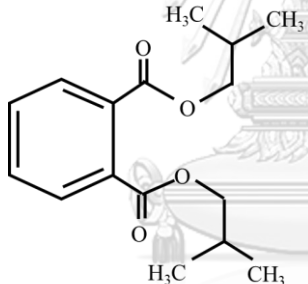
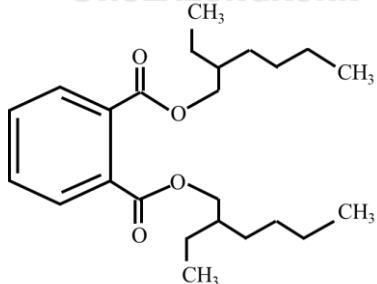
LITERATURE REVIEW

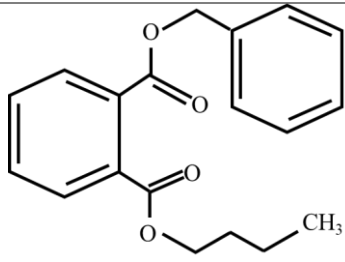
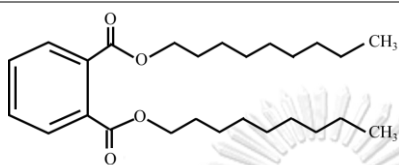
2.1 Phthalate esters: types, uses, and properties

Phthalate esters can be of different types depending on the length and structure of its two alkyl chains. The properties of some commonly used PAEs and their uses are listed in Table 1. Low molecular weight PAEs have alkyl chains with 1-4 carbon atoms, while the alkyl chains of high molecular weight PAEs contain 7 or more carbon atoms. High molecular weights PAEs are typically used as plasticizers; however, dibutyl phthalate is sometimes used as plasticizer in conjunction with high molecular weight PAEs such as DEHP (Cousins et al 2003). Phthalate plasticizers account for approximately 65% of the global plasticizer consumption and DEHP and DBP are two of the most widely used PAE plasticizers (Wright et al 2020).

Table 1 Properties and uses of commonly used phthalate esters (adapted from Boll et al (2020), Baloyi et al (2021), and Cousins et al (2003)).

Phthalate ester	Chemical structure	Properties	Uses
Dimethyl phthalate, DMP (C ₁₀ H ₁₀ O ₄)		Molecular weight: 194.19 g/mol Log K _{ow} : 1.46-1.90; Solubility in water: 2810-4320 mg/L	Insecticides, shampoo, room fresheners, etc.

Diethyl phthalate, DEP (C ₁₂ H ₁₄ O ₄)		Molecular weight: 222.24 g/mol Log Kow: 2.21-3.0; Solubility in water: 680-1080 mg/L	Cosmetics, fragrances, deodorants, nail polish, pharmaceuticals, etc.
Di-n-butyl phthalate, DBP/DnBP (C ₁₆ H ₂₂ O ₄)		Molecular weight: 278.35 g/mol Log Kow: 3.74-5.15; Solubility in water: 9.15-13 mg/L	Plasticizer, printer inks, adhesives, cosmetics, pharmaceuticals, and aftershave, etc.
Di-isobutyl phthalate, DiBP (C ₁₆ H ₂₂ O ₄)		Molecular weight: 278.35 g/mol Log Kow: 4.11; Solubility in water: 6.2-20.3 mg/L	Plasticizer, cosmetics, adhesives, sealants, etc.
Di-(2-ethylhexyl) phthalate, DEHP (C ₂₄ H ₃₈ O ₄)		Molecular weight: 390.56 g/mol Log Kow: 5.11-8.35; Solubility in water: 1.9×10 ⁻³ -0.4 mg/L	Plasticizer in medical devices, food packaging materials, home furnishings, automobile upholstery, pipes, wire and cable sheathing, etc.

Benzyl butyl phthalate, BBP (C ₁₉ H ₂₀ O ₄)		Molecular weight: 312.36 g/mol Log K _{ow} : 3.57- 4.91; Solubility in water: 0.7- 40.2 mg/L	Plasticizer, traffic cones, artificial leather, vinyl flooring, etc.
Diisononyl phthalate, DINP (C ₂₆ H ₄₂ O ₄)		Molecular weight: 312.36 g/mol Log K _{ow} : 8.8; Solubility in water: 0.09 mg/L	Plasticizer, clothing, paints, electronic products, in construction materials, etc.

2.2 Phthalate esters in the marine ecosystem

PAEs in the marine environment primarily originate from plastic waste, discharge from polluted rivers, wastewater from cities and industries, and atmospheric deposition ((Hidalgo-Serrano et al 2022, Mi et al 2019, Paluselli & Kim 2020). Jambeck et al (2015) reported that 1.7 to 4.6% of the total plastic waste generated in coastal regions worldwide in 2010 (99.5 million metric tons) entered the marine ecosystem. Furthermore, a 2021 report by the International Union for Conservation of Nature (IUCN) estimated that 14 million tons of plastic waste end up in the marine ecosystem annually (IUCN 2021). A number of toxic additives such as plasticizers, stabilizers, and flame retardants are added during the manufacture of plastics to impart characteristics such as flexibility, durability, and color (Baini et al 2017). Phthalate acid esters, especially DEHP and DBP, are the most widely used plasticizers and account for more than half of the global plasticizer consumption. These

plasticizers can easily leach into the environment as they are not chemically bound to plastic polymers. It is estimated that plastic waste may contain up to 2700 mg/kg of DEHP and 360 mg/kg of DBP (Wright et al 2020). Thus, the widespread pollution of marine environments by plastic waste has in turn led to the pervasive detection of phthalate plasticizers in seawater, sediment, and even in marine biota including in edible fish varieties (Table 2). The partitioning of phthalate esters amongst different environmental matrices depends on physical and chemical properties such as octanol-water partition coefficient (K_{ow}). The K_{ow} values of phthalate esters increase with increase in alkyl chain lengths and is an indicator of how a chemical compound will partition between animal and plant lipids and organic matter in sediment and soil (Das et al 2021).

Mi et al (2019) quantified levels of DEP, di-isobutyl phthalate (DiBP), di-n-butyl phthalate (DnBP), benzylbutyl phthalate (BBP), dicyclohexyl phthalate (DCHP) and DEHP in sediments collected from the Bohai and Yellow Seas and detected total concentrations ranging from 0.0014 to 0.0246 mg/kg sediment. Furthermore, DEHP was present in the highest concentration in the sediment samples. Furthermore, Kim et al (2020) studied phthalate and non-phthalate plasticizer levels in sediment from two semi-enclosed bays in Korea and detected phthalates and non-phthalate plasticizers in the ranges of 0.0475-46.2 mg/kg-dw (mean: 10 mg/kg-dw) and 0.0277-3.44 (0.77 mg/kg-dw), respectively. DEHP was the predominant phthalate in all tested sediment, and was attributable for 48% of total PAEs. Similarly, several researchers have reported DEHP to be the predominant PAE in marine sediment samples from different areas (Table 2). Phthalate plasticizers have also been detected in sediment samples collected from aquaculture farms. Zhang et al (2021) reported

total PAE concentrations of 0.19 to 2.43 mg/kg-dw in sediment samples from a marine aquaculture area in China, and observed that DEHP and DBP were major PAEs.

According to the sediment quality guidelines developed by MacDonald et al (1996), threshold effect level (TEL) and probable effect level (PEL) of DEHP are 0.182 mg/kg-dw and 2.647 mg/kg-dw, respectively. When DEHP concentration is below the TEL, adverse biological effects may be rare. If concentration is equal to or greater than the TEL but less than the PEL, adverse biological effects may be possible. Finally, DEHP concentrations equal to or above the PEL indicate the likelihood of frequent negative biological effects. As shown in Table 2, the concentrations of DEHP in sediment is higher than the PEL in sediment from Hangzhou Bay, China (collected in summer) (Wang et al 2021a), the Persian Gulf (Arfaenia et al 2019), the Tunisian coast (Jebara et al 2021), East China Sea and Korean South Sea (Paluselli & Kim 2020), and Masan and Haengam Bays, Korea (Kim et al 2020), while DEHP levels in sediment collected from the Hanzhou Bay (collected in autumn) (Wang et al 2021a), eastern coast of Thailand (Malem et al 2019), exceeded the TEL but was below the PEL.

Phthalates present in the seawater and sediment can enter the marine food web and accumulate in marine biota (Baini et al 2017). PAEs have indeed been detected in marine biota, and DEHP, DnBP, and DiBP are the most frequently detected PAEs in marine biota. Fish samples from a mariculture area in China contained 0.82 to 4.93 mg/kg-dw of total PAEs, and DEHP and DBP were the major PAE types (Zhang et al 2021). Hu et al (2016) analyzed levels of DMP, DEP, DBP, and DEHP and their

monoesters in 69 fish, 20 prawn, and 6 mollusks samples collected from the East China Sea. DEHP (maximum mean of 1.941 mg/kg wet weight in fish) and DBP (0.0787 mg/kg) were the predominant PAEs. Similarly, DEHP and DBP monoesters were predominant at maximum mean concentrations of 0.0616 mg/kg and 0.049 mg/kg (wet weight of prawns), respectively. Lo Brutto et al (2021) detected the presence of DEHP (mean concentration: 0.046 mg/kg-wet weight), DiBP (0.097 mg/kg), DnBP (0.023 mg/kg), and DEP (0.108 mg/kg) in five species of amphipod crustaceans sampled from the north-western coast of Sicily. DEHP and its monoester MEHP were the predominant phthalates detected in all neustonic or planktonic organisms collected from the Mediterranean Sea, with maximum concentrations of 2.7 mg/kg-dw and 2.71 mg/kg-dw, respectively (Baini et al 2017). Phthalate plasticizers, especially DEHP (1.2-1.6 mg/kg-dw) and DEP (0.06-3.4 mg/kg-dw), have all been detected in seafood species such as mackerel, shrimp, and salmon bought from local Spanish markets (Hidalgo-Serrano et al 2020).

Table 2 Phthalate ester levels in the marine ecosystem.

Region and environmental matrix	PAE type and level (mg/kg-dry weight or mg/L)	Reference
Bohai Sea (Sediment)	DEHP: 0.00004-0.0159; DnBP: 0.00035-0.00224, DiBP: 0.00077-0.00258; DEP: 0.00008-0.00112	Mi et al (2019)
Northern Yellow Sea (Sediment)	DEHP: 0.00193-0.0156; DnBP: 0.00055-0.00679, DiBP: 0.00072-0.00408; DEP: ND-0.00029	Mi et al (2019)
Southern Yellow Sea (Sediment)	DEHP: ND-0.0104; DnBP: ND-0.00385, DiBP: 0.00022-0.00640; DEP: ND-0.00250	Mi et al (2019)

Hangzhou Bay, China (Sediment)	Summer DEHP: 0.0031- 2.414 ; DnBP: 0.0019-1.458; DiBP: 0.0219-0.336; DEP: 0.00248-1.778; DMP: 0.00608-1.483 Autumn DEHP: 0.0613- 1.114 ; DnBP: 0.00017-1.346; DiBP: 0.00178-2.175; DEP: 0.00317-0.219; DMP: 0.00402-0.189	Wang et al (2021a)
Persian Gulf (Sediment)	DEHP: 1.99-30.25 ; DnBP: 0.91-11.97; DiBP: 0.33-3.64; DEP: 0.43-5.83; DMP: 0.19-5.68	Arfaeinia et al (2019)
Tunisian coast (Seawater)	DEHP: ND-0.168; DBP: ND-0.0305; DiBP: ND-0.106; DEP: ND-0.0170	Jebara et al (2021)
Tunisian coast (Sediment)	DEHP: 4.15-5.24 ; DBP: 0.043-0.0824; DiBP: 0.152-0.394; DEP: 0.0644-0.142	Jebara et al (2021)
Tunisian coast (Fish)	DEHP: 0.772-1.46; DBP: ND-2.99; DiBP: 0.434-1.48; DEP: 0.561-2.70	Jebara et al (2021)
Eastern coast of Thailand (Seawater)	DEHP: 0.00031-0.00091; DBP: 0.00023-0.00077	Malem et al (2019)
Eastern coast of Thailand (Sediment)	DEHP: ND- 1.65 ; DBP: ND-0.80	Malem et al (2019)
East China Sea and Korean South Sea (Sediment)	DEHP: 0.015- 8.30 ; DnBP: 0.003-0.51; DiBP: 0.002-0.63; DEP: ND-0.08; DMP: ND-0.03	Paluselli and Kim (2020)
Coastal aquaculture area, China (Seawater)	DEHP: 3.09×10^{-5} -0.0026; DnBP: 1.93×10^{-5} -0.0014; DiBP: 2.36×10^{-5} -0.0013; DEP: 2.03×10^{-6} -0.0015; DMP: 0.93×10^{-6} -0.0008	Zhang et al (2021)
Coastal aquaculture area, China (Sediment)	DEHP: 4.52×10^{-5} -0.0016; DnBP: 4.43×10^{-5} -0.0009; DiBP: 3.42×10^{-5} -0.0014; DEP: ND- 1.6×10^{-5} ; DMP: 0.93×10^{-6} - 2.07×10^{-5}	Zhang et al (2021)
Coastal aquaculture area, China (Biological sample)	DEHP: 7.5×10^{-5} -0.0022; DnBP: 4.15×10^{-5} -0.0016; DiBP: 3.6×10^{-5} -0.0019; DEP: 0.83×10^{-6} - 4.8×10^{-5} ; DMP: 3×10^{-6} - 3.2×10^{-4}	Zhang et al (2021)

Masan and Haengam Bays, Korea	DEHP: 0.0235- 3.57 ; 0.0708; DiBP: 0.0005- ⁶ -0.006; DMP: 0.0003-0.046	DnBP: 0.0012- 0.0096; DEP: 4×10 ⁻⁶	Kim et al (2020)
-------------------------------	--	--	---------------------

2.3 Toxicity of phthalate esters

PAEs in the environment can be ingested by aquatic organisms and move through the food chain. Most PAEs are known to have endocrine disrupting effects and prolonged exposure to these toxic chemicals affect the development and reproductive systems of organisms (Hidalgo-Serrano et al 2020). Once ingested, PAEs can be hydrolyzed to their monoesters, which is further metabolized into oxidative intermediates, which are lipophilic and hence accumulate in the fat tissues of aquatic organisms. Phthalate monoesters like monobutyl phthalate are known to persist in aquatic organisms for up to six months and exert toxic effects (Jiao et al 2020). PAEs have also been reported to exert immune toxicity, oxidative stress toxicity and metabolic toxicity. Exposure of common carp to DEHP for 2 h resulted in suppressed immune response of neutrophils (Wang et al 2020). Yang et al (2018c) exposed medaka fish to DEHP concentrations of 20, 100, and 200 µg/L for 21 d and observed significant reduction in body weight and length of the exposed fish via combined effects of oxidative stress, apoptosis, and neurotoxicity. Furthermore, the exposure of African sharptooth catfish to DEHP concentrations of up to 400 µg/L for 14 d had endocrine disrupting effects (Adeogun et al 2018).

The toxic effects of phthalate plasticizers and their metabolites on mammals including humans have been widely studied. Humans may be exposed to PAEs via consumption of contaminated food or drinks, personal care products, pharmaceuticals, and healthcare devices and/or inhalation of PAEs in air or dust (Chang et al 2021b,

Wang & Qian 2021). Studies have reported on the endocrine disrupting and carcinogenic effects, reproductive toxicity, mutagenicity, and teratogenicity of PAEs. PAEs and their metabolites have been detected in breast milk, saliva, semen, and in the circulatory system. Wang et al (2016) studied the associations between the presence of eight phthalate metabolites in human semen and semen quality and reproductive hormones and found that exposure to phthalates could affect the quality of human semen. Meanwhile, Amin et al (2018) reported that urinary concentrations of phthalate metabolites were significantly associated with obesity, high blood pressure and high levels of triglyceride in a study conducted in children and adolescents between the ages of 6 and 18 years. Furthermore, Grindler et al (2018) found that maternal phthalate exposure altered the methylation and expression of several placental genes, thus indicating potential impacts of phthalates on placental function.

Owing to these toxic effects of PAEs, the use of PAEs have been restricted in several countries such as the USA, Canada, Europe, Australia, Japan, and China. The USA and Canada have restricted the use of benzyl butyl phthalate, DEHP, DnBP, and DiBP in children's items and toys under the Consumer Product Safety Improvement Act (2008) and Hazardous Products Act (2010), respectively. Australia has also introduced bans on products that contain levels of DEHP higher than 1% by weight in products that children of 3 years or younger could put in their mouths. In 2017, China introduced new regulations that limit the presence of several phthalates in food and food containers and in childcare products. Several organizations have also established limits concerning the intake of phthalate esters. For instance, tolerable daily intakes for DnBP (0.01 mg/kg body weight) and DEHP (0.05 mg/kg body weight) have been

established by the European Food Safety Agency (EFSA Panel on Food Contact Materials et al 2019).

2.4 Phthalate ester degradation processes

2.4.1 Abiotic processes for phthalate ester degradation

A number of abiotic strategies for the degradation of phthalate esters such as coagulation, advanced oxidation processes, and photocatalysis, have been reported. Abiotic methods are typically used for the remediation of PAE-contaminated wastewater. Dong et al (2020) used iron-cerium bimetallic catalysts prepared with sodium persulfate as the oxidation agent to degrade phthalate esters in marine sediment (total PAE concentration 19.5 ± 2.1 mg/kg) and found that pH 2, 86% of the total PAEs could be degraded in 6 h. Furthermore, Mansouri et al (2019) compared the efficiencies of DEP removal from water (200 mg/L) of several advanced oxidation processes and reported that ozonation with 2 g/L of Al_2O_3 could achieve complete DEP degradation within 30 min. In contrast, Mansouri et al (2019) observed that less than 1% DEP degradation could be achieved in 60 min via oxidation using only H_2O_2 at pH of 3 and 7, while UV treatment with TiO_2 (1 g/L) could achieve 19-26% DEP degradation. Therefore, effective PAE degradation via abiotic processes typically involves high financial investments (for chemical reagents and light sources). Furthermore, it has reported that pollutant degradation via ozonation results in the formation of intermediates that are recalcitrant to ozonation, thus necessitating the use of other follow-up degradation strategies (Mecha & Chollom 2020).

2.4.2 Biodegradation of phthalate esters

Degradation of PAEs can take place via abiotic processes such as hydrolysis and photolysis, or via biotic processes such as degradation by bacteria, fungi, or algae. However, photolysis of PAEs in aquatic systems due to low penetration by UV light, while abiotic hydrolysis of PAEs is typically sterically hindered by the alkyl chains. Due to the slow rate of phthalate ester degradation by abiotic processes such as photolysis and hydrolysis and the cost and chemical reagents involved, much focus has been paid to the microbial metabolism of phthalate esters (Das et al 2021).

2.4.2.1 Biodegradation of phthalate esters by fungi and algae

Several fungal and algal species with the ability to degrade a variety of PAEs have been reported, although bacterial-mediated PAE degradation is more extensively studied. For instance, a fungal strain, *Pleurotus ostreatus*, could degrade 99.3% and 98.4% of 500 mg/L and 1000 mg/L DEHP concentrations, respectively, in 21 d. The degradation intermediates detected were MEHP, phthalic acid, hexanal, ethanol, acetaldehyde, acetic acid, and butanediol (Ahuactzin-Perez et al 2018). Chi et al (2019) identified three marine algae, *Chaetoceros muelleri*, *Cylindrotheca closterium*, and *Dunaliella salina*, that could degrade DBP (22.5%, 91.4%, and 34.5% degradation of 0.1 mg/L of DBP in 4 d).

2.4.2.2 Biodegradation of phthalate esters by bacteria

Most of the bacteria capable of DEHP degradation have been isolated from activated sludge, landfill soil or agricultural soil (Table 3). *Rhodococcus pyridinivorans* XB isolated from activated sludge could completely degrade up to 400 mg/L of DEHP within 72 h in aqueous medium via de-esterification and β -oxidation.

DBP, PA, and 2-ethyl-1-hexanol were identified as intermediates of DEHP degradation. Strain XB could however not utilize 2-ethylhexanol, indicating that this DEHP intermediate (Zhao et al 2018a) is toxic to the strain. Wang et al (2019b) isolated *Gordonia* sp. Lff from river sludge enriched with up to 2000 g/L of DEHP. This strain could degrade over 91.43% of 2000 mg/L of DEHP within 72 h in mineral salt medium. Furthermore, *Achromobacter* sp. RX isolated from activated sludge could degrade 99.3% of DEHP (50-300 mg/L) in mineral salt medium within 96 h. It could also utilize phthalic acid as the sole source of carbon and MEHP, butyl (2-ethylhexyl) phthalate, 2-ethylhexyl pentyl phthalate, and monobutyl phthalate were the DEHP intermediates detected (Wang et al 2021b). *Bacillus mojavensis* B1811 isolated from oil-polluted soil could degrade PAEs with longer alkyl chains like DEHP and DBP (100%) more effectively than PAEs with shorter alkyl chains like DMP (5.9%) and DEP (40%). This could be because PAEs with longer alkyl chains could induce stronger specific esterase activity from B1811 than PAEs with shorter alkyl chains. This enzyme catalyzes the break-down of PAEs to phthalate monoesters and then to phthalic acid (Zhang et al 2018).

Despite the widespread pollution of the marine environment by phthalate esters (Table 2), only a few marine bacterial isolates have been reported for the degradation of phthalate esters (Ren et al 2021, Wright et al 2020, Yang et al 2018b). Therefore, very little known about the PAE-degrading potential of marine bacteria and the associated pathways and enzymes. *Mycobacterium phocaicum* RL-HY01, isolated from intertidal sediment samples, could degrade DEHP, DBP, DMP and DEP at pH of 5.0 to 9.0, temperature of 20 °C to 40 °C, and salinity of 4 to 8%. Intermediates identified during DEHP degradation by RL-HY01 were di-n-hexyl

phthalate, di-(2-ethylbutyl) phthalate, DBP, DEP, phthalic acid, salicylic acid, and gentisic acid (Ren et al 2021). Wright et al (2020) enriched and isolated two DBP- and DEHP-degrading bacteria, *Halomonas* sp. ATBC28 and *Mycobacterium* sp. DBP42, from marine plastic debris. The pathway of DBP and DEHP degradation by ATBC28 and DBP42 was investigated using a multi-OMIC approach. The DBP intermediates identified for *Mycobacterium* sp. DBP42 were monobutyl phthalate, phthalic acid, phthalic anhydride, butanol, butyl benzoate, 3,4-dihydroxy phthalate, protocatechuate, β -carboxy muconate, γ -carboxymuconolactone, 3-oxoadipate-enolactone, and 3-oxoadipate; however, no intermediates were detected during DEHP degradation. Similarly, none of the targeted intermediates were detected during degradation of DEHP and DBP by *Halomonas* sp. ATBC28. *Rhodococcus ruber* YC-YT1 isolated from marine plastic debris collected from coastal seawater could degrade 100 mg/L of DEHP in 3 d and MEHP, phthalic acid and benzoic acid were the intermediates detected (Yang et al 2018b).

Although the degradation of phthalate esters by single bacterial strains has been extensively studied, degradation by bacterial consortia has received considerably less attention. The bioremediation efficiency of single bacterial strains is generally considered to be lower and more restrictive (in terms of metabolite utilization) than that of bacterial consortia (Qian et al 2020). A halotolerant bacterial consortium enriched from sewage activated sludge could degrade up to 93.84% of DEHP (1000 mg/L) in mineral salt medium within 48 h. 2-Ethylhexyl pentyl phthalate, butyl (2-ethylhexyl) phthalate, MEHP, and monobutyl phthalate were identified as degradation metabolites. *Gordonia*, *Rhodococcus*, and *Achromobacter* were the main genera in the consortium (Li et al 2018). Furthermore, a consortium (CM9) enriched from

contaminated farmland soil could degrade 98.80% of DEHP (200–1000 mg/L) in mineral salt medium within 72 h (Bai et al 2020). Although the dominant bacterial members in enriched consortium CM9 during DEHP degradation were determined, dominant members (and likely key degraders) for DEHP metabolites of concern such as MEHP and 2-ethyl hexanol were not explored. This information can guide the creation of bacterial consortia for complete DEHP biodegradation. Further, studying dominant bacteria during degradation of PAE mixtures (of varying structure and alkyl chain lengths), will lay the background for application in contaminated sites where different PAEs exist as complex mixtures. A few researchers have also investigated the use of bacterial co-cultures for PAE degradation. For instance, monobutyl phthalate and phthalic acid were detected as intermediates during DBP degradation by a co-culture of *Microbacterium* sp. PAE-1 and *Pandoraea* sp. PAE-2 (Lu et al 2020). Furthermore, Chatterjee and Dutta (2008) reported that a co-culture of *Arthrobacter* sp. WY and *Acinetobacter* sp. FW could degrade 140 μmol (in 50 mL) of butyl benzyl phthalate completely within 44 d. Degradation of butyl benzyl phthalate by *Arthrobacter* sp. WY occurred via ester bond hydrolysis yielding mono-n-butyl phthalate, monobenzyl phthalate, and phthalic acid, while the alcohols produced during degradation by strain WY was utilized by *Acinetobacter* sp. FW.

Table 3 Bacterial strains reported for phthalate ester degradation.

Bacteria	Degradation conditions	Degradation efficiency	Metabolites detected	Reference
<i>Acinetobacter</i> sp. SN13;	400 mg/L DEHP, 30°C, Gram-	Specific degradation rate:	MEHP, diethyl	Xu et al (2017)

negative;	pH 6-9, basal	21.71 × 10 ⁻⁷ mg/d.	hexanoic
Activated sludge	salt medium	Improved	acid, β-
		degradation and	carboxy-
		cell growth with	cis,cis-
		ferric ion	muconic
			acid, 3-
			ketoadipate
<i>Rhodococcus</i>	200 mg/L	99.1% degradation	DBP, PA, 2-
<i>pyridinivorans</i>	DEHP, pH	in 2 d	EHA, (2018a)
XB;	Gram-	7.04, 30.4°C,	MEHP,
positive,	OD ₆₀₀	0.6,	PCA, di-
facultative	mineral salt		hydroxy
anaerobic;	medium		phthalic
Activated sludge,			acid
sewage treatment			
plant			
<i>Bacillus</i>	500 mg/L	100% degradation	MEHP, 2-
<i>mojavensis</i>	DEHP, 30-	in 4 d. Better	EHA, PA, al (2018)
B1811;	Gram-	40°C, pH 7-	degradation of long
positive;	Oil	8, mineral	chain PAEs. Yeast
polluted soil	salt medium	extract	enhances
			degradation.
<i>Microbacterium</i>	pH 8.3, 32°C,	91.8% degradation	MEHP, PA, Zhao et al

sp. J-1; Gram-positive; Landfill soil	OD ₆₀₀ 0.8, in 10 d	1200 mg/L DEHP, Mineral salt medium	PCA, and 2-EHA	(2017)
<i>Gordonia alkanivorans</i> YC-RL2; Gram-positive; Petroleum-contaminated soil, China	pH 8, 30°C, 98.7% degradation	180 rpm, in 7 d	DEHP 100 mg/L, Trace mineral medium	BA, MEHP, Nahurira et al (2017)
<i>Gordonia</i> sp. Lff; Gram-positive; Contaminated-river sludge, China	pH 7, DEHP 1000 mg/L in half-life; 0.599 to 0.746 d.	Biodegradation	MEHP, MBP, butyl ethylhexyl phthalate, 2-ethylhexyl pentyl phthalate	Wang et al (2019b)
<i>Burkholderia pyrrocinia</i> B1213; Gram-positive	500 mg/L 98.05% degradation	180 rpm, 30°C, 6	DEHP, Mineral salt	Li et al (2019)

negative; soil	d	medium (MSM);	oxohexanoic			
		little degradation in	acid			
		MSM.				
<i>Acromyces</i> sp.	DEHP (200 mg/L), 150 rpm, 30°C, Landfill soil	(200 mg/L), 150 rpm, 30°C, Mineral salt medium	100% degradation in 7 d	MEHP, PA	Zhao et al (2016)	
<i>Rhodococcus</i> sp.	LW-XY12; Gram positive; Activated sludge	DEHP (500 mg/L), 30 °C, pH 8.5, Inoculum size 2.1×10^8 CFU, Minimum salt medium	96.91 ± 0.68% degradation within 32 h	MEHP, 2-EHA, MMP, DBP, DEP, DMP, PA, BA, catechol	Song et al (2022)	
<i>Mycolicibacterium phocaicum</i> RL-HY01;	Gram positive; Intertidal sediment	DEHP (500-1000 mg/L); 30 °C, pH 7.0; Inoculum size 7.0×10^7 cells/mL	100% degradation within 3 d	Di-n-hexyl phthalate; di-(2-ethylbutyl) phthalate; DBP, DEP, PA, salicylic	Ren et al (2021)	

	Mineral salt medium	acid, gentisic acid
Enriched consortium CM9;	DEHP, DMP, DEP, DBP and DEHP	Bai et al (2020)
Farmland soil (1000 mg/L)	degradation of MEHP, DMP, DEP, PA, phthalic acid (2-ethyl hexyl-methyl ester), phthalic acid (2-ethyl hexyl-butyl ester), phthalic acid (2-ethyl hexyl-amyl acetate), and phthalic acid (2-ethyl hexyl-hexyl ester)	



<i>Rhodococcus</i>	DEHP (500 mg/L)	99.75% degradation within 3 d	DMP, PA, BA, 2-ethylhexyl benzoate	Wang et al (2022)
<i>pyridinovorans</i>	DNHP-S2; Gram-positive; Soil	pH 7.0; 35 °C;		

MEHP: mono (ethylhexyl) phthalate; PCA: protocatechuic acid; PA: phthalic acid; BA: benzoic acid; MBP: monobutyl phthalate; 2-EHA: 2-ethylhexanol; MMP: monomethyl phthalate; DBP: dibutyl phthalate, DMP: dimethyl phthalate: DEP: diethyl phthalate

2.5 Biodegradation of phthalate esters in soil and sediment

2.5.1 Biodegradation of phthalate esters by indigenous soil/sediment bacteria

Zhu et al (2018) studied DEHP (200 mg/kg) degradation by indigenous bacteria in twelve agricultural soil samples (pH: 5.0 to 9.0). Less than 50% of DEHP was degraded in all soil samples after 35 d and degradation was more efficient in soils with near-neutral pH (pH 6.0 to 8.0) than in acidic or alkaline soils. Intermediates detected were MEHP, 2-ethylhexanoic acid, phthalic acid, protocatechuic acid, and benzoic acid. It was observed that under acidic conditions, DEHP metabolites, MEHP and 2-ethylhexanol, accumulated at higher levels than under alkaline or near-neutral conditions. This implies that pH influences the rate and extent of DEHP degradation. Additionally, soil pH affected soil bacterial community, pollutant binding, and hydrolase activity, while bacterial population and soil organic carbon influenced DEHP degradation in all the soils tested. The response of soil bacterial communities to DEHP contamination was also examined. Acidic soils had lower bacterial diversity and richness. Additionally, in one of the acidic soils, DEHP exposure significantly

reduced richness and diversity, implying that DEHP may have different impacts in different soils.

Zhu et al (2019a) studied DEHP (100 to 1000 mg/kg) degradation and microbial response to DEHP contamination in aerobic and anaerobic flooded soils. After 42 d, DEHP degradation was below 40%, and MEHP accumulation was much lower in aerobic soil (20-31 $\mu\text{g}/\text{kg}$) than in anaerobic soil (300-600 $\mu\text{g}/\text{kg}$). Further, MEHP tended to migrate from the solid to the liquid phase, while 2-ethylhexanol adsorbed onto soil particles. This raises environmental concerns as some soils such as acidic soil accumulate high levels of monoester phthalates, which may be readily released into the surrounding water, posing risks for aquatic and terrestrial life. In this study, high levels of 2-ethylhexanol were detected in both aerobic and anaerobic soils, indicating that the soil used lacked efficient degraders. Analysis of soil bacterial community revealed that under both aerobic and anaerobic conditions, Firmicutes was inhibited by DEHP, while Actinobacteria, Gemmatimonadaceae, and β -Proteobacteria populations were enhanced by DEHP exposure.

Zhu et al (2020) studied indigenous bacteria involved in aerobic and anaerobic DEHP degradation in agricultural soil (spiked with 1000 mg/kg DEHP). After 21 d, 31.3% and 23.0% degradation were observed under aerobic and anaerobic conditions, respectively. MEHP, phthalic acid, and 2-ethylhexanol were detected, indicating that DEHP degradation was via hydroxylation (Figure 1). Both benzoic acid (~22 mg/g) and protocatechuate (~3 $\mu\text{g}/\text{kg}$) were detected in aerobic microcosms on Day 5, indicating that DEHP degradation might have occurred via multiple pathways. Bacterial community composition was significantly altered under both aerobic and

anaerobic conditions. Actinobacteria (*Pimelobacter*, *Nocardioides*, *Gordonia*, *Nocardia*, *Rhodococcus*, and *Mycobacterium*) and Proteobacteria (*Ramlibacter* and *Burkholderia*) were enriched under aerobic conditions, with highest enrichment observed for *Nocardioides* (from 2.30% to 9.79%) and *Pimelobacter* (from 0.05% to 1.13%). Under anaerobic conditions, Gemmatimonadetes, Proteobacteria, Acidobacteria, and Bacteroidetes, were enriched in the presence of DEHP.

2.5.2 Biodegradation of phthalate esters via bioaugmentation with exogenous bacteria

Bai et al (2020) studied DEHP degradation by consortium CM9 (enriched from contaminated soil) in DEHP-spiked soil (100 mg/kg). After 42 d, indigenous soil microorganisms degraded 49.39% of DEHP, while CM9 could achieve 83.48%–87.53% degradation. The dominant genera in consortium CM9 were *Rhodococcus*, *Niabella*, *Sphingopyxis*, *Achromobacter*, *Tahibacter*, and *Xenophilus*. Proteobacteria, Bacteroidetes, and Actinobacteria were the dominant phyla in bioaugmented soil after 42 d; *Pigmentiphaga* and *Sphingopyxis* relative abundances decreased sharply, while those of *Tahibacter*, *Terrimonas*, and *Niabella* increased in bioaugmentation treatments. In treatments with indigenous microbes, Firmicutes, Chloroflexi, and Acidobacteria relative abundances decreased with DEHP degradation, while those of *Bacillus*, *Pseudomonas*, and *Noviherbaspirillum* increased at 7 d, but decreased sharply thereafter. The relative abundances of *Sphingomonas*, *Phenylobacterium*, and *Flavisolibacter* increased gradually.

Rhodococcus pyridinivorans XB was applied for bioremediation of DEHP-contaminated soil (strain XB inoculation, planting maize, and combined treatment).

Treatment with either strain XB inoculation or planting maize could degrade 67.55% and 73.11% of DEHP (100 mg/kg) within 50 d, respectively, while degradation efficiency of combined treatment was 78.45%. Evidently, the degradation performance of strain XB is much lower in soil than in liquid medium, wherein 100% degradation of 400 mg/L DEHP could be achieved in 3 d (Zhao et al 2018a). Similarly, *Gordonia* sp. Lff could degrade 90% of DEHP (100 mg/kg) in contaminated soil in 35 d although this strain could degrade up to 91.43% of 100-2000 mg/L DEHP in mineral salt medium in just 3 d (Wang et al 2019b).

Ren et al (2021) used *Mycolicibacterium phocaicum* RL-HY01 to bioaugment DEHP-degradation in three types of intertidal sediment (50 mg/kg DEHP), namely muddy, sandy, and mixed sediment. In the DEHP-spiked sediment, complete degradation by RL-HY01 could be achieved within 3 d. Indigenous microbes in the muddy, sandy, and mixed intertidal sediments could degrade 5.7, 2.1, and 8.9% of DEHP on Day 21, indicating that different sediment types harbor microbes with varying PAE-degrading capabilities. In the bioaugmented muddy, sediment, and mixed sediment microcosms, DEHP degradation efficiencies of 57.6, 79.3, and 92.5%, respectively, could be achieved within 21 d. The effect of bioaugmentation on the indigenous microbial community was not investigated in this study. Hu et al (2022) used a bacterial strain *Gordonia* sp. GZ-YC7 isolated from landfill soil to bioaugment the degradation of DEHP in garden soil spiked with 500 mg/kg of DEHP. Strain GZ-YC7 could degrade 45% and 47.33% of DEHP in non-sterile soil and sterile soil, respectively.

Gordonia terrae RL-JC02 was inoculated in red soil spiked with 50 mg/kg of DEHP and incubated for 30 d at 30°C (Zhang et al 2020). Only 1.5% DEHP degradation could be achieved by indigenous soil microbe, while abiotic DEHP degradation was just 0.6%. In microcosms with sterile red soil inoculated with strain RL-JC02, 88.4% DEHP degradation was observed, while in microcosms with non-sterile red soil (harboring indigenous microbes) bio-augmented with strain RL-JC02, 91.8% DEHP degradation was recorded. As hydrolysis of the ester bonds of DEHP is typically the first step of DEHP degradation, soil hydrolase activities were determined using the fluorescein diacetate (FDA) method, and it was observed that in DEHP-spiked soils bio-augmented with strain RL-JC02, FDA hydrolysis activity increased rapidly during first 3 d, and then decreased slowly to a steady value, while no changes were observed in non-DEHP spiked soils. This implies that FDA hydrolysis activity is induced by both the presence of DEHP and strain RL-JC02.

Zhao et al (2017) conducted a pot experiment using soil spiked with 50 mg/kg of DEHP to investigate the effect of bioaugmentation with *Microbacterium* sp. J-1 (isolated from landfill soil) on vegetable biomass (soils were planted with Chinese flowering cabbage) and DEHP levels in soil and the planted vegetable. At the end of the experiment on Day 35, DEHP degradation efficiencies in soils bio-augmented with strain J-1, soils cultivated with Chinese flowering cabbage, and soils with combined bioaugmentation and cultivation were 88, 62, and 97%, respectively. Peroxidase and polyphenol oxidase enzyme activities in the soils under different treatments were investigated and it was found that soil polyphenol oxidase activity was enhanced by strain J-1. Polyphenol oxidase is an important oxidoreductase involved in the oxidation of aromatic compounds such as PAEs.

Lastly, the ability of the inoculated strain to survive in the soil was monitored and it was observed that strain J-1 survivability decreased from Day 7 to Day 21, and the bioaugmented bacteria was no longer detected on Day 35.

2.6 Mechanism of bacteria-mediated phthalate ester degradation

2.6.1 Pathway of bacteria-mediated phthalate ester degradation

A generalized PAE biodegradation pathway under aerobic condition based on PAE intermediates reported in literature (Das et al 2021, Ren et al 2018a, Song et al 2022, Zhao et al 2018a) is shown in Figure 1. The ester side chains of PAEs are typically hydrolyzed to form phthalic acid, which is then further hydrolyzed to 3,4-dihydroxy phthalate or 4,5-dihydroxy phthalate, which are converted to protocatechuate via decarboxylation. The cleavage of protocatechuate can take place via the *meta* and *ortho* cleavage pathways. However, some exceptions to this typical pathway have been reported. Even under aerobic conditions, the conversion of phthalic acid to benzoic acid and the conversion of phthalate monoesters to benzoic acid has been reported (Song et al 2022, Wright et al 2020). Although benzoic acid is used as an antimicrobial agent, bacterial degradation of benzoic acid formed during PAE metabolism has been reported (Zhang et al 2018; Wright et al 2020).

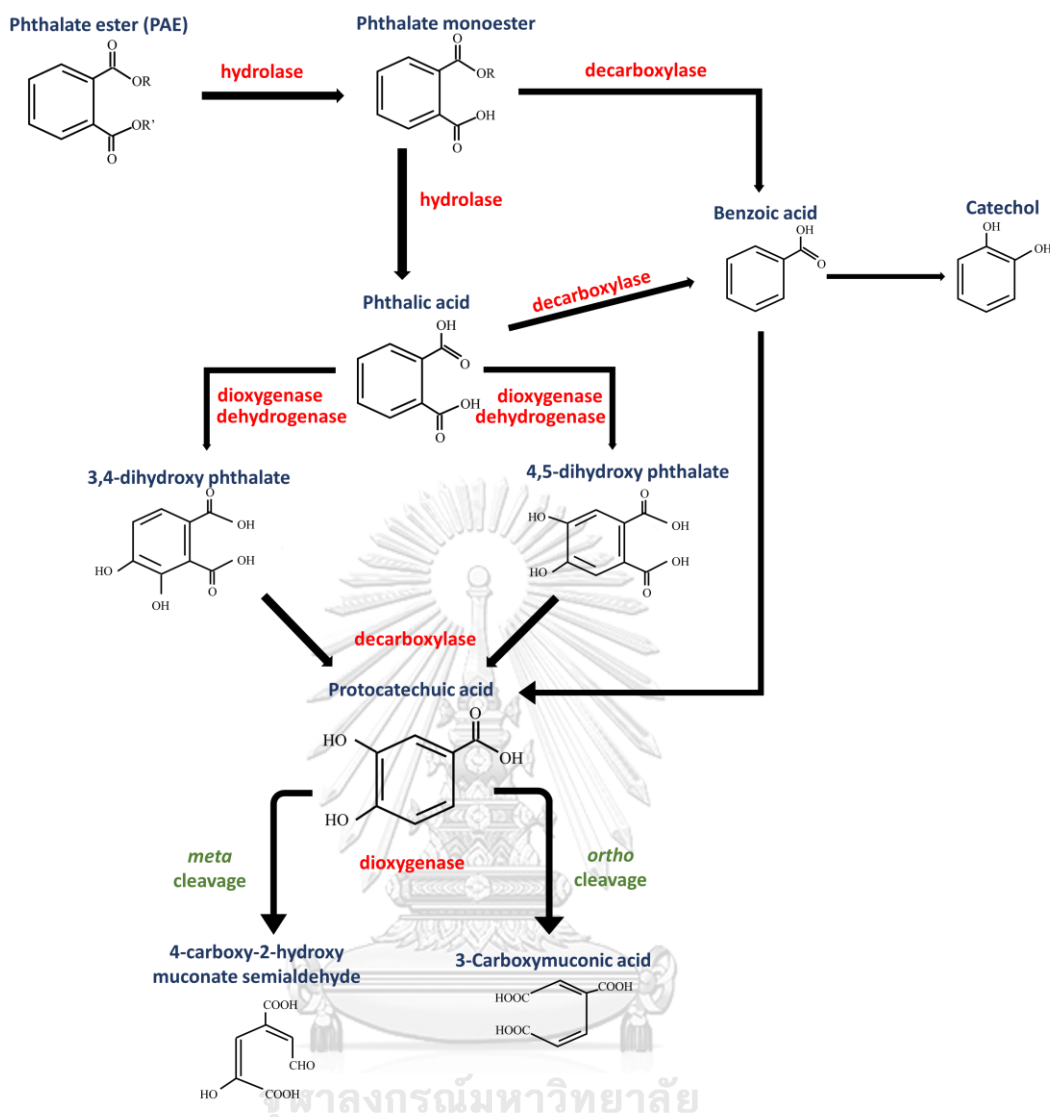


Figure 1 Generalized pathway for the biodegradation of phthalate esters under aerobic conditions adapted from literature.

2.6.2 Enzymes and genes involved in bacteria-mediated phthalate ester biodegradation

Bacterial degradation of phthalate esters is typically initiated by ester bond hydrolyses, which are catalyzed by phthalate hydrolases. The hydroxylation of phthalic acid to protocatechuate is known to be catalyzed by phthalate 3,4-dioxygenase (in Gram-positive bacteria) or phthalate 4,5-dioxygenase (in Gram-

negative bacteria), while *ortho* and *meta* cleavage of protocatechuate is catalyzed by protocatechuate 3,4-dioxygenase and protocatechuate 4,5-dioxygenase, respectively (Das et al 2021). Genes/enzymes reported to be involved in the degradation of phthalate esters are listed in Table 4.

Wright et al (2020) isolated several bacterial strains that could grow on various plasticizers, including DEHP, from bulk marine plastic debris and two best degraders, *Mycobacterium* sp. DBP42 and *Halomonas* sp. ATBC28, were selected. Both strains encoded genes involved in phthalate degradation and for enzymes such as esterases, cutinases, and lipases or those involved in the β -oxidation of fatty acids (removal of the ester side chains from phthalates). Proteomic and metabolomic studies were conducted to determine degradation pathways. Strain DBP42 degraded DBP through sequential removal of ester side chains, producing monobutyl phthalate, phthalic acid, and two butanol molecules. Side chain cleavage may be catalyzed by cutinase as it was strongly upregulated. Phthalic acid is then likely converted to protocatechuate, which can then enter the β -ketoacid pathway. Metabolomic analysis indicate accumulation of butyl benzoate (from monobutyl phthalate decarboxylation) and phthalic anhydride (detoxification of phthalic acid). Unlike DEHP, DBP could strongly induce phthalate catabolism in strain DBP42. Degradation of DEHP by strain DBP42 may occur via β -oxidation of the fatty acid side chains as enzymes for long chain fatty acid β -oxidation were strongly induced by DEHP. DEHP degradation is hypothesized to start with ester side chain hydroxylation by a monooxygenase. During degradation by strain ATBC28, build-up of degradation intermediates was not detected, and so degradation pathways could not be confirmed.

Genomic and proteomic analyses suggest that hydrolysis of the butyl side chains of DBP is catalyzed by esterase 4375, which was upregulated by DBP and DEHP.

Zhu et al (2020) studied the presence and abundance of 15 genes encoding for enzymes involved in the degradation of DEHP to phthalic acid (upper pathway) during DEHP degradation in soil. Genes encoding putative phthalate ester hydrolase PehA and MEHP hydrolase, from unclassified Actinomycetales and *Gordonia*, respectively, were enriched by DEHP under aerobic conditions. Enzymes reported to be involved in upstream DEHP degradation are esterase, lipase, carboxylesterase, unclassified hydrolases, cytochrome P450, laccase, and cutinase. Genes encoding for these enzymes, except unclassified hydrolases, were tested. Under aerobic conditions, all analyzed genes were enriched by DEHP, with the greatest enrichment for cytochrome P450 (from Actinomycetales), lipase (Actinomycetales, unidentified microorganisms and β -Proteobacteria), and esterase (Actinomycetales and unidentified microorganisms) genes. About 50% of enriched functional gene reads under aerobic conditions were from *Nocardioide*s. It was hypothesized that *Nocardioide*s, carrying lipase, esterase, and cytochrome P450 genes, degrades DEHP to its monoester using lipase (or esterase) and then metabolizes the monoester with cytochrome P450. Under anaerobic condition, only abundance of esterase genes from Bacteroidetes, β -Proteobacteria, Gemmatimonadetes, and unidentified microbes increased significantly with DEHP. Only four strains belonging to *Bacillus* (Firmicutes) and *Streptomyces* (Actinobacteria) could be isolated in mineral agar medium with DEHP as sole source of carbon. Genes involved in phthalic acid and benzoic acid degradation were significantly more abundant in the presence of DEHP under aerobic conditions, while under anaerobic condition, abundance of benzoate

metabolism genes increased only slightly. The authors propose that under aerobic conditions, phthalic acid was oxidized by phthalate 3,4-dioxygenase (Actinomycetales) and phthalate 4,5-dioxygenase (β -Proteobacteria) to phthalate 3,4-cis-dihydrodiol and phthalate 4,5-cis-dihydrodiol, respectively. Unidentified microorganisms and Actinomycetales were involved in later phthalic acid degradation steps, such as formation and breakdown of protocatechuate. Protocatechuate, catechol, and benzoyl-CoA were the major metabolites of benzoic acid, and were further degraded to succinyl-CoA or acetyl-CoA, which could then enter the tricarboxylic acid (TCA) cycle.

A phthalic acid catabolic gene cluster (*phtBAabcdCR*) was identified in PAE-degrading *Gordonia* sp. strain HS-NH1 via genomic analysis and cloning and gene expression studies (Li et al 2016). This gene cluster has been reported to be involved in the degradation of phthalic acid to protocatechuic acid. The *pht* cluster in *Gordonia* sp. strain HS-NH was comprised of 8 genes, *phtB*, *phtAa*, *phtAb*, *phtU*, *phtAc*, *phtAd*, *phtC*, and *phtR*. The gene products of *phtB*, *phtAa*, *phtAb*, *phtU*, *phtAc*, *phtAd*, *phtC*, and *phtR* predicted by BlastP are 3,4-dihydroxy-3,4-dihydrophthalate dehydrogenase, 3,4-phthalate dioxygenase large subunit, 3,4-phthalate dioxygenase small subunit, hypothetical protein, 3,4-phthalate dioxygenase ferredoxin subunit, 3,4-phthalate dioxygenase reductase subunit, 3,4-dihydroxyphthalate decarboxylase, and IclR family transcriptional regulator, respectively. Phthalic acid could be degraded by a mixture of PhtAab and PhtAc, although PhtAab and PhtAc separately could not degrade phthalic acid.

Huang et al (2020) identified a gene *baces04* in the genome of *Bacillus velezensis* SYBC H47. This gene encodes for a carboxylesterase (BaCEs04), a novel phthalate hydrolase belonging to esterase family VI. The amino acid sequence of this carboxylesterase shared less than 45% identity with the amino acid sequence of all experimentally proven PAE hydrolases. The activity of this carboxylesterase was investigated at different pH values and temperatures, and activity was maintained at pH 5.5–8.0 and temperatures 10°C to 40°C. After a 5-h treatment of DMP, DEP, dipropyl phthalate, DBP (1 mM each) with the carboxylesterase (BaCEs04), degradation efficiencies of 32.42, 50.48, 77.85, and 86.79%, respectively, were recorded. The monoesters of all four PAEs (monomethyl phthalate, monoethyl phthalate, monopropyl phthalate, and monobutyl phthalate) were identified as the corresponding degradation intermediates.

Song et al (2022) carried out genomic analysis and annotation of a DEHP-degrading bacterial strain *Rhodococcus* sp. LW-XY12. Furthermore, levels of gene expression in the presence of DEHP was analyzed. A carboxylesterase-encoding gene, a putative PAE esterase (Group I) gene, and a putative monoalkyl phthalate hydrolase (Group II enzyme) gene were identified and these enzymes were revealed to belong to hydrolase family VII, IV, and V, respectively based on an analysis of evolutionary relationship. Furthermore, homologous modeling and molecular docking showed that DEHP and MEHP can bind to this putative carboxylesterase via hydrogen and hydrophobic bonding. Additionally, gene annotation of *Rhodococcus* sp. LW-XY12 revealed a protocatechuate degradation gene cluster (*pcaGHBCDLIJ-fadA*), a benzoic acid degradation cluster (*benABCD*), and catechol degradation gene clusters for *meta* cleavage (*xylEGHI-mhpDEF*) and *ortho* cleavage (*catABC-pcaLIJ*). The expression

levels of protocatechuate 3,4-dioxygenase subunit alpha (*pcaG*), 3-oxoadipate CoA-transferase subunit alpha (*pcaI*), benzoate 1,2-dioxygenase subunit alpha (*benA-xylX*), catechol 1,2-dioxygenase (*catA*), and catechol 2,3-dioxygenase (*xylE*) in *Rhodococcus* sp. LW-XY12 cultured with DEHP were upregulated 1499, 675, 33, 32, and 461 folds, respectively, compared to expression levels in *Rhodococcus* sp. LW-XY12 of the control (grown with citrate). This indicates that these genes are involved in the degradation of DEHP by *Rhodococcus* sp. LW-XY12.



Table 4 Genes/enzymes with reported role in phthalate ester degradation.

Gene/Enzyme	Role in PAE degradation	Accession number	Host bacteria	References
<i>carEW</i> /Carboxylesterase	Degradation of diisobutyl phthalate to monoisobutyl phthalate and phthalic acid (Upper pathway)	AIZ00845	<i>Bacillus</i> sp. K91	Ding et al (2015a)
<i>pehA</i> /PAEs hydrolase	Hydrolysis of phthalate esters (Upper pathway)	AAK16532	<i>Arthrobacter keyseri</i> 12B	Eaton (2001)
<i>mehpH</i> /Mono-2-ethylhexyl phthalate hydrolase	Degradation of mono-2-ethylhexyl phthalate to phthalic acid (Upper pathway)	LC094142.1	<i>Rhodococcus</i> sp. EG-5	Iwata et al (2016)
<i>estSI</i> /Esterase	Degradation of phthalate esters to corresponding phthalate monoesters (Upper pathway)	AEW03609.1	<i>Sulfobacillus acidophilus</i> DSM10332	Zhang et al (2014)
<i>hyd</i> /PAE-hydrolyzing esterase	Hydrolysis of dibutyl phthalate (Upper pathway)	MH507318.1	<i>Rhodococcus</i> sp. 2G	Du et al (2021)
<i>dpeH</i> /Esterase for dialkyl PAEs	Hydrolysis of phthalate esters to phthalate monoesters (Upper pathway)	MK165156	<i>Microbacterium</i> sp. PAE-1	Lu et al (2020)
<i>mpeH</i> /Esterase for mono alkyl esterase	Hydrolysis of phthalate mono esters to phthalic acid (Upper pathway)	MK165157	<i>Microbacterium</i> sp. PAE-1	Lu et al (2020)
<i>patE</i> /Putative phthalate ester hydrolase	Hydrolysis of phthalic monoesters to phthalic acid (Upper pathway)	ABH00399.1	<i>Rhodococcus jostii</i> RHA1	Hara et al (2010)
<i>mphGI</i> /Hydrolase for	Hydrolysis of monoethyl phthalate, mono-n-butyl	MH674097.1	<i>Gordonia</i> sp. YC-	Fan et al (2018b)

monoalkyl ester	phthalate, mono-n-hexyl phthalate, and monoethylhexyl phthalate to phthalic acid (Upper pathway)	JH1	
<i>goEst15</i> /DEHP hydrolase	Degradation of phthalate esters to phthalate monoesters (Upper pathway)	MH513611.1	<i>Gordonia</i> sp. F5 Huang et al (2019)
<i>phtAa</i> /Phthalate dioxygenase large subunit	Degradation of phthalic acid to protocatechuic acid (Lower pathway)	AAQ91914.2	<i>Mycobacterium vanbaalenii</i> PYR-1 Stingley et al (2004)
<i>phtAb</i> /Phthalate dioxygenase small subunit	Degradation of phthalic acid to protocatechuic acid (Lower pathway)	AAQ91915.1	<i>Mycobacterium vanbaalenii</i> PYR-1 Stingley et al (2004)
<i>phtB</i> /Phthalate dihydrodiol dehydrogenase	Degradation of phthalic acid to protocatechuic acid (Lower pathway)	AAQ91917.1	<i>Mycobacterium vanbaalenii</i> PYR-1 Stingley et al (2004)
<i>phtAc</i> /Phthalate dioxygenase ferredoxin subunit	Degradation of phthalic acid to protocatechuic acid (Lower pathway)	AAQ91918.1	<i>Mycobacterium vanbaalenii</i> PYR-1 Stingley et al (2004)
<i>phtAd</i> /Phthalate dioxygenase ferredoxin reductase	Degradation of phthalic acid to protocatechuic acid (Lower pathway)	AAQ91919.1	<i>Mycobacterium vanbaalenii</i> PYR-1 Stingley et al (2004)

2.7 Microbial co-occurrence networks

Bacteria like all microbes in the environment exist as part of a complex community. Advances in sequencing technology, such as 16S rRNA gene amplicon sequencing and shot metagenomic sequencing, has allowed for the effective characterization of complex bacterial communities in terms of community composition. However, these results do not provide information about potential interactions or associations amongst members of the community (Berry & Widder 2014). Organisms in a community are constantly interacting with each other, to compete for resources or synergize their activities, thus contributing to the overall functionality and robustness of the community. A number of network-based analytical methods have been developed for predicting microbial interactions using microbial community composition data. However, the sparse and compositional nature of microbial abundance data presents challenges in inferring microbial interactions in complex communities. Furthermore, it may not be possible to differentiate between direct and indirect interactions. Additionally, the interactions predicted using network-based approaches are rarely validated due to the challenges associated with studying complex microbial communities (Berry & Widder 2014).

Network analysis methods based on Spearman and Pearson correlations are among the most popular methods for the prediction of bacterial co-occurrence patterns. However, correlation-based network analyses such as the Molecular Ecological Network Analysis Pipeline, MENAP (Deng et al 2012) do not consider the compositionality of microbial abundance data and hence may lead to the prediction of false interactions or associations (Matchado et al 2021). Compositionality refers to the fact that microbial numbers obtained via sequencing methods such as 16S rRNA gene

amplicon sequencing represent proportions or relative abundance of a fixed total number. This means that the microbial count values are not independent and must add up to a fixed total. Therefore, Schwager et al (2020) developed an R package for the determination of associations, such as Pearson and Spearman correlations, between features in sparse and compositional data. CCREPE accounts for compositional bias and avoids the prediction of spurious correlations, generating p and q values that have been corrected for compositionality bias.

Recently, several studies have carried out co-occurrence network analyses to better understand the effects of various pollutants on microbial interactions and changes in microbial interaction or co-occurrence patterns with time and changing conditions, and to predict co-operators of pollutant degraders in complex bacterial communities. Sun et al (2022) conducted soil incubation experiments to investigate the effects of conventional and biodegradable microplastics on the co-occurrence relationships of the indigenous soil bacterial community. They used the MENAP (Deng et al 2012) to infer bacterial interactions based on Spearman correlations. Sun et al (2022) observed more complex bacterial networks in soil incubated with biodegradable microplastics than in soil with conventional microplastics. Furthermore, more keystone species were predicted in bacterial networks influenced by biodegradable microplastics and the networks influenced by biodegradable microplastics were more robust.

Huang et al (2021) used a network analysis method based on Spearman correlations to study bacterial interactions in an DBP-degrading bacterial consortium enriched from activated sludge of a wastewater treatment plant. They predicted

mutualistic interactions amongst bacterial genera, which could be indicative of cross-feeding of metabolites. Furthermore, competitive interactions were predicted amongst the bacterial genera with DBP-degrading potential, which could be attributable to the competition for the carbon source (DBP). Furthermore, Meng et al (2022) used network analysis to investigate how microbial interactions influence lignocellulose degradation during composting. They predicted that approximately 20 to 80% of lignocellulose degradation was attributable to interactions between bacterial and fungal species in the compost and analysis of keystone taxa in the network revealed that low-abundance microbial taxa impacted the microbial interactions attributable to lignocellulose degradation. A network-based approach was used by Wang et al (2021c) to identify potential cooperators of a DBP-degrading bacterium *Arthrobacter nicotiniana* ZM05, which was sensitive to pH, temperature, and heavy metal stress. Strain ZM05 was inoculated in soils spiked with high concentrations of DBP (up to 3000 mg/kg) and network analysis of the bacterial community in the soil revealed positive interactions with several bacterial taxa including *Pseudomonas*. Through targeted isolation methods, *Pseudomonas aeruginosa* ZM03, was isolated from the DBP-spiked and ZM05-inoculated soils. Experimental results showed that a co-culture of *Pseudomonas aeruginosa* ZM03 and *Arthrobacter nicotiniana* ZM05 had a high DBP degradation activity even under acidic conditions (pH 5.5), while the DBP-degradation activity of ZM05 was significantly inhibited at pH 5.5. This provides direct evidence of the positive interaction between ZM03 and ZM05, and implies that network-based approaches could be used for reliable predictions of microbial interactions.

Song et al (2019) studied the interactions between DEHP-degrading indigenous bacteria and non-degraders in agricultural soils spiked with 10 mg/kg of DEHP via stable isotope probing and co-occurrence network analysis. DEHP degradation efficiencies by indigenous soil microbes on days 3 and 6 were approximately 30% and 80%, respectively. Based on relative abundance information, active DEHP-degraders were bacterial strains from genera *Singulisphaera*, *Dyella*, *Brevundimonas*, and *Sphingobacterium*, uncultured bacterium belonging to class Ktedonobacteria, two *Bacillus* strains belonging to family Planococcaceae, and a bacterial genus belonging to class *Spartobacteria*. However, DEHP-degrading bacteria isolated from the soil belonged to the genera *Rhizobium* and *Ensifer* (belonging to phylum Proteobacteria and class Alphaproteobacteria). The predicted interactions amongst the active DEHP-degraders and the major bacterial family Oxalobacteraceae (non-degrader) were mostly negative, which are generally attributed to predation amongst bacterial species and competition for carbon and nitrogen. These negative interactions could be why the active DEHP-degraders predicted based on community analysis could not be isolated in this study.

CHAPTER 3

MATERIALS AND METHODS

3.1 Chemicals and materials

Nine marine sediment samples collected from the Gulf of Thailand (sampling locations and depths are available in Table 5 and a map showing the sampling sites is shown in Figure 2) were used in Phase I of this study for the enrichment of DEHP-degrading bacterial consortia. DEHP, DBP, DEP, and DMP were purchased from Tokyo Chemical Industry Co., Ltd. (Tokyo, Japan). Zobell marine broth was purchased from HiMedia. 2-ethylhexanol and MEHP were purchased from Sigma Aldrich (Missouri, USA). Phthalic acid was purchased from Kanto Chemical Co., Inc. (Tokyo, Japan), and protocatechuic acid was obtained from Wako Pure Chemical Industries Ltd. (Tokyo, Japan). All PAEs and metabolites used here were >99.0% pure. Dichloromethane (99.5%), methanol was purchased from Loba Chemie Pvt. Ltd (Mumbai, India). All the reagents used in this study were of analytical grade. The sediment used in Phase III of the study to investigate the degradation of DEHP in microcosms was collected from a shrimp farm in Rayong (12.7504840, 101.6617480).

Table 5 Sampling locations of the nine marine sediment samples used for enrichment.

Station ID	Collection date	Longitude (°)	Latitude (°)	Water Depth (m)
3	19-08-18	100.2642	12.72727	23.9
8	21-08-18	101.7586	12.25625	30.2
10	23-08-18	100.769	11.74502	44
13	21-08-18	102.2563	11.73568	46
14	26-08-18	99.75413	11.2347	42
22	2-9-2018	99.67372	10.39833	46.8
27	1-9-2018	100.2747	9.774583	30.4
32	8-9-2018	101.0739	9.236367	60
33	9-9-2018	100.3231	8.7074	24

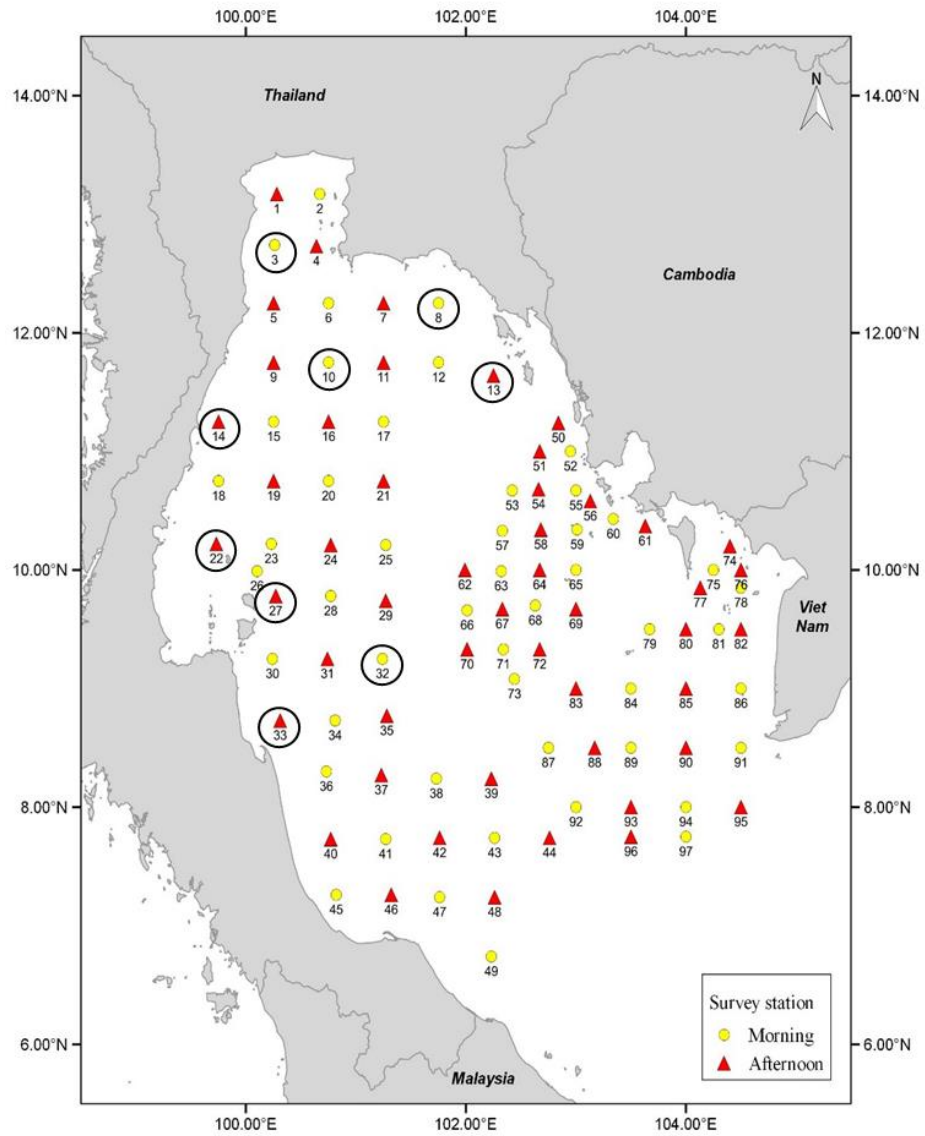


Figure 2 Map showing the sampling sites (in the Gulf of Thailand) of the marine sediment samples used in this study.

3.2 Experimental procedure

The experiments conducted for this research project can be divided into three phases (as shown in Section 1.5). Phase I experiments focused on obtaining potential DEHP-degrading bacterial consortia from marine sediment through enrichment with DEHP as the carbon source. The bacterial communities of the marine sediment samples and the corresponding DEHP-enriched consortia were compared based on 16S rRNA gene amplicon sequencing to identify bacterial members that are induced by DEHP exposure and hence likely to be DEHP-degraders. A prediction of key PAE-degraders was made through network analysis based on bacterial community dynamics of the enriched consortia in the presence of PAEs and their intermediates. In Phase II, the predicted degraders were selectively isolated using different isolation media and substrates, followed by determination of their abilities to degrade DEHP and utilize DEHP metabolites as carbon source for growth. In the last phase of this study (Phase III), a defined consortium of the key degraders was created and genomic analysis was done to reveal genes encoding potential PAE-degrading genes and predict synergistic role of each member of the consortium in DEHP degradation. The DEHP-degrading capabilities of this defined consortium was investigated in sediment microcosms, coupled with monitoring of the bacterial community dynamics through metagenomic analysis.

All experiments in this study were performed in triplicates. Statistical analysis was carried using the one-way analysis of variance (ANOVA) and Tukey's test on GraphPad Prism 8.4.2. All data are presented as mean \pm deviation of triplicate readings (unless indicated otherwise) and different letters indicate statistically significant differences at p value < 0.05 .

3.3 Phase I

3.3.1 Enrichment of bacterial consortia from marine sediment with DEHP as a carbon source

Nine surface sediment samples collected from the Gulf of Thailand were selected for enrichment. Information about the sampling locations and depths are available in Table 5. Enrichment was carried out over a period of 35 d. In brief, 5 g of sediment was transferred to 125 mL Erlenmeyer flasks containing 45 mL of nutrient sea water (NSW) spiked with 50 mg/L DEHP as a carbon source and incubated for 7 d at room temperature (RT; 30 ± 2 °C) and 200 rpm. The composition of NSW was NH_4NO_3 (1 g), K_2HPO_4 (0.02 g), $\text{C}_6\text{H}_5\text{FeO}_7$ (0.02 g), and yeast extract (0.5 g) in 1000 mL of filtered seawater (using a cellulose acetate filter, 0.45 μm). After every 7 d, 5 mL of the culture was transferred to fresh NSW with DEHP (50 mg/L for enrichment cycles 1 and 2 and 100 mg/L thereafter) and incubated under the same conditions. DEHP was dissolved in dichloromethane and filter-sterilized (through 0.2 μm PTFE filters) prior to use. The cultures obtained at the end of the fifth enrichment cycle on Day 35 (enriched consortia) were lyophilized and stored at 4 °C for further use.

3.3.2 Preparation of inoculum for enriched bacterial consortia

As shown in Figure 3, to prepare inoculum for degradation and growth experiment, the enriched bacteria consortia were cultured in 50 mL of NSW spiked with 25 mg/L DEHP for 3 d at 200 rpm and RT. Cells were harvested by centrifuging at 8000 rpm (10 min, 4 °C), the supernatant was discarded, and the cell pellet was washed with 30 mL 0.85% (w/v) NaCl solution and centrifuged again. This washing step was repeated twice. Then, the washed cell pellets were resuspended in 0.85%

(w/v) NaCl solution to obtain a cell concentration of $\log 8$ CFU/mL and starved for 1 d at 200 rpm and RT. This was then used as inoculum for further experiments.

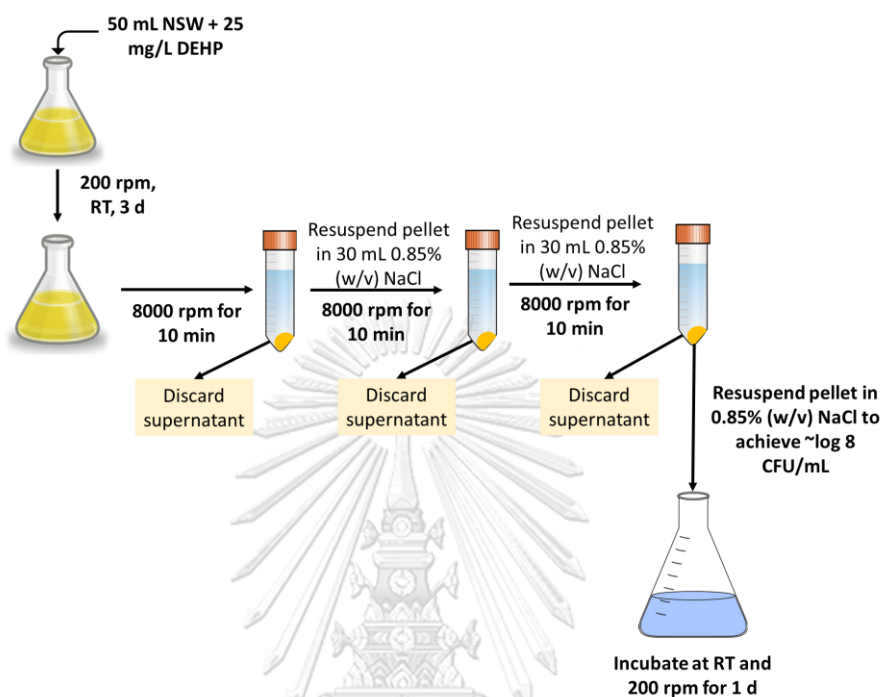


Figure 3 Schematics of bacterial inoculum preparation.

3.3.3 Preliminary investigation of the DEHP-degrading capabilities of the nine enriched consortia

DEHP degradation experiments were performed in test tubes containing NSW (4.5 mL) spiked with 100 mg/L DEHP. The prepared inoculum (0.5 mL) was transferred into experimental test tubes to obtain an initial cell count of $\sim \log 7$ CFU/mL, while tubes without inoculum served as the abiotic control. Experimental and control tubes were incubated at 200 rpm and RT. All the experiments were performed in triplicate. The samples were sacrificed on days 4 and 6. Cell growth was determined via serial dilution (in 0.85% (w/v) NaCl) and viable cell count (plating on 0.25X Zobell marine agar (ZMA)). As illustrated in Figure 4, the remaining

concentration of DEHP in the culture medium was extracted using DCM (1:1 v/v) by vortexing for 1 min. The solvent fraction was collected and dried in a fume hood. The extracts were resuspended in dichloromethane, and the DEHP concentration was quantified via gas chromatography with flame ionization detection (GC-FID; AGILENT series 6890) equipped with an HP-5 column (30 m × 0.25 mm × 0.25 μm). The oven temperature was programmed to increase from 50 °C (hold time: 1 min) to 280 °C at a rate of 30 °C/min and then to 310 °C (hold time: 6 min) at a rate of 15 °C/min. Helium was used as the carrier gas at a flow rate of 2.1 mL/min. The samples were injected in split mode. The injection volume was 1 μL, and the FID temperature was set at 290 °C. Percent degradation was calculated using Eq. 1.

$$\text{Percent degradation} = [(C_0 - C_t) / C_0 \times 100] \dots\dots\dots(1)$$

where C_0 is the concentration (mg/L) at time 0 and C_t is the concentration (mg/L) remaining at time t.

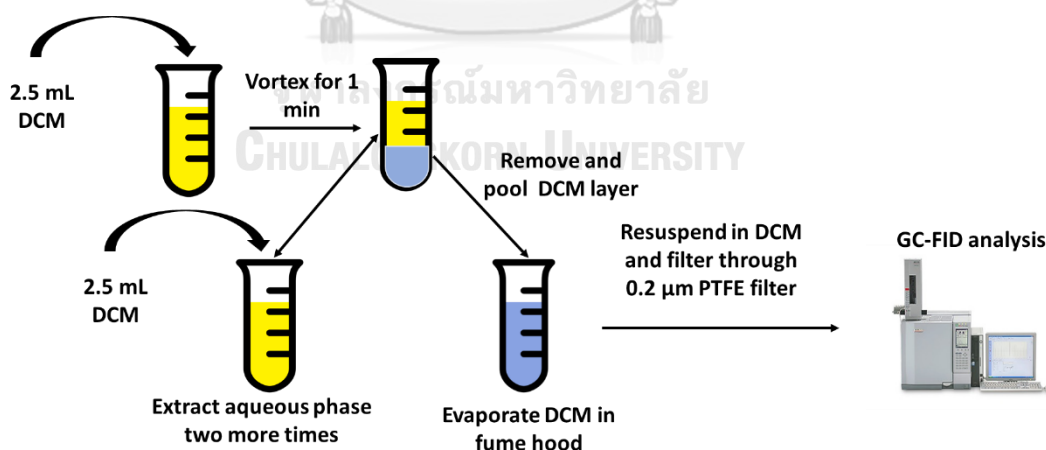


Figure 4 Schematics of residual DEHP extraction from the degradation medium.

3.3.4 Degradation of other phthalate esters by the enriched consortia and growth on DEHP intermediates

C10, C22, and C33 (which were determined to have the highest DEHP degradation activities based on Section 3.3.3) were tested for their abilities to degrade other PAEs of varying alkyl chain lengths (as mixtures and separately). For this purpose, the inoculum of the three enriched consortia (prepared as described in Section 3.3.2) were cultured in NSW spiked separately with 100 mg/L each of DBP, DEP, and DMP. For the degradation of the PAE mixture, 100 mg/L of DEHP, DBP, DEP, and DMP were added to NSW to obtain a total PAE concentration of 400 mg/L. Experiments were performed at RT and 200 rpm shaking in triplicate, and abiotic controls were set up. The remaining concentrations of the PAEs were extracted and quantified via GC-FID analysis using the same protocol described for DEHP in Section 3.3.3.

The growth of C10 on DEHP metabolites (MEHP, 2-ethylhexanol, phthalic acid, and protocatechuic acid) as the sole carbon source was also monitored. Filter-sterilized solutions (using a 0.2 μ PTFE filter) of MEHP, 2-ethylhexanol, phthalic acid, and protocatechuic acid dissolved in methanol were added to modified NSW (without yeast extract) to achieve a concentration of 100 mg/L for MEHP, phthalic acid, and protocatechuic acid and 200 mg/L for 2-ethylhexanol. C10 inoculum was added to obtain an initial cell concentration of $\log 7$ CFU/mL. A biological control (BC) containing modified NSW and C10 inoculum, without the addition of any carbon substrate, was set up. All the experiments were conducted in triplicate and incubated at RT and 200 rpm for 5 d. Samples were withdrawn every 24 h, and the viable cell count was determined via serial dilution and plating on 0.25X ZMA.

3.3.5 Taxonomic classification of the bacterial communities in the enriched consortia and sediment samples

DNA was extracted from the nine marine sediment samples (referred to as S3, S8, S10, S13, S14, S22, S27, S32, and S33) using the Qiagen DNeasy PowerSoil Kit (Qiagen, Hilden, Germany) following manufacturer's protocol. Meanwhile, for the corresponding nine enriched bacterial consortia (C3, C8, C10, C13, C14, C22, C27, C32, and C33), cells were harvested on Day 4 of DEHP (100 mg/L) degradation, DNA was extracted using the GenUP™ Bacteria gDNA Kit (Biotechrabbit, Berlin, Germany) according to the manufacturer's protocol.

Furthermore, the bacterial communities of C10 (on days 2, 4, and 6), C22 (days 2, 4, 6, and 8), and C33 (days 2, 4, 6, and 8) during the degradation of the PAE mixture (DEHP, DBP, DEP, and DMP) were monitored. During degradation, cells were harvested (by centrifuging at 8000 rpm) and DNA was extracted using the GenUP™ Bacteria gDNA Kit. For C10, cells were harvested on Day 4 of the degradation of the other three PAEs (DBP, DEP, and DMP) and growth on DEHP metabolites (MEHP, 2-ethylhexanol, phthalic acid, and protocatechuic acid) as well. DNA was extracted using the GenUP™ Bacteria gDNA Kit (Biotechrabbit, Berlin, Germany) according to the manufacturer's protocol. All extractions were carried out in triplicates and the triplicate DNA for each sample was pooled and submitted for 16S rRNA gene amplicon sequencing to the Omics Sciences and Bioinformatics Center (Chulalongkorn University, Thailand).

3.3.6 16S rRNA gene amplicon sequencing

The V3-V4 regions of the 16S rRNA gene were amplified using 341F and 805R primers, and high-throughput 16S rRNA gene amplicon sequencing was performed as detailed by Muangchinda et al (2018). Cluster generation and 250-bp paired-end read sequencing were performed on an Illumina MiSeq platform (Illumina, CA, USA) at Omics Sciences and Bioinformatics Center (Bangkok, Thailand). Sequence processing was performed on QIIME 2 (Bolyen et al 2019). Raw sequence data were demultiplexed and quality filtered using q2-demux, while DADA2 (Callahan et al 2016) was employed for denoising. Phylogenetic tree construction was performed with the SATé-enabled phylogenetic placement (SEPP) q2-plugin (Janssen et al 2018). The samples were rarefied through subsampling without replacement, and the alpha diversity and beta diversity indices were estimated using q2-diversity. A taxonomic classification of the amplicon sequence variants (ASVs) was performed using q2-feature-classifier (Bokulich et al 2018) against the SILVA ribosomal RNA gene database (Quast et al 2013). All high-throughput 16S rRNA gene amplicon sequences obtained are available at the Sequence Read Archive database (project accession number PRJNA816432). For species-level taxonomic identification of the bacterial community of C10, long-read sequencing of the 16S rRNA genes of the C10 bacterial community on Day 4 of mix PAE degradation was also carried out on the Pac Bio HiFi sequencing platform at the National Science and Technology Development Agency (NSTDA), Thailand.

3.3.7 Kinetics of DEHP degradation by C10

C10 inoculum (0.5 mL) prepared as described in Section 3.3.2 was added to 4.5 mL of NSW (final cell count: $\log 7$ CFU/mL) supplemented with initial DEHP

concentrations of 50, 100, 200, 500, and 800 mg/L in glass test tubes. Abiotic controls were set up. Test and control tubes were incubated at RT and 200 rpm shaking. Samples were sacrificed every 24 h for 8 d, and residual DEHP was quantified using GC-FID. All the experiments were performed in triplicate. Percent DEHP degradation was calculated using Eq. 1 and the first-order kinetic model (Eq. 2) was used to determine the biodegradation kinetics of different initial concentrations of DEHP. Lastly, the biodegradation half-life of DEHP was determined using Eq. 3.

$$\ln C = -kt + A \dots\dots\dots(2)$$

$$t_{\frac{1}{2}} = \ln 2/k \dots\dots\dots(3)$$

where \ln refers to the natural logarithm, C refers to the initial DEHP concentration (mg/L), k is the first-order rate constant (d^{-1}), t is the time in days (d), A is a constant, and $t_{1/2}$ refers to the half-life (d).

3.3.8 Bacterial co-occurrence patterns and prediction of bacterial community function

Pearson correlations among the relative abundances of bacterial taxa were calculated using the Compositionality Corrected by PERmutation and RENormalization (CCREPE) R Package (Schwager et al 2020). Positive and negative Pearson correlations ≥ 0.7 and compositionality-corrected p values < 0.05 were used network construction. Cytoscape 3.8.2 was used for network visualization and analysis (Shannon et al 2003). Predictions of bacterial metabolic pathways and functions were performed using Tax4Fun2 (Wemheuer et al 2020) based on the Kyoto Encyclopedia of Genes and Genomes (KEGG) database.

3.4 Phase II

3.4.1 Selective isolation of bacterial strains in C10 and identification of isolated bacterial stains

To isolate bacterial strains from C10, the following agar media were used: 0.25XZMA, DEHP (50 mg/L)-spiked modified nutrient seawater agar (without yeast extract), ATCC medium 159, *Sporosarcina halophila* agar, ATCC medium 589, *Bacillus* agar, sea water-yeast extract agar, and 0.5× tryptic soy agar with 4% NaCl (the compositions are detailed in the Appendix A). To obtain bacterial isolates capable of degrading DEHP and other PAEs (DBP, DMP, and DEP), as well as DEHP metabolites (MEHP, 2-ethylhexanol, phthalic acid, and protocatechuic acid), C10 was cultured separately in NSW spiked with these target substrates (100 mg/L), and samples were periodically withdrawn and plated on the different agar media mentioned above for single strain isolation. Once pure cultures were obtained, their genomic DNA was extracted using the GenUP™ Bacteria gDNA kit following manufacturer's instructions. The 16S rRNA gene was sequenced by ATGC Co. Ltd. (Thailand). These sequences were characterized via a similarity search using EzBioCloud's 16S database.

3.4.2 Preparation of inoculum for single bacterial strains

To prepare inoculum for degradation and growth experiments for single bacterial strains, a loopful of each bacterial isolate streaked on 0.25X ZMA plates was cultured in 50 mL of 0.25X Zobell marine broth spiked with 25 mg/L DEHP for 3 d at 200 rpm and RT. Cells were harvested by centrifuging at 8000 rpm (10 min, 4 °C), the supernatant was discarded, and the cell pellet was washed with 30 mL 0.85% (w/v) NaCl solution and centrifuged again. This washing step was repeated twice.

Then, the washed cell pellets were resuspended in 0.85% (w/v) NaCl solution to obtain a cell concentration of log 8 CFU/mL and starved for 1 d at 200 rpm and RT. This was then used as inoculum for further experiments.

3.4.3 Characterization of the bacterial isolates from C10

The DEHP degradation activities of the isolates were determined as described in Section 3.3.3. To check the growth of the bacterial isolates obtained from C10 on commonly reported DEHP metabolites, MEHP, monobutyl phthalate, 2-ethylhexanol, phthalic acid, and protocatechuic acid, modified NSW (without yeast extract) was prepared. The bacterial inoculum was prepared as described in Section 3.4.2, and 20 μ L was added to 96-well plates containing 180 μ L of modified NSW to achieve an initial cell count of ~ 7 log CFU/mL. The modified NSW was supplemented with target metabolites (100 mg/L for MEHP, monobutyl phthalate, phthalic acid, and protocatechuic acid; and 100 and 200 mg/L for 2-ethylhexanol) as the sole carbon source. The plates were incubated at RT for 5 d and wells containing only bacterial inoculum and modified NSW with no additional substrates were set as biotic controls. Number of viable cells in the wells on Day 0 and Day 5 were determined via serial dilution in 0.85% (w/v) NaCl solution and plating on 0.25X ZMA. Isolates were qualitatively screened for biosurfactant production ability using oil displacement test. In brief, isolates were cultured in productive medium containing 2% v/v soybean oil (Khondee et al 2015) for 5 d at RT and 200 rpm shaking. Then, 10 μ L of the culture broth was added at the center of crude oil layer (20 μ L) formed over distilled water (10 mL) in a petri dish. Displacement of oil forming a clear zone (≥ 1.5 cm in diameter) is considered positive for biosurfactant production (Rani et al 2020).

Distilled water and 10 mg/mL of Triton X-100 were used as the negative and positive controls, respectively.

3.5 Phase III

3.5.1 Creation of defined bacterial consortia and screening their PAE degradation activities

Selection of bacterial strains for defined consortia creation was based on DEHP degradation activity, growth of isolates of DEHP intermediates (MEHP, 2-ethylhexanol, phthalic acid, protocatechuic acid, and monobutyl phthalate) as sole sources of carbon, qualitative biosurfactant productivity (crude oil displacement activity), predicted interactions based on network analysis, and information on pathogenicity. The selected bacterial isolates from C10 were screened for any antagonistic effects against each other, prior to creation of defined consortia, through cross streaking on 0.25X ZMA. Then, the selected strains were cultured in 0.25X Zobell marine broth spiked with 25 mg/L of DEHP (200 rpm shaking for 3 d at RT). Cells were harvested via centrifugation at 8000 rpm and the cell pellets were resuspended in 0.85 % (w/v) NaCl to obtain bacterial inoculum containing log 8 CFU/mL. The inoculum was rested for 1 d at 200 rpm and RT. Bacterial inoculum were mixed at equal volumetric ratios to prepare the defined consortia. Then, 0.5 mL of the created consortia was added to 4.5 mL of NSW spiked with DEHP, DBP, DEP, and DMP separately (100 mg/L) and as a mixture (100 mg/L each; total concentration: 400 mg/L) to achieve an initial cell count of log 7 CFU/mL. Degradation efficiencies were investigated determined as described in Section 3.3.3.

3.5.2 Whole genome sequencing

Genomic DNA of each member of the selected bacterial consortium was extracted using the GenUP™ Bacteria gDNA Kit and submitted for whole genome sequencing to Omics Sciences and Bioinformatics Center (Bangkok, Thailand). Library preparation was performed using sparQ Frag & DNA Library Prep (QuantaBio, USA). The qualitative and quantitative determination of the indexed libraries were done using Agilent 2100 Bioanalyzer and Denovix fluorometer. Cluster generation and paired end (2×250 bp) sequencing were performed on an Illumina MiSeq sequencer. The FASTQC software was used to check the quality of the raw reads and adaptors and poor-quality reads were removed using Fastp. Unicycler was used for genome assembly and the assembled genome was annotated using the PATRIC RASTtk-enabled Genome Annotation Service (Brettin, et al. 2015). Average nucleotide identity (ANI) was calculated and compared on the JSpecies web server (Richter et al 2015). Further, amino acid sequences of enzymes reported to be involved in phthalate degradation were retrieved from the NCBI's Protein database and used to query the CDS of the genomes. Genes encoding for enzymes involved in the catabolism of DEHP and its metabolites were identified using the BlastP algorithm and default parameters.

3.5.3 Degradation of DEHP intermediates

Degradation of DEHP metabolites, MEHP, 2-ethylhexanol, phthalic acid, and protocatechuic acid, was investigated in NSW. In summary, MEHP, phthalic acid, and protocatechuic acid (100 mg/L) was added separately to test tubes containing NSW (4.5 mL). Bacterial inoculum (0.5 mL, prepared as described in Section 3.4.2) was added to achieve an initial cell count of log 7 CFU/mL. Abiotic controls containing

substrate and NSW (without inoculum) were set up. All experiments were conducted in triplicates and incubated at 200 rpm and RT. Tubes were sacrificed on Day 4 (for phthalic acid and protocatechuic acid) and Day 8 (for MEHP) and remaining concentrations of substrates were extracted and number of viable cells in the tubes were determined via serial dilution and plating on 0.25X ZMA. Extraction of MEHP was carried out by vortexing with dichloromethane as the solvent and quantification was done via GC-FID analysis using the protocol described in Section 3.3.3. Remaining concentrations of phthalic acid and protocatechuic acid were extracted by vortexing using ethyl acetate as solvent (at equal volumetric ratio) after acidification of the medium of pH 2.0 using 1 M HCl. This extraction step was repeated three times, and the solvent fractions (top layer) were collected after each extraction, pooled, and allowed to evaporate in a fume hood. The dried extracts were then resuspended in methanol and quantification was done by measuring the absorption of the resuspended at 276 nm for phthalic acid (Ebenau-Jehle et al 2017) and 236 nm for protocatechuic acid using a UV-Vis spectrophotometer (BioMate 3S, Thermo Scientific, USA). A UV spectral scan of different concentrations of phthalic acid and protocatechuic acid was carried out to determine the wavelength of interest for each compound.

3.5.4. Sediment microcosm study

3.5.4.1 Microcosm setup

Sediment used in the microcosm was collected from a shrimp farm in Rayong, Thailand, and stored at 4°C till use. The sediment was sieved through a 10 mm sieve prior to use and its physical and chemical characteristics were determined at Department of Soil Science, Faculty of Agriculture, Kasetsart University (Thailand).

As shown in Figure 5, three sets of microcosms were set up: Abiotic control, Natural attenuation, and Bioaugmentation. For the Abiotic control, sediment was sterilized at 121°C and 15 psi for 15 min for three consecutive days. The sediment (20 g) was added to glass jars, spiked with 100 mg/kg of DEHP, and filtered seawater was added until the sediment was completely submerged. Sediment in the bioaugmentation experiments were inoculated with the selected consortium (final concentration: log 7 CFU/g). The control and experiment microcosm jars were incubated at RT and 100 rpm shaking to maintain aerobic conditions.

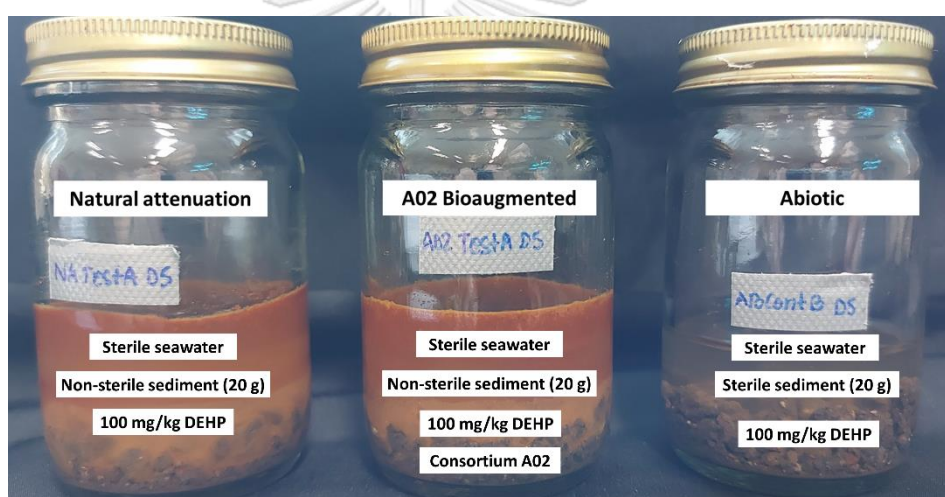


Figure 5 Set-up of the sediment microcosm study.

3.5.4.2 Quantification of DEHP concentrations and bacterial numbers

Microcosm jars were sacrificed on days 0, 5, 8, 11, 16, 21, and 26. The sediment and seawater fractions were separated via centrifugation at 4000 rpm for 10 min. DEHP in the sediment fraction was extracted with dichloromethane at an equal weight/volume ratio via shaking (200 rpm for 30 min) followed by sonication for 20 min. The solvent fraction was removed, while the sediment fraction was extracted two more times. Solvent fractions from all extractions were pooled, allowed to dry in a

fume hood, resuspended in dichloromethane, and quantified via GC-FID analysis (Section 3.3.3). To recover DEHP in the seawater fraction, extraction was carried out using dichloromethane at an equal volumetric ratio and shaking at 200 rpm for 30 min. The extraction was repeated three times, the solvent fractions were pooled, dried under a fume hood, resuspended in dichloromethane, and quantified via GC-FID analysis (Section 3.3.3).

Total heterotrophic bacteria in the microcosms were enumerated. In summary, 1 g of sediment was mixed well with 9 mL of 0.25X Zobell marine broth and then diluted 10^3 times. Then, 20 μL of this solution was transferred to 96-well plates containing 180 μL 0.25X Zobell marine broth, creating 10^1 to 10^{10} fold serial dilutions (eight replicates for each dilution). Wells containing only 0.25X Zobell marine broth served as the control. Cultures were incubated in dark at RT for 24 h. Positive wells were detected by measuring absorbance at 600 nm on Day 0 and 1 using a microplate reader (Benchmark Plus, BIO-RAD, US). Viable bacterial numbers were estimated using the most probable number (MPN) method (Eq. 4). The lowest dilution with at least one negative well and the highest dilution with at least one positive well were selected.

$$\frac{\text{MPN}}{g} = \frac{\sum g_j}{(\sum t_j m_j \sum (t_j - g_j) m_j)^{0.5}} \dots\dots\dots(4)$$

where summation is over the selected dilutions, $\sum g_j$ is the number of positive wells in the selected dilution, $\sum t_j m_j$ is g of sediment in all wells of the selected dilutions, and $\sum (t_j - g_j) m_j$ is g of sediment in negative wells of the selected dilutions.

3.5.4.3 Studying the bacterial community in sediment microcosms during DEHP degradation

DNA was extracted from the sediment fractions (on days 0, 5, 16, and 26) of the natural attenuation and bioaugmentation experiments using the Qiagen DNeasy PowerSoil Pro Kit (Qiagen, Hilden, Germany). DNA extracted from triplicate samples were pooled prior to submission to Omics Sciences and Bioinformatics Center (Chulalongkorn University, Thailand) for metagenomic analyses. Bacterial co-occurrence patterns will be determined using Compositionality Corrected by PERmutation and RENormalization (CCREPE) R Package (Schwager, et al. 2020) as described in Section 3.3.8. Annotation of the metagenome-assembled genomes and prediction of genes involved in phthalate ester degradation will be carried out using the PATRIC RASTtk-enabled Genome Annotation Service (Brettin et al 2015) and eggNOG 4.5 (Huerta-Cepas et al 2016).

CHAPTER 4

RESULTS AND DISCUSSION

4.1 Phase I

4.1.1 Enrichment of bacterial consortia from marine sediment with DEHP as a carbon source

Eight DEHP-enriched bacterial consortia (referred to as C3, C8, C13, C14, C22, C27, and C32, and C33) were obtained in this study. Another DEHP-enriched bacterial consortium (referred to as C10) obtained from a previous study was also used. The physical and chemical properties of the nine marine sediment samples (S3, S8, S10, S13, S14, S22, S27, S32, and S33) used for enrichment are provided in the Appendix C. As the sediment samples (S3, S8, S10, S13, S14, S22, S27, S32, and S33) were stored at 4°C, prior to DEHP-enrichment in this study, the total heterotrophic bacteria (log MPN/g) in the sediment samples were enumerated and high viable bacterial counts (greater than log 8 MPN/g) were observed for all the eight sediment samples (Appendix C).

4.1.2 Preliminary investigation of the DEHP-degrading capabilities of the nine enriched consortia

The DEHP-degradation efficiencies of the nine enriched bacterial consortia were determined on days 4 and 6 as shown in Figure 6. All the nine enriched consortia showed DEHP degradation activity, achieving 37% to 100% degradation of 100 mg/L DEHP on Day 6. C10 had the highest DEHP degradation efficiency (96.5% degradation on Day 4 and 100% degradation on Day 6), followed by C22 and C33, which could degrade 81.9% and 82.7%, respectively, of 100 mg/L DEHP on Day 6. As shown in Figure 7, viable bacterial cell counts of all the enriched consortia on days

4 and 6 of DEHP degradation were slightly elevated from those on Day 0. C10, C22, and C33 were selected for further degradation studies as they had the highest DEHP degradation performance.

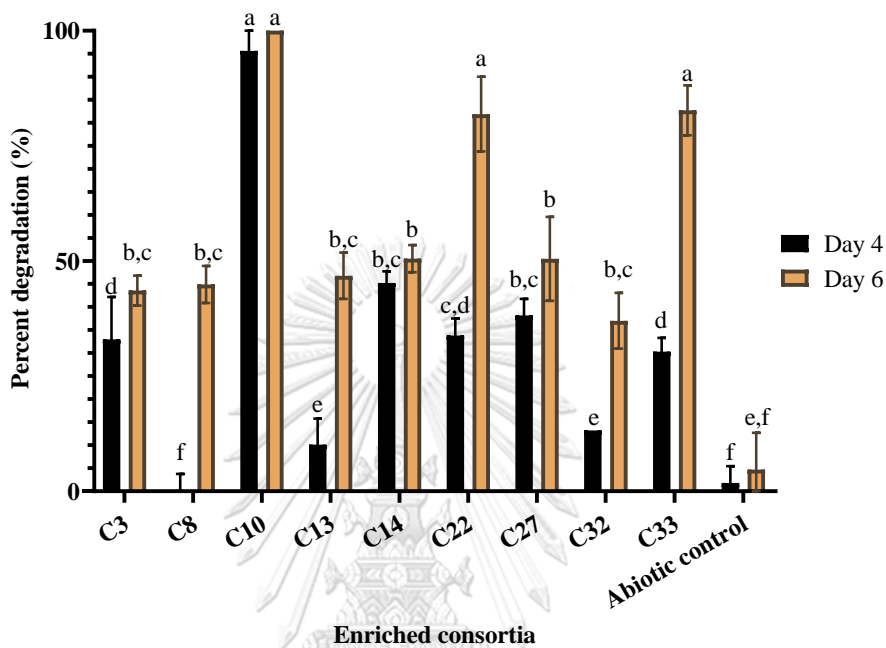


Figure 6 DEHP (100 mg/L) degradation efficiencies of the nine enriched bacterial consortia on days 4 and 6. Different letters indicate significantly different ($p < 0.05$) average percent DEHP degradation values.

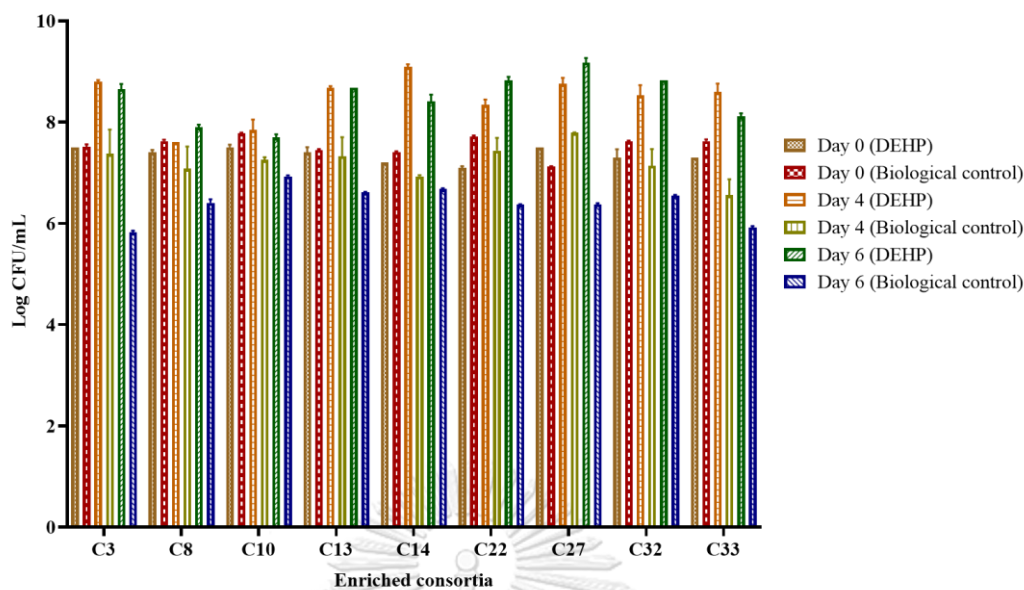


Figure 7 Viable cell counts of the nine enriched bacterial consortia on days 4 and 6 of DEHP degradation and in the biological control.

The DEHP degradation efficiencies of all the nine enriched consortia are generally lower than relevant reports in literature (Table 3). For instance, Bai et al (2020) obtained an enriched consortium CM9 from farmland soil that could completely degrade 1000 mg/L of DEHP in 3 d. Consortium CM9 was enriched with up to 1000 mg/L of DEHP, which is much higher than the DEHP concentration (100 mg/L) used for bacterial enrichment in this study. This could be attributable for the lower DEHP degradation efficiencies observed in this study. As shown in Table 2 and as reviewed by Hidalgo-Serrano et al (2022), the highest reported DEHP concentration in marine sediment is approximately 30 mg/kg (Arfaenia et al 2019). Therefore, a relatively low DEHP concentration (100 mg/L) was used for bacterial enrichment in this study. Nevertheless, this is the first study to enrich DEHP/PAE-degrading bacteria from marine sediment, and hence studying the enriched consortia

obtained in this study could reveal new insights into the DEHP/PAE-degrading potential of marine sediment bacteria.

4.1.3 Degradation of other phthalate esters by C10, C22, and C33

As several types of PAEs such as DEHP, DBP, DEP, and DMP are used in various commercial products, in actual PAE-contaminated sites, several types of PAEs occur simultaneously (Bringer et al 2021, Paluselli & Kim 2020). However, most studies focus on the biodegradation of a single type of PAE (Feng et al 2021, Wang et al 2021d). Therefore, the abilities of the three selected enriched consortia (C10, C22, and C33) to degrade other PAE types were also investigated. As shown in Figure 8a, all the three enriched consortia could completely degrade DMP and DEP (100 mg/L) within 4 d. C22 could completely degrade DBP (100 mg/L) as well, while C10 and C33 could achieve 88.38% and 84.11% degradation, respectively. All three enriched consortia could degrade PAEs with shorter alkyl chains (DMP and DEP) much faster than the PAEs with longer alkyl chains (DBP and DEHP). Longer alkyl chains may create steric hindrance for hydrolytic enzymes (Chen et al. 2021), thus inhibiting the hydrolysis of side chains of PAEs.

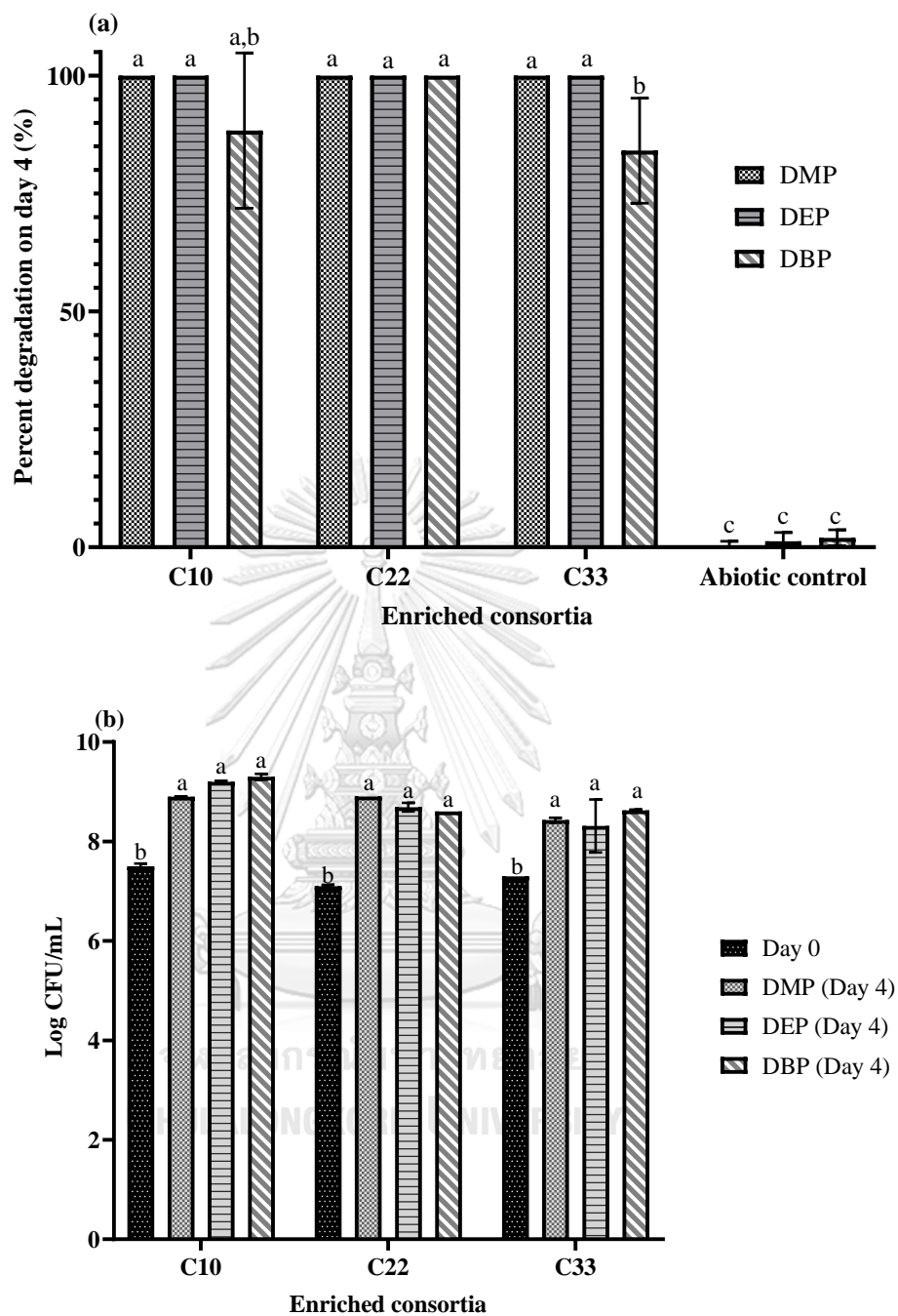
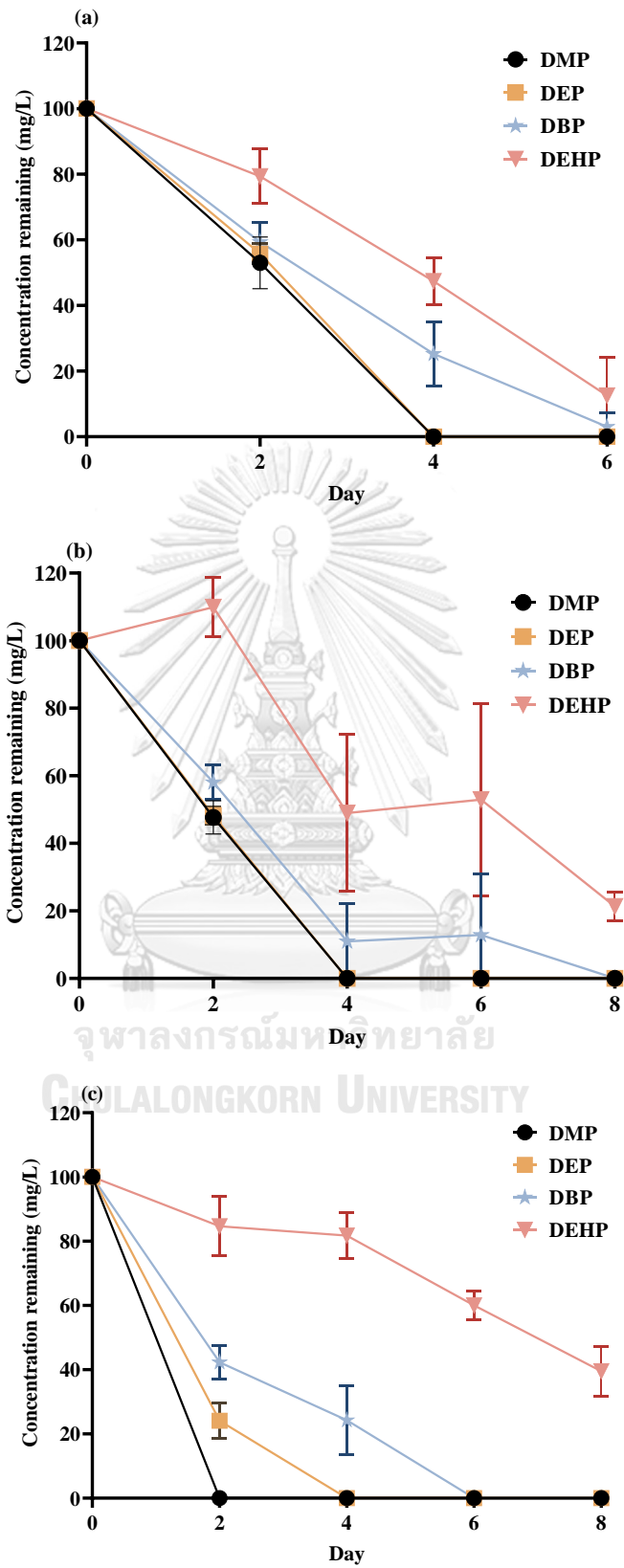


Figure 8 a) Percent degradation of DMP, DEP, and DBP (100 mg/L each) by C10, C22, and C33 on Day 4; (b) Viable cell counts of C10, C22, and C33 on Day 0 and Day 4 of degradation of DMP, DEP, and DBP. Different letters indicate statistically different average percent degradation and log CFU/mL values.

Furthermore, the abilities of the three selected consortia to degrade a mixture of PAEs of varying alkyl chain lengths (100 mg/L each of DEHP, DBP, DEP, and DMP) was also investigated (Figure 9a-c). All the three selected consortia could degrade DMP and DEP within 4 d. Complete DBP degradation was observed within 6 d for C10 and C33 and within 8 d for C22, while 87%, 79%, and 60% DEHP degradation was observed by C10 (on Day 6), C22, and C33 (on Day 8), respectively. As in the case of degradation of different PAEs separately, the faster degradation of PAEs with shorter alkyl chains is evident in this case as well; such a trend has been observed in other studies as well (Kanaujiya et al 2022). Nevertheless, the PAE mixture degradation efficiencies of the three enriched consortia are comparable to relevant reports in literature. For instance, Ren et al (2016) reported 86.3 – 100% degradation of a mixture of DEHP, DMP, dicyclohexyl phthalate, DBP, and DEP (total concentration: 250 mg/L) in 5 d by *Mycobacterium* sp. YC-RL4. Furthermore, 6.4 – 94.1% degradation of DMP, DEP, DBP, and DEHP (total concentration: 300 mg/L) could be achieved in 2 d by a bacterial consortium enriched from activated sludge (He et al 2013). C10, C22, and C33 could degrade 87 – 100%, 47 – 100%, and 40-100%, respectively of the mixture of DEHP, DBP, DEP, and DMP (total concentration: 400 g/L) in 6 d. In this study, PAE degradation in the abiotic control (Figure 9d) was negligible. Viable cell counts of all three enriched consortia increased during the degradation of the PAE mixture (Figure 9e). This shows that the three enriched consortia obtained in this study can degrade mixtures of several kinds of PAEs effectively.



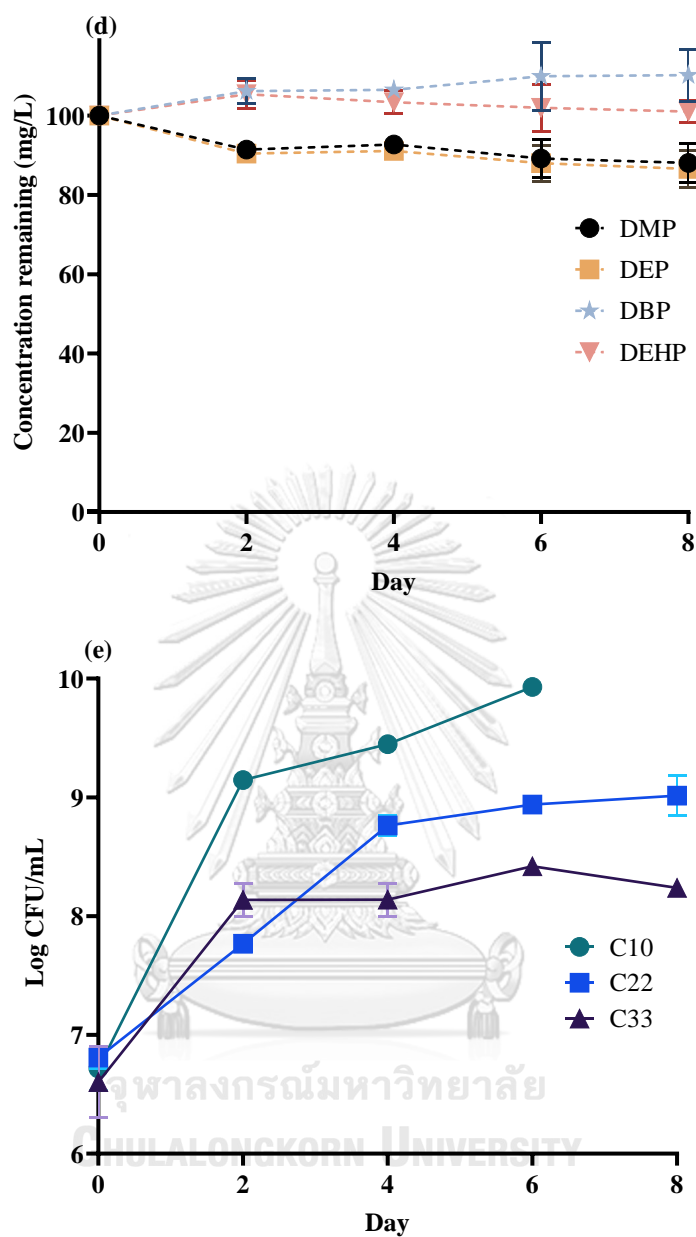


Figure 9 PAE concentration remaining during degradation of a mixture of DEHP, DBP, DEP, and DMP (100 mg/L each; total concentration: 400 mg/L) by C10 (a); C22 (b); C33 (c); and in the abiotic control (d); and viable cells counts (log CFU/mL) of C10, C22, and C33 during degradation of the PAE mixture (e).

As C10 showed the best PAE degradation performance from amongst the three selected enriched consortia, it was selected for further experiments. The kinetics of degradation of different initial concentrations of DEHP (50 – 800 mg/L) by C10 was investigated (Figure 10). As shown in Table 6, the kinetics of DEHP degradation by C10 fitted the first-order kinetic equation: $\ln C = -Kt + A$, where C is the initial DEHP concentration, K is the first-order kinetic constant, T is time, and A is a constant. DEHP half-lives were in the range of 1.28-3.06 d for initial DEHP concentrations of 50-800 mg/L. It is apparent that the DEHP degradation rate is dependent on the initial DEHP concentration – DEHP half-lives increased with increase in the initial DEHP concentration from 100 to 800 mg/L. Conversely, the slower degradation at the initial concentration of 50 mg/L could be because DEHP degraders in C10 are not effectively induced at lower concentrations (Ren et al 2018a). It is expected that biodegradation of high initial concentrations of DEHP will be a challenge due to toxic effects on bacterial growth (Kanaujiya et al 2022). However, lower PAE concentrations may present their own set of biodegradation challenges, such as low bioavailability, insufficient substrate for cell growth, and inability to induce the expression of PAE degradative enzymes (Ren et al 2018a, Yang et al 2018a).

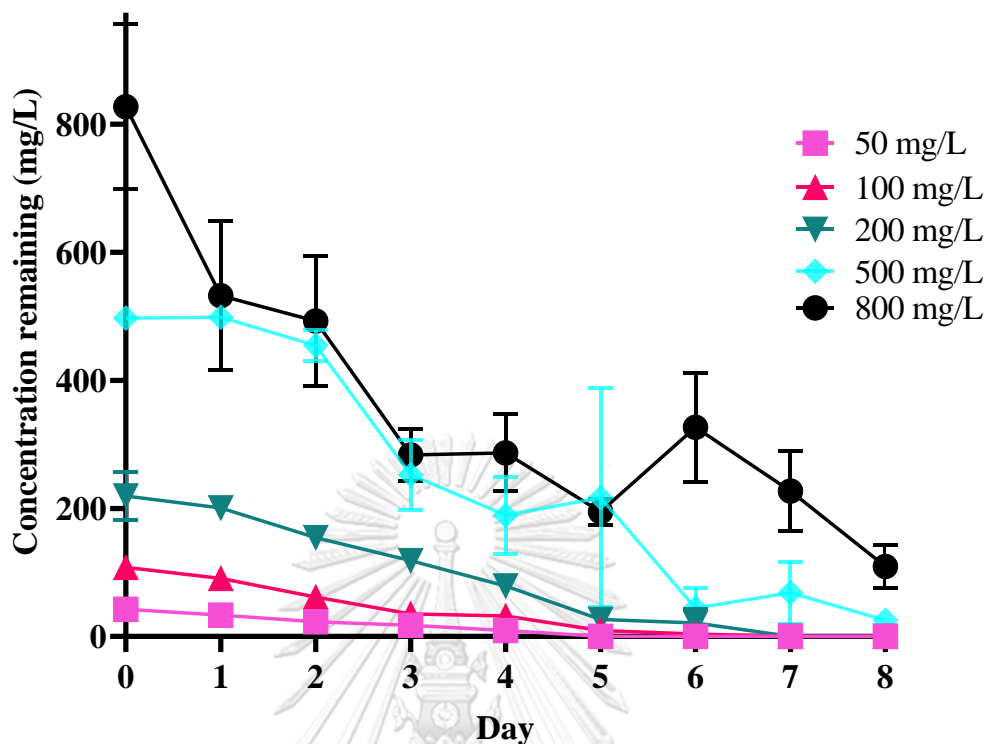


Figure 10 Degradation of different concentrations of DEHP (50 – 800 mg/L) by C10.

Table 6 Kinetic equations of the degradation of different initial DEHP concentrations by C10.

Initial concentration	Zero order			First order			Second order		
	Kinetic equation	R ²	t _{1/2} (d)	Kinetic equation	R ²	t _{1/2} (d)	Kinetic equation	R ²	t _{1/2} (d)
800 (mg/L)	C = -76.853t + 652.88	0.84	5.38	lnC = -0.2265t + 6.5683	0.95	3.06	1/C = 0.0008t + 0.0007	0.89	1.51

500 (mg/L)	C = -	0.	3.	lnC = -	0.	1.	1/C =	0.	0
	67.253t +	9	70	0.3786t +	8	83	0.0038t -	6	.
	518.64	2		6.6182	8		0.0046	6	5
									3
200 (mg/L)	C = -	0.	3.	lnC = -	0.	1.	1/C =	0.	0
	30.659t +	9	58	0.4195t +	9	65	0.0071t -	7	.
	213.75	5		5.7165	1		0.004	7	6
									5
100 (mg/L)	C = -	0.	3.	lnC = -	0.	1.	1/C =	0.	0
	16.046t +	9	36	0.5415t +	9	28	0.0157t -	6	.
	98.764	4		5.0444	2		0.0058	6	6
									2
50 (mg/L)	C = -	0.	2.	lnC = -	0.	1.	1/C =	0.	1
	9.3471t +	9	67	0.398t +	9	74	0.0199t +	8	.
	45.571	7		3.9276	8		0.0115	7	0
									1

As shown in Figure 1, the degradation of DEHP leads to the formation of several intermediates, some of which are reported to be toxic and difficult to biodegrade. The growth of C10 was monitored on four such commonly reported DEHP intermediates, MEHP, 2-ethylhexanol, phthalic acid, and protocatechuic acid, as the sole source of carbon (Figure 11). From days 1 to 5, the viable cell count of C10 (log CFU/mL) was higher with MEHP, phthalic acid, and protocatechuic acid as the carbon source than in the biological control (no carbon source added). Furthermore, in the C10 cultured with MEHP, phthalic acid, and protocatechuic acid as carbon source, a greater than 10-fold increase in CFU/mL by Day 5 compared to that on Day 0 was observed. This indicates that C10 can utilize these three DEHP intermediates as carbon source for growth, and consequently degrade them. However,

on days 1 and 2, viable cell count of C10 growing on 2-ethylhexanol as the sole carbon source was lower than that in the biological control, while from Day 3 onwards, growth of C10 on 2-ethylhexanol was similar to that in the biological control. This may be because 2-ethylhexanol exerts toxic effects on C10 and/or a higher concentration (200 mg/L) of 2-ethylhexanol used. Nevertheless, although growth of C10 is initially inhibited by 2-ethylhexanol, the bacterial members of C10 seem to eventually resist the toxicity of 2-ethylhexanol as indicated by the similar viable cell counts observed on 2-ethylhexanol and in the biological control from Day 3 to Day 5.

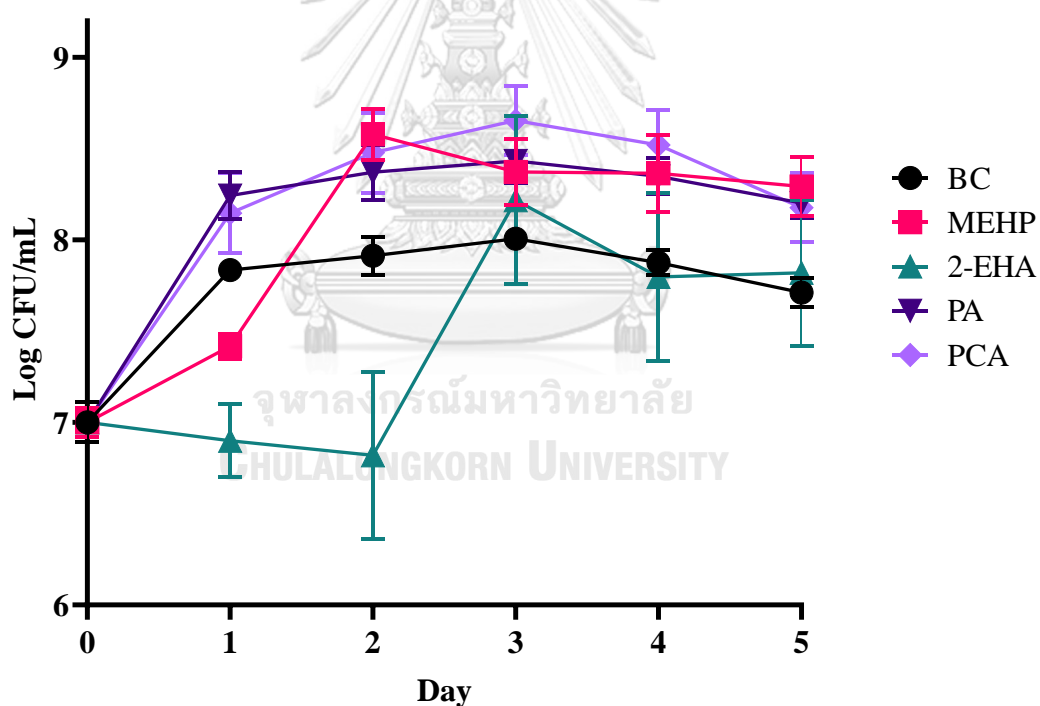


Figure 11 Viable cell numbers of C10 cultured with MEHP, 2-ethylhexanol (2-EHA), phthalic acid (PA), and protocatechuic acid (PCA) as the sole source of carbon. BC refers to the biological control wherein C10 was cultured without the addition of any carbon source.

4.1.4 Taxonomic classification of the bacterial communities in the enriched consortia and sediment samples

4.1.4.1 Bacterial communities in the marine sediment and corresponding enriched consortia

The bacterial communities of the marine sediment samples and enriched bacterial consortia were studied through 16S rRNA gene amplicon sequencing. As shown in Table 7, the alpha diversity indices (Shannon index, Faith's phylogenetic diversity, and observed operational taxonomic units (OTUs)) of the enriched consortia are markedly lower than those of the corresponding marine sediment samples. Beta diversity principal coordinate analysis based on weighted UniFrac distances (Figure 12) revealed differences among the bacterial communities of the enriched consortia, which may in turn explain the variations in their DEHP degradation activities.

Table 7 Alpha diversity indices (Shannon index, Faith's phylogenetic diversity, and observed OTUs) of the bacterial communities of the nine marine sediment samples and corresponding enriched consortia.

Sediment	Shannon index	Faith's PD	Observed OTUs	Enriched consortia	Shannon index	Faith's PD	Observed OTUs
S3	8.9	41.5	767.9	C3	3.1	3.9	36
S8	8.9	45.3	838	C8	3.3	3.8	40
S10	9.5	51.4	1041.8	C10	1.7	3.4	25
S13	9.3	48.3	943	C13	2.4	7.4	55.9
S14	9.3	52.1	1051.8	C14	2.5	4.2	42.2
S22	9.3	50.5	1052.5	C22	2.9	7.3	55.5
S27	9.3	52.9	1118.5	C27	2.1	6.1	52.2

S32	8.6	40.8	724.2	C32	2.4	3.8	26.8
S33	9.3	52.8	1151.2	C33	2.1	6.2	38.9

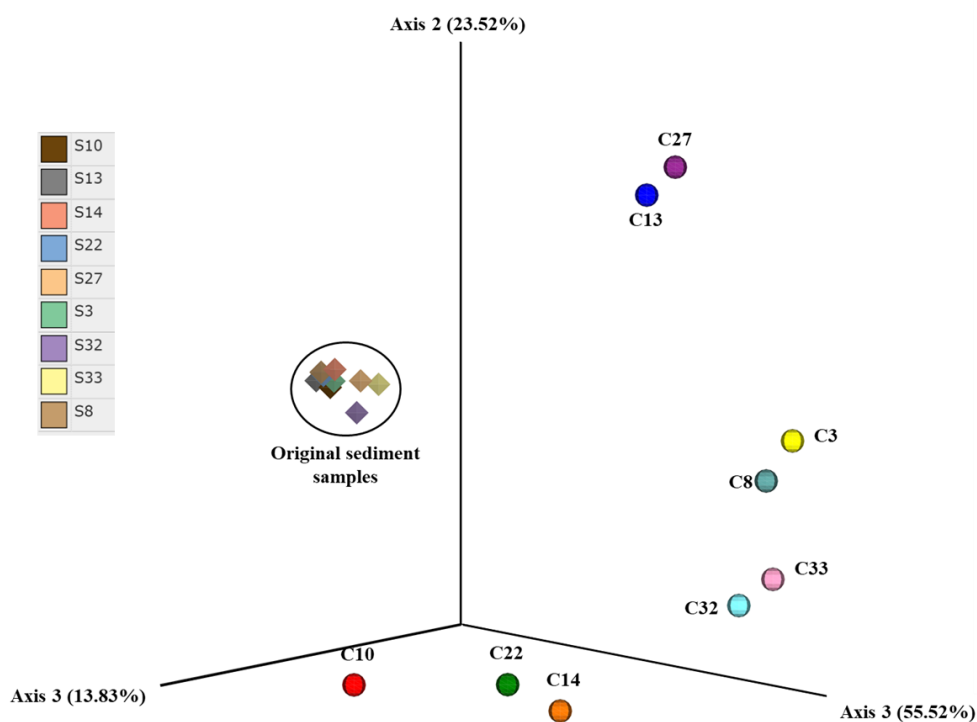


Figure 12 Principal coordinate analysis plot of beta diversity based on weighted UniFrac distances between the bacterial communities of the nine marine sediment samples and corresponding enriched consortia.

Deltaproteobacteria (19.5 – 30.5%), Gammaproteobacteria (19.5 – 29.6%), and Alphaproteobacteria (4.8 – 9.3%) were the dominant classes of bacteria in all the nine marine sediment samples (Figure 13). In the DEHP-enriched consortia C3, C8, C13, and C27, major bacterial classes (Figure 14) were Bacteroidia (20.6 – 64.6%), Gammaproteobacteria (17.4 – 62.1%), and Bacilli (8.3 – 18.4%), while in C10, C14, C22, C32, and C33, Bacilli (10.3 – 81.8%), Gammaproteobacteria (6.5 – 75.5%), and Alphaproteobacteria (4.9 – 12.3%) were the dominant bacterial classes. In six of the

nine DEHP-enriched bacteria consortia, Gammaproteobacteria populations were highly enhanced, while Bacilli was enriched by DEHP exposure in all the nine enriched bacterial consortia. This may indicate that bacteria from these classes are important PAE-degraders in marine sediment.

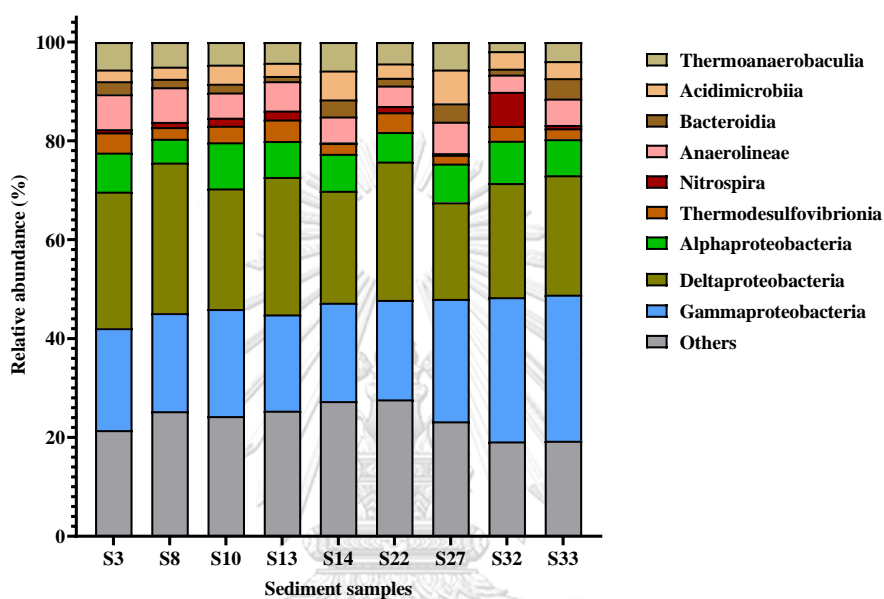


Figure 13 Bacterial communities of the nine marine sediment samples at the class level.

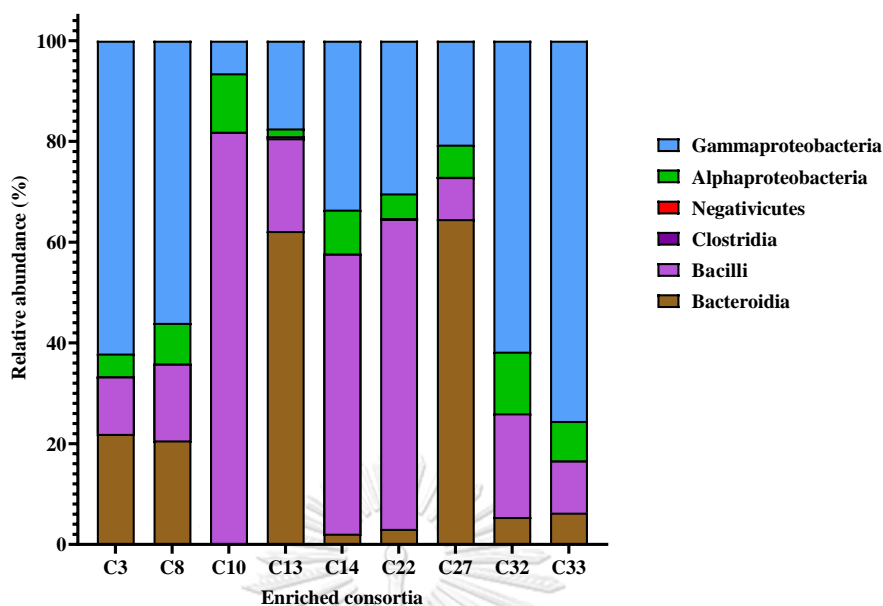


Figure 14 Bacterial communities of the enriched bacterial consortia at the class level.

At the genus level, much of the taxa in the marine sediment samples were unclassified. *Bacillus* was detected at high relative abundances in all nine enriched consortia (8.3% to 81.62%). Several species of *Bacillus*, such as *Bacillus subtilis* (Xu et al 2021), *Bacillus mojavensis* (Zhang et al 2018), and *Bacillus amyloliquefaciens* (Liu et al 2022), are known to degrade phthalate esters. In enriched consortium C10, *Bacillus* (81.6%), *Ochrobactrum* (10.2%), and *Stenotrophomonas* (5.7%) were the dominant genera (Figure 15). *Ochrobactrum* and *Stenotrophomonas* were detected only in C10, which has the highest DEHP degradation efficiency, indicating that bacteria belonging to these genera may be the key DEHP-degraders in C10. *Ochrobactrum* spp. that can degrade DBP (Wu et al 2010) and DEHP (Nshimiyimana et al 2020) have been reported. Wu et al (2022) isolated a *Stenotrophomonas acidaminiphila* strain capable of degrading DBP from pyrethroid pesticide-contaminated soil.

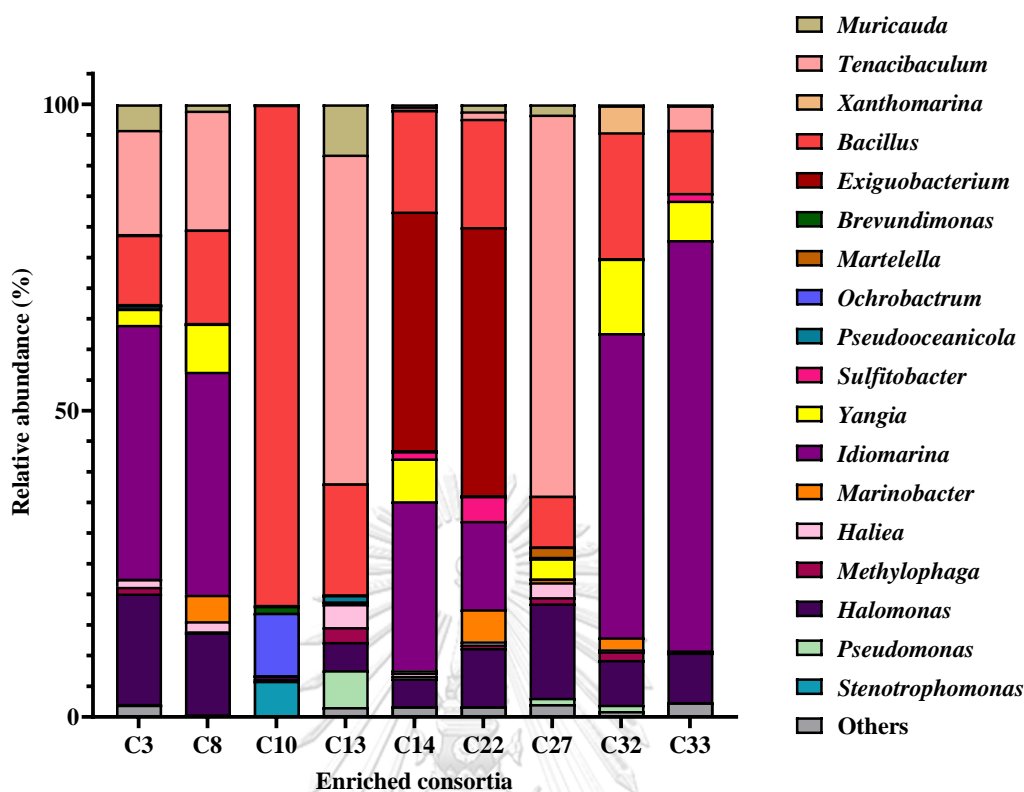


Figure 15 Bacterial communities of the enriched bacterial consortia at the genus level.

Exiguobacterium (43.8%), *Bacillus* (17.7%), and *Idiomarina* (14.4%) were the most abundant genera in C22, while in C33, *Idiomarina* (67%), *Bacillus* (10.3%), and *Halomonas* (8.1%) were dominant. Yastrebova et al (2019) isolated phthalate-degrading *Idiomarina* spp. and *Halomonas* spp. from sediment and soil in a salt mining area. Although *Exiguobacterium* spp. have not been reported for phthalate ester degradation, they are known to degrade various xenobiotics such as dyes, aromatic hydrocarbons, and phenolic and heterocyclic compounds (Kasana & Pandey 2018). *Tenacibaculum* and *Muricauda* are some of the other major genera in the enriched consortia. Members of *Tenacibaculum*, a marine bacterial genus, can degrade polyesters (Sekiguchi et al 2011) and dyes (Yang et al 2019), while

Muricauda is a common marine bacterium that has been identified as a critical member of a crude-oil degrading bacterial consortium (Uribe-Flores et al 2019).

4.1.4.2 Bacterial communities of C10, C22, and C33 during degradation of the PAE mixture

As shown in Figure 16a, at the class level, during degradation of the PAE mixture by C10, Gammaproteobacteria was the most abundant up to Day 4 (40%), while Actinobacteria relative abundance was the highest on Day 6, increasing from 30.9% and 35.4% on days 2 and 4, respectively, to 60.8% on Day 6. Alphaproteobacteria was the third most abundant class (19.4, 20.1, and 8.3% on days 2, 4, and 6, respectively). At the genus level (Figure 16b), *Glutamicibacter* relative abundance increased only slightly from Day 2 (30.8%) to Day 4 (35.4%), but increased sharply to 60.7% on Day 6. Meanwhile, *Ochrobactrum* population was almost stable from Day 2 (17.9) to Day 6 (18.7%), but reduced to 7.5% on Day 8. The PAE degradation activity of C10 was at its peak up to Day 4, during which DMP and DEP were completely degraded, while 75% and 53% of DBP and DEHP, respectively, were degraded. *Pseudomonas* (10.8% - 15.4%) was also a major genus in C10 throughout the PAE degradation period, while *Stenotrophomonas* relative abundance showed only slight changes (2.8% - 3.6%). It is conceivable that *Glutamicibacter* and *Ochrobactrum* rapidly degraded lower-molecular-weight PAEs such as DEP, DMP, and DBP during the first 4 d. The increase in *Glutamicibacter* on Day 6 could be due to the generation of PAE degradation products. Wang et al (2021d) reported that *Glutamicibacter nicotianae* ZM05 could degrade short-chain PAEs such as DBP, DEP, and DMP. Further, strain ZM05 could utilize PAE metabolites, monoethyl phthalate, monobutyl phthalate, phthalic acid, and

protocatechuic acid, as carbon source. The bacterial community of C10 on Day 4 of the degradation of the PAE mixture was studied using long-read 16S rRNA gene amplicon sequencing as well (Table 8). Unlike short-read 16S rRNA gene amplicon sequencing (simply referred to as 16S rRNA gene amplicon sequencing here), long-read 16S rRNA gene amplicon sequencing allows for reliable bacterial taxonomic classification up to the species level.



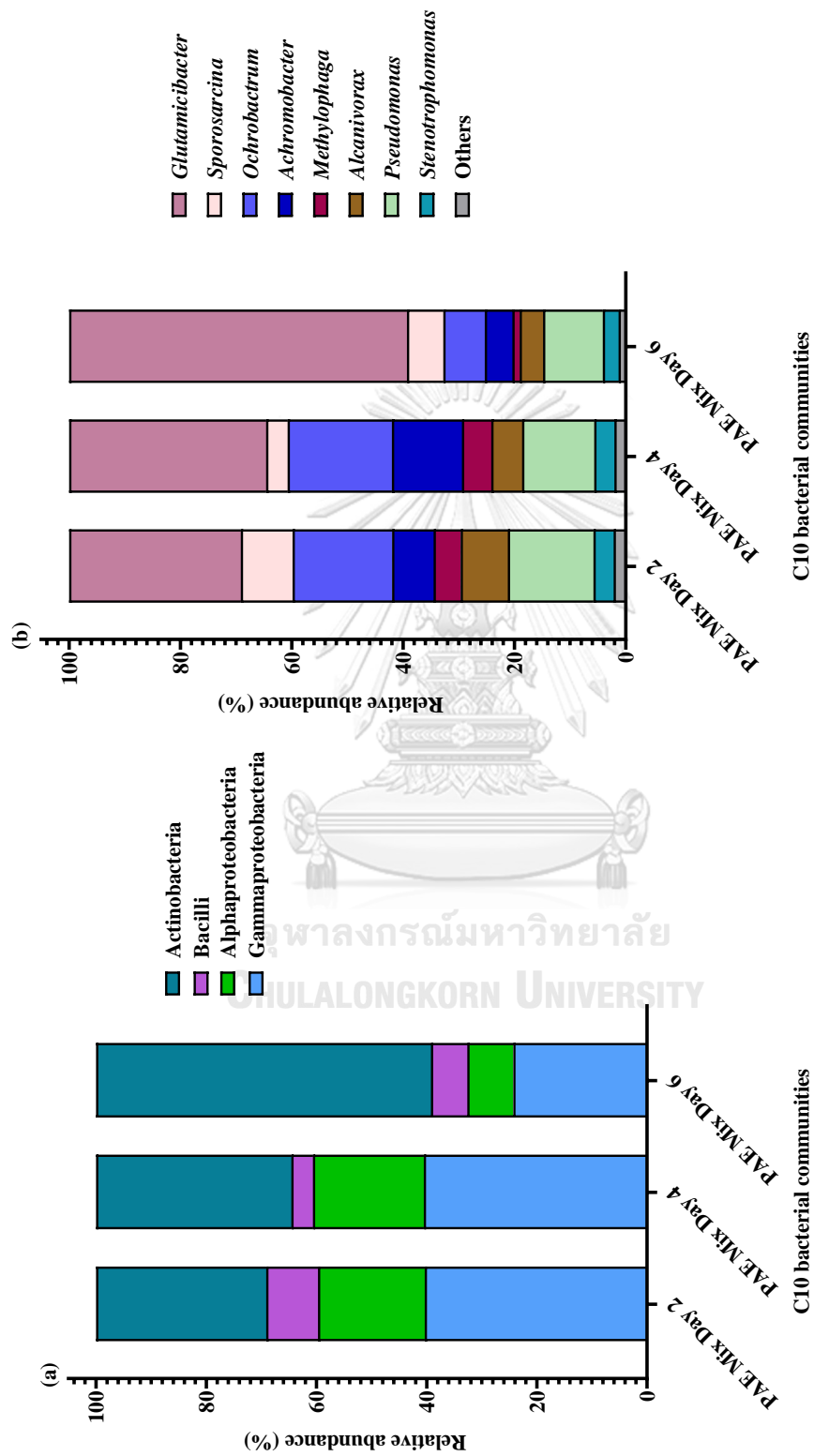


Figure 16 Bacterial communities of C10 on days 2, 4, and 6 of the degradation of a mixture of DEHP, DBP, DEP, and DMP at the class level (a) and the genus level (b).

Table 8 Taxonomic classification of the bacterial community of C10 on Day 4 of degradation of the PAE mixture based on long-read 16S rRNA gene amplicon sequencing.

Taxonomic classification	Relative abundance (%)
<i>Glutamicibacter nicotianae</i>	38.6
<i>Pseudomonas stutzeri</i>	28.7
<i>Brucella intermedia</i>	5.0
<i>Sporosarcina saromensis</i>	5.0
<i>Brucella pseudintermedia</i>	5.0
<i>Alcanivorax pacificus</i>	4.0
<i>Methylophaga nitratireducenticrescens</i>	3.5
<i>Pseudomonas</i> sp.	2.0
<i>Achromobacter veterisilvae</i>	1.5
<i>Achromobacter xylooxidans</i>	1.5
<i>Microbacterium esteraromaticum</i>	1.5
<i>Glutamicibacter halophytocola</i>	1.0
<i>Stenotrophomonas acidaminiphila</i>	1.0
<i>Achromobacter pulmonis</i>	1.0
<i>Microbacterium paraoxydans</i>	0.5
<i>Methylophaga muralis</i>	0.5

During degradation of the PAE mixture by C22, Gammaproteobacteria and Bacilli were the dominant bacterial classes (Figure 17a). The relative abundance of Gammaproteobacteria increased from 37.2% on Day 2 to 82.9% on Day 8, while that of Bacilli decreased from 60.6% on Day 2 to 10.7% on Day 8. At the genus level, *Bacillus*, *Exiguobacterium*, *Alcaligenes*, and *Stenotrophomonas* were the major genera in C22 during degradation of PAE mixture (Figure 17b). *Bacillus* relative abundance was the highest on Day 2 during active degradation of all four PAEs, while *Stenotrophomonas* abundance changed only slightly during active DEHP degradation by C22 on Day 2 (22.25%), Day 4 (22.85%), and Day 6 (30.42%). *Alcaligenes* relative abundance increased sharply from 14.6% – 32.8% on Day 2 to Day 6 to 71.4% on Day 8, when all the other PAEs in the mixture except DEHP (remaining concentration: 21 mg/L) were completely degraded. It is possible that, in C22, *Alcaligenes* spp. utilize the PAE degradation products generated. *Alcaligenes* sp. has been reported to possess the gene for protocatechuate 3,4-dioxygenase (Tian et al. 2017), which catalyzes the cleavage of protocatechuate.

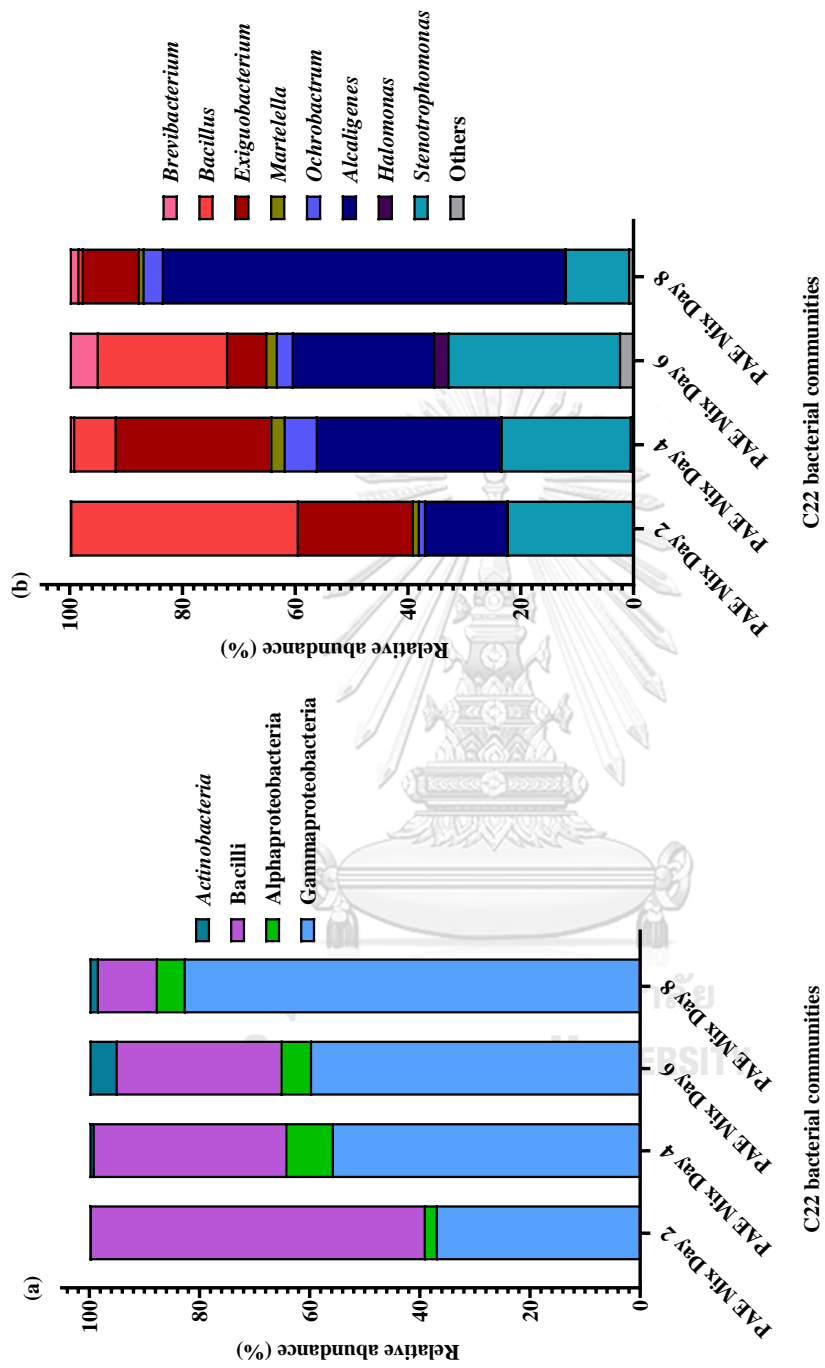


Figure 17 Bacterial communities of C22 on days 2, 4, 6, and 8 of the degradation of a mixture of DEHP, DBP, DEP, and DMP at the class level (a) and the genus level (b).

In C33, during degradation of the PAE mixture, relative abundance of Gammaproteobacteria decreased from 68.9% on Day 2 to 47.33% on Day 8, while that of Bacteroidia increased from 14.62% to 23.39% (Figure 18a). Alphaproteobacteria was also a major bacterial class in C33 during the degradation period (7% – 24.8%). As shown in Figure 18b, *Halomonas* was the major genera on days 2, 4, and 6 (37.2, 28.9, and 40.8%), while *Tenacibaculum* changed slightly throughout the degradation period (11.8 – 19.5%). Similarly, *Stenotrophomonas* relative abundance changed only slightly till Day 6 (6 – 9.2%) but increased to 16.2% on Day 8. Although only 40% DEHP degradation by C33 was observed during the first 6 d, 21% degradation could be achieved within the subsequent 2 d. This suggest that *Stenotrophomonas* spp. in C33 may be good DEHP degraders. Table 9 lists the alpha diversity indices of the bacterial communities of C10, C22, and C33 during degradation of the PAE mixture, while the principal coordinate analysis plot in Figure 19 depicts the differences amongst the bacterial communities based on weighted UniFrac distances.

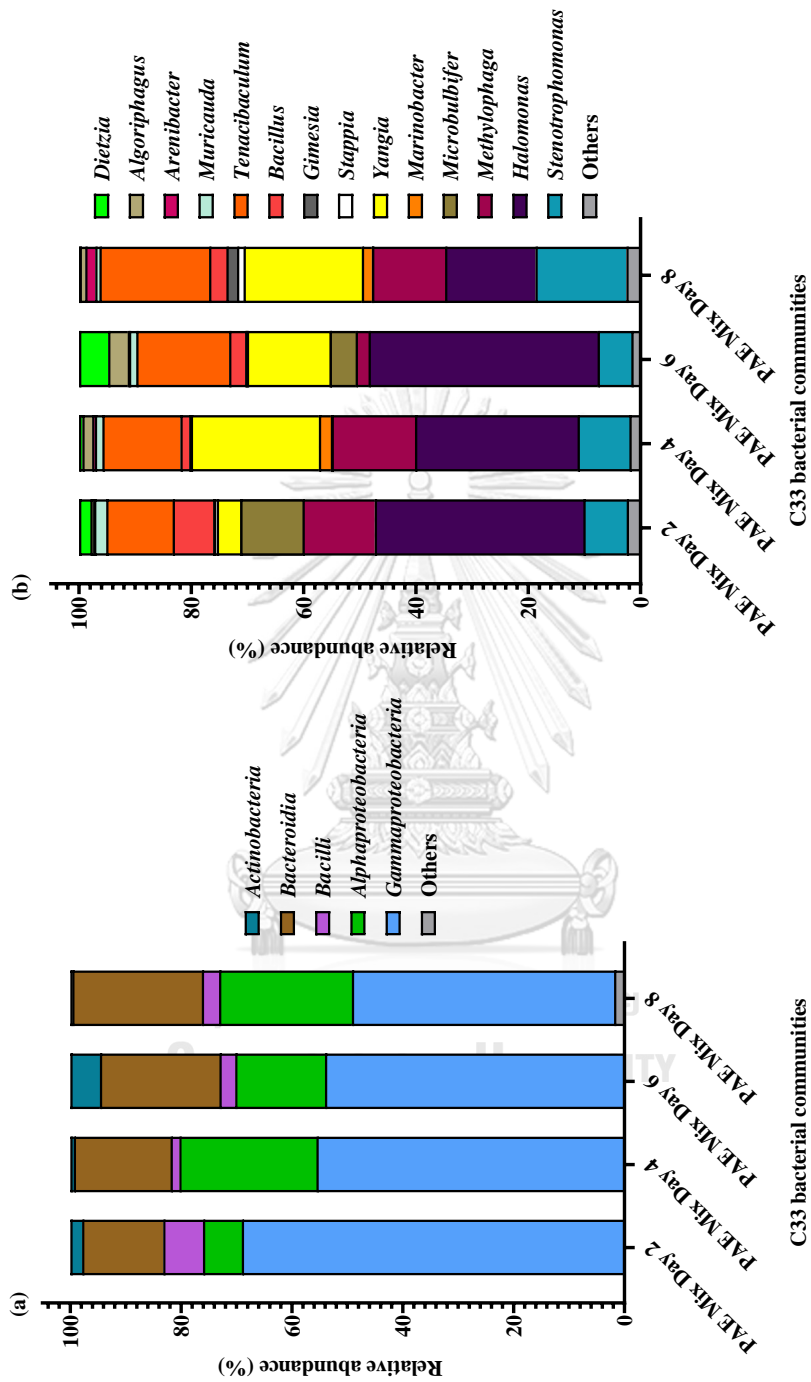


Figure 18 Bacterial communities of C33 on days 2, 4, 6, and 8 of the degradation of a mixture of DEHP, DBP, DEP, and DMP at the class level (a) and the genus level (b).

Table 9 Alpha diversity indices (Shannon index, Faith's phylogenetic diversity, and observed OTUs) of C10, C22, and C33 bacterial communities in the presence of different substrates.

Sample	Shannon index	Faith's PD	Observed OTUs
C10 Day 2 PAE Mixture	3.2	3.5	32
C10 Day 4 PAE Mixture	3.1	3.2	28
C10 Day 6 PAE Mixture	2.3	3.5	31.2
C10 DBP	3.4	3.6	32.3
C10 DEP	2.7	3.3	34.9
C10 DMP	3	3	29.9
C10 EHA	2.5	6.3	24.7
C10 MEHP	2.4	5.6	22
C10 PA	2.2	2.1	22.9
C10 PCA	1.8	2.2	24.6
C22 Day 2 PAE Mixture	2.1	3.1	23.2
C22 Day 4 PAE Mixture	2.5	6	35.6
C22 Day 6 PAE Mixture	3	2.9	34.9
C22 Day 8 PAE Mixture	1.5	2.5	26.4
C33 Day 2 PAE Mixture	3.1	8	32.2
C33 Day 4 PAE Mixture	3	5.1	33.3
C33 Day 6 PAE Mixture	2.9	5.1	32.6
C33 Day 8 PAE Mixture	3.3	5.2	35.6

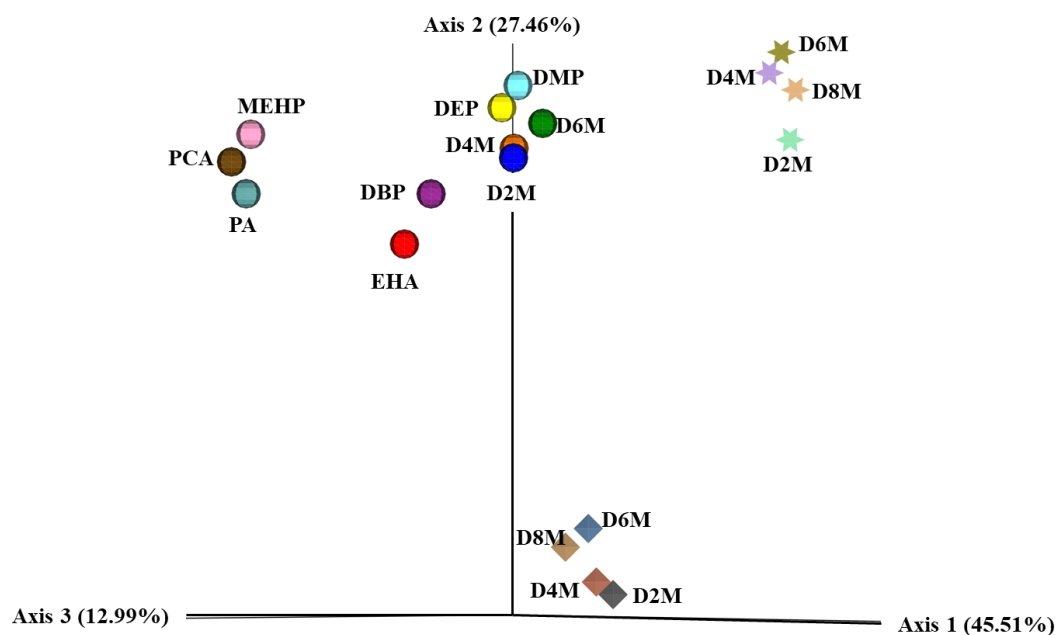


Figure 19 Principal coordinate analysis plot of beta diversity based on a weighted UniFrac of the bacterial communities of C10 (circle), C22 (diamond), and C33 (star) in the presence of different substrates. D2M, D4M, D6M, and D8M indicate bacterial communities on days 2, 4, 6, and 8 of the degradation of a mixture of DEHP, DBP, DEP, and DMP.

4.1.4.3 Bacterial communities of C10 during degradation of different PAEs and growth on DEHP intermediates.

As shown in Figure 20a, Actinobacteria (40.7% and 46.6%), Gammaproteobacteria (32.4% and 25.01%), and Alphaproteobacteria (21.7% and 19.8%) were the dominant bacterial classes of C10 during the degradation of DMP and DEP, respectively. Meanwhile, during the degradation of DBP and DEHP by C10, relative abundances of Bacilli (11.6 and 81.9%, respectively), Alphaproteobacteria (39.2 and 11.6%), and Gammaproteobacteria (38 and 6.5%) were the highest. At the genus level (Figure 20b), *Bacillus* (81.6%), *Ochrobactrum* (10.2%), and *Stenotrophomonas* (5.7%) were dominant during DEHP degradation, while *Ochrobactrum* (34.6%), *Pseudomonas* (19.1%), and *Sporosarcina* (11.3%) were the major genera of C10 during DBP degradation. During the degradation of DEP and DMP the major genera were *Glutamicibacter* (46.4%), *Ochrobactrum* (18.2%), and *Pseudomonas* (13.8%); and *Glutamicibacter* (40.5%), *Ochrobactrum* (19.8%), and *Methylophaga* (12.1%), respectively.

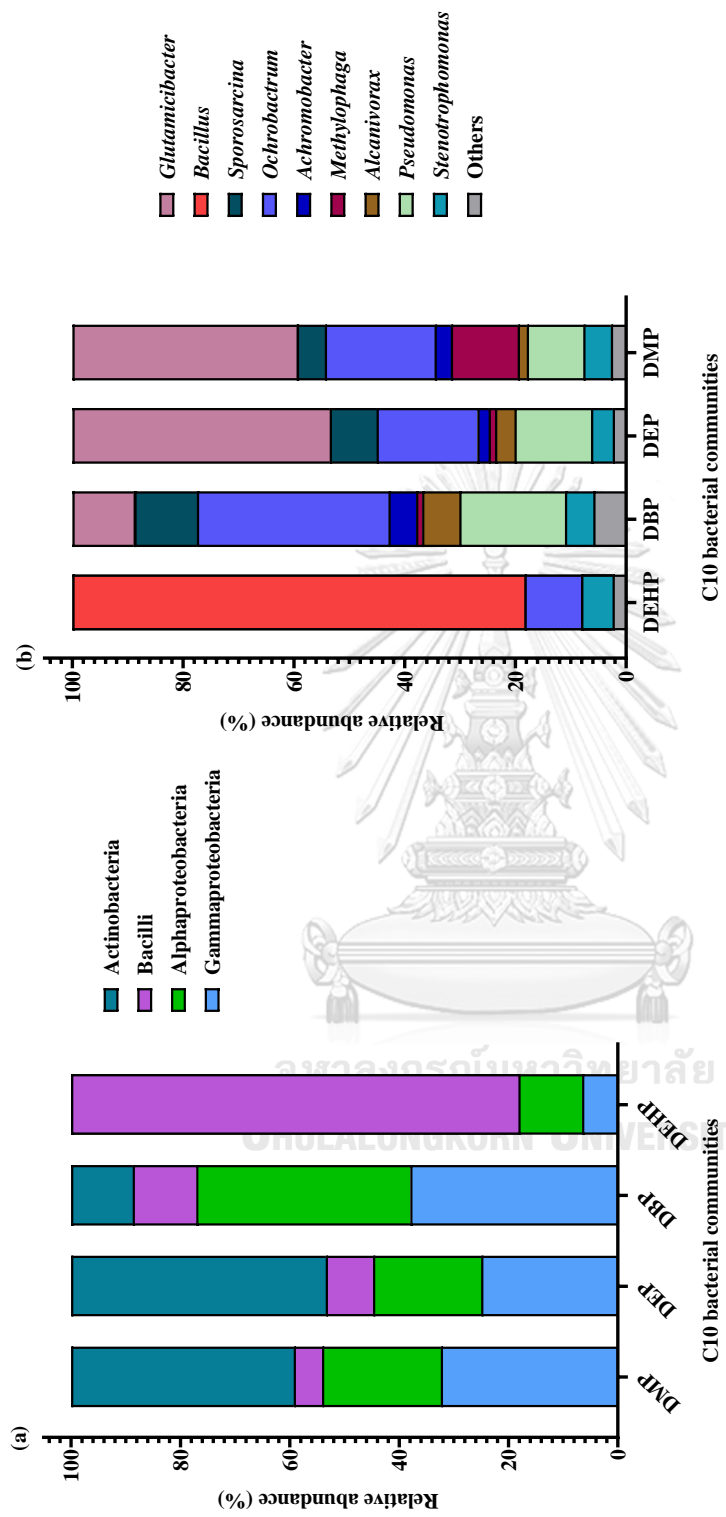


Figure 20 Bacterial communities of C10 on Day 4 of DEHP, DBP, DEP, and DMP degradation at the class level (a) and the genus level (b).

Changes in the bacterial community of C10 induced by exposure to four commonly reported DEHP intermediates was also monitored (Figure 21). Actinobacteria (49.3, 12.9, and 15%), Gammaproteobacteria (17.7, 12.6, 9.3%) and Alphaproteobacteria (17.7, 68.9, and 71.3%) were the dominant bacterial classes of C10 cultured with 2-ethylhexanol, phthalic acid, and protocatechuic acid, respectively, as the sole source of carbon. Meanwhile, in C10 cultured with MEHP as the sole carbon source, Alphaproteobacteria (52.8%), Actinobacteria (33.2%), and Bacilli (12.8%) were the major classes. Interestingly, in C10 cultured with the DEHP intermediates, some bacterial genera that were not detected (or present at very low levels) during degradation of PAEs, such as *Brevibacterium* and *Microbacterium* were observed at increased abundances (Figure 21b). *Ochrobactrum* (52.5%), *Brevibacterium* (33.1%), and *Bacillus* (12.6%) were the dominant genera of C10 cultured with MEHP, while C10 cultured with 2-ethylhexanol was primarily comprised of *Brevibacterium* (46.8%), *Achromobacter* (17.4%), and *Ochrobactrum* (15%). Furthermore, *Ochrobactrum*, *Brevibacterium*, and *Achromobacter* were the major genera of C10 cultured with phthalic acid (65.5, 12.3, and 8.9%, respectively) and protocatechuic acid (69.6, 14.6, and 6%, respectively) as the sole source of carbon. It is worth noting that the highest relative abundance of *Microbacterium* and *Sporosarcina* were observed in the presence of 2-ethylhexanol.

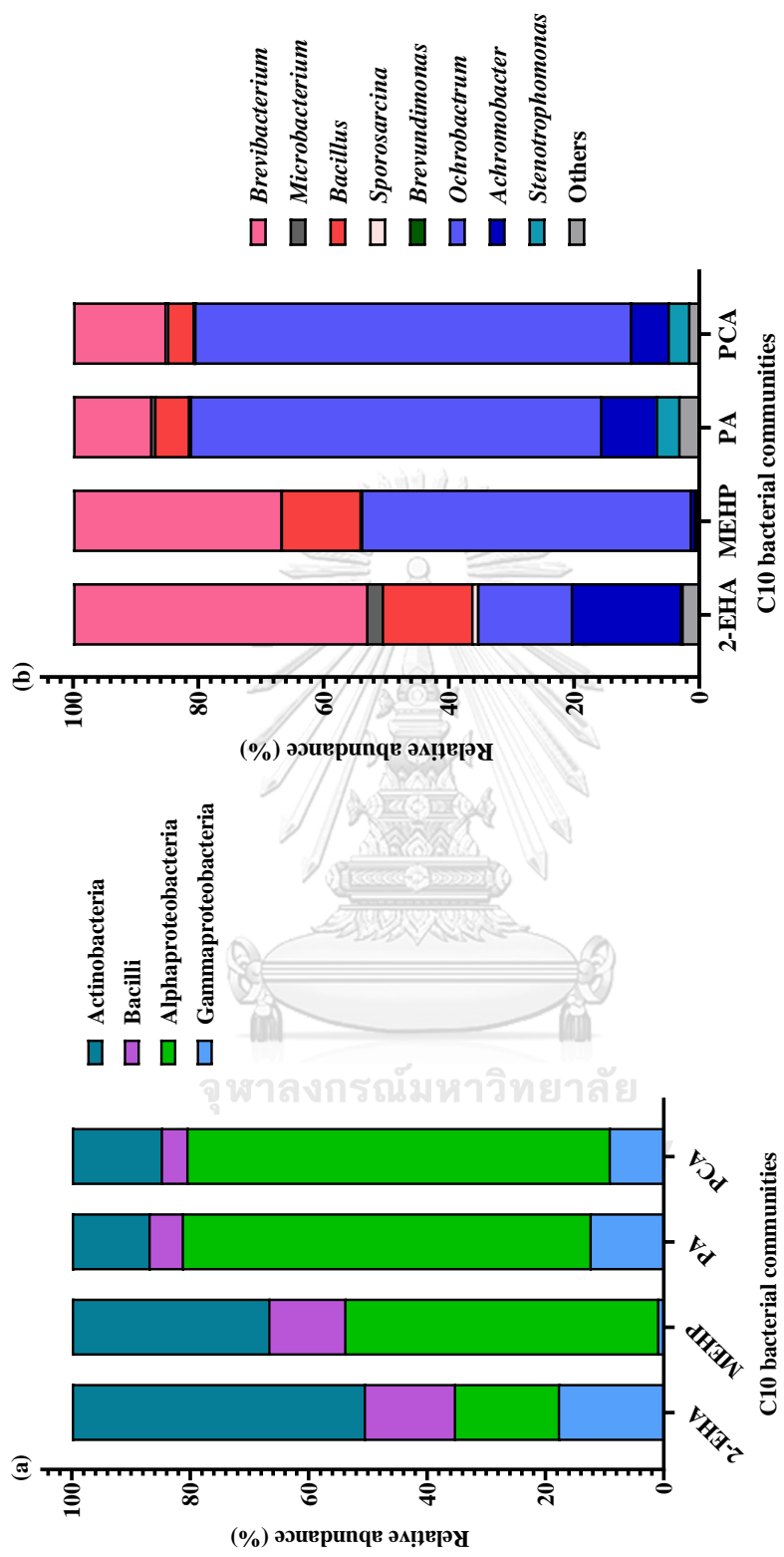


Figure 21 Bacterial communities of C10 on Day 4 of growth on MEHP, 2-ethylhexanol (2-EHA), phthalic acid (PA), and protocatechuic acid (PCA) at the class level (a) and the genus level (b).

It is important to acknowledge that not all the bacterial taxa identified must be directly involved in the degradation of PAEs and/or their intermediates. Some of the bacterial members may supply nutrients essential for the functions of the bacterial members and/or confer interactions that ensure the stability of the bacterial community (Bai et al 2020). Another possible scenario is that some bacterial members are “cheaters” and not involved in biodegradation (Kang et al 2019). Furthermore, bacterial taxa present in low numbers have been reported to surprisingly contribute greatly to the activity of the bacterial community (Meng et al 2022). As shown in Table 9, alpha diversity indices for C10 in the presence of DEHP intermediates are lower than those for C10 in the presence of PAEs (both single type and mixture). This may indicate that fewer bacterial members are capable of degrading DEHP intermediates. The beta diversity principal coordinate analysis plot based on weighted UniFrac distances of the bacterial communities of C10 during degradation of the different PAEs and growth on DEHP intermediates is shown in Figure 19.

4.1.5 Changes in the predicted metabolic potential of the bacterial communities of C10 induced by PAEs and DEHP intermediates

The 16S rRNA gene amplicon sequencing data obtained in Phase I was used to predict shifts in the metabolic potential of C10 using Tax4Fun2 (Wemheuer et al 2020) against the Kyoto encyclopedia of genes and genomes (KEGG) orthology database (Kanehisa et al 2015). This database assigns functions/pathways at levels 1 to 3, becoming more specific as one moves through the levels. Categories of functions at level 1 are Metabolism, Genetic information processing, Environmental information processing, Cellular processes, Organismal systems, Human diseases, and Drug development. At level 2, each of these broad pathways are divided into more specific functions/pathways. For instance, at level 2, the Metabolism function can be further categorized into Carbohydrate metabolism, Energy metabolism, Xenobiotics degradation and metabolism, and so on.

Global and overview maps was the most abundant KEGG level 2 function (36.1 to 38.1%) assigned to the bacterial communities of C10 during degradation of the different PAEs (separately and as a mixture) and when cultured with the four DEHP intermediates as the sole source of carbon. The functions assigned at level 3 under Global and overview maps is illustrated in Figure 22. The subsequent top nineteen metabolic pathways (Global and overview maps has been excluded so that differences in the relative abundances of the other pathways are clearly visible) are shown in Figure 23. Carbohydrate metabolism (8.7 – 9.8%) and Amino acid metabolism (7.9 – 9.5%) were the second and third most abundant KEGG level 2 pathways, respectively. The Amino acid metabolism pathway could be partly related to the production of enzymes involved in the degradation of PAEs and DEHP

intermediates (Huang et al 2021), such as phthalate hydrolases and phthalate dioxygenases involved in the degradation of PAEs and their intermediates. It is clear from the heatmap in Figure 23, that the Amino acid metabolism pathway is more abundant in C10 cultured with the four DEHP intermediates as the sole source of carbon, than in C10 during PAE degradation. Conversely, the signal transduction pathway is more abundant in C10 during PAE degradation than in the presence of the four DEHP intermediates, which could be attributable to higher interactions within the C10 bacterial community during the degradation of more complex substrates (PAEs). Furthermore, the Membrane transport pathway was another major function assigned to the bacterial communities of C10, with slightly higher abundance of this pathway in the bacterial communities of C10 cultured with phthalic acid and protocatechuic acid as the sole source of carbon. These findings suggest that bacterial community functions change in response to the type of substrate. Nevertheless, the functions discussed in this section are predictions based on 16S rRNA gene amplicon sequencing. Therefore, more studies, such as meta-transcriptomic analyses, must be conducted to confirm the actual functions of the C10 bacterial community in the presence of different substrates. The functions assigned to the C10 bacterial communities under Xenobiotics degradation and metabolism, at KEGG level 3 are shown in Figure 24. Benzoate degradation and chloroalkane and chloroalkene degradation were the most dominant sub-pathways assigned to C10 under Xenobiotics degradation and metabolism.

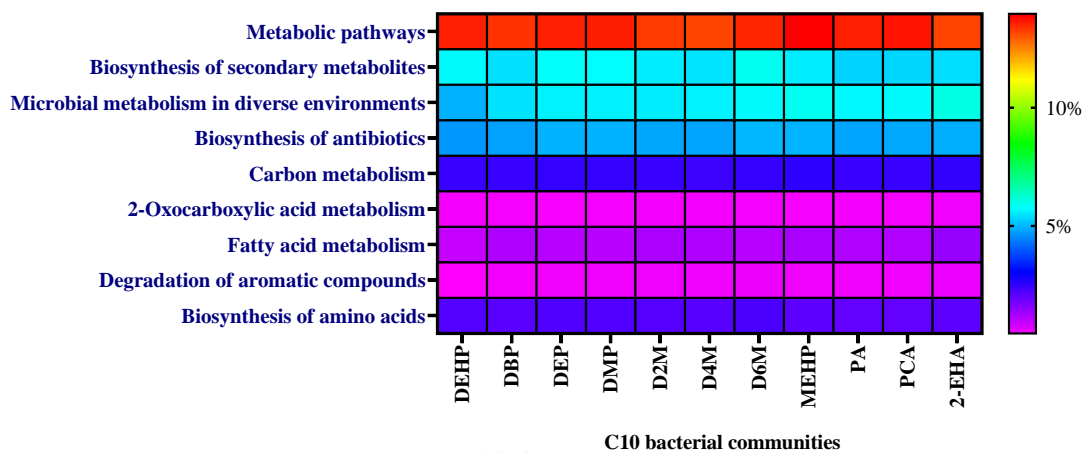


Figure 22 Level 3 KEGG functions under Global and overview maps assigned to the bacterial communities of C10 during degradation of DEHP, DBP, DEP, and DMP, on days 2, 4, and 6 of the degradation of the PAE mixture (D2M, D4M, and D6M, respectively), and cultured with MEHP, 2-ethylhexanol (2-EHA), phthalic acid (PA), and protocatechuic acid (PCA) as sole source of carbon.

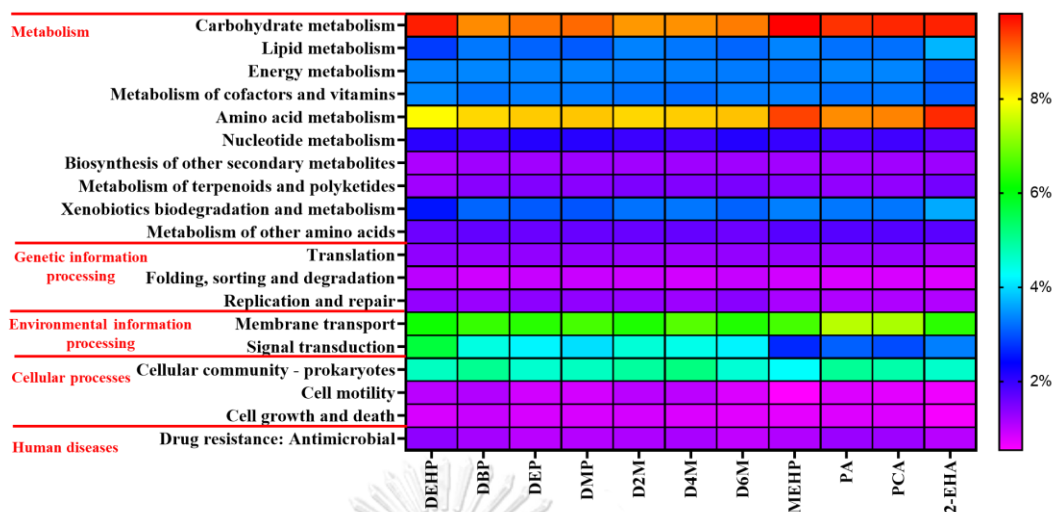


Figure 23 Top nineteen KEGG level pathways (excluding Global and overview maps) assigned to the bacterial communities of C10 during degradation of DEHP, DBP, DEP, and DMP, on days 2, 4, and 6 of the degradation of the PAE mixture (D2M, D4M, and D6M, respectively), and cultured with MEHP, 2-ethylhexanol (2-EHA), phthalic acid (PA), and protocatechuic acid (PCA) as sole source of carbon.

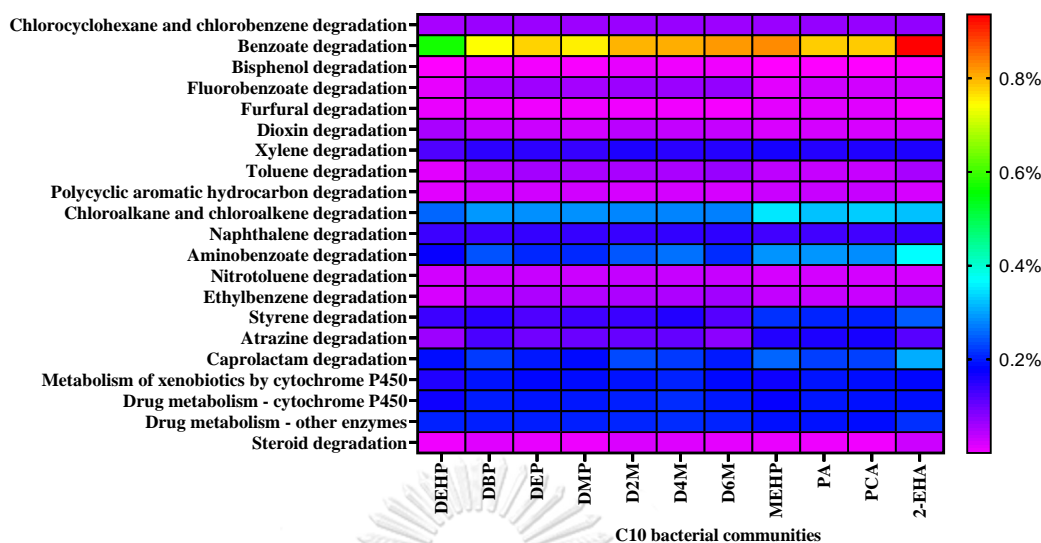


Figure 24 Level 3 KEGG functions under Xenobiotics degradation and metabolism assigned to the bacterial communities of C10 during degradation of DEHP, DBP, DEP, and DMP, on days 2, 4, and 6 of the degradation of the PAE mixture (D2M, D4M, and D6M, respectively), and cultured with MEHP, 2-ethylhexanol (2-EHA), phthalic acid (PA), and protocatechuic acid (PCA) as sole source of carbon.

4.1.6 Co-occurrence patterns of C10 at the genus level and prediction of key degraders

Network-based analyses of bacterial co-occurrence patterns are increasingly being used to understand interactions within complex bacterial communities and predict key bacterial taxa (Huang et al 2021, Ishimoto et al 2021). In this study, bacterial co-occurrence patterns in C10 at the genus level was predicted using significant Pearson correlations ($p < 0.05$) amongst the different bacterial genera of C10. These correlations were generated using the CCREPE package on R (Schwager et al 2020). The overall bacterial network of C10 (based on bacterial community information of C10 during PAE degradation and growth on DEHP intermediates)

comprises 12 nodes and 15 edges (Figure 25a). Nodes represent bacterial genera, while the edges represent significant positive (green) and negative (red) Pearson correlations amongst the bacterial genera. Figure 25b illustrates the bacterial interactions predicted in C10 cultured with DEHP intermediates, while Figure 25c displays the network of bacterial interactions predicted in C10 during degradation of PAEs (separately and as a mixture). Network and node statistics of the bacterial network in Figure 25a are detailed in Tables 10 and 11, respectively.



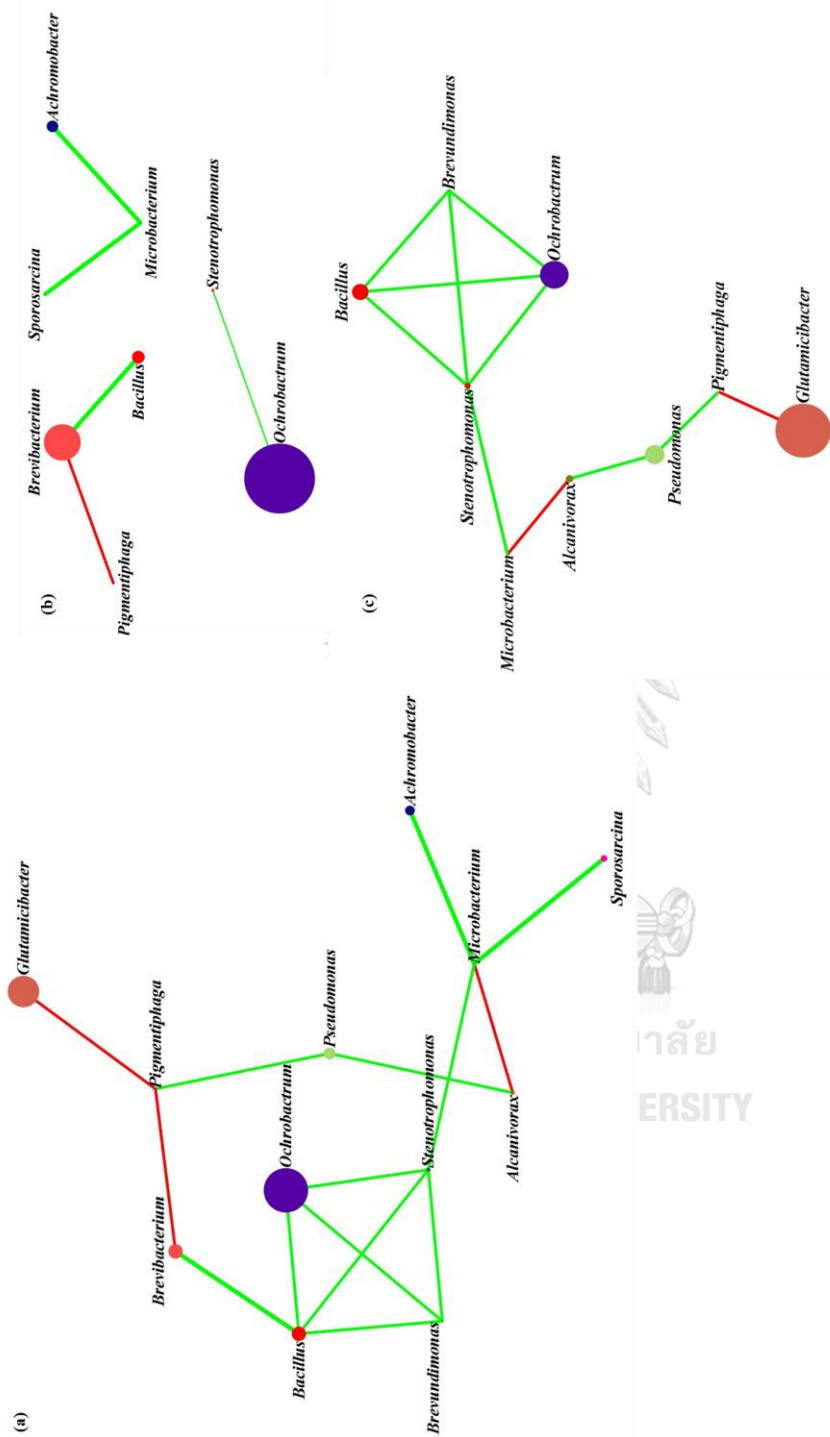


Figure 25 Predicted co-occurrence patterns of C10 bacterial community members at the genus level: (a) overall network in the presence of DEHP intermediates and PAEs, (b) subnetwork in the presence of DEHP intermediates, and (c) subnetwork in the presence of DEHP, DEP, and DMP (separately and as a mixture).

Table 10 Co-occurrence network parameters of C10 at the genus level observed in the presence of DEHP, DBP, DEP, and DMP (separately and as a mixture) and MEHP, 2-ethylhexanol, phthalic acid, and protocatechuic acid).

Parameter	Value
Number of nodes	12
Number of edges	15
Average number of neighbors	2.5
Network diameter	5
Characteristic path length	2.485
Clustering coefficient	0.250
Network density	0.227
Network heterogeneity	0.447
Network centralization	0.164

Table 11 Node parameters of the co-occurrence network of C10 at the genus level in the presence of DEHP, DBP, DEP, and DMP (separately and as a mixture) and MEHP, 2-ethylhexanol, phthalic acid, and protocatechuic acid.

Node or Taxa	Degree	Betweenness Centrality	Closeness Centrality	Clustering Coefficient	Eccentricity
<i>Achromobacter</i>	1	0	0.34375	0	5
<i>Microbacterium</i>	4	0.454545	0.5	0	4
<i>Bacillus</i>	4	0.236364	0.478261	0.5	3
<i>Brevibacterium</i>	2	0.181818	0.423077	0	4
<i>Pigmentiphaga</i>	3	0.254545	0.407407	0	4
<i>Sporosarcina</i>	1	0	0.34375	0	5
<i>Ochrobactrum</i>	3	0	0.407407	1	4

<i>Stenotrophomonas</i>	4	0.290909	0.5	0.5	4
<i>Alcanivorax</i>	2	0.2	0.44	0	3
<i>Pseudomonas</i>	2	0.163636	0.392857	0	4
<i>Brevundimonas</i>	3	0	0.407407	1	4
<i>Glutamicibacter</i>	1	0	0.297297	0	5

More than half of the nodes belong to the phylum Proteobacteria. Bacteria belonging to this phylum are reported to be associated with tolerance to and/or degradation of PAEs (Huang et al 2021, Zhu et al 2020). As shown in Table 11, *Bacillus*, *Stenotrophomonas*, and *Microbacterium* have the highest degree (number of predicted interactions with other genera in the community) among the nodes in the network, indicating that bacteria from these genera could be the key degraders in C10 (Banerjee et al 2018, Yan et al 2019). Positive interactions were predicted between *Ochrobactrum* and *Stenotrophomonas* and between *Brevibacterium* and *Bacillus* in C10 cultured with the DEHP intermediates as the sole carbon source. Meanwhile, *Microbacterium* was predicted to be positively correlated with *Sporosarcina* and *Achromobacter*. On the other hand, positive interactions were predicted amongst *Ochrobactrum*, *Bacillus*, *Stenotrophomonas*, and *Brevundimonas* in C10 during PAE degradation. Wang et al (2021c) used a network-based approach to identify the cooperators of a DBP-degrading bacterium, *Arthrobacter nicotianae* ZM05, which showed inhibited DBP degradation activity at low pH. A predicted cooperator, *Pseudomonas aeruginosa* ZM03, was isolated. It was observed that co-cultures of ZM05 and ZM03 enhanced DBP degradation even at low pH, thus proving the predicted cooperative interaction between the two strains. Therefore, the bacterial

interactions predicted in this study and the information on predicted key degraders could be used to guide the creation of simpler defined bacterial consortia capable of efficient PAE degradation.

4.2 Phase 2

4.2.1 Selective isolation of bacterial strains in C10 and identification of isolated bacterial stains

Twenty-one bacterial isolates were obtained from C10 using different agar media (Appendix A) for the selective isolation of the key degraders predicted via network analysis, such as *Bacillus*, *Stenotrophomonas*, and *Microbacterium*. DNA was extracted from these isolates, the 16S rRNA gene was amplified and purified and submitted for sequencing. The obtained sequences were searched against the EzBioCloud 16S database for taxonomic identification of the isolates (Table 12). Bacterial strains belonging to some of the predicted key and dominant genera observed in Phase I, such as *Bacillus*, *Stenotrophomonas*, *Ochrobactrum*, *Microbacterium*, and *Sporosarcina*, could be successfully isolated. However, some major bacterial genera observed in C10 in Phase I such as *Brevibacterium*, *Glutamicibacter*, and *Pseudomonas* could not be isolated in this study. Obtaining bacterial isolates from complex bacterial communities is a common challenge (Zhu et al 2020). This could be attributed to the lack of selective media for the target bacterial group (e.g., *Glutamicibacter*) and/or metabolic dependencies among the members of a bacterial community (Wilhelm et al 2021).

Table 12 Taxonomic identification of the bacterial isolates from C10.

Strain	Top hit bacterial strain on EzBioCloud	Accession no.	Similarity %	Variation ratio
OR01	<i>Bacillus cereus</i> ATCC 14579(T)	AE016877	100	0/1245
OR02	<i>Bacillus cereus</i> ATCC 14579(T)	AE016877	100	0/542
OR03	<i>Microbacterium esteraromaticum</i> DSM 8609(T)	Y17231	99.7	2/660
OR04	<i>Microbacterium esteraromaticum</i> DSM 8609(T)	Y17231	99.7	2/665
OR05	<i>Sporosarcina saromensis</i> HG645(T)	AB243859	100	0/659
OR06	<i>Microbacterium esteraromaticum</i> DSM 8609(T)	Y17231	99.71	2/682
OR07	<i>Sporosarcina saromensis</i> HG645(T)	AB243859	100	0/655
OR08	<i>Microbacterium paraoxydans</i> NBRC 103076(T)	BCRH01000180	99.48	3/579
OR09	<i>Microbacterium esteraromaticum</i> DSM 8609(T)	Y17231	99.7	2/656
OR10	<i>Micrococcus luteus</i> NCTC 2665(T)	CP001628	99.7	2/662
OR11	<i>Microbacterium esteraromaticum</i> DSM 8609(T)	Y17231	99.67	2/601
OR12	<i>Ochrobactrum intermedium</i>	NR113812	99.93	1/1369

NBRC 15820				
OR13	<i>Stenotrophomonas acidaminiphila</i> SUNE0	CP019797	100	0/1252
OR14	<i>Microbacterium paraoxydans</i> NBRC 103076(T)	BCRH01000180	100	0/1324
OR15	<i>Stenotrophomonas acidaminiphila</i> SUNE0	CP019797	100	0/1365
OR16	<i>Microbacterium esteraromaticum</i> DSM 8609(T)	Y17231	99.78	3/1364
OR17	<i>Microbacterium esteraromaticum</i> DSM 8609(T)	Y17231	99.7	2/666
OR18	<i>Alcaligenes faecalis</i> subsp. phenolicus DSM 16503(T)	AUBT01000026	99.85	2/1371
OR19	<i>Sporosarcina saromensis</i> HG645(T)	AB243859	100	0/632
OR20	<i>Cytobacillus firmus</i> NBRC 15306(T)	BCUY01000205	99.49	7/1365
OR21	<i>Microbacterium esteraromaticum</i> DSM 8609(T)	Y17231	99.63	5/1339

4.2.2 Characterization of the bacterial isolates from C10

4.2.2.1 DEHP degradation activities of the isolates from C10

The DEHP degradation efficiencies of the twenty-one isolates from C10 (Figure 26; Table 13) and viable cell counts of the isolates on Day 0 and Day 8 of DEHP degradation (Figure 27) were investigated. Twenty-one bacterial strains with distinct colony morphologies were isolated and identified from enriched consortium

C10. *Microbacterium* sp. OR21 was identified to be the best DEHP degrader among the isolates, achieving 84.5% degradation of 100 mg/L DEHP in 8 d. This is interesting because *Microbacterium* spp. were detected at very low levels in C10 during degradation of the four PAEs (separately and as a mixture). Similarly, although *Stenotrophomonas* spp. accounted for only 5.7% of the C10 bacterial community during DEHP degradation, *Stenotrophomonas acidaminiphila* OR13 was identified to be one of the best DEHP degraders (83.68%) among the isolates. It could be that growth of *Stenotrophomonas* spp. and *Microbacterium* spp. in C10 is slower than that of the more dominant bacterial genera such as *Bacillus*, although still metabolically active (Lempp et al 2020). It is worth noting that *Stenotrophomonas acidaminiphila* was detected in C10 on Day 4 of PAE mixture degradation (Table 8) through long-read 16S rRNA gene amplicon sequencing. *Stenotrophomonas acidaminiphila* was first identified by Assih et al (2002) in a reactor treating wastewater from a terephthalic acid plant. The next best DEHP degrader was *Microbacterium* sp. OR16 (59.1% degradation of 100 mg/L DEHP in 8 d), followed by *Sporosarcina* sp. OR19 (43.4%), *Cytobacillus firmus* OR20 (40.6%), and *Alcaligenes faecalis* subsp. phenolicus OR18 (38.8%). *Stenotrophomonas acidaminiphila*, *Sporosarcina* sp., and *Cytobacillus firmus* have so far not been reported for DEHP degradation. However, a *Stenotrophomonas acidaminiphila* strain capable of degrading DBP was isolated from pyrethroid pesticide-contaminated soil by Wu et al (2022). Meanwhile, *Microbacterium* sp. J-1 isolated from landfill soil has been reported to degrade DEHP (Zhao et al 2017), while *Microbacterium* sp. USTB-Y isolated from activated sludge was reported to degrade DBP (Zhao et al 2021). Interestingly, although *Bacillus* was a major genus of C10 during DEHP degradation (Phase I), the *Bacillus* isolates

obtained in Phase II showed relatively low DEHP degradation activities. It is possible that the *Bacillus* spp. of C10 grew rapidly on the metabolites formed during DEHP degradation by the other members of the C10 bacterial community. Although not all the predicted degraders and cooperators of C10 could be isolated, it will be interesting to study if smaller consortia comprised of a few of the isolated degraders and cooperators can parallel the degradation performance of the source enriched consortium.

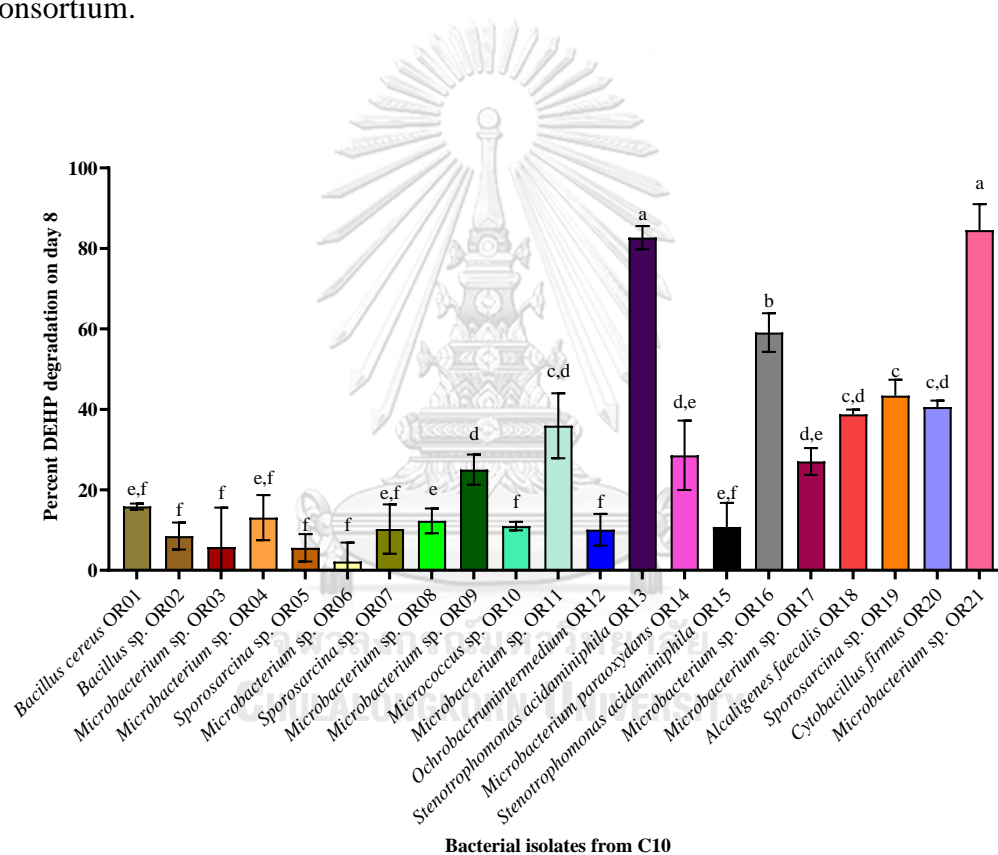


Figure 26 Percent DEHP (100 mg/L) degradation by the twenty-one isolates from C10 on Day 8. The different letters significantly different ($p < 0.05$) percent DEHP degradation values.

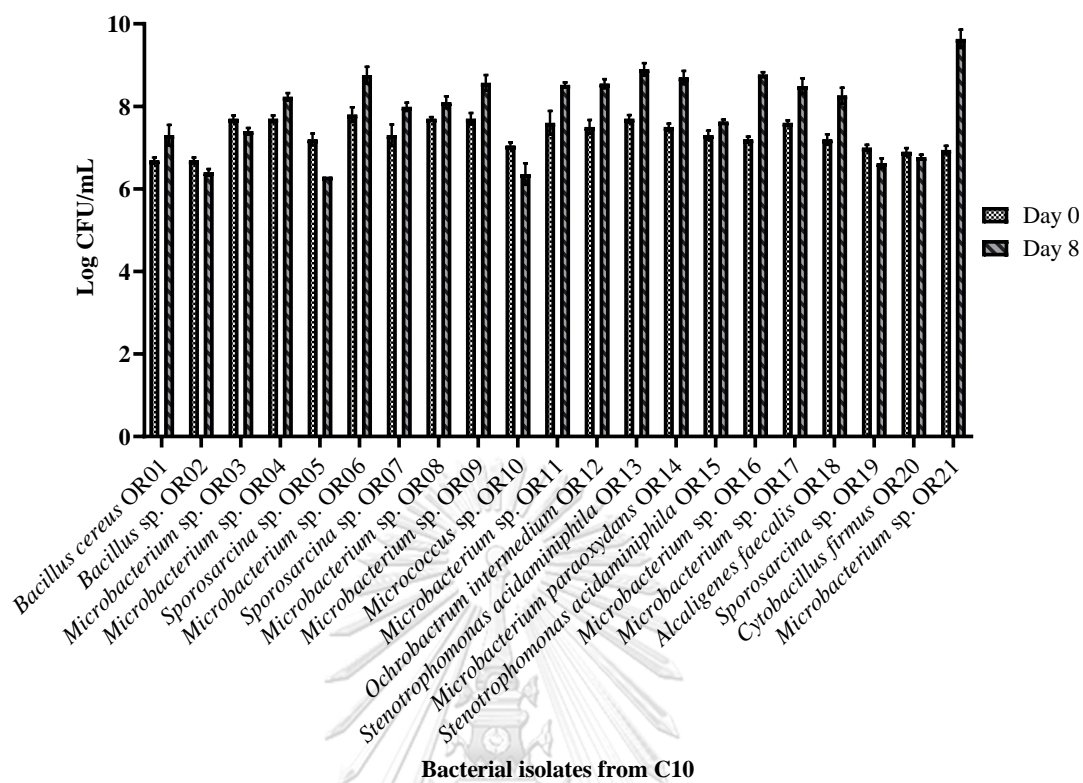


Figure 27 Viable cell counts of the bacterial isolates from C10 on Day 0 and Day 8 of DEHP degradation.

Table 13 Overview of the DEHP degradation activities, growth characteristics and oil displacement abilities of the isolates from C10.

Strain/MSCU Code	Accession number	DEHP degradation %	Growth > BC	Growth ≤ BC	Oil displacement diameter (cm)
<i>Bacillus cereus</i> OR01 MSCU 1259	OM970879	15.86 ± 0.74 ^{e,f}	DEHP, MEHP	EHA-100, PA, PCA, MBP	-
<i>Bacillus</i> sp. OR02 MSCU 1260	OM971006	8.51 ± 3.36 ^f	-	PCA	-
<i>Microbacterium</i> sp. OR03 MSCU 1261	OM971068	5.78 ± 9.79 ^f	PCA	-	-
<i>Microbacterium</i> sp. OR04 MSCU 1262	OM971707	13.09 ± 5.61 ^{e,f}	-	-	-
<i>Sporosarcina</i> sp. OR05 MSCU 1263	OM971708	5.59 ± 3.43 ^f	EHA-200	PA, MBP	2.2 ± 0.1
<i>Microbacterium</i> sp. OR06 MSCU 1264	OM971711	2.18 ± 4.71 ^f	-	EHA-200, PA, PCA, MEHP, MBP	4 ± 0.05

<i>Sporosarcina</i> sp. OR07 MSCU 1265	OM971814	10.25 ± 6.13 ^{e,f}	-	-	2.5 ± 0.05
<i>Microbacterium</i> sp. OR08 MSCU 1266	OM971850	12.29 ± 3.08 ^e	-	-	4 ± 0.1
<i>Microbacterium</i> sp. OR09 MSCU 1267	OM971884	25.02 ± 3.74 ^d	-	-	-
<i>Micrococcus</i> sp. OR10 MSCU 1268	OM972018	10.98 ± 1.04 ^f	-	EHA-100, DEHP, MBP	1.5 ± 0.1
<i>Microbacterium</i> sp. OR11 MSCU 1269	OM972660	35.92 ± 8.09 ^{c,d}	-	MBP	1.5 ± 0.2
<i>Ochrobactrum</i> <i>intermedium</i> OR12 MSCU 1270	OM972664	10.08 ± 3.93 ^f	-	All tested intermediates	2.1 ± 0.2
<i>Stenotrophomonas</i> <i>acidaminiphila</i> OR13	OM987444	82.68 ± 2.9 ^a	-	All tested intermediates	2.5 ± 0.4
<i>Microbacterium</i>	OM987443	28.58 ± 8.62 ^{d,e}	-	PA	1.6 ± 0.3

<i>paraoxydans</i> OR14 MSCU 1271	OM972734	10.77 ± 5.97 ^{e,f}	MBP	EHA, PA, PCA	5 ± 0.3
<i>Stenotrophomonas acidaminiphila</i> OR15 MSCU 1272	OM972735	59.1 ± 4.8 ^b	-	PA, MEHP	-
<i>Microbacterium</i> sp. OR16 MSCU 1273	OM972851	27.03 ± 3.33 ^{d,e}	-	-	-
<i>Microbacterium</i> sp. OR17 MSCU 1274	OM972852	38.77 ± 1.18 ^{c,d}	-	All tested intermediates	-
<i>Alcaligenes faecalis</i> OR18 MSCU 1275	OM972885	43.4 ± 3.97 ^c	-	PCA, MEHP, MBP	2.7 ± 0.05
<i>Sporosarcina</i> sp. OR19 MSCU 1276	OM972903	40.57 ± 1.62 ^{c,d}	-	All tested intermediates	-
<i>Cytobacillus firmus</i> OR20 MSCU 1277					

<i>Microbacterium</i> sp.	84.5 ± 6.5 ^a	DEHP, PCA,	1.6 ± 0.3
OR21		MEHP	
MSCU 1278			

Percent DEHP degradation is reported as the means ± standard deviation of triplicate degradation recorded on Day 8 of incubation and different letters indicate significantly ($p < 0.05$) different values. BC refers to the biological control. Growth refers to a positive value of log CFU/mL (Day 5- Day 0). Growth > BC refers to growth that is significantly ($p \leq 0.05$) higher than the BC. Growth \leq BC refers to growth that is not statistically different from that in the BC. EHA: 2-ethylhexanol; MEHP: monoethylhexyl phthalate; MBP: monobutyl phthalate; PA: phthalic acid; PCA: protocatechuic acid.

4.2.2.2 Growth of the isolates from C10 on DEHP intermediates as sole source of carbon

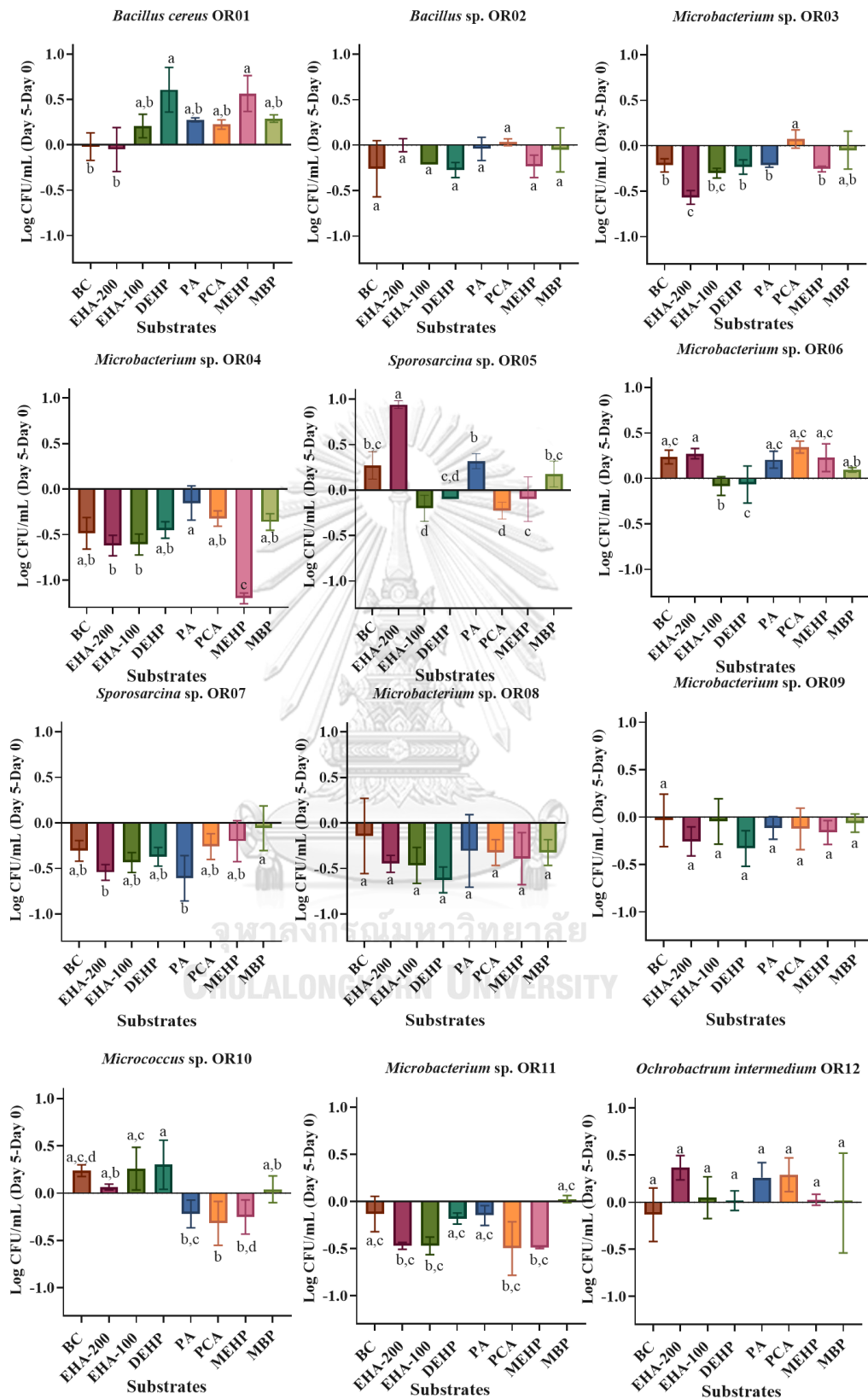
The abilities of the twenty-one isolates from C10 to grow on DEHP intermediates as sole source of carbon was studied as a preliminary screening step to shortlist isolates with the potential to degrade DEHP intermediates (Figure 28). The following DEHP intermediates were used: MEHP, 2-ethylhexanol, monobutyl phthalate, phthalic acid, and protocatechuic acid. Growth was determined by measuring the viable cell counts of the isolates cultured in modified NSW (without yeast extract) supplemented with the different intermediates as sole source of carbon on Day 0 and Day 5. A positive value of log CFU/mL on Day 5 minus log CFU/ml on Day 0 was considered as growth. Biological controls were set up for each isolate (cultured in modified NSW without the addition of any carbon source) to confirm that growth is primarily attributable to the DEHP intermediate supplied as carbon source. *Stenotrophomonas acidaminiphila* OR13 showed growth on DEHP and all the tested intermediates (except 200 mg/L of 2-ethylhexanol), although the growth observed was not significantly different ($p < 0.05$) from that in the biological control, while growth of *Stenotrophomonas acidaminiphila* OR15 on monobutyl phthalate was significantly higher than that in the biological control and the other tested substrates. Although *Ochrobactrum* spp. accounted for a major fraction of the C10 bacterial community cultured with MEHP, phthalic acid, and protocatechuic acid as carbon sources (Phase I), growth of *Ochrobactrum intermedium* OR12 on phthalic acid and protocatechuic acid was not significantly different from that in the biological control, while no growth was observed with MEHP as the carbon source. Interestingly, *Bacillus cereus* OR01 could grow significantly better on MEHP than in the biological

control, while growth of *Microbacterium* sp. OR16 on phthalic acid and MEHP as carbon sources was significantly higher than that in the biological control. Furthermore, growth of *Microbacterium* sp. OR21 was significantly better with MEHP and protocatechuic acid as carbon source than in the biological control, while its growth was significantly inhibited in the presence of phthalic acid. *Sporosarcina* sp. OR05 was the only isolate from C10 that showed significantly higher growth on 2-ethylhexanol than in the biological control. This is noteworthy as *Sporosarcina* relative abundance was enhanced when C10 was cultured in medium containing 2-ethylhexanol (Phase I). The growth results obtained in this study could be used as an indicator of the potential of the isolates to degrade the DEHP intermediates on which growth of the isolates was significantly higher than in the biological control (Wang et al 2021c).

Although some major bacterial genera of C10 such as *Brevibacterium* and *Glutamicibacter* could not be isolated, the techniques used in this study were successful in predicting and isolating key PAE-degraders of C10. Therefore, these techniques could potentially be applied with some refinements for the prediction and isolation of key pollutant-degraders from complex and dynamic bacterial communities such as those found in an enriched bacterial consortium. It is recommended that the bacterial community of an enriched consortium be monitored at different points during degradation of the target substrate and using different initial concentrations of the target substrate. The bacterial abundance data obtained can then be used to predict key members of the community during degradation by applying network analyses techniques. Selective isolation conditions and media can then be designed to target for the predicted degraders. Information about bacterial community

composition during degradation can also be used to determine appropriate time points at which bacterial culture should be collected for plating on different isolation media. The isolation of effective pollutant-degraders from bacterial consortia is a challenge (Zhu et al 2020, Wilhelm et al 2021) and, therefore, developing a streamlined strategy for the prediction and isolation of key degraders is important.





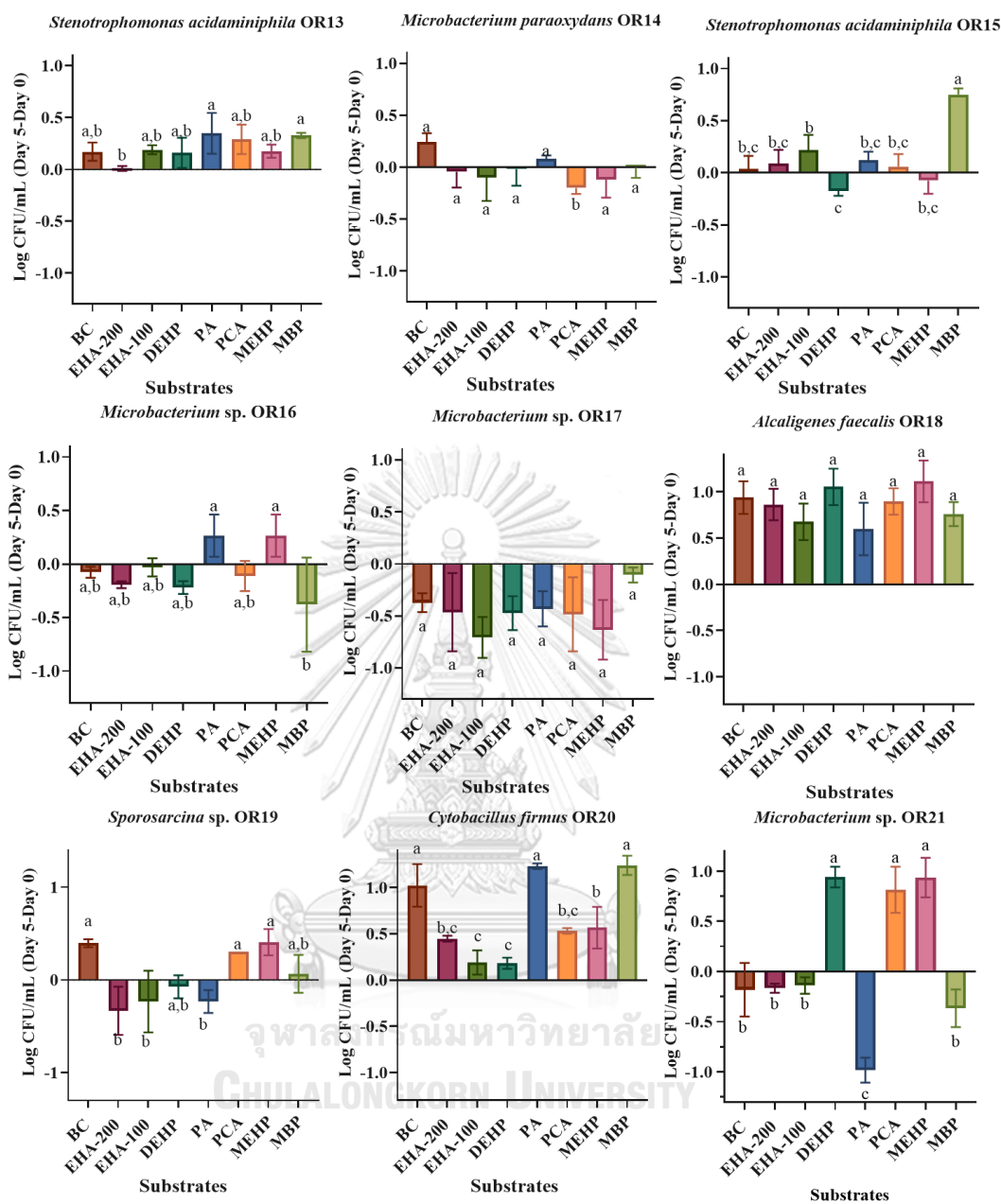


Figure 28 Growth of the bacterial isolates from C10 on 100 mg/L DEHP, MEHP, monobutyl phthalate (MBP), phthalic acid (PA), and protocatechuic acid (PCA) and 100 and 200 mg/L 2-ethylhexanol (EHA-100 and EHA-200) as the sole carbon source. Different letters indicate significantly different ($p < 0.05$) log CFU/mL (Day 5-Day 0) values.

4.2.2.3 Oil displacement activities of the isolates from C10

Qualitative screening of the biosurfactant productivity of the isolates from C10 was carried out using the oil displacement method (Khondee et al 2015). Most commonly used PAE plasticizers such as DEHP and DBP are hydrophobic as indicated by their limited water solubility and octanol-water partition coefficients (Table 1). Such PAEs tend to migrate and adsorb onto organic particulates and sediments, thereby limiting their bioavailability, which could explain their slow degradation in soil and sediment (Kastner et al 2012). Biosurfactants are surface active compounds that can enhance desorption of hydrophobic chemicals, thus facilitating microbial uptake (Ren et al 2018b) and the use of such compounds or microbes that can produce them may solve the problem of limited DEHP bioavailability in soil and sediment. Twelve of the twenty-one isolates obtained from C10 showed biosurfactant production potential (diameter of oil displacement zone \geq 1.5 cm) as shown in Table 13. The negative control (distilled water) did not cause any oil displacement, while the diameter of the oil displacement zone created by the positive control (10 mg/mL Triton X-100) was 7.5 cm.

4.2.3 Selection of isolates for defined consortia creation

Although *Stenotrophomonas acidaminiphila* OR13 was initially selected for defined consortia creation on the basis of its DEHP degradation efficiency (82.68%), this strain was lost during the course of the project. Hence, *Microbacterium* sp. OR21, with similar DEHP degradation efficiency (84.5%), was used instead. OR21 could also grow well on MEHP and protocatechuic acid as sole source of carbon, indicating that it could be able to degrade these DEHP intermediates. The next best DEHP degrader among the isolates was *Microbacterium* sp. OR16 (59.1%); this strain could

also grow on phthalic acid and MEHP as sole source of carbon, although this growth was not significantly different than that in the biological control. OR16 was, therefore, selected for defined consortia creation as it may share the burden of DEHP degradation with OR21 and may potentially be able to utilize MEHP and phthalic acid generated during DEHP degradation. Although *Sporosarcina* sp. OR05 did not show DEHP degradation activity, it could grow very well on 2-ethylhexanol. As it was the only strain among the isolates that could grow on this DEHP intermediate, it was selected for defined consortia creation in Phase III. Furthermore, in C10, *Sporosarcina* spp. were predicted to positively interact with *Microbacterium* spp. as shown in the overall bacterial co-occurrence network of C10 (Figure 22a). As *Bacillus* spp. was observed to be the dominant genera of C10 in the presence of DEHP and its intermediates, *Bacillus cereus* OR01 was also selected for defined consortia creation. Furthermore, although the DEHP degradation activity of OR01 is low (15.86%), it showed significantly higher growth with MEHP as the carbon source compared to that in the biological control. *Bacillus* spp. could also potentially exhibit indirect cooperative interactions with *Microbacterium* spp. in C10 as shown in Figure 22a.

4.3 Phase III

4.3.1 Phthalate ester degradation efficiencies of defined bacterial consortia

The selected bacterial strains (OR01, OR05, OR16, and OR21) did not exhibit any antagonistic effects against each other. Two defined bacterial consortia A01 (comprised of *Bacillus cereus* OR01, *Sporosarcina* sp. OR05, *Microbacterium* sp. OR16, and *Microbacterium* sp. OR21) and A02 (comprised of strains OR05, OR16, and OR21) were created and their PAE degradation efficiencies were investigated. Additionally, PAE degradation experiments were carried out with co-cultures of OR05 and OR21 (referred to as OR05 + OR21) in order to confirm the role of OR16 in PAE degradation. As shown in Figure 29, complete degradation DBP, DEP, and DMP by consortia A01 and A02, OR05 + OR21, and OR21 was achieved on Day 4 and hence no significant difference in degradation performance was observed. However, for DEHP, which has longer alkyl chains than the other three PAEs, the degradation efficiencies of A01, A02, and OR05 + OR21 on Day 4 were significantly higher than that of OR21. Therefore, more in-depth DEHP degradation experiments were carried out as shown in Figure 30. On Day 8, the DEHP degradation efficiencies (initial DEHP concentration: 100 mg/L) of OR21 ($84.5 \pm 6.5\%$), OR05 + OR21 ($90.7 \pm 2.4\%$) and Consortium A02 ($91.3 \pm 8.1\%$) were not significantly different, but were significantly higher than the DEHP degradation efficiency of Consortium A01 ($74.5 \pm 0.8\%$). However, DEHP degradation by Consortium A02 on Day 2 ($64.8 \pm 8.5\%$) was significantly higher than those by OR05 + OR21 ($50 \pm 0.7\%$), Consortium A01 ($35.8 \pm 2.4\%$), and OR21 ($24.9 \pm 2.1\%$). This indicates that the co-occurrence of OR05, OR16, and OR21 in Consortium A02 promotes DEHP degradation, which in turn

implies that all three strains have important roles in the DEHP degradation process of Consortium A02.

It has to be acknowledged that although the genus *Bacillus* was predicted to interact positively with *Sporosarcina* and *Microbacterium* in enriched consortium C10, the defined consortium comprising strains belonging to the three genera (A01) isolated from C10 displayed slower DEHP degradation performance than the defined consortium comprised of just *Microbacterium* and *Sporosarcina*. This could be because although *Bacillus cereus* OR01 could grow well on DEHP, it has low DEHP degradation activity; this means that OR01 would compete with the other strains for essential elements, such as nitrogen, for growth without contributing to the degradation of DEHP. Furthermore, as shown in Figure 22a, the positive interaction predicted between the *Bacillus* spp. and *Microbacterium* spp. in C10 is indirect, and, therefore, cooperative interactions between bacteria from these two genera may require the presence of *Stenotrophomonas* spp. It is also possible that the OR01 is not the main PAE-degrading strain of *Bacillus* in C10 and hence its contribution to the predicted positive interaction between *Bacillus* and the other strains of C10 is insignificant.

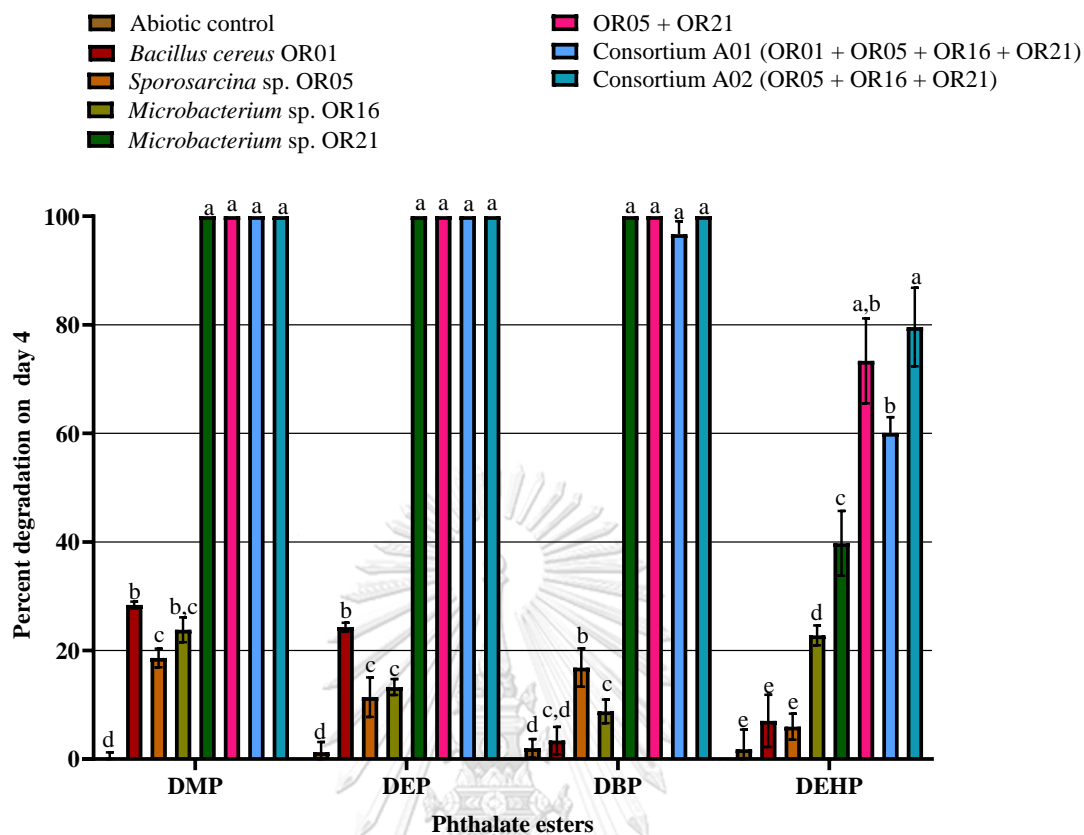


Figure 29 Degradation efficiencies of 100 mg/L of DMP, DEP, DBP, and DEHP (separately) on Day 4. The different letters indicate significantly different ($p < 0.05$) percent degradation values for each PAE type.

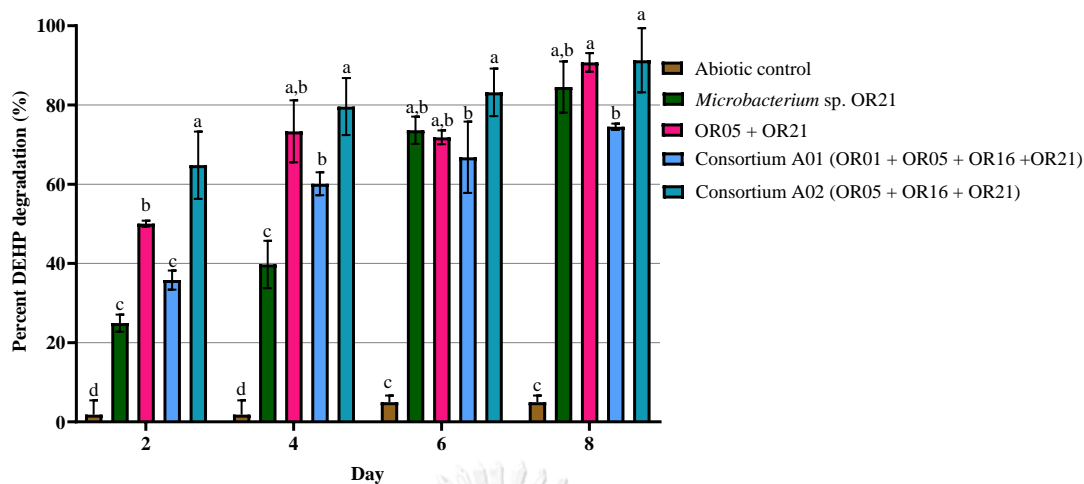
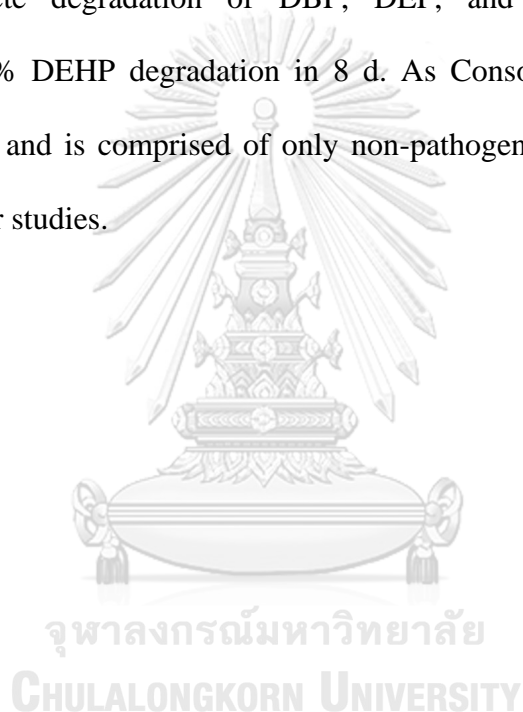


Figure 30 DEHP (100 mg/L) degradation efficiencies of OR21, OR05 +OR21, Consortium A01, and Consortium A02 on days 2, 4, 6, and 8. Different letters indicate significantly different ($p < 0.05$) percent degradation values.

The degradation of a mixture of 100 mg/L each of DEHP, DBP, DEP, and DMP by OR21, OR05 + OR21, Consortium A01, and Consortium A02 was also investigated (Figure 31a-d). As in the case of the degradation of individual PAEs, PAEs with shorter alkyl chain lengths in the mixture (DBP, DEP, and DMP) were completely degraded in all four treatment types within 2 d. Meanwhile, DEHP degradation was slower as expected. The DEHP degradation efficiencies on Day 2 were in the order of $A02 \approx A01 > OR05+OR21 \approx OR21$, while those on days 4, 6, and 8 were in the order of $A02 \approx A01 > OR05+OR21 \approx OR21$, $A02 \approx OR05+OR21 \approx A01 \approx OR21$, and $A02 \approx OR05+OR21 \approx A01 > OR21$, respectively. Thus, degradation of DEHP in the PAE mixture by Consortium A02 was faster. It is worth noting that although OR05 on its own does not exhibit DEHP degradation activity (as shown in Table 13), it enhances the DEHP degradation efficiency of OR21; in the PAE mixture, OR21 could degrade about 58% of DEHP in 8 d, while OR05 + OR21 could

degrade about 89% of DEHP. This implies the potential role of OR05 in the degradation of DEHP intermediates such as 2-ethylhexanol as OR05 could utilize 2-ethylhexanol as sole source of carbon for growth (Table 13). Some researchers have reported the limited degradation performance of single bacterial strains in the degradation of multiple PAE types (Fan et al 2018a, Zhang et al 2018). However, Consortium A02 could degrade a mixture of different PAE types (400 mg/L) well, achieving complete degradation of DBP, DEP, and DMP within 2 d and approximately 80% DEHP degradation in 8 d. As Consortium A02 could achieve faster degradation and is comprised of only non-pathogenic bacterial strains, it was selected for further studies.



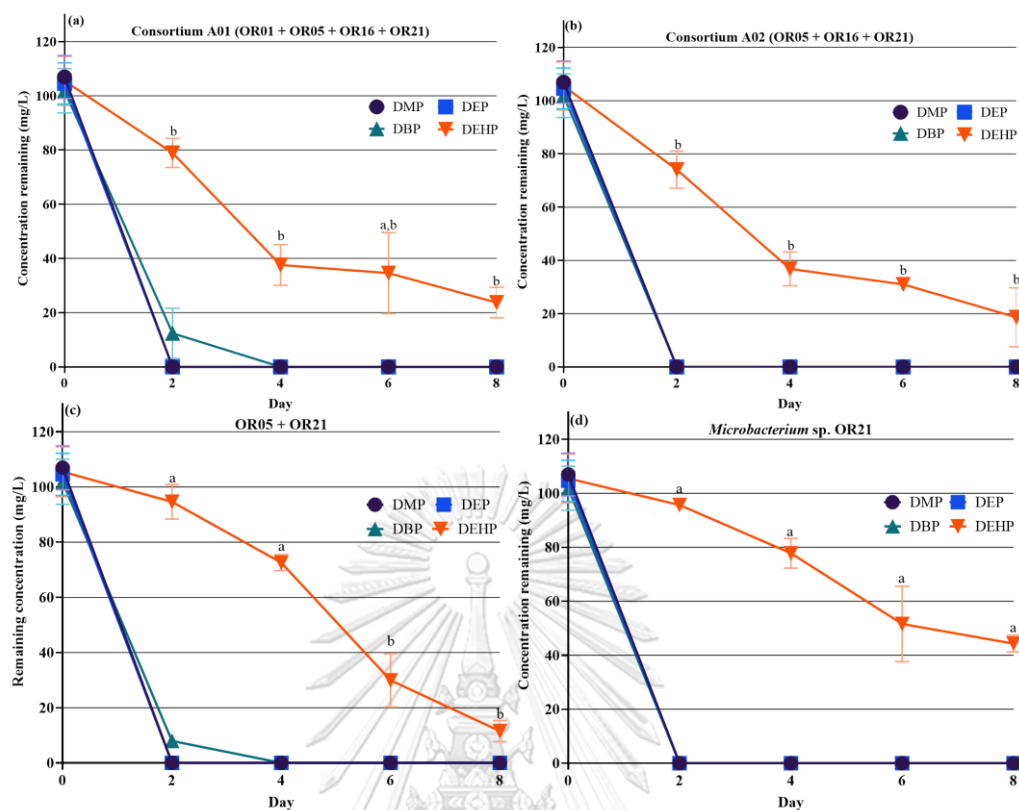
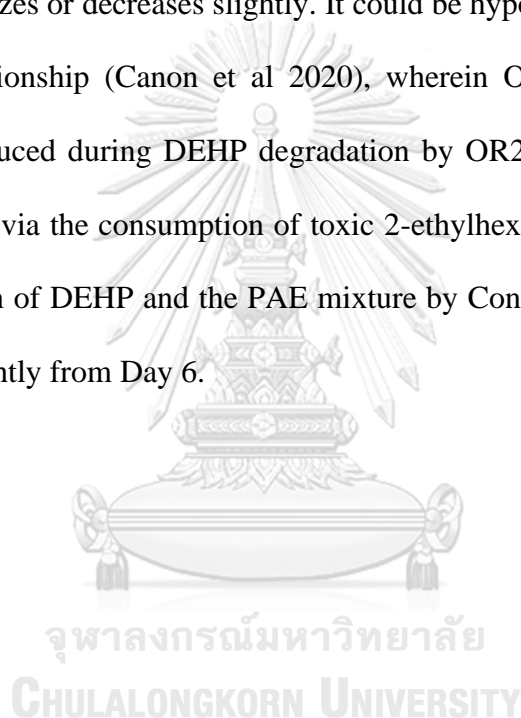


Figure 31 Remaining PAE concentrations during degradation of a mixture of DEHP, DBP, DEP, and DMP (100 mg/L each) by Consortium A01 (a), Consortium A02 (b), OR05 + OR21 (c), and OR21 (d). The different letters indicate significantly different ($p < 0.05$) DEHP concentrations in the different treatments (a-d) at each sampling point.

Cell numbers of the individual strains in Consortium A01, Consortium A02, and OR05 + OR21 during degradation of DEHP and the PAE mixture were monitored (Figure 32). Increase in the total number of viable cells from that on Day 0 is observed during degradation in all cases. This is primarily attributable to the increase in viable cell numbers of OR16 and OR21 during the degradation period in all cases. This result is noteworthy because it implies that although OR16 and OR21 use the same carbon source (DEHP), they do not inhibit each other's growth. This could

imply a homotypic cooperative interaction between OR16 and OR21. Homotypic cooperative interaction refers to bidirectional interactions between bacteria that share the same genotype and resources such as carbon source (Canon et al 2020, Rodríguez Amor & Dal Bello 2019). During degradation of DEHP and the PAE mixture by Consortium A02 and OR05 + OR21, slight increase in the viable cell counts of OR05 can be observed during initial degradation (Day 2). After this initial increase, the cell count either stabilizes or decreases slightly. It could be hypothesized that OR05 shares a syntrophic relationship (Canon et al 2020), wherein OR05 benefits from the 2-ethylhexanol produced during DEHP degradation by OR21 and OR16, while OR21 and OR16 benefit via the consumption of toxic 2-ethylhexanol by OR05. In contrast, during degradation of DEHP and the PAE mixture by Consortium A01, cell numbers of OR01 drop slightly from Day 6.



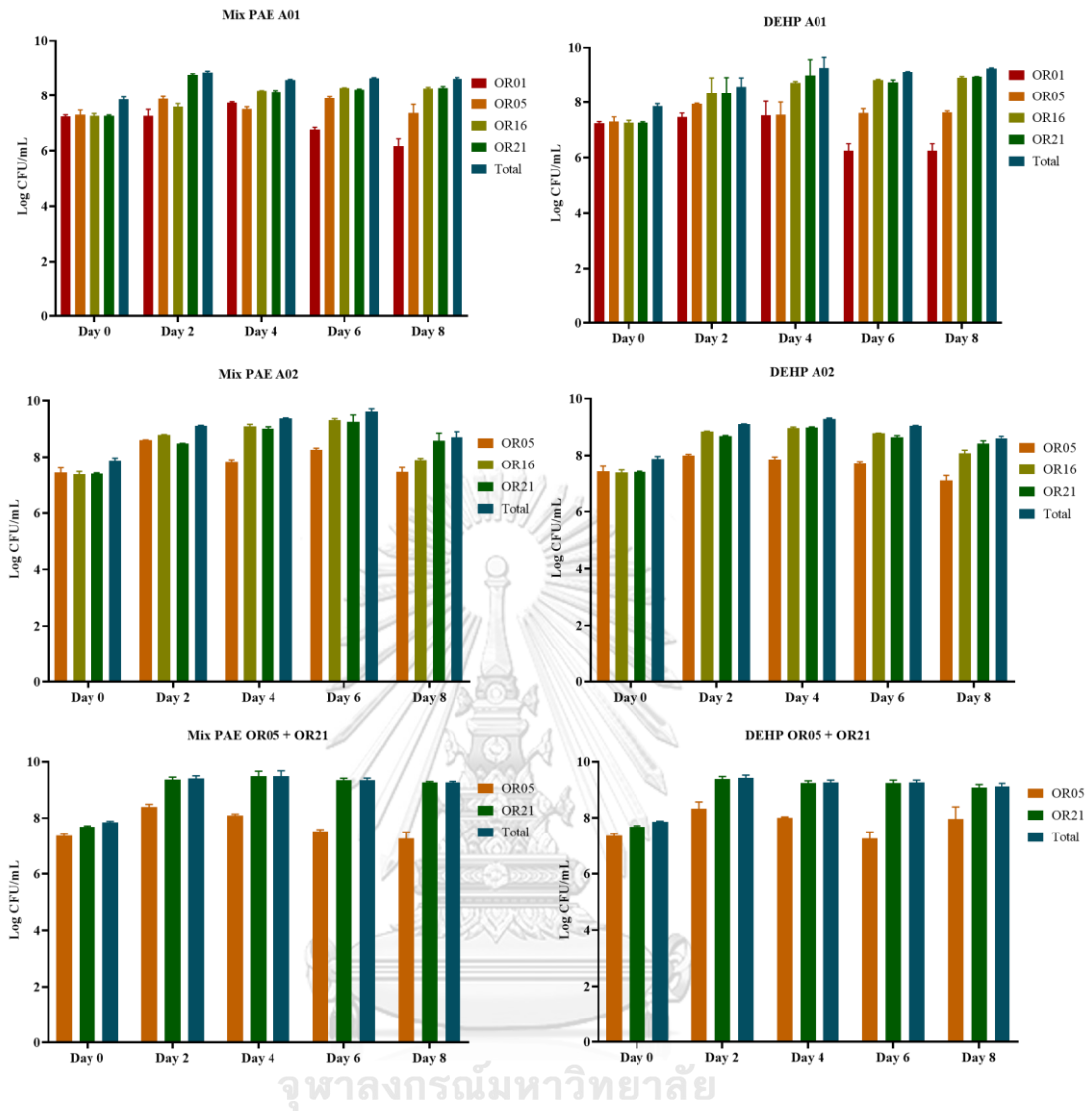


Figure 32 Viable cell counts of Consortium A01, Consortium A02, and OR05 + OR21 during degradation of the PAE mixture (Mix PAE) and DEHP.

4.3.1.1 Comparison of the PAE degradation efficiencies of enriched consortium C10 and defined consortia created using bacterial isolates of C10

In Phase I, enriched consortium C10 was observed to degrade 91% of 100 mg/L DEHP in 4 d, while complete degradation of DBP, DEP, and DMP by C10 was observed within the same time period. Meanwhile, the defined consortia created using bacterial isolates from C10, A01 (OR01 + OR05 + OR16 + OR21) and A02 (OR05 + OR16 + OR21) could degrade about 66 and 80% of DEHP (100 mg/L) in 4 d. However, like enriched consortium C10, defined consortia A01 and A02 exhibited almost complete degradation (97 – 100%) of DBP, DEP, and DMP in 4 d. This indicates that for PAEs with longer alkyl chains, like DEHP, enriched consortium C10 has a higher degradation efficiency than the much simpler defined consortia A01 and A02. In terms of degradation of the mixture of DEHP, DBP, DEP, and DMP (PAE mixture; total concentration: 400 mg/L), C10 showed 20 – 47% degradation of each PAE type on Day 2, while defined consortia A01 and A02 could achieve 18 – 100% and 30 – 100% degradation of the PAE mixture within the same time. On Day 6, C10 could degrade 90 – 100% degradation of the PAE mixture, while 67 – 100% and 70 – 100% degradation could be achieved by A01 and A02, respectively. This indicates that although the PAE degradation efficiency of enriched consortia C10 is higher for longer incubation periods, PAE degradation by the defined consortia is faster. Nevertheless, the slightly lower PAE degradation efficiency of the defined consortia than that of the enriched consortium is outweighed by the advantages it offers. First, the dynamic nature of enriched bacterial consortia presents challenges, such as variations in biodegradation capacity with change in bacterial community (Mendes et

al 2021). Furthermore, enriched bacterial consortia contain unknown bacteria with metabolic and functional interactions that are difficult to understand (Gilmore et al 2019). Additionally, unlike enriched bacterial consortia, defined bacterial consortia can be designed with only non-pathogenic bacterial strains.

4.3.2 Degradation of DEHP intermediates

The degradation of three commonly reported and toxic DEHP intermediates by Consortium A02, OR05 + OR21, OR05 + OR16, OR05, OR16, and OR21 was investigated. As shown in Figure 33, OR21, OR05 + OR21, and Consortium A02 could achieve complete degradation of 100 mg/L of MEHP within 8 d. Although OR05, OR16, and OR05 + OR16 also exhibited MEHP degradation ability, degradation efficiencies were much lower (below 40%). In the case of phthalic acid (Figure 34a), on Day 4, the highest degradation efficiency was achieved by Consortium A02 (10.7%), while degradation by all three single strains and the two co-cultures were below 10% and not significantly different from that in the abiotic control. However, although not statistically significant, phthalic acid degradation by OR16 and OR05 + OR16 is slightly higher than that by OR05, OR21, and OR05 + OR21. The low phthalic acid degradation efficiencies observed in all the treatments could be because phthalic acid is toxic to bacterial cells at the concentration used (100 mg/L). Protocatechuic acid degradation efficiencies on Day 4 are shown in Figure 34b. Highest degradation efficiency was achieved by Consortium A02, followed by OR05 + OR21 and OR21. Although 2-ethylhexanol is also a commonly reported DEHP intermediate and is known to have toxic properties, its degradation could not be studied as 2-ethylhexanol could not be extracted from the degradation medium used in this study. More extraction solvents and conditions will need to be

investigated in the future to quantify the 2-ethylhexanol degradation efficiency of Consortium A02. Furthermore, it would be interesting to explore degradation of varying concentrations of MEHP, phthalic acid, and protocatechuic acid at various time intervals.

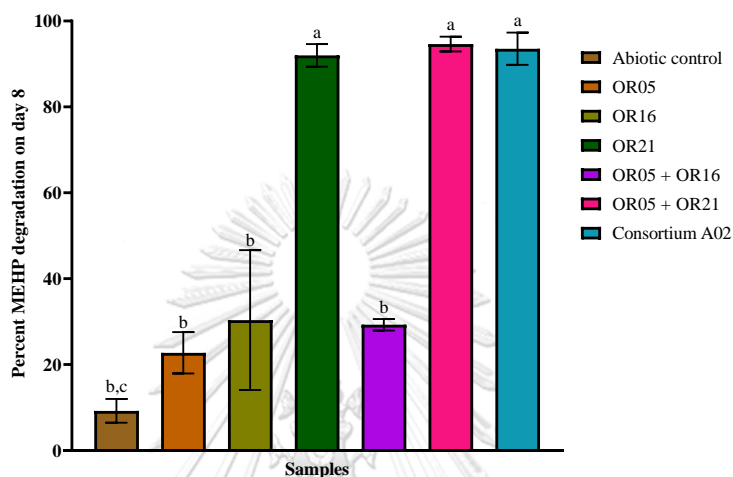


Figure 33 Percent degradation of MEHP on Day 8 by OR05, OR16, OR21, OR05+OR16, OR05+OR21, and Consortium A02. Different letters indicate significantly ($p < 0.05$) different values.

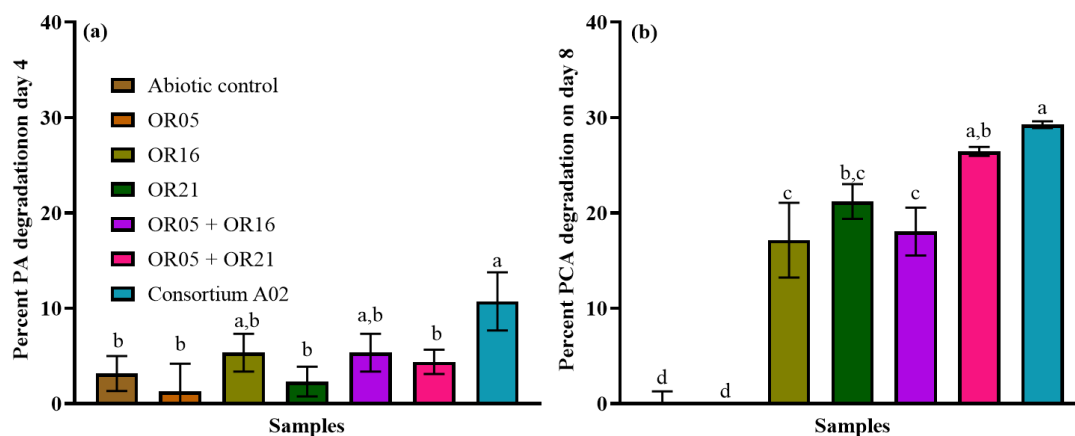


Figure 34 Percent degradation of phthalic acid (a) and protocatechuic acid (b) on Day 4 by OR05, OR16, OR21, OR05+OR16, OR05+OR21, and Consortium A02. Different letters indicate significantly ($p < 0.05$) different values.

4.3.3 Genome sequencing and functional annotation

A circular genome comprising 51 contigs and spanning a length of 3,626,936 bp with a GC content of 41.9% was obtained for *Sporosarcina* sp. OR05 (Figure 35). The features of this genome are summarized in Table 14. Based on the KEGG database, 44 genes in this genome were assigned to 75 pathways under Xenobiotics biodegradation and metabolism.

Table 14 Genomic and annotation features of OR05, OR16, and OR21.

Features	<i>Sporosarcina</i> sp.	<i>Microbacterium</i> sp.	<i>Microbacterium</i> sp.
	OR05	OR16	OR21
CDS	3743	2647	2959
tRNA	64	45	46
rRNA	6	6	3
Hypothetical	1439	842	994

proteins				
Proteins	with	2304	1805	1965
functional assignments				
Proteins with EC		750	715	761
number assignments				
Proteins mapped		565	563	585
to	KEGG			
pathways				

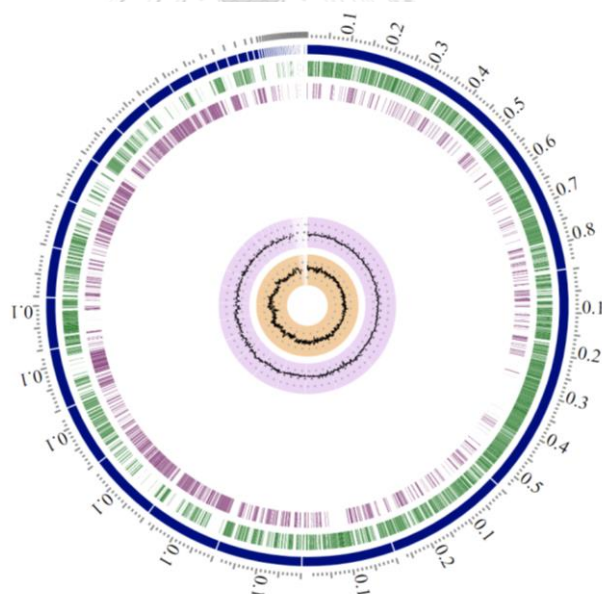


Figure 35 Circular map of *Sporosarcina* sp. OR05 based on genome sequencing and annotation. The inner to outer circles represent GC skew, GC content, CDS on the reverse strand, CDS on the forward strand, and contigs.

The full length of the assembled genome of *Microbacterium* sp. OR16 (3 contigs) spans a length of 2785191 bp, with a GC content of 69.14%. The annotated features of this genome are listed in Table 14, while the circular genome map of OR16 is shown in Figure 36. Furthermore, 32 genes in the genome of OR16 were assigned to 69 pathways under the KEGG Xenobiotics biodegradation and metabolism pathway. The assembled genome of *Microbacterium* sp. OR21 comprises 18 contigs, spans a total length of 3042717 bp and has a GC content of 69.47%. The annotation and protein features of this genome are available in Table 14, while the circular genome of OR21 is displayed in Figure 37. In the genome of OR21, 38 genes were assigned to 72 pathways in the KEGG Xenobiotics biodegradation and metabolism pathway. Although OR16 and OR21 belong to the same genus, *Microbacterium*, the average nucleotide identity of OR16 and OR21 was 87.9% (Appendix F), indicating variations in their genomic potential. Average nucleotide identities of all three genomes with genomes of closely related type strains in public databases are listed in Appendix F.

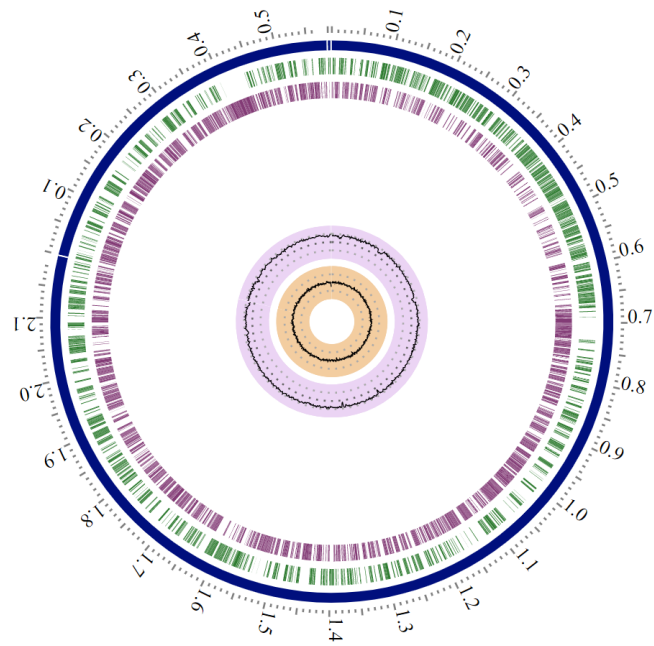


Figure 36 Circular map of *Microbacterium* sp. OR16 based on genome sequencing and annotation. The inner to outer circles represent GC skew, GC content, CDS on the reverse strand, CDS on the forward strand, and contigs.

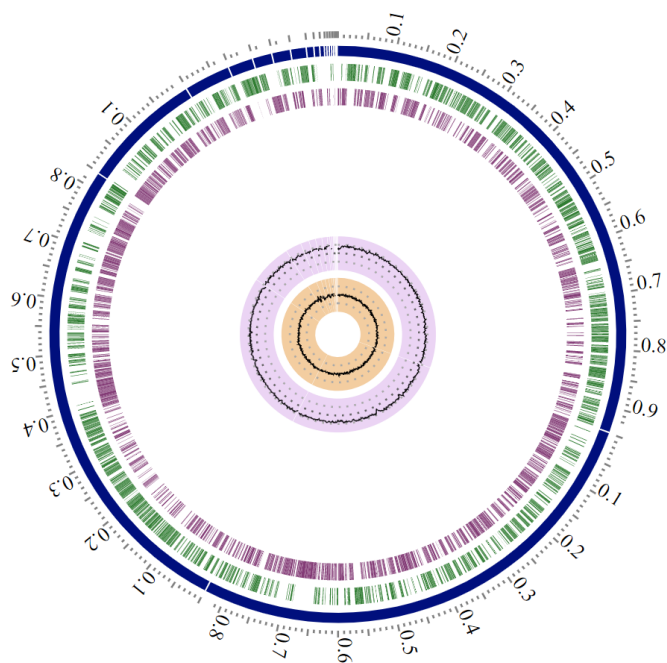


Figure 37 Circular map of *Microbacterium* sp. OR21 based on genome sequencing and annotation. The inner to outer circles represent GC skew, GC content, CDS on the reverse strand, CDS on the forward strand, and contigs.

The KEGG pathways assigned to genes present in the genomes of the three bacterial strains of Consortium A02 are displayed in Figure 38a, while the Xenobiotics biodegradation and metabolism roles mapped to the genes are displayed in Figure 38b. The maximum number of genes in all three genomes were mapped to the Amino acid metabolism and Carbohydrate metabolism KEGG pathways. Several carbohydrate metabolism pathways, such as glycolysis/gluconeogenesis, tricarboxylic acid cycle, pentose phosphate pathway, pyruvate metabolism, and butanoate metabolism, were assigned to all three genomes. Diversity of carbohydrate metabolism pathways facilitate the utilization and metabolism of organic pollutants like PAEs (Chen et al 2021). Several genes were also mapped to stress response and ABC transport systems as shown in Figure 39a-b.

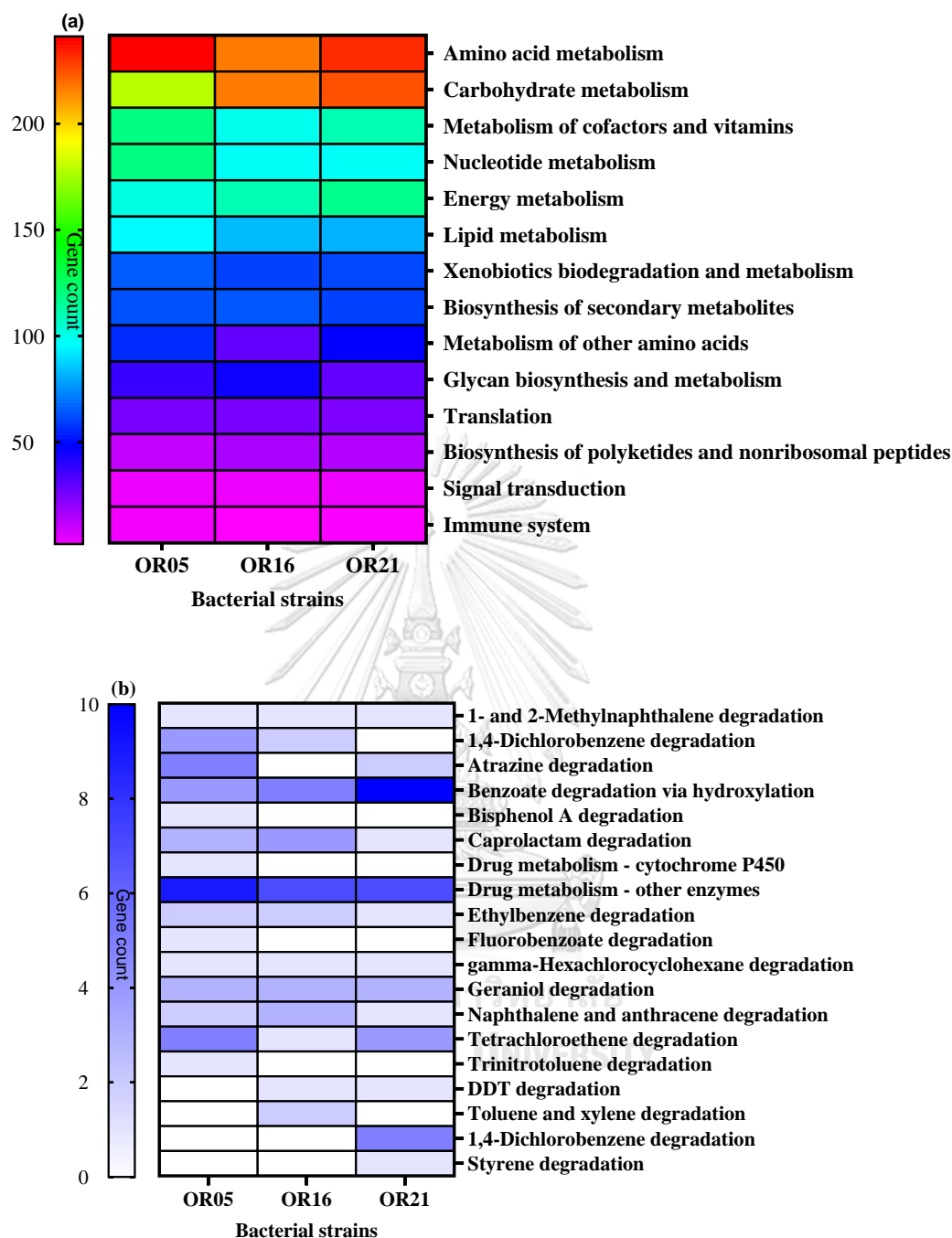


Figure 38 KEGG pathways mapped to genes in the genomes of OR05, OR16, and OR21 (a) and sub-division of the Xenobiotics biodegradation and metabolism pathway (b) assigned to genes in OR05, OR16, and OR21.

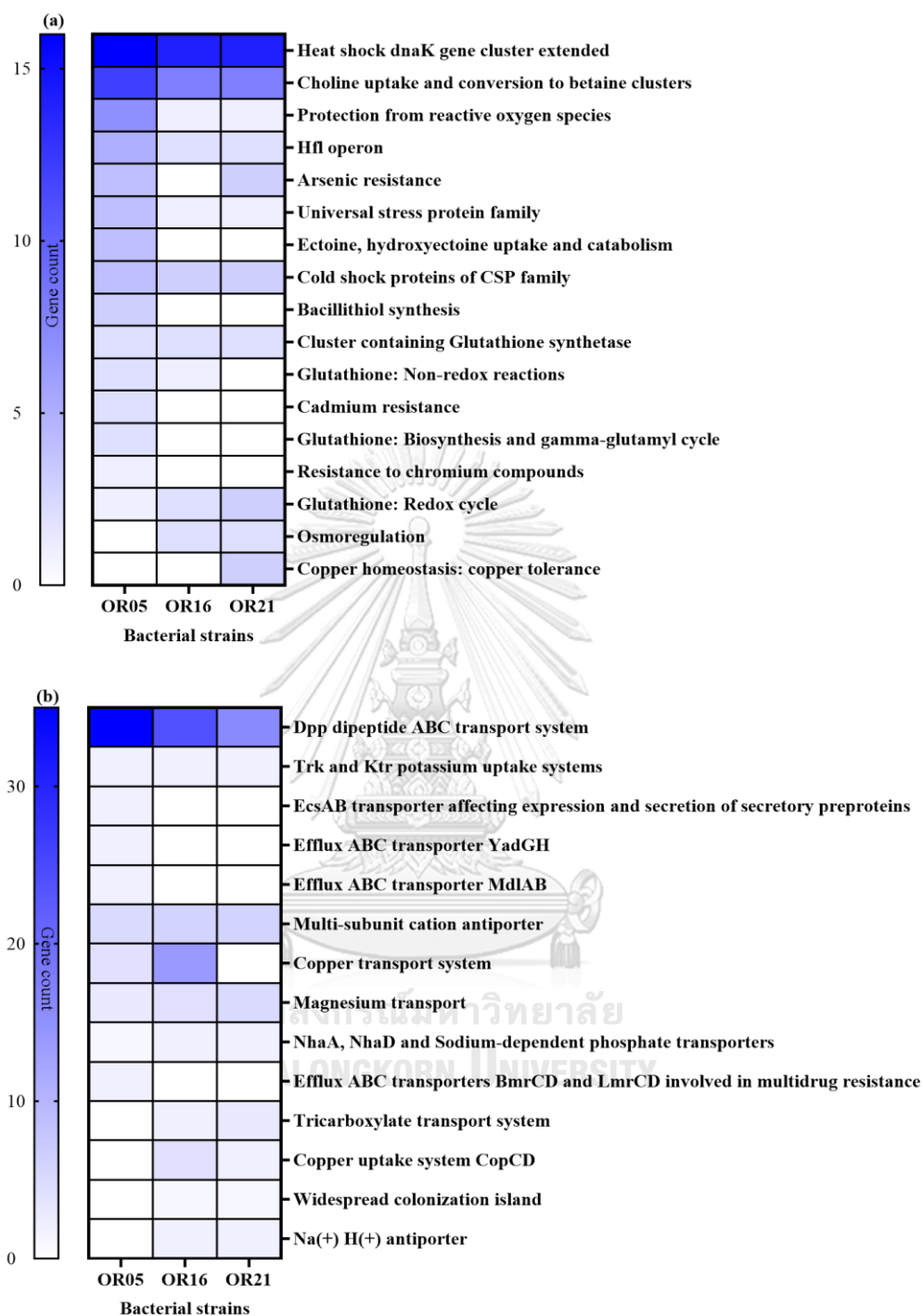


Figure 39 Stress response (a) and membrane transport (b) KEGG pathways assigned to genes in the genomes of OR05, OR16, and OR21.

4.3.3.1 Detection of genes encoding potential phthalate degradation enzymes

Table 15 lists the putative phthalate degradation genes annotated in the genomes of *Sporosarcina* OR05, *Microbacterium* sp. OR16, and *Microbacterium* sp. OR21 using the RAST tool kit via the genome annotation service on PATRIC. Various genes with significant similarities to genes reported to code for several enzymes involved in the degradation of phthalate esters and its metabolites were detected in the genomes of the three bacterial strains comprising Consortium A02. Furthermore, local BLAST searches were carried out on the three genomes with amino acid sequences of various relevant phthalate ester-degrading enzymes reported in literature as query sequences and significant hits in the subject genomes are listed in Table 16.

As shown in Table 16, the amino acid sequence of the CDS at 11_2811-723 of OR21 is 97% identical to DpeH from *Microbacterium* sp. PAE-1 (Lu et al 2020), while the amino acid sequence of the CDS at 11_2072-915 shows a 99% identity with MpeH of the same strain. DpeH is an esterase that catalyzes the hydrolysis of PAEs to their monoesters, while MpeH is able to hydrolyze phthalate monoesters to phthalic acid (Lu et al 2020). However, in OR16, the protein sequence of the putative esterase coded by the gene at 1_900612+696 shares only a 29% identity with DpeH, while no significant matches were found for MpeH in OR16. Two genes in the genome of OR05 (3_77852+747 and 4_61817+603) were annotated to encode for the carboxylesterase (Table 15). Carboxylesterases, which catalyze the hydrolysis and formation of carboxylic acid ester bonds, have been reported to be involved in the degradation of PAEs to their monoesters and finally to phthalic acid (Chen et al 2021,

Ding et al 2015b, Huang et al 2020). Song et al (2022) reported that a carboxylesterase (KXC42_04905) from *Rhodococcus* sp. LW-XY12 could catalyze the hydrolysis of the ester bonds in DEHP and MEHP to ultimately form phthalic acid. Furthermore, the genomes of OR05, OR16, and OR21 possess genes whose protein sequences have high similarities with various hydrolases belonging to the alpha/beta fold family, including esterases (Table 15). Phthalate hydrolases belong to the alpha/beta family of hydrolases (Bhattacharyya et al 2022). Three genes in OR21 were annotated to code for alpha/beta hydrolases, while the gene at 5_859+666 was annotated to code for a phthalate ester hydrolase. As expected, a much higher number of putative phthalate hydrolase encoding genes were observed in the genome of OR21, which demonstrated the highest PAE degradation efficiencies among the three strains. As studies on the genomic potentials of *Microbacterium* spp. and *Sporosarcina* spp., in terms of their genomic potential for the degradation of PAEs and their intermediates, have been rarely studied, the specific roles of most of these alpha/beta hydrolase genes are still unclear.

Additionally, the protein sequences encoded by the genes at 11_7431-1290 and 5_20415-1395 of OR21 have similarities of 74% and 71%, respectively, to phthalate 3,4-dioxygenase (ALT56978.1) from *Microbacterium* sp. J-1 (Zhao et al 2017). Furthermore, two putative phthalate 3,4-dioxygenase genes and aromatic-ring-hydroxylating-dioxygenase genes were identified in the genome of OR21. Phthalate 3,4-dioxygenase is known to catalyze the conversion of phthalic acid to protocatechuic acid in Gram-positive bacteria. Genes annotated to code for several enzymes that catalyze the further degradation of protocatechuic acid, such as protocatechuate dioxygenase, 2-pyrone-4,6-dicarboxylic acid hydrolase, and 4-

oxalomesaconate hydratase, were detected in the genome of OR21. As shown in Table 15, the protocatechuate dioxygenase identified in OR21 shares 100% and 94.3% identities with protocatechuate 4,5-dioxygenase alpha subunit from *Microbacterium laevaniformans* OR221 and protocatechuate 3,4-dioxygenase from *Microbacterium* sp. Root180, respectively. The protein sequence coded by the gene at 2_304660-924 of OR16 has a 75.52% identity to the protein sequence of phthalate dioxygenase reductase (PDR)/VanB family oxidoreductase from *Microbacterium marinilacus* YM11-607 (MBY0687621.1). This implies that both OR16 and OR21 possess the genomic potential to catalyze the degradation of phthalic acid; however, no phthalate dioxygenase gene was detected in the genome of OR05. Nevertheless, gene expression studies would need to be conducted to confirm that the potential phthalate degradation genes detected in the genomes are involved in degradation.

It is widely reported that phthalate 3,4-dioxygenase produced by Gram-positive bacteria catalyze the conversion of phthalic acid to protocatechuic acid (Li et al 2016, Song et al 2022). However, a different degradation pathway may be adopted by bacteria that do not produce phthalate 3,4-dioxygenase. The formation of benzoic acid via decarboxylation of phthalic acid during bacterial degradation of phthalate esters has been reported (Wright et al 2020, Zhang et al 2018). The benzoate 1,2-dioxygenase from strain LW-XY12 shared 30%, 30%, and 31% sequence similarities with the proteins coded by genes at 5_20415-1395, 11_7431-1290 (OR21) and 4_180244+975 (OR05). Several genes of OR05 were annotated to encode for putative ring-cleaving dioxygenases and other enzymes, such as catechol 1,2-dioxygenase, muconate cycloisomerase and 3-oxoadipate enol-lactonase, reported to be involved in the degradation of benzoic acid and its metabolites. Alcohol dehydrogenase and

aldehyde dehydrogenase, which have been reported to be involved in the initial steps of 2-ethylhexanol degradation (Wyatt et al 1987), were detected in the genomes of all the three bacterial strains used in this study. Wright et al (2020) reported that alcohol and aldehyde dehydrogenases (followed by fatty acid-CoA ligase) from *Mycobacterium* sp. DBP42 metabolized the butanol molecules generated via side chain hydrolysis of DBP.



Table 15 Functional annotation of the CDS in the genomes of OR05, OR16, and OR21.

<i>Sporosarcina</i> sp. OR05						
Gene location	PATRIC annotation	Top hit protein(s)	Host of top hit protein	Protein identity	Hit protein accession	
1_19189	3-Oxoadipate enol-lactonase,	Alpha/beta hydrolase	<i>Sporosarcina</i> sp.	77.13%	MBD7985	
6+888	alpha/beta hydrolase fold family		Sa2YVA2		151.1	
1_19279	Oxidoreductase, short-chain	3-oxoacyl-ACP reductase FabG	<i>Sporosarcina</i> sp.	90.65%	MBD7985	
6+741	dehydrogenase/reductase family		Sa2YVA2		150.1	
1_21302	Oxidoreductase, short-chain	SDR family oxidoreductase	<i>Sporosarcina</i> sp.	80.15%	MBO0600	
4+810	dehydrogenase/reductase family		E16_3		096.1	
1_23549	Putative esterase YitV	Putative esterase YitV	<i>Sporosarcina</i>	84.31%	GEN8294	
8+768			<i>luteola</i> NBRC 105378		0.1	
1_26506	Putative acetyl esterase YjcH	Esterase family protein	<i>Sporosarcina</i> sp.	85.06%	MBD7985	
4-726			Sa2YVA2		081.1	
1_48518	Alcohol dehydrogenase	Zinc-binding dehydrogenase	<i>Sporosarcina</i>	75.46%	MCM374	
2+981			<i>luteola</i> MER 47		3583.1	
1_55865	Aldehyde dehydrogenase	Aldehyde dehydrogenase family	<i>Sporosarcina</i> sp.	79.59%	KAA0964	

1+1458		protein	ANT_H38	993.1
1_82940	Hydrolase, alpha/beta fold family	Alpha/beta hydrolase	<i>Sporosarcina</i> sp.	78.33% QTD4190
0+840			Te-1	5.1
2_12519	Aldehyde dehydrogenase	Aldehyde dehydrogenase	<i>Sporosarcina</i> sp.	75.27% MBD7983
3+1386			Sa2YVA2	338.1
2_42236	3-ketoacyl-CoA thiolase; Acetyl-CoA C-acyltransferase	Acetyl-CoA C-acyltransferase	<i>Sporosarcina</i> sp.	86.80% MBD7983
8+1185	CoA acetyltransferase		Sa2YVA2	623.1
3_77852	Carboxylesterase	Carboxylesterase	<i>Sporosarcina</i> sp.	84.27% MBD7985
+747			Sa2YVA2	716.1
4_55161	Hydrolase, alpha/beta fold family	Alpha/beta hydrolase	<i>Sporosarcina</i>	80.39% MCM371
+936			<i>Luteola</i> MER 9	0528.1
4_61817	Carboxylesterase	Alpha/beta hydrolase	<i>Sporosarcina</i> sp.	79% MBD7983
+603			Sa2YVA2	968.1
		Carboxylesterase	<i>Sporosarcina</i>	79.40% GEN8354
			<i>Luteola</i> NBRC 105378	3.1
4_70376	Aldehyde dehydrogenase	Aldehyde dehydrogenase family	<i>Sporosarcina</i> sp.	97.86% MBD7983
+1542		protein	Sa2YVA2	961.1
4_14717	Putative ring-cleaving dioxygenase	Glyoxalase	<i>Sporosarcina</i>	85.71% KON9008

4+945	MhqA		<i>glibispora</i> DSM 4	3.1	
Ring-cleaving dioxygenase					
			<i>Sporosarcina</i>	83.11%	MCM363
			<i>Luteola</i> MERTA48		7786.1
5_29379	Aldehyde dehydrogenase		<i>Sporosarcina</i> sp.	89.78%	PIC76073.
+1473			P19		1
5_58830	Hydrolase of unknown specificity		<i>Sporosarcina</i> sp.	76.19%	MBD7986
-801	RsbQ		Sa2YVA2		267.1
5_18360	Aldehyde dehydrogenase		<i>Sporosarcina</i> sp.	78.51%	MBD7985
2+1449			Sa2YVA2		041.1
6_96801	Carboxymuconolactone		<i>Sporosarcina</i> sp.	84.21%	QTD4009
+351	decarboxylase		Te-1		2.1
7_13392	Oxidoreductase, short-chain		<i>Sporosarcina</i> sp.	82.07%	NYF2393
9-756	dehydrogenase/reductase family		JAI121		6.1
(short-subunit alcohol dehydrogenase family)					
7_15440	Oxidoreductase, short-chain		<i>Sporosarcina</i>	90.72%	GEN8433
9+879	dehydrogenase/reductase family		<i>Luteola</i> NBRC		4.1
			105378		
8_64058	Muconate cycloisomerase		<i>Sporosarcina</i>	82.43%	MCM363
+1116			<i>Luteola</i> MERTA48		6257.1
Muconate cycloisomerase family protein					

8_66393 +792	Catechol 1,2-dioxygenase	Catechol 1,2-dioxygenase	<i>Sporosarcina</i> <i>luteola</i> MER 47	92.40%	MCM374 4367.1
13_1619 1-1200	Alcohol dehydrogenase	Iron-containing alcohol dehydrogenase	<i>Sporosarcina</i> <i>luteola</i> MERT A48	73.37%	MCM363 8974.1
15_3414 2-798	Beta-ketoacidate enol-lactone hydrolase, putative	Alpha/beta hydrolase	<i>Sporosarcina</i> sp. Sa2YVA2	85.28%	MBD7983 884.1
17_4426 -1167	Long-chain-alcohol dehydrogenase	Putative beta-ketoacidate enol-lactone hydrolase	<i>Cytobacillus firmus</i> I-1582	57.25%	KAF0823 981.1
19_7900 +693	Hydrolase, alpha/beta fold family	Iron-containing alcohol dehydrogenase Carboxylesterase	<i>Sporosarcina</i> sp. ACRS <i>Sporosarcina</i> <i>luteola</i> NBRC 105378	80.15%	MCG7346 575.1 GEN8480 5.1
24_5731 -1479	Aldehyde dehydrogenase	Alpha/beta fold hydrolase Aldehyde dehydrogenase	<i>Sporosarcina</i> sp. Sa2YVA2 <i>Sporosarcina</i> <i>luteola</i> NBRC 105378	79.57%	MBD7983 931.1 GEN8306 8.1

<i>Microbacterium</i> sp. OR16						
Gene location	PATRIC annotation	Top hit protein(s)	Host of top hit protein	Protein identity	Hit protein	Hit accession
1_90061 2+696	Putative esterase	Alpha/beta hydrolase	<i>Microbacterium esteraromaticum</i> MM1	89.61%	PYD0100	4.1
1_8745- 1167	Catechol 2,3-dioxygenase	3,4-dihydroxyphenylacetate 2,3-dioxygenase	<i>Microbacterium esteraromaticum</i> MM1	97.42%	PYD0199	0.1
1_63345 1+1158	Hydrolase	Alpha/beta hydrolase	<i>Microbacterium</i> sp. Re1	95.25%	WP_1917	13054.1
1_65634 3+687	Hydrolase	HAD superfamily hydrolase (TIGR01509 family)	<i>Microbacterium esteraromaticum</i>	85.78%	MBM7464	479.1
1_69277 1-792	Hydrolase, alpha/beta hydrolase fold family	Alpha/beta hydrolase	<i>Microbacterium esteraromaticum</i> MM1	77.19%	PYD0114	8.1
1_90061 2+696	Putative esterase	Alpha/beta hydrolase	<i>Microbacterium esteraromaticum</i>	89.61%	PYD0100	4.1

		MM1	
1_95939	Putative hydrolase	Alpha/beta hydrolase	93.28%
9+723		<i>Microbacterium esteraromaticum</i>	0.1
		B24	
1_13266	Alpha/beta hydrolase fold	Alpha/beta hydrolase	94.38%
06+750		<i>Microbacterium esteraromaticum</i>	1.1
		MM1	
1_15856	Hydrolase, putative isochorismatase	Isochorismatase family protein	87.78%
21+543		<i>Microbacterium esteraromaticum</i>	5.1
		MM1	
1_18303	Benzoate transport protein	Benzoate/H(+) symporter BenE	95.70%
54+408		family transporter	4.1
		B24	
1_19375	Putative oxidoreductase	Putative 4,5-dihydroxyphthalate	27.66%
34+1209		dehydrogenase	.1
		12510	
1_20077	Alcohol dehydrogenase	NAD(P)-dependent alcohol	97.67%
89+1035		dehydrogenase	4.1
		<i>Microbacterium esteraromaticum</i>	
		MM1	

1_20109	Aldehyde dehydrogenase	Aldehyde dehydrogenase	<i>Microbacterium</i>	99.42%	PYD0071
01-1548			<i>esteraromaticum</i> MM1		6.1
1_21052	Acetyl xylan esterase	Acetyl xylan esterase	<i>Microbacterium</i>	99%	PYD0084
59-969			<i>esteraromaticum</i> MM1		2.1
2_26599	Aldehyde dehydrogenase B	Aldehyde dehydrogenase family protein	<i>Microbacterium</i>	75.10%	QPZ38097
3-1440			<i>chengjingii</i> HY60		.1
2_30466	Flavodoxin reductases (ferredoxin- PDR/VanB family oxidoreductase		<i>Microbacterium</i>	75.52%	MBY0687
0-924	NADPH reductases) family 1; Vanillate O-demethylase oxidoreductase		<i>marinilacus</i> YM11- 607		621.1
1_12531	Hypothetical protein	Flavodoxin reductase	<i>Microbacterium</i> sp.	89.82%	MBD8012
31-1575			Re1		743.1
1_72533	Rieske 2Fe-2S family protein	(2Fe-2S)-binding protein	<i>Microbacterium</i> sp.	98.45%	OIU87088
6-1593			AR7-10		.1

Microbacterium sp. OR21

Gene location	PATRIC annotation	Top hit protein(s)	Host of top hit protein	Protein identity	Hit protein accession
1_10048 6+969	Acetyl xylan esterase	Acetyl xylan esterase	<i>Microbacterium esteraromaticum</i> MM1	95.03%	PYD0084 2.1
1_38953 4-825	Hydrolase (HAD superfamily)	HAD family phosphatase	<i>Microbacterium esteraromaticum</i> MM1	97.76%	PYD0044 2.1
1_66999 2-543	hydrolase, putative isochorismatase	Isochorismatase family protein	<i>Microbacterium esteraromaticum</i> MM1	96.11%	PYD0159 5.1
		Hydrolase, putative isochorismatase	<i>Microbacterium esteraromaticum</i> B Mb 05.01	82.58%	SJN16629. 1
2_18515 1-846	Hydrolase, alpha/beta fold family	Alpha/beta hydrolase	<i>Microbacterium esteraromaticum</i> MM1	100%	PYD0220 8.1

3_34273	Hydrolase	Alpha/beta hydrolase	<i>Microbacterium esteraromaticum</i> MM1	98%	PYD0119
6+903					8.1
3_36523	Hydrolase	HAD family phosphatase	<i>Microbacterium esteraromaticum</i> MM1	99.56%	PYD0117
9+687					9.1
		HAD superfamily hydrolase	<i>Microbacterium esteraromaticum</i> DSM 8609	86.67%	MBM7464
					479.1
3_40705	Putative hydrolase/acyltransferase	Alpha/beta hydrolase	<i>Microbacterium esteraromaticum</i> MM1	99.10%	PYD0114
1-666					9.1
3_40783	Hydrolase, alpha/beta hydrolase fold	Alpha/beta hydrolase	<i>Microbacterium esteraromaticum</i> MM1	93.16%	PYD0114
9-792	family				8.1
3_60143	Putative esterase	Alpha/beta hydrolase	<i>Microbacterium esteraromaticum</i> MM1	98.27%	PYD0100
5+696					4.1
		Esterase	<i>Microbacterium</i>	68.56%	GGD7938

		<i>aerolatum</i> NBRC	0.1
		103071	
3_65923	Putative hydrolase	<i>Microbacterium</i>	96.10% PYD0194
9+774		<i>esteraromaticum</i>	8.1
		MM1	
4_19448	Alpha/beta hydrolase fold	<i>Microbacterium</i>	99.20% PYD0213
4+750		<i>esteraromaticum</i>	1.1
		MM1	
5_859+6	Phthalate ester hydrolase	<i>Microbacterium</i>	100% EIC07821.
66	(isochorismatase hydrolase)	<i>laevaniformans</i>	1
		OR221	
		<i>Rhodococcus</i> sp.	74.65% AAR9018
		DK17	0.1
5_22965	Salicylate esterase	<i>Microbacterium</i>	99.16% MCC4268
-714		<i>schleiferi</i> FXH-	654.1
		192	
2_24625	Catechol 2,3-dioxygenase (EC	<i>Microbacterium</i>	98.71% PYD0199
0+1167	1.13.11.2)	<i>esteraromaticum</i>	0.1
		MM1	

	Catechol 2,3-dioxygenase	<i>Microbacterium aerolatum</i> NBRC 103071	93.30%	9.1	GEK8703
5_19024-594	Aromatic-ring-hydroxylating dioxygenase, beta subunit	<i>Microbacterium laevaniformans</i> OR221	100.00%	1	EIC07797.
	Phthalate 3,4-dioxygenase, beta subunit	<i>Mycolicibacterium gilvum</i> PYR-GCK	70.11%	.1	ABP43171
5_20415-1395	Phthalate 3,4-dioxygenase alpha subunit	<i>Microbacterium laevaniformans</i> OR221	100.00%	1	EIC07796.
	Rieske (2Fe-2S) iron-sulfur domain-containing protein	<i>Saccharomonospora azurea</i> SZMC 14600	82.67%	1.1	EHK8771
5_73659+1353	Protocatechuate 4,5-dioxygenase beta chain	<i>Microbacterium laevaniformans</i> OR221	100%	1	EIC07241.
	Protocatechuate 3,4-dioxygenase	<i>Microbacterium</i> sp. Root180	94.93%	7.1	KRB3840

11_6145	Aromatic-ring-hydroxylating dioxygenase, beta subunit	Aromatic-ring-hydroxylating dioxygenase beta subunit	<i>Microbacterium laevaniformans</i> OR221	100%	EIC06397.
-588					1
		Phthalate 3,4-dioxygenase, beta subunit (plasmid)	<i>Arthrobacter</i> sp. FB24	73%	ABK0580
11_7431	Phthalate 3,4-dioxygenase alpha subunit	Aromatic-ring-hydroxylating dioxygenase, alpha subunit	<i>Microbacterium laevaniformans</i> OR221	99.76%	EIC06398.
-1290					1
		Phthalate 3,4-dioxygenase, alpha subunit	<i>Saccharomonospora ra azurea</i> SZMC 14600	85.64%	EHK8771
5_20561	Phenanthrene-4,5-dicarboxylate 5- decarboxylase; 3,4- dihydroxyphthalate decarboxylase	Class II aldolase/adducin family protein	<i>Microbacterium laevaniformans</i> OR221	100%	EIC07795.
+729					1
		3,4-dihydroxyphthalate decarboxylase	<i>Streptomyces mirabilis</i> OK461	54.67%	SFH11172
1_47502	2-hydroxyhepta-2,4-diene-1,7-dioate isomerase/ 5-carboxymethyl-2-oxo- hex-3-ene-1,7-dioate decarboxylase	FAA hydrolase family protein	<i>Microbacterium esteraromaticum</i> MM1	99.30%	PYD0245
6-861					6.1

	2-hydroxyhepta-2,4-diene-1,7-dioate isomerase / 5-carboxymethyl-2-oxo-hex-3-ene-1,7-dioate decarboxylase	<i>Microbacterium esteraromaticum</i> B Mb 05.01	88.81%	SJN40062.
	2-hydroxyhepta-2,4-diene-1,7-dioate isomerase	<i>Microbacterium aerolatum</i> NBRC 103071	81.82%	GEK8586
1_18314 8+1059	Alkanal monooxygenase alpha chain Alkane 1-monooxygenase	<i>Microbacterium esteraromaticum</i> MM1	99.43%	PYD0072
5_68317 -1185	P-hydroxybenzoate hydroxylase Monooxygenase FAD-binding protein	<i>Microbacterium laevaniformans</i> OR221	100%	EIC07248.
	p-hydroxybenzoate hydroxylase	<i>Microbacterium trichothecenolyticum</i> m DSM 8608	88.30%	KJL42958
1_19504 3+1548	Aldehyde dehydrogenase	<i>Microbacterium esteraromaticum</i> MM1	99.81%	PYD0071
1_19815	Alcohol dehydrogenase	<i>Microbacterium</i>	98%	PYD0071

5-1035	dehydrogenase	<i>esteraromaticum</i> MM1	4.1
3_71052	Aldehyde dehydrogenase	<i>Microbacterium</i> <i>esteraromaticum</i> MM1	100% 8.1
3_71196	Aldehyde dehydrogenase	<i>Microbacterium</i>	98.75%
3-1443	Betaine-aldehyde dehydrogenase	<i>esteraromaticum</i> MM1	7.1
5_70954	Aldehyde dehydrogenase	<i>Microbacterium</i> <i>esteraromaticum</i> B Mb 05.01	94.79% 1
+1029	Amidohydrolase 2	<i>Microbacterium</i> <i>laevaniformans</i> OR221	100% 1
5_72002	4-oxalomesaconate hydratase	<i>Microbacterium</i> <i>saccharophilum</i> UNC380MFSHa3. 1	92.40% 1
	4-carboxy-4-hydroxy-2-oxoadipate	<i>Microbacterium</i>	100%
	4-carboxy-4-hydroxy-2-oxoadipate		EIC07243.

+699	aldolase	aldolase/oxaloacetate decarboxylase	<i>laevaniformans</i> OR22	100%	1
5_72703	2-pyrone-4,6-dicarboxylic acid	Amidohydrolase 2	<i>Microbacterium</i>	100%	EIC07242.
+954	hydrolase		<i>laevaniformans</i> OR22		1
		2-pyrone-4,6-dicarboxylate hydrolase	<i>Microbacterium</i> sp. 67-17	91.96%	OJV99931 .1
5_75008	4-carboxy-2-hydroxymuconate-6-	Oxidoreductase domain protein	<i>Microbacterium</i>	100%	EIC07240.
+954	semialdehyde dehydrogenase		<i>laevaniformans</i> OR221		1
		4-carboxy-2-hydroxymuconate-6- semialdehyde dehydrogenase	<i>Microbacterium</i> <i>hydrocarbonoxyda</i> <i>ns</i> SA35	90.07%	KJL47309 .1

Table 16 Hits for phthalate ester-degradative genes reported in literature in the genomes of *Microbacterium* sp. OR16 and *Microbacterium* sp. OR21 via local BLAST searches.

Subject genome	Gene location in subject genome	PATRIC annotation	Query protein GenBank accession number and host	Query protein description	Query coverage (%)	Subject coverage (%)	E value	Protein identity (%)	Query reference
OR16	1_90061	Putative	<i>Microbacte</i>	DpeH	90	89	6.00E	29	Lu et al
	2+696	esterase	<i>rium</i> sp.	(hydrolyzes			-10		(2020)
			PAE-1 AZP89727. 1	dialkyl phthalate esters)					
OR21	11_2811	hypothetical	<i>Microbacte</i>	DpeH	100	100	7.00E	97	Lu et al
	-723	1 protein	<i>rium</i> sp.	(hydrolyzes			-154		(2020)
OR21	5_22965	salicylate	PAE-1 AZP89727. 1	dialkyl phthalate esters)					
			<i>Microbacte</i>	DpeH	100	100	1.00E	54	Lu et al

-714	esterase	<i>rium</i> sp.	(hydrolyzes dialkyl phthalate esters)	100	100	0	-68	(2020)
OR21	11_2072	hypothetica <i>Microbacte</i>	MpeH	100	100	0		Lu et al (2020)
-915	1 protein	<i>rium</i> sp.	(hydrolyzes monoalkyl phthalate esters)	1				
		PAE-1						
		AZP89726.						
OR21	5_22255	hypothetica <i>Microbacte</i>	MpeH	95	93	1.00E		Lu et al (2020)
-915	1 protein	<i>rium</i> sp.	(hydrolyzes monoalkyl phthalate esters)	1		-58		
		PAE-1						
		AZP89726.						
OR21	11_7431	Phthalate	Phthalate	100	57	1.00E		Zhao et al (2017)
-1290	3,4-dioxygenas	<i>rium</i> sp. J-1	dioxygenase large subunit, partial	1		-133		
		ALT56978.						
	e alpha subunit							

OR21	5_20415	Phthalate	<i>Microbacte</i>	Phthalate	100	52	4.00E	71	Zhao et al
	-1395	3,4-dioxygenas	<i>rium</i> sp. J-1	dioxygenase			-128		(2017)
		e alpha	ALT56978.	large					
		subunit	1	subunit,					
		subunit		partial					
OR16	2_30466	Flavodoxin	<i>Microbacte</i>	Phthalate dio	94	98	2.00E	35	
	0-924	reductases	<i>rium</i>	xygenase red			-35		
		(ferredoxin-	<i>oxydans</i>	uctase					
		NADPH	BEL4b						
		reductases)	KJL29263.						
		family 1	1						
OR21	2_22646	1,2-	<i>Microbacte</i>	Phthalate dio	84	79	7.00E	28	
	2+1164	phenylacety	<i>rium</i>	xygenase red			-10		
		l-CoA	<i>oxydans</i>	uctase					
		epoxidase,	BEL4b						
		subunit E	KJL29263.						
			1						
OR21	11_7431	Phthalate	<i>Mycobacter</i>	Phthalate	96	66	1.00E	80	Stingley et
	-1290	3,4-	<i>ium</i> sp.	dioxygenase			-176		al (2004)

	dioxygenas	PAH2.135	large						
	e alpha subunit	AAQ93688	subunit, partial						
OR21	Phthalate 3,4-dioxygenas	<i>Mycobacterium</i> sp. PAH2.135	Phthalate dioxygenase large subunit, partial	100	63	1.00E-176	77	Stingley et al (2004)	
OR21	oxidoreductase of aldo/keto reductase family, subgroup 1	<i>Gordonia</i> sp. HS-NH1 AIU94734.1	Phthalate dihydrodiol dehydrogenase	95	97	9.00E-124	60	Li et al (2016)	
OR16	2,5-didehydrogluconate reductase (2-dehydro-	<i>Gordonia</i> sp. HS-NH1 AIU94734.1	Phthalate dihydrodiol dehydrogenase	98	97	5.00E-67	40	Li et al (2016)	

subunit												
OR21	5_19024	Aromatic- ring- hydroxylati ng dioxygenas e, beta subunit	<i>Gordonia</i> sp. HS- NH1 AIU94732. 1	Phthalate dioxygenase small subunit	96	96	1.00E -92	68	Li et al (2016)			
OR21	11_5231 -198	hypothetica I protein	<i>Gordonia</i> sp. HS- NH1 AIU94735. 1	Phthalate dioxygenase ferredoxin subunit	100	97	1.00E -21	78	Li et al (2016)			
OR21	5_18105 -195	Ferredoxin	<i>Gordonia</i> sp. HS- NH1 AIU94735. 1	Phthalate dioxygenase ferredoxin subunit	100	98	2.00E -17	67	Li et al (2016)			
OR21	11_5037	Ferredoxin	<i>Gordonia</i> 1	Phthalate	97	56	7.00E	47	Li et al			

	se; 3,4-									
	dihydroxyp									
	hthalate									
	decarboxyla									
	se									
OR16	1_21794	Ribulose-5-	<i>Gordonia</i>	Dihydroxyp	80	85	2.00E	25	Li et al	
	78+636	phosphate	sp. HS-	hthalate			-10		(2016)	
		4-epimerase	NH1	decarboxylas						
		and related	AIU94737.	e						
		epimerases	1							
		and								
		aldolases								
OR21	5_20415	Phthalate	<i>Rhodococc</i>	benzoate	80	80	6.00E	30	Song et al	
	-1395	3,4-	<i>us</i> sp. LW-	1,2-			-47		(2022)	
		dioxygenas	XY12	dioxygenase						
		e alpha	QXU53417	large subunit						
		subunit	.1							
OR21	11_7431	Phthalate	<i>Rhodococc</i>	benzoate	75	82	1.00E	30	Song et al	
	-1290	3,4-	<i>us</i> sp. LW-	1,2-			-42		(2022)	

dioxygenas	XY12	dioxygenase
e alpha	QXU53417	large subunit
subunit	.1	



Table 17 Genes in OR05, OR16, and OR21 mapped to the benzoate degradation via hydroxylation pathway.

Genome Name	Gene location	Gene product
<i>Sporosarcina</i> sp. OR05	8_64058+1116	Muconate cycloisomerase (EC 5.5.1)
<i>Microbacterium</i> sp. OR16	1_57554-759	Enoyl-CoA hydratase (EC 4.2.1.17)
<i>Microbacterium</i> sp. OR16	1_890211+891	Acyl-CoA thioesterase II (EC 3.1.2.-)
<i>Sporosarcina</i> sp. OR05	1_535016+774	Enoyl-CoA hydratase (EC 4.2.1.17)
<i>Microbacterium</i> sp. OR21	3_591196+861	Acyl-CoA thioesterase II (EC 3.1.2.-)
<i>Sporosarcina</i> sp. OR05	1_159864-777	Enoyl-CoA hydratase (EC 4.2.1.17)
<i>Sporosarcina</i> sp. OR05	3_29262+780	Enoyl-CoA hydratase (EC 4.2.1.17)
<i>Sporosarcina</i> sp. OR05	2_223398+936	Enoyl-CoA hydratase (EC 4.2.1.17)
<i>Microbacterium</i> sp. OR21	2_203230+759	Enoyl-CoA hydratase (EC 4.2.1.17)
<i>Microbacterium</i> sp. OR21	2_449681-822	Enoyl-CoA hydratase (EC 4.2.1.17)
<i>Microbacterium</i> sp. OR21	5_70954+1029	4-oxalomesaconate hydratase (EC 4.2.1.83)
<i>Microbacterium</i> sp. OR16	1_781538+2160	3-ketoacyl-CoA thiolase (EC 2.3.1.16)
<i>Sporosarcina</i> sp. OR05	7_67634-1188	Acetyl-CoA acetyltransferase (EC 2.3.1.9)
<i>Microbacterium</i> sp. OR16	2_268514-804	Enoyl-CoA hydratase (EC 4.2.1.17)
<i>Microbacterium</i> sp. OR16	2_175651-810	Enoyl-CoA hydratase (EC 4.2.1.17)
<i>Microbacterium</i> sp. OR21	5_68317-1185	P-hydroxybenzoate hydroxylase (EC 1.14.13.2)
<i>Sporosarcina</i> sp. OR05	7_66419-852	3-hydroxybutyryl-CoA dehydrogenase (EC 1.1.1.157)
<i>Microbacterium</i> sp. OR21	2_246250+1167	Catechol 2,3-dioxygenase (EC 1.13.11.2)
<i>Microbacterium</i> sp. OR21	3_496856+1206	3-ketoacyl-CoA thiolase (EC 2.3.1.16)
<i>Sporosarcina</i> sp. OR05	1_768396+909	Branched-chain phosphotransacylase

		(EC 2.3.1.-)
<i>Microbacterium</i> sp. OR16	1_8745-1167	Catechol 2,3-dioxygenase (EC 1.13.11.2)
<i>Microbacterium</i> sp. OR21	5_73659+1353	Protocatechuate 4,5-dioxygenase beta chain (EC 1.13.11.8)
<i>Microbacterium</i> sp. OR16	2_79735-510	Ribosomal-protein-S18p-alanine acetyltransferase (EC 2.3.1.-)
<i>Sporosarcina</i> sp. OR05	3_267420+1176	3-ketoacyl-CoA thiolase [fadN-fadA-fadE operon] (EC 2.3.1.16)
<i>Sporosarcina</i> sp. OR05	6_106003+1413	Probable poly(beta-D-mannuronate) O-acetylase (EC 2.3.1.-)
<i>Microbacterium</i> sp. OR21	2_332883-600	Ribosomal-protein-S18p-alanine acetyltransferase (EC 2.3.1.-)
<i>Microbacterium</i> sp. OR21	5_72703+954	2-pyrone-4,6-dicarboxylic acid hydrolase (EC 3.1.1.57)
<i>Microbacterium</i> sp. OR21	5_72002+699	4-carboxy-4-hydroxy-2-oxoadipate aldolase (EC 4.1.3.17)
<i>Microbacterium</i> sp. OR16	1_664514+1524	Apolipoprotein N-acyltransferase (EC 2.3.1.-) in lipid-linked oligosaccharide synthesis cluster
<i>Microbacterium</i> sp. OR16	2_314712-1581	Apolipoprotein N-acyltransferase (EC 2.3.1.-) in lipid-linked oligosaccharide synthesis cluster
<i>Microbacterium</i> sp. OR21	2_592145-1578	Apolipoprotein N-acyltransferase (EC 2.3.1.-) in lipid-linked oligosaccharide synthesis cluster
<i>Microbacterium</i> sp. OR21	3_373392+1524	Apolipoprotein N-acyltransferase (EC 2.3.1.-) in lipid-linked oligosaccharide synthesis cluster
<i>Microbacterium</i> sp. OR16	1_486553+1179	3-ketoacyl-CoA thiolase (EC 2.3.1.16); Acetyl-CoA

		acetyltransferase (EC 2.3.1.9)
<i>Microbacterium</i> sp. OR16	1_928484-768	3-ketoacyl-CoA thiolase (EC 2.3.1.16); Acetyl-CoA acetyltransferase (EC 2.3.1.9)
<i>Microbacterium</i> sp. OR16	1_1724422-1179	3-ketoacyl-CoA thiolase (EC 2.3.1.16); Acetyl-CoA acetyltransferase (EC 2.3.1.9)
<i>Sporosarcina</i> sp. OR05	8_38517+1149	3-ketoacyl-CoA thiolase (EC 2.3.1.16); Acetyl-CoA acetyltransferase (EC 2.3.1.9)
<i>Sporosarcina</i> sp. OR05	8_65189+1200	3-ketoacyl-CoA thiolase (EC 2.3.1.16); Acetyl-CoA acetyltransferase (EC 2.3.1.9)
<i>Sporosarcina</i> sp. OR05	2_422368+1185	3-ketoacyl-CoA thiolase (EC 2.3.1.16); Acetyl-CoA acetyltransferase (EC 2.3.1.9)
<i>Microbacterium</i> sp. OR21	3_216318+1179	3-ketoacyl-CoA thiolase (EC 2.3.1.16); Acetyl-CoA acetyltransferase (EC 2.3.1.9)
<i>Microbacterium</i> sp. OR21	3_629163-768	3-ketoacyl-CoA thiolase (EC 2.3.1.16); Acetyl-CoA acetyltransferase (EC 2.3.1.9)
<i>Microbacterium</i> sp. OR21	1_508745+1179	3-ketoacyl-CoA thiolase (EC 2.3.1.16); Acetyl-CoA acetyltransferase (EC 2.3.1.9)
<i>Microbacterium</i> sp. OR21	1_524549+777	Enoyl-CoA hydratase (EC 4.2.1.17)
<i>Microbacterium</i> sp. OR21	2_203985+855	3-hydroxybutyryl-CoA dehydrogenase (EC 1.1.1.157); 3-hydroxyacyl-CoA dehydrogenase (EC 1.1.1.35)
<i>Microbacterium</i> sp. OR16	1_56799-855	3-hydroxybutyryl-CoA

		dehydrogenase (EC 1.1.1.157); 3-hydroxyacyl-CoA dehydrogenase (EC 1.1.1.35)
<i>Microbacterium</i> sp. OR16	1_150143+861	3-hydroxybutyryl-CoA dehydrogenase (EC 1.1.1.157); 3-hydroxyacyl-CoA dehydrogenase (EC 1.1.1.35)
<i>Microbacterium</i> sp. OR16	1_1708646-801	Enoyl-CoA hydratase (EC 4.2.1.17)
<i>Microbacterium</i> sp. OR16	1_58737-1191	3-oxoadipyl-CoA thiolase (EC 2.3.1.174); 3-oxo-5,6-dehydrosuberil-CoA thiolase (EC 2.3.1.223)
<i>Microbacterium</i> sp. OR16	2_304660-924	Flavodoxin reductases (ferredoxin-NADPH reductases) family 1; Vanillate O-demethylase oxidoreductase (EC 1.14.13.-)
<i>Sporosarcina</i> sp. OR05	3_265007+2385	3-hydroxyacyl-CoA dehydrogenase [fadN-fadA-fadE operon] (EC 1.1.1.35) / Enoyl-CoA hydratase [fadN-fadA-fadE operon] (EC 4.2.1.17)
<i>Microbacterium</i> sp. OR21	3_498067+2160	Enoyl-CoA hydratase (EC 4.2.1.17) / 3-hydroxyacyl-CoA dehydrogenase (EC 1.1.1.35) / 3-hydroxybutyryl-CoA epimerase (EC 5.1.2.3)
<i>Microbacterium</i> sp. OR16	1_781538+2160	Enoyl-CoA hydratase (EC 4.2.1.17) / 3-hydroxyacyl-CoA dehydrogenase (EC 1.1.1.35) / 3-hydroxybutyryl-CoA epimerase (EC 5.1.2.3)

4.3.3.2 Predicted pathway of DEHP biodegradation by Consortium A02 based on genomic analysis

The pathway of PAE biodegradation is typically divided into two phases. The first phase encompasses the conversion of phthalate esters to phthalic acid through sequential hydrolysis of the two ester bonds of PAEs or reduction of the alkyl chain length of PAEs via β -oxidation (Ren et al 2018a, Xu et al 2021). Based on the genomic analyses of OR05, OR16, and OR21, the pathway of DEHP biodegradation by Consortium A02 was predicted (Figure 40). The enzymes with potential to catalyze the different degradation steps, and for which genes were detected in the genomes of the three bacterial strains of Consortium A02 are represented by numbers (Table 18).

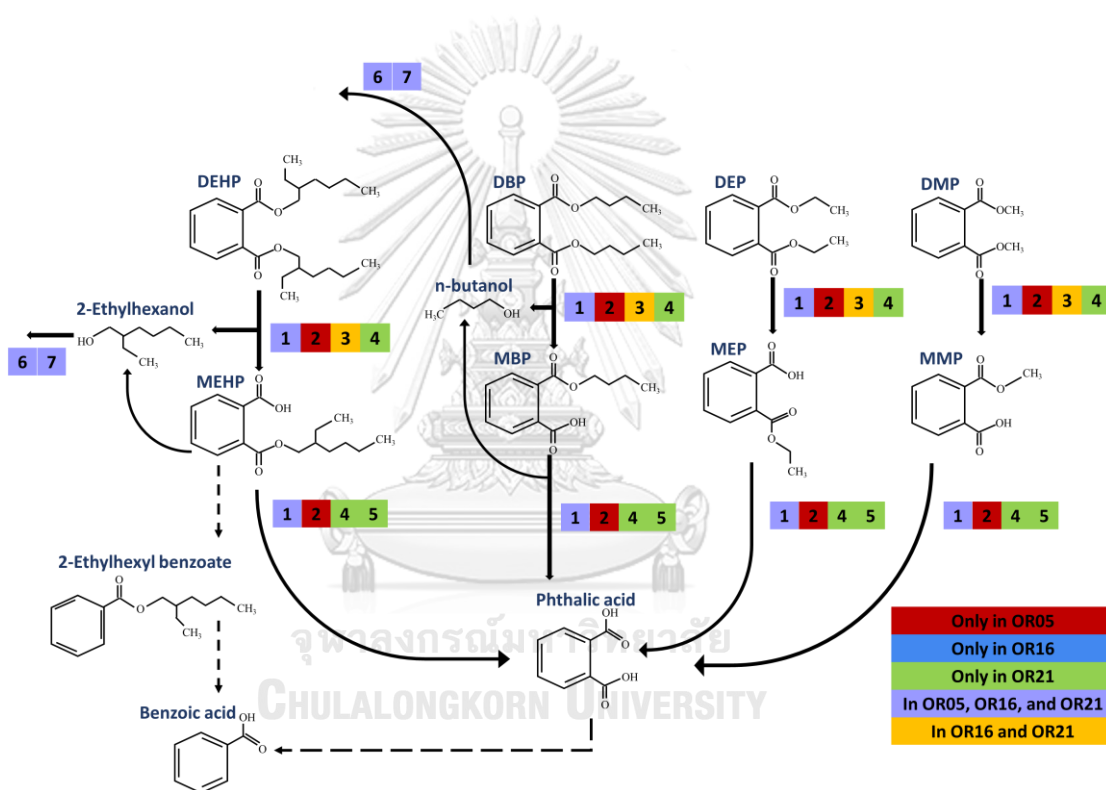
It is expected that DEHP will be transformed to its monoester MEHP and one molecule of 2-ethylhexanol via side chain hydrolysis. MEHP is then likely to undergo another side chain hydrolysis step to yield phthalic acid and one molecule of 2-ethylhexanol. These side chain hydrolysis steps are expected to be catalyzed by enzymes belonging to the alpha/beta fold superfamily of hydrolases, including phthalate ester hydrolase, carboxylesterase and other putative phthalate esterases. As shown in Table 15, OR05 has two genes encoding carboxylesterase and two genes encoding other esterases. The genomes of OR21 and OR16 contain three and two genes, respectively, that encode for esterases. Furthermore, all three genomes carry genes for hydrolase (alpha/beta fold family). This information indicates that all the three members of Consortium A02 have the genomic potential to degrade PAEs; however, this potential translates to actual PAE degradation ability for only OR16 and OR21.

Microbacterium sp. OR21, a Gram-positive bacterium, harbors genes whose amino acid sequences have high degrees of similarities with phthalate 3,4-dioxygenase-encoding genes in literature (Table 15). Phthalate 3,4-dioxygenase catalyzes the conversion of phthalic acid to 3,4-dihydroxy phthalate, which is then transformed to protocatechuic acid by the action of 3,4-dihydroxy phthalate decarboxylase. Furthermore, OR16 possess genes encoding for PDR/VanB family oxidoreductase. The protocatechuic acid formed is then expected to be transformed via the *meta* (catalyzed by protocatechuate 4,5-dioxygenase) or *ortho* (catalyzed by protocatechuate 3,4-dioxygenase) pathways to form 4-carboxy-2-hydroxy muconate semialdehyde or 3-carboxymuconic acid, respectively. As mentioned in Section 4.3.3.1, the protocatechuate dioxygenase in OR21 shares high similarities with the amino acid sequences of both protocatechuate 4,5-dioxygenase and protocatechuate 3,4-dioxygenase from *Microbacterium* spp. Although genes encoding for protocatechuate dioxygenase was not detected in the genome of OR16, this strain could degrade about 17% of 100 mg/L protocatechuic acid in 4 d. It is possible that general aromatic-ring hydroxylating dioxygenase catalyzes the degradation of protocatechuic acid by OR16. OR21 possesses the genomic potential for hydrolysis of the *meta* cleavage product, 4-carboxy-2-hydroxy muconate semialdehyde, which is expected to be further hydrolyzed by 2-pyrone-4,6-dicarboxylate hydrolase to 4-oxalomesaconate, which will then be converted to 4-carboxy-4-hydroxy-2-oxoadipate by 4-oxalomesaconate hydratase. Finally, 4-carboxy-4-hydroxy-2-oxoadipate is expected to be cleaved by 4-carboxy-4-hydroxy-2-oxoadipate aldolase to produce pyruvate and oxaloacetate (Hara et al 2000). For the *ortho* cleavage pathway, 3-carboxymuconic acid is expected to be transformed to 3-oxoadipate; however, no

genes encoding for the enzymes (3-carboxymuconate cycloisomerase and 4-carboxymuconolactone decarboxylase) that catalyze this transformation was detected. Investigations into the role of the protocatechuate dioxygenase gene during PAE degradation by OR21 through gene expression studies coupled with monitoring of intermediates formed during PAE degradation can, therefore, reveal interesting new insights into PAE biodegradation by *Microbacterium* sp. OR21 and are worthwhile future investigations.

Although it has been widely reported that decarboxylation of phthalic acid to benzoic acid occurs anaerobically (Zhao et al 2018b), some studies have found that facultative anaerobic bacteria can catalyze this reaction under aerobic conditions (Xu et al 2021). Song et al (2022) proposed that *Rhodococcus* sp. LW-XY12 converts phthalic acid generated during DEHP degradation to benzoic acid via decarboxylation. Zhang et al (2018) also detected the formation of benzoic acid during degradation of seven phthalate esters, including DEHP, DBP, DEP, and DMP, by *Bacillus mojavensis* B1811 isolated from oil-polluted soil. A benzoate transporter protein was annotated in the genome of OR16. Furthermore, several genes in the genomes of OR05, OR16, and OR21 were mapped to the benzoate degradation pathway (Table 17). Wright et al (2020) reported that three pathways of benzoate degradation to form catechol, gentisate, or protocatechuate. The cleavage of catechol can occur via the *ortho* or *meta* cleavage pathways, which are catalyzed by catechol 1,2-dioxygenase and catechol 2,3-dioxygenase, respectively (Song et al 2022). The genomes of OR16 and OR21 possess the gene for catechol 2,3-dioxygenase, while OR05 possesses the gene for catechol 1,2-dioxygenase. This indicates that catechol degradation by Consortium A02 may be via the *ortho*- or *meta*- cleavage pathways. It

has to be noted that PAE degradation pathway predicted for Consortium A02 in this study is based the detection of phthalate-degradation genes in the genomes of its three component strains. More studies such as analysis of the expression of the phthalate-degradative genes through real time quantitative PCR (Wang et al 2022), transcriptome sequencing (Wang et al 2021d), and metabolomic analysis (Wright et al 2020) are needed to confirm the roles of the different genes detected.



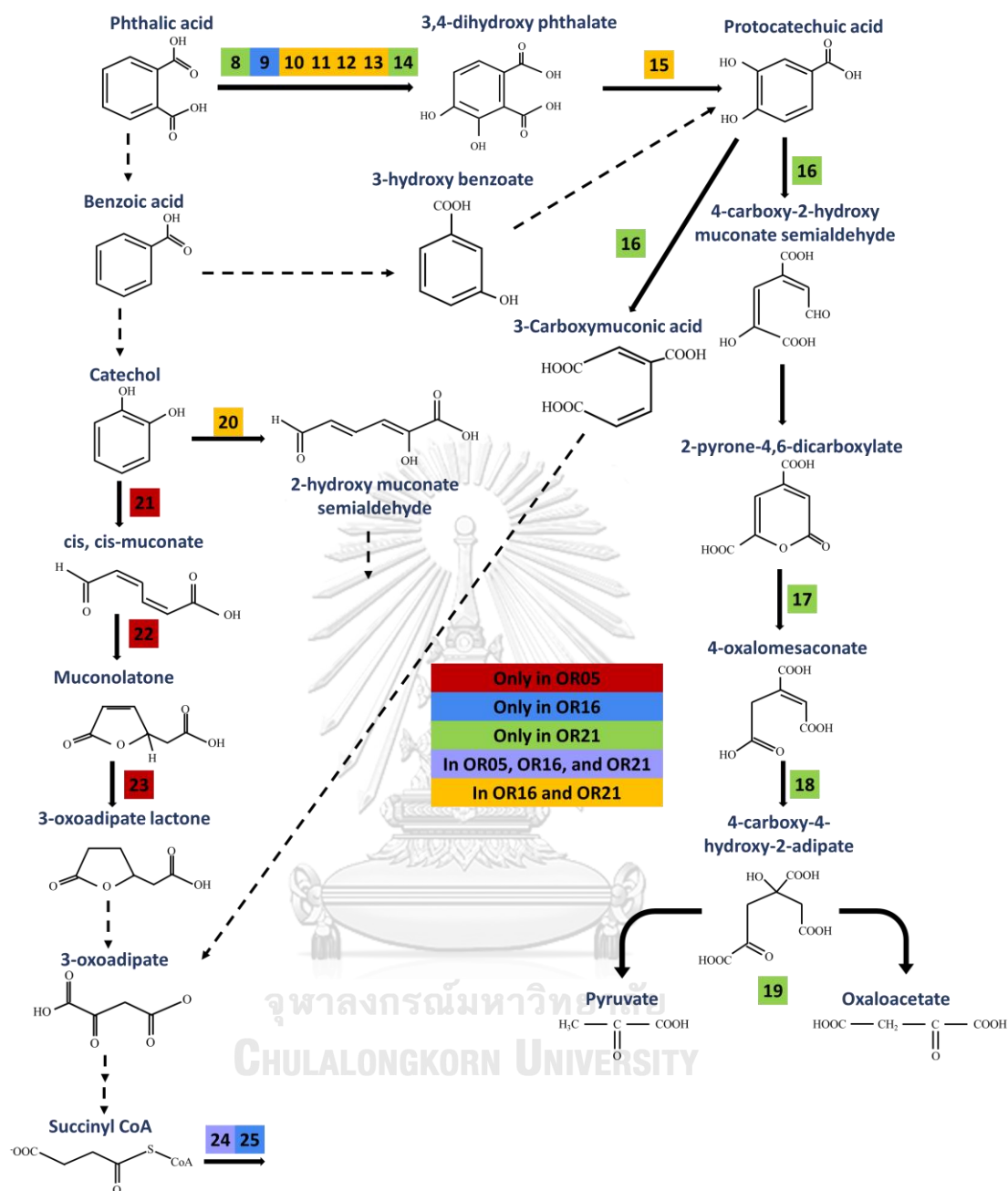


Figure 40 PAE degradation pathway predicted based on genomic analysis on OR05, OR16, and OR21. The dashed lines represent degradation steps for which enzymes are unknown or have not been detected in the genomes of OR05, OR16, and OR21. The numbers within the boxes represent the potential degradation enzymes detected in the genomes of OR05, OR16, and OR21 (Table 18).

4.3.3.3 Predicted roles of OR05, OR16, and OR21 in DEHP degradation by Consortium A02

In Phase II, it was found that both OR16 and OR21 showed DEHP degradation activity (59.1 and 84.5% degradation of 100 mg/L DEHP in 8 d). In Phase III, Consortium A02 (comprised of OR05, OR16, and OR21) showed faster DEHP degradation (both in degradation of DEHP separately and as a mixture with other PAEs) than the co-culture of OR05 and OR21. This implies that both OR16 and OR21 contributes to DEHP degradation by Consortium A02. This coupled with the lack of antagonistic interaction (via cross-streak method) and the increase in viable cell counts of both OR16 and OR21 during DEHP and mix PAE degradation by Consortium A02, implies that OR16 and OR21 share a homotypic cooperative interaction (Rodríguez Amor & Dal Bello 2019), wherein they share the load of DEHP degradation. The genome analysis and experimental results indicate that OR21 would be primarily attributable for MEHP degradation by Consortium A02. The 2-ethylhexanol molecules generated via DEHP and MEHP degradation could then be degraded by OR05 as OR05 could grow on 2-ethylhexanol as sole carbon source. This indicates that OR05 shares a syntrophic relationship with the other members of Consortium A02 (Canon et al 2020). OR16 could utilize phthalic acid as carbon source for growth. Furthermore, both the genomes of OR16 and OR21 possess the genomic potential for phthalic acid degradation (Tables 15 and 16). However, OR16 and OR21 could degrade only about 5% and 2.3%, respectively of 100 mg/L of phthalic acid in 4 d. This discrepancy between the genomic degradation potential and the experimental degradation efficiency could be because expression of the genes encoding for phthalate-degradation enzyme could not be efficiently induced under the

conditions used (Wright et al 2020). It is also possible that degradation of PAEs by OR16 and OR21 does not proceed via phthalic acid; the degradation of PAEs via the decarboxylation of phthalate monoesters to form benzoic acid has been reported (Song et al 2022). However, the specific decarboxylase responsible for this degradation step is still unclear. Therefore, more in-depth studies such as transcriptomic analyses and detection of metabolites during PAE degradation are needed for a better understanding of the enzymes involved in PAE degradation. Meanwhile, Consortium A02, OR05 + OR16, and OR05 + OR21 could degrade about 10%, 5%, and 4%, respectively of phthalic acid. This indicates that the co-occurrence of OR16 and OR21 enhances phthalic acid degradation. Lastly, as both OR16 and OR21 have protocatechuic acid degradation activity (17 and 21% in 4 d), it can be hypothesized that both strains contribute to protocatechuic acid degradation by Consortium A02 (29%).

Table 18 Enzymes used for the prediction of the PAE degradation pathway of Consortium A02.

Enzyme	OR05	OR16	OR21
1 Alpha/beta hydrolase	+	+	+
2 Carboxylesterase	+		
3 Protein similar to DpeH (hydrolyzes dialkyl phthalate ester) from <i>Microbacterium</i> sp. J-1			+
4 Phthalate ester hydrolase (isochorismatase hydrolase)			+
5 Protein similar to MpeH (hydrolyzes monoalkyl phthalate ester) from <i>Microbacterium</i> sp. J-1			+
6 Alcohol dehydrogenase	+	+	+
7 Aldehyde dehydrogenase	+	+	+

8	Phthalate 3,4-dioxygenase alpha subunit			+
9	Phthalate dioxygenase reductase (PDR)/VanB family oxidoreductase		+	
10	Protein similar to phthalate dioxygenase reductase from <i>Microbacterium</i> sp. J-1		+	+
11	Protein similar to phthalate dihydrodiol dehydrogenase from <i>Gordonia</i> sp. HS-NH1		+	+
12	Aromatic ring-hydroxylating dioxygenase, beta subunit similar to phthalate dioxygenase from <i>Gordonia</i> sp. HS-NH1		+	+
13	Protein similar to phthalate dioxygenase ferredoxin subunit from <i>Gordonia</i> sp. HS-NH1		+	+
14	Protein similar to phthalate dioxygenase ferredoxin reductase subunit from <i>Gordonia</i> sp. HS-NH1			+
15	Protein similar to dihydroxyphthalate decarboxylase from <i>Gordonia</i> sp. HS-NH1		+	+
16	Protocatechuate dioxygenase			+
17	2-pyrone-4,6-dicarboxylic acid hydrolase			+
18	4-oxalomesaconate hydratase			+
19	4-carboxy-4-hydroxy -2-oxoadipate aldolase			+
20	Catechol 2,3-dioxygenase		+	+
21	Catechol 1,2-dioxygenase	+		
22	Muconate cycloisomerase	+		
23	3-oxoadipate enol-lactonase	+		
24	3-ketoacyl-CoA thiolase	+	+	+
25	3-oxoadipyl-CoA thiolase		+	

4.3.4 Sediment microcosm study

Most studies on bacteria-mediated PAE degradation focus on PAE degradation in aqueous media, and only a handful of studies have investigated the PAE-degrading efficiencies of bacterial strains in PAE-contaminated soil or sediment (Zhang et al 2018, Zhao et al 2018a). However, commonly used PAEs like DBP and DEHP are present in higher concentrations and frequencies in soil or sediment, owing to their hydrophobicity (Hidalgo-Serrano et al 2022). Therefore, in this study, the applicability of Consortium A02 for DEHP degradation in sediment microcosms was investigated. The sediment used for the microcosm experiment was obtained from a shrimp farm. It was mainly composed of sand, had a neutral pH, and was highly saline as indicated by its high electrical conductivity (EC) value (Table 19).

Table 19 Physical and chemical properties of sediment used in the microcosm study.

Parameter	Unit	Value
pH	-	6.76
Sand	%	64
Silt	%	17
Clay	%	19
Organic matter	g/kg	54
Available phosphorus	mg/kg	170
Available potassium	mg/kg	189
Available calcium	mg/kg	7145
Available magnesium	mg/kg	1141
Electrical conductivity (saturated with water)	dS/m	35.48
Organic carbon	%	3.14
Total nitrogen	g/kg	1.12

Total potassium	g/kg	5.13
Moisture	%	26.15
C/N ratio		28.09

Figure 41a shows the concentration of DEHP (mg/kg) remaining in the sediments of the abiotic control, natural attenuation, and A02 bioaugmented experiments from Day 0 to Day 26, while Figure 41b shows the percent DEHP degradation observed in the sediment. Till Day 11, DEHP degradation by indigenous sediment microbes (Natural attenuation) and in the A02 bioaugmented sediment were not significantly different. However, from Day 16 onwards, the bioaugmentation of indigenous microbes with Consortium A02 promotes DEHP degradation over that by indigenous microbes alone. This may indicate that the bioaugmented consortium undergoes an initial lag period, during which cell resources are directed towards adaptation to the new environment and hence no contribution is made to DEHP degradation. Nevertheless, by the end of the microcosm study on Day 26, 80% degradation of 100 mg/kg of DEHP was achieved in the A02 bioaugmented sediment, while only 53% DEHP degradation could be achieved by the indigenous sediment microbes alone. DEHP degradation in the sediment of the abiotic control on Day 26 was 4%. Thus, the bioaugmentation of indigenous sediment microbes with Consortium A02 significantly enhances DEHP degradation efficiency. As shown in Table 20, similar DEHP degradation efficiencies were achieved in sediment spiked with 100 mg/kg DEHP using consortium A02 in a shorter time than reports in literature. For instance, Bai et al (2020) reported 87.53% degradation of 100 mg/kg of DEHP in farmland soil treated with an enriched bacterial consortium and biochar in 42 d. It is worth noting that the sediment used in this microcosm study is highly saline

as indicated by its high EC (35.48 dS/m). Researchers have reported decrease in the PAE-degradation efficiencies of bacteria with increase in salinity (Zhang et al 2020). Li et al (2018) observed that DEHP degradation by a halotolerant bacterial consortium LF decreased dramatically at NaCl concentrations higher than 4%. Therefore, Consortium A02 shows high potential applicability for the bioremediation of PAE-contaminated sites with high salinity. Very low DEHP concentrations were detected in the seawater fraction of the abiotic control (Table 21), while DEHP was not detected in seawater of the natural attenuation and A02 bioaugmented experiments.

Table 20 DEHP degradation efficiencies in soil/sediment microcosms by augmentation with bacteria in literature.

Bioaugmentation agent	Initial concentration	Soil/sediment	Degradation	Reference
<i>Microbacterium</i> sp. J-1 isolated from landfill soil	50 mg/kg	Agricultural soil	88% degradation in 35 d	Zhao et al (2017)
Consortium CM9 enriched from farmland soil + biochar	100 mg/kg	Farmland soil	87.53% in 42 d	Bai et al (2020)
<i>Gordonia</i> sp. Lff isolated from river sludge	100 mg/kg	Soil	86.5% in 35 d	Wang et al (2019b)
<i>Gordonia terrae</i> RL-JC02 isolated from soil with history of plastic mulch use	50 mg/kg	Garden soil	91.8% in 30 d	Zhang et al (2020)
<i>Rhodococcus</i>	25 mg/kg	Soil from an	59.9% in 25 d	Zhao et al

<i>pyridinivorans</i> XB isolated from activated sludge		experimental field		(2018a)
<i>Rhodococcus pyridinivorans</i> XB isolated from activated sludge	100 mg/kg	Soil from an experimental field	53.63% in 25 d	Zhao et al (2018a)
<i>Mycolicibacterium phocaicum</i> RL-HY01 from intertidal sediment	50 mg/kg	Muddy sediment	57.6% in 21 d	Ren et al (2021)
<i>Mycolicibacterium phocaicum</i> RL-HY01 from intertidal sediment	50 mg/kg	Sandy sediment	79.3% in 21 d	Ren et al (2021)
<i>Mycolicibacterium phocaicum</i> RL-HY01 from intertidal sediment	50 mg/kg	Mixed sediment	92.5% in 21 d	Ren et al (2021)
Defined consortium A02 comprised of three bacteria strains isolated from marine sediment	100 mg/kg	Saline shrimp farm sediment	76% in 21 d 80% in 26 d	This study

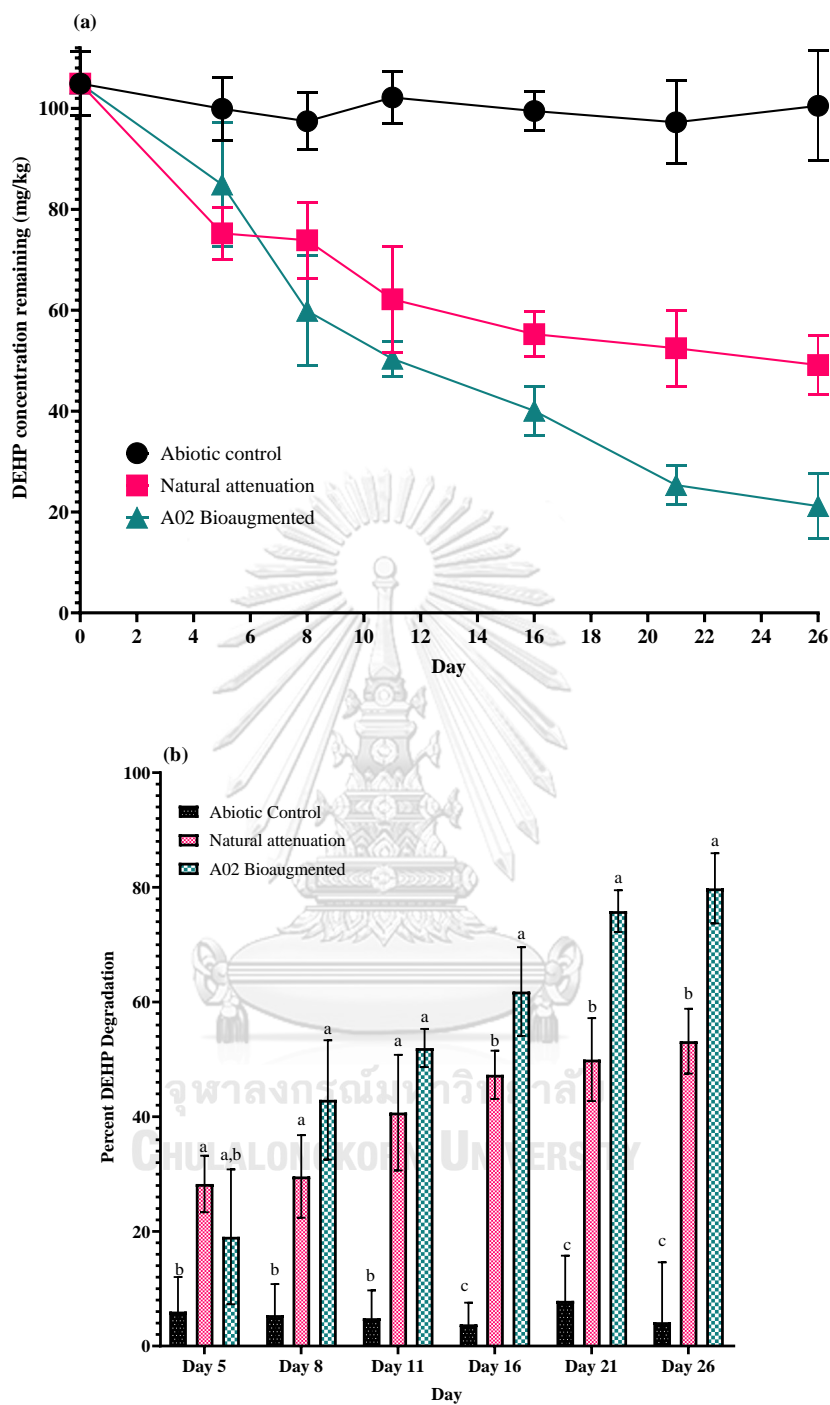


Figure 41 Remaining DEHP concentration (a) and percent DEHP degradation (b) in sediment of abiotic control, natural attenuation, and A02 bioaugmented microcosms. Different letters indicate significantly different ($p < 0.05$) percent DEHP degradation.

Table 21 DEHP levels in the seawater fraction of the abiotic control, natural attenuation, and A02 bioaugmented microcosms.

	Abiotic control (mg/L)	Natural attenuation (mg/L)	A02 Bioaugmented (mg/L)
Day 0	ND	ND	ND
Day 5	1.5 ± 2.2	ND	ND
Day 8	1.8 ± 0.7	ND	ND
Day 11	1.06 ± 0.8	ND	ND
Day 16	2.3 ± 0.7	ND	ND
Day 21	1.9 ± 0.6	ND	ND
Day 26	2.5 ± 0.9	ND	ND
ND: Not detected			

CHAPTER 5

CONCLUSIONS AND RECOMMENDATIONS

5.1 Conclusions

In this study, nine DEHP-degrading bacterial consortia were enriched from marine sediment collected from the Gulf of Thailand. Bacterial community analyses of the marine sediment and corresponding enriched bacterial consortia revealed enhanced populations of Gammaproteobacteria and Bacilli after enrichment with DEHP as a carbon source, indicating that bacteria from these classes may play a role in phthalate ester degradation in marine sediment. Enriched consortium C10 could almost completely degrade DEHP, DBP, DEP, and DMP within 4 d, while about 96% of a mixture of the four PAEs (DEHP, DBP, DEP, and DMP) could be degraded by C10 within 6 d. Growth of C10 on MEHP, phthalic acid, and protocatechuic acid as sole source of carbon was higher than that in the biological control (without carbon source), indicating that C10 has the potential to degrade these DEHP intermediates. Meanwhile, growth of C10 on 2-ethylhexanol was initially delayed, indicating potential toxicity of this DEHP intermediate. The bacterial community composition of C10 was observed to shift in response to the type of substrate (PAEs and DEHP intermediates) added to the culture medium, indicating the different roles of the bacterial members of C10 during DEHP/PAE degradation. Similarly, shifts in predicted bacterial community functions, especially functions related to amino acid metabolism and signal transduction, in response to the type of substrate were observed. Based on network analyses of the bacterial composition and abundance data, it was predicted that the *Bacillus* spp., *Stenotrophomonas* spp., and *Microbacterium* spp. in C10 are the key PAE-degraders in this enriched consortium.

Twenty-one bacterial isolates were obtained from C10, of which *Microbacterium* sp. OR21 (84.5%), *Stenotrophomonas acidaminiphila* OR13 (82.7%), *Microbacterium* sp. OR16 (59.1%), *Sporosarcina* sp. OR19 (43.4%), and *Cytobacillus firmus* OR20 (40.6%) showed the highest DEHP degradation activities. Several *Bacillus*, *Microbacterium*, and *Stenotrophomonas* isolates from C10 also showed the ability to utilize DEHP intermediates MEHP, protocatechuic acid, and monobutyl phthalate for growth. This lends support to the prediction of key PAE-degraders based on network analyses. Furthermore, it was predicted that bacteria belonging to genera like *Sporosarcina*, *Achromobacter*, and *Ochrobactrum* could play supporting roles, such as degradation of intermediates, during PAE-degradation by C10. Although *Achromobacter* isolates could not be obtained from C10, *Sporosarcina* sp. OR05 isolated from C10 could utilize 2-ethylhexanol as sole source of carbon for growth. Moreover, *Sporosarcina* strains OR05 and OR07, and *Ochrobactrum intermedium* OR12 showed biosurfactant production ability. A defined consortium comprising *Microbacterium* sp. OR21, *Microbacterium* sp. OR16, and *Sporosarcina* sp. OR05 (referred to as Consortium A02) could effectively degrade DEHP, DBP, DEP, and DMP (separately and as a mixture). Consortium A02 could also degrade MEHP, protocatechuic acid, and phthalic acid. Genomic analyses of the three strains in Consortium A02 revealed the presence of several genes encoding for PAE-degrading enzymes such as phthalate hydrolase and carboxylesterase. Genes encoding for other enzymes involved in the PAE degradation pathway such as phthalate, protocatechuate, and catechol dioxygenases and alcohol and aldehyde dehydrogenases were also detected. A pathway for PAE degradation by Consortium A02 was predicted based on genome analyses; however, more in-depth analyses such as

detection of metabolites formed and gene expression studies during PAE degradation are needed to validate this predicted PAE degradation pathway. Bioaugmentation of indigenous microbes with Consortium A02 could also greatly enhance DEHP-degradation in a saline sediment microcosm. Therefore, this study reveals as yet unknown insights into the PAE-degrading potential of marine sediment bacteria. For instance, this is the first report of DEHP degradation by *Stenotrophomonas acidaminiphila*, *Sporosarcina* sp., and *Cytobacillus firmus*. Furthermore, this study demonstrates a simple and easy approach for the prediction and isolation of key pollutant-degraders from complex bacterial communities. Lastly, a defined consortium created using isolated non-pathogenic key degraders could effectively enhance DEHP-degradation in a microcosm of saline shrimp farm sediment, indicating the potential applicability of this consortium for PAE-degradation in marine environment. An overview of the research results obtained is shown in Figure 42.

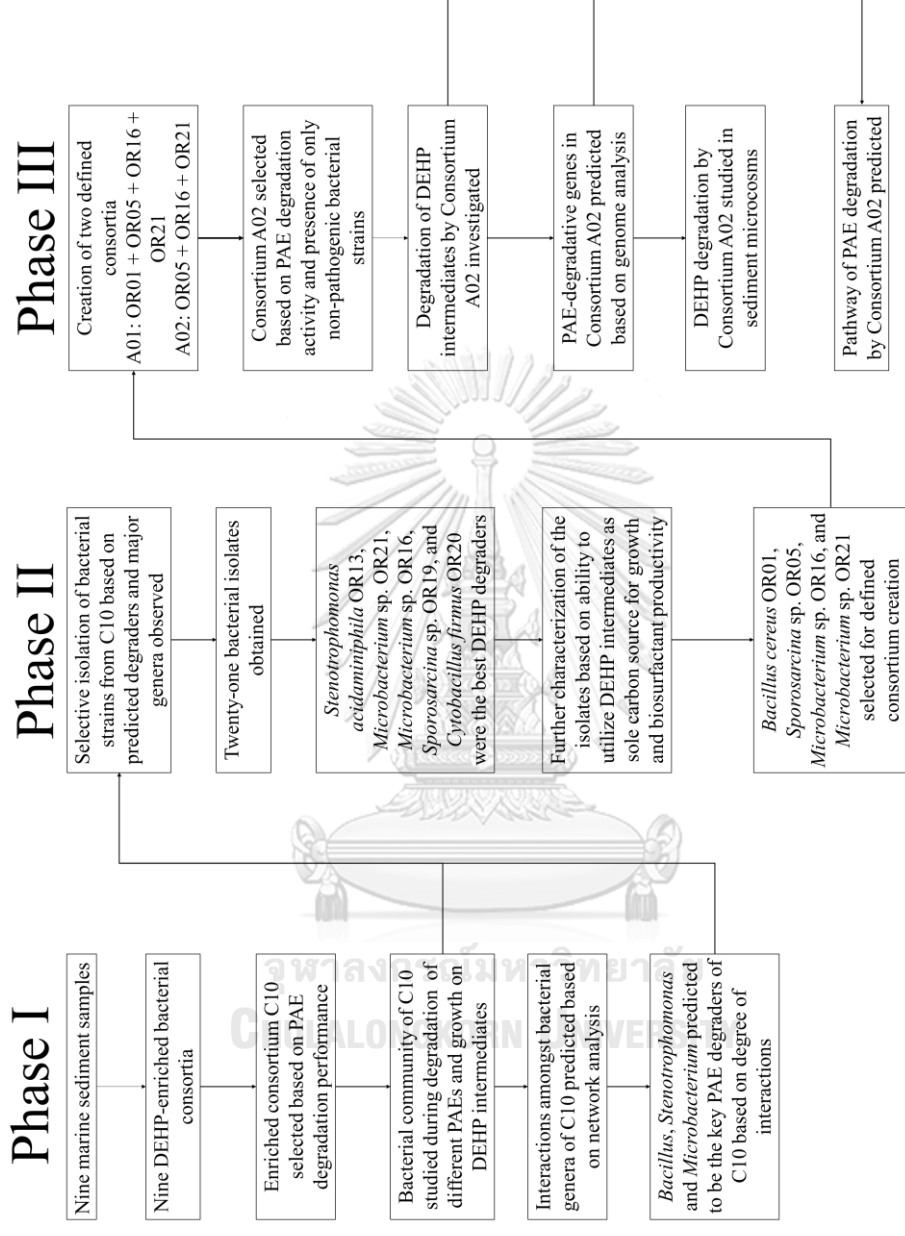


Figure 42 Overview of research results.

The conclusions derived for the hypotheses of these study are:

1. Marine sediment contains bacteria that can degrade DEHP and/or its metabolites such as mono-ethylhexyl phthalate, 2-ethylhexanol, and phthalic acid.
 - a. All nine bacterial consortia enriched from marine sediment showed DEHP-degradation activities.
 - b. Nine of the twenty-one isolates obtained from the enriched marine sediment bacterial consortium C10 showed DEHP degradation efficiencies greater than 20%.
 - c. Fourteen of the twenty-one isolates from C10 showed ability to utilize DEHP intermediates as sole carbon source for growth. For five of these fourteen isolates, growth on DEHP intermediate was significantly higher than in the biological control.
2. A defined bacterial consortium of key degraders isolated from a DEHP-enriched consortium will be able to degrade DEHP and its metabolites.
 - a. Defined consortium A02 comprised of *Sporosarcina* sp. OR05, *Microbacterium* sp. OR16, and *Microbacterium* sp. OR21 could degrade DEHP, DBP, DEP, and DMP (separately and as a mixture).
 - b. Defined consortium A02 could degrade MEHP, phthalic acid, and protocatechuic acid.
3. DEHP biodegradation in sediment microcosms bioaugmented with the defined bacterial consortium will be higher than DEHP biodegradation by natural attenuation.

- a. In DEHP-spiked sediment microcosm experiments, bioaugmentation with defined consortium A02 could degrade 80% of 100 mg/kg DEHP in 26 d, while natural attenuation by indigenous microbes could degrade only 53% DEHP within the same time period.

5.2 Recommendations

1. In this study, bacterial consortia were enriched from marine sediment using just DEHP. Furthermore, a relatively low concentration of DEHP (100 mg/L) was used during enrichment. Most relevant studies in literature use a much higher concentration of DEHP/PAE during bacterial enrichment (Bai et al 2020). This could explain the generally lower DEHP degradation efficiency of the enriched bacterial consortia and bacterial isolates obtained in this study. It would, therefore, be interesting to study if bacterial consortia enriched with higher DEHP concentrations and/or using multiple types of PAEs such as benzyl butyl phthalate, diisononyl phthalate, and DBP would result in higher and broader PAE degradation activities.
2. In contrast, it will be also be interesting to study if using environmentally relevant levels (with respect to the target site) of DEHP/PAE for bacterial enrichment will result in bacterial consortia with better degradation performance in the target environmental site.
3. In this study, bacterial communities of the original sediment samples were compared to the bacterial communities of the final enriched bacterial consortia. However, it will be interesting to study how the bacterial community composition changes during the enrichment process (Huang et al

2021). Furthermore, this will help identify the point of bacterial community stabilization during the enrichment process.

4. This study investigated the bacterial community of C10 on Day 4 of the degradation of DEHP, DBP, DEP, and DMP (separately). At this point, C10 could almost completely degrade all the four PAE types. Therefore, the major bacterial members observed may not be truly reflective of the key PAE-degraders in the enriched bacterial community. Studying the bacterial community of C10 at different points of degradation could, thus, reveal additional insights into the PAE-degrading potential of bacteria in C10.
5. The functional/metabolic potential of C10 was predicted based on 16S rRNA gene amplicon sequencing information. It would be worthwhile to confirm the bacterial community functions predicted for the C10 bacterial communities through meta-transcriptomic analyses (Wei et al 2021).
6. Some of the dominant genera and key degraders observed in C10 such as *Brevibacterium*, *Glutamicibacter*, and *Achromobacter* could not be isolated. This indicates that applying more selective isolation techniques, such as more specific selective media (Wang et al 2021c), could be help in obtaining additional isolates from C10.
7. The species level identification of the bacterial community of C10 based on long-read 16S rRNA gene amplicon sequencing could be used to design more specific bacterial isolation techniques.
8. Defined consortia could be created using additional strains from C10 such as *Microbacterium* sp. OR03, *Stenotrophomonas acidaminiphila* OR15, *Cytobacillus firmus* OR20. Then, the DEHP/PAE degradation efficiencies of

the defined consortia created using different combinations of strains could be compared.

9. In this study, bacterial strains were mixed at equal volumetric ratio to create defined consortia. The ratio at which the bacterial strains are mixed could be varied to optimize DEHP/PAE degrading efficiency (Gao et al 2020).
10. The role of *Sporosarcina* OR05, *Microbacterium* sp. OR16, and *Microbacterium* sp. OR21 in DEHP/PAE degradation could be confirmed by removing one strain at a time and monitoring the intermediates formed during PAE degradation in each case.
11. It will be interesting to study the PAE degradation performances of the source enriched consortium (C10), isolated single strains, and created defined consortia under various environmental conditions, such as pH and salinity, to compare the robustness of the different bacterial systems. Furthermore, the metabolites formed during PAE degradation by the different bacterial systems could be compared.
12. In this study, several genes encoding for potential PAE-degrading enzymes were detected in the genomes of OR05, OR16, and OR21 through genome sequencing and annotation. However, the presence of genes does not necessarily translate to the involvement of the gene in PAE degradation. Therefore, the expression of the potential PAE-degradative genes detected through whole genome sequencing should be studied during PAE degradation (Wang et al 2022). Metabolomic and proteomic analyses could also be carried out for clearer elucidation of the PAE degradation pathways (Wright et al 2020). In addition to identifying the genes involved in PAE degradation, this

will also provide a better understanding of the roles of the different bacterial strains during PAE degradation by Consortium A02. The expression of genes related to stress response during PAE degradation could also be studied for insights into how the bacterial strains adapt to the presence of PAEs.

13. The experimental degradation results and genome analyses indicate that Consortium A02 may have the potential to degrade other environmental pollutants, such as polycyclic aromatic hydrocarbons (PAHs), that share chemical structure similarity with PAEs. Investigating the degradation efficiencies of Consortium A02 for such environmental pollutants that are also commonly reported in the marine environment will therefore be a worthwhile future endeavor.
14. The DEHP degradation performance of *Microbacterium* sp. OR21 and Consortium A02 in sediment microcosms could be compared for a better understanding of the contribution of the other bacterial strains in Consortium A02. Monitoring the survival of the strains during PAE degradation could be useful in comparing the potential applicability of bioaugmentation with single bacterial strains and consortia of multiple strains (Dueholm et al 2015).
15. In this study, only DEHP concentrations were monitored in the sediment and seawater fractions of the microcosm. The formation of metabolites in the sediment and seawater fractions of the microcosm during DEHP degradation could be monitored to understand the DEHP degradation pathway in simulated environmental conditions (Zhu et al 2018) and the partitioning of DEHP and its metabolites in different environmental compartments. As the different metabolites of DEHP, such as MEHP, 2-ethylhexanol, and phthalic acid have

significantly different aqueous solubilities, investigating how the metabolites generated during DEHP/PAE degradation are distributed in different environmental media would be a worthwhile endeavor.

16. To assess the potential applicability of Consortium A02 for remediation of PAE-contaminated marine environments, the effect of Consortium A02 on aquatic biota could be assessed. Furthermore, the toxicities on aquatic life of the DEHP-spiked microcosms with and without bioaugmentation with Consortium A02 could be compared (Kögel et al 2020).
17. In this study, analyses of the bacterial communities in the sediments of the microcosm experiments could not be completed. However, shotgun metagenome analyses of the sediment samples from the natural attenuation and bioaugmented microcosms are being carried out. Further analyses will be carried out to understand the effect of the bioaugmented consortium in terms of interactions with indigenous microbes and influence on bacterial community composition and function.
18. Bacterial isolates OR16 and OR21 were initially classified as *Microbacterium esteraromaticum* based on 16S rRNA gene-based identification. However, identification based on the whole genome sequences of OR16 and OR21, revealed that the average nucleotide identities between the genome of *M. esteraromaticum* type strain DSM 8609 and the genomes of OR16 and OR21 were 85.77% and 84.91%, respectively. Since these values are below 95%; bacteria belonging to the same species show $\geq 95\%$ ANI. Therefore, the classification of *Microbacterium* sp. OR16 and *Microbacterium* sp. OR21 at the species level is recommended.

5.3 Research benefits

PAE contamination in the marine environment, especially in the sediment fraction, is widespread and researchers have even reported PAEs and their metabolites in marine biota. Despite this, very little is known about the PAE-degrading potential of marine sediment bacteria. Our study identifies some marine sediment bacteria that have as yet not been known to possess PAE-degradation ability, thus shedding some light on PAE-degrading bacterial groups in marine sediment. Furthermore, the study demonstrates a simple approach for the prediction and isolation of pollutant degraders from complex and dynamic bacterial communities such as those found in enriched consortia. Through this study, a defined consortium A02 that could enhance DEHP degradation over that by indigenous microbe in DEHP-spiked saline shrimp farm sediment was developed. This consortium, thus, has potential applicability for use in the remediation of DEHP-contaminated saline environments. Lastly, through genomic analyses, several genes that potentially encode for phthalate-degrading enzymes were identified in marine sediment bacterial isolates, *Sporosarcina* sp. OR05, *Microbacterium* sp. OR16, and *Microbacterium* sp. OR21. Hence, this study expands on the limited literature on the distribution of PAE-degradation genes in marine bacteria.

REFERENCES



จุฬาลงกรณ์มหาวิทยาลัย
CHULALONGKORN UNIVERSITY

1. Adeogun AO, Ibor OR, Imiuwa ME, Omogbemi ED, Chukwuka AV, et al. 2018. Endocrine disruptor responses in African sharptooth catfish (*Clarias gariepinus*) exposed to di-(2-ethylhexyl)-phthalate. *Comp Biochem Physiol C Toxicol Pharmacol* 213: 7-18
2. Ahuactzin-Perez M, Tlecuitl-Beristain S, Garcia-Davila J, Santacruz-Juarez E, Gonzalez-Perez M, et al. 2018. A novel biodegradation pathway of the endocrine-disruptor di(2-ethyl hexyl) phthalate by *Pleurotus ostreatus* based on quantum chemical investigation. *Ecotoxicol Environ Saf* 147: 494-99
3. Amin MM, Ebrahimpour K, Parastar S, Shoshtari-Yeganeh B, Hashemi M, et al. 2018. Association of urinary concentrations of phthalate metabolites with cardiometabolic risk factors and obesity in children and adolescents. *Chemosphere* 211: 547-56
4. An XJ, Cheng Y, Miao L, Chen X, Zang HL, Li CY. 2020. Characterization and genome functional analysis of an efficient nitrile-degrading bacterium, *Rhodococcus rhodochrous* BX2, to lay the foundation for potential bioaugmentation for remediation of nitrile-contaminated environments. *J Hazard Mater* 389
5. Arfaeina H, Fazlzadeh M, Taghizadeh F, Saeedi R, Spitz J, Dobaradaran S. 2019. Phthalate acid esters (PAEs) accumulation in coastal sediments from regions with different land use configuration along the Persian Gulf. *Ecotox Environ Safe* 169: 496-506
6. Assih EA, Ouattara AS, Thierry S, Cayol JL, Labat M, Macarie H. 2002. *Stenotrophomonas acidaminiphila* sp nov., a strictly aerobic bacterium isolated from an upflow anaerobic sludge blanket (UASB) reactor. *Int J Syst Evol Micr* 52: 559-68
7. Bai NL, Li SX, Zhang JQ, Zhang HL, Zhang HY, et al. 2020. Efficient biodegradation of DEHP by CM9 consortium and shifts in the bacterial community structure during bioremediation of contaminated soil. *Environ Pollut* 266
8. Bainsi M, Martellini T, Cincinelli A, Campani T, Minutoli R, et al. 2017. First detection of seven phthalate esters (PAEs) as plastic tracers in

- superficial neustonic/planktonic samples and cetacean blubber. *Analytical Methods* 9: 1512-20
9. Baloyi ND, Tekere M, Maphangwa KW, Masindi V. 2021. Insights Into the Prevalence and Impacts of Phthalate Esters in Aquatic Ecosystems. *Frontiers in Environmental Science* 9
 10. Banerjee S, Schlaeppi K, van der Heijden MGA. 2018. Keystone taxa as drivers of microbiome structure and functioning. *Nat Rev Microbiol* 16: 567-76
 11. Berry D, Widder S. 2014. Deciphering microbial interactions and detecting keystone species with co-occurrence networks. *Front Microbiol* 5: 219
 12. Bhattacharyya M, Basu S, Dhar R, Dutta TK. 2022. Phthalate hydrolase: distribution, diversity and molecular evolution. *Environ Microbiol Rep* 14: 333-46
 13. Bokulich NA, Kaehler BD, Rideout JR, Dillon M, Bolyen E, et al. 2018. Optimizing taxonomic classification of marker-gene amplicon sequences with QIIME 2 's q2-feature-classifier plugin. *Microbiome* 6
 14. Boll M, Geiger R, Junghare M, Schink B. 2020. Microbial degradation of phthalates: biochemistry and environmental implications. *Env Microbiol Rep* 12: 3-15
 15. Bolyen E, Rideout JR, Dillon MR, Bokulich NA, Abnet CC, et al. 2019. Reproducible, interactive, scalable and extensible microbiome data science using QIIME 2. *Nat Biotechnol* 37: 852-57
 16. Brettin T, Davis JJ, Disz T, Edwards RA, Gerdes S, et al. 2015. RASTtk: a modular and extensible implementation of the RAST algorithm for building custom annotation pipelines and annotating batches of genomes. *Scientific Reports*
 17. Bringer A, Le Floch S, Kerstan A, Thomas H. 2021. Coastal ecosystem inventory with characterization and identification of plastic contamination and additives from aquaculture materials. *Mar Pollut Bull* 167: 112286
 18. Callahan BJ, McMurdie PJ, Rosen MJ, Han AW, Johnson AJA, Holmes SP. 2016. DADA2: High-resolution sample inference from Illumina amplicon data. *Nat Methods* 13: 581-+

19. Canon F, Nidelet T, Guillardon E, Thierry A, Gagnaire Vr. 2020. Understanding the Mechanisms of Positive Microbial Interactions That Benefit Lactic Acid Bacteria Co-cultures. *Front Microbiol* 11
20. Chang WH, Herianto S, Lee CC, Hung H, Chen HL. 2021a. The effects of phthalate ester exposure on human health: A review. *Sci Total Environ* 786: 147371
21. Chang WH, Herianto S, Lee CC, Hung H, Chen HL. 2021b. The effects of phthalate ester exposure on human health: A review. *Sci Total Environ* 786
22. Chatterjee S, Dutta TK. 2008. Complete degradation of butyl benzyl phthalate by a defined bacterial consortium: Role of individual isolates in the assimilation pathway. *Chemosphere* 70: 933-41
23. Chen FY, Chen YC, Chen C, Feng L, Dong YQ, et al. 2021. High-efficiency degradation of phthalic acid esters (PAEs) by *Pseudarthrobacter defluvii* E5: Performance, degradative pathway, and key genes. *Sci Total Environ* 794
24. Cheng Z, Liu JB, Gao M, Shi GZ, Fu XJ, et al. 2019. Occurrence and distribution of phthalate esters in freshwater aquaculture fish ponds in Pearl River Delta, China (& z.star;). *Environ Pollut* 245: 883-88
25. Chi J, Li Y, Gao J. 2019. Interaction between three marine microalgae and two phthalate acid esters. *Ecotoxicol Environ Saf* 170: 407-11
26. Cousins IT, Mackay D, Parkerton TF. 2003. Physical-Chemical Properties and Evaluative Fate Modelling of Phthalate Esters In *Series Anthropogenic Compounds: Phthalate Esters*, ed. CA Staples, pp. 57-84. Berlin, Heidelberg: Springer Berlin Heidelberg
27. Das MT, Kumar SS, Ghosh P, Shah G, Malyan SK, et al. 2021. Remediation strategies for mitigation of phthalate pollution: Challenges and future perspectives. *J Hazard Mater* 409
28. Deng Y, Jiang Yh Fau - Yang Y, Yang Y Fau - He Z, He Z Fau - Luo F, Luo F Fau - Zhou J, Zhou J. 2012. Molecular ecological network analyses. *BMC Bioinformatics*

29. Ding J, Wang C, Xie Z, Li J, Yang Y, et al. 2015a. Properties of a Newly Identified Esterase from *Bacillus* sp. K91 and Its Novel Function in Diisobutyl Phthalate Degradation. *Plos One* 10: e0119216
30. Ding JM, Wang CF, Xie ZR, Li JJ, Yang YJ, et al. 2015b. Properties of a Newly Identified Esterase from *Bacillus* sp K91 and Its Novel Function in Diisobutyl Phthalate Degradation. *Plos One* 10
31. Dong CD, Chen CW, Nguyen TB, Huang CP, Hung CM. 2020. Degradation of phthalate esters in marine sediments by persulfate over Fe-Ce/biochar composites. *Chem Eng J* 384
32. Douglas GM, Maffei VJ, Zaneveld JR, Yurgel SN, Brown JR, et al. 2020. PICRUSt2 for prediction of metagenome functions. *Nat Biotechnol* 38: 685-88
33. Du H, Hu R-W, Zhao H-M, Huang H-B, Xiang L, et al. 2021. Mechanistic insight into esterase-catalyzed hydrolysis of phthalate esters (PAEs) based on integrated multi-spectroscopic analyses and docking simulation. *J Hazard Mater* 408: 124901
34. Dueholm MS, Marques IG, Karst SM, D'Imperio S, Tale VP, et al. 2015. Survival and activity of individual bioaugmentation strains. *Bioresour Technol* 186: 192-99
35. Eaton RW. 2001. Plasmid-encoded phthalate catabolic pathway in *Arthrobacter keyseri* 12B. *Journal of Bacteriology*
36. Ebenau-Jehle C, Mergelsberg M, Fischer S, Bruls T, Jehmlich N, et al. 2017. An unusual strategy for the anoxic biodegradation of phthalate. *Isme J* 11: 224-36
37. Efsa Panel on Food Contact Materials E, Processing A, Silano V, Barat Baviera JM, Bolognesi C, et al. 2019. Update of the risk assessment of di-butylphthalate (DBP), butyl-benzyl-phthalate (BBP), bis(2-ethylhexyl)phthalate (DEHP), di-isononylphthalate (DINP) and di-isodecylphthalate (DIDP) for use in food contact materials. *EFSA J* 17: e05838

38. Fan S, Wang J, Li K, Yang T, Jia Y, et al. 2018a. Complete genome sequence of *Gordonia* sp. YC-JH1, a bacterium efficiently degrading a wide range of phthalic acid esters. *J Biotechnol* 279: 55-60
39. Fan SH, Wang JH, Yan YC, Wang JY, Jia Y. 2018b. Excellent Degradation Performance of a Versatile Phthalic Acid Esters-Degrading Bacterium and Catalytic Mechanism of Monoalkyl Phthalate Hydrolase. *Int J Mol Sci* 19
40. Feng NX, Feng YX, Liang QF, Chen X, Xiang L, et al. 2021. Complete biodegradation of di-n-butyl phthalate (DBP) by a novel *Pseudomonas* sp. YJB6. *Sci Total Environ* 761
41. Festa S, Coppotelli BM, Madueno L, Loviso CL, Macchi M, et al. 2017. Assigning ecological roles to the populations belonging to a phenanthrene-degrading bacterial consortium using omic approaches. *Plos One* 12
42. Gao DW, Wen ZD. 2016. Phthalate esters in the environment: A critical review of their occurrence, biodegradation, and removal during wastewater treatment processes. *Sci Total Environ* 541: 986-1001
43. Gao N, Zhang J, Pan Z, Zhao X, Ma X, Zhang H. 2020. Biodegradation of Atrazine by Mixed Bacteria of *Klebsiella variicola* Strain FH-1 and *Arthrobacter* sp. NJ-1. *B Environ Contam Tox* 105: 481-89
44. Gilmore SP, Lankiewicz TS, Wilken SE, Brown JL, Sexton JA, et al. 2019. Top-Down Enrichment Guides in Formation of Synthetic Microbial Consortia for Biomass Degradation. *ACS Synthetic Biology* 8: 2174-85
45. Grindler NM, Vanderlinden L, Karthikraj R, Kannan K, Teal S, et al. 2018. Exposure to Phthalate, an Endocrine Disrupting Chemical, Alters the First Trimester Placental Methylome and Transcriptome in Women. *Sci Rep* 8: 6086
46. Hara H, Masai E, Katayama Y, Fukuda M. 2000. The 4-oxalomesaconate hydratase gene, involved in the protocatechuate 4,5-cleavage pathway, is essential to vanillate and syringate degradation in *Sphingomonas paucimobilis* SYK-6. *J Bacteriol* 182: 6950-7
47. Hara H, Stewart GR, Mohn WW. 2010. Involvement of a Novel ABC Transporter and Monoalkyl Phthalate Ester Hydrolase in Phthalate Ester

- Catabolism by *Rhodococcus jostii* RHA1. *Appl Environ Microb* 76: 1516-23
48. He Z, Xiao H, Tang L, Min H, Lu Z. 2013. Biodegradation of di-n-butyl phthalate by a stable bacterial consortium, HD-1, enriched from activated sludge. *Bioresource Technol* 128: 526-32
 49. Hidalgo-Serrano M, Borrull F, Marcé RM, Pocurull E. 2022. Phthalate esters in marine ecosystems: Analytical methods, occurrence and distribution. *TrAC Trends in Analytical Chemistry* 151
 50. Hidalgo-Serrano Mr, Borrull F, Pocurull E, Marcé RM. 2020. Pressurised Liquid Extraction and Liquid Chromatography-High Resolution Mass Spectrometry for the Simultaneous Determination of Phthalate Diesters and Their Metabolites in Seafood Species. *Food Analytical Methods* 13: 1442-53
 51. Hu H, Fang S, Zhao M, Jin H. 2020. Occurrence of phthalic acid esters in sediment samples from East China Sea. *Sci Total Environ* 722: 137997
 52. Hu T, Yang C, Hou Z, Liu T, Mei X, et al. 2022. Phthalate Esters Metabolic Strain *Gordonia* sp. GZ-YC7, a Potential Soil Degradator for High Concentration Di-(2-ethylhexyl) Phthalate. *Microorganisms* 10
 53. Hu XL, Gu YY, Huang WP, Yin DQ. 2016. Phthalate monoesters as markers of phthalate contamination in wild marine organisms. *Environ Pollut* 218: 410-18
 54. Huang HA-O, Zhang XY, Chen TL, Zhao YL, Xu DS, Bai YA-OX. 2019. Biodegradation of Structurally Diverse Phthalate Esters by a Newly Identified Esterase with Catalytic Activity toward Di(2-ethylhexyl) Phthalate. *Journal of agricultural and food chemistry*
 55. Huang L, Meng D, Tian Q, Yang S, Deng H, et al. 2020. Characterization of a novel carboxylesterase from *Bacillus velezensis* SYBC H47 and its application in degradation of phthalate esters. *J Biosci Bioeng* 129: 588-94
 56. Huang X-J, Du H, Deng X-L, Chen Y-H, Xiang L, et al. 2021. New insights into the evolution of bacterial community during the domestication of phthalate-degrading consortium. *Journal of Cleaner Production* 303

57. Huerta-Cepas J, Szklarczyk D, Forslund K, Cook H, Heller D, et al. 2016. eggNOG 4.5: a hierarchical orthology framework with improved functional annotations for eukaryotic, prokaryotic and viral sequences.
58. Ishimoto CK, Aono AH, Nagai JS, Sousa H, Miranda ARL, et al. 2021. Microbial co-occurrence network and its key microorganisms in soil with permanent application of composted tannery sludge. *Sci Total Environ* 789: 147945
59. IUCN. 2021. Marine plastic pollution. International Union for Conservation of Nature
60. Iwata M, Imaoka T, Nishiyama T, Fujii T. 2016. Re-characterization of mono-2-ethylhexyl phthalate hydrolase belonging to the serine hydrolase family. *Journal of Bioscience and Bioengineering* 122: 140-45
61. Jambeck JR, Geyer R, Wilcox C, Siegler TR, Perryman M, et al. 2015. Plastic waste inputs from land into the ocean. *Science* 347: 768-71
62. Janssen S, McDonald D, Gonzalez A, Navas-Molina JA, Jiang L, et al. 2018. Phylogenetic Placement of Exact Amplicon Sequences Improves Associations with Clinical Information. *Msystems* 3
63. Jebara A, Albergamo A, Rando R, Potorti AG, Lo Turco V, et al. 2021. Phthalates and non-phthalate plasticizers in Tunisian marine samples: Occurrence, spatial distribution and seasonal variation. *Mar Pollut Bull* 163: 111967
64. Jiao Y, Tao Y, Yang Y, Diogene T, Yu H, et al. 2020. Monobutyl phthalate (MBP) can dysregulate the antioxidant system and induce apoptosis of zebrafish liver. *Environ Pollut* 257
65. Kanaujiya DK, Sivashanmugam S, Pakshirajan K. 2022. Biodegradation and toxicity removal of phthalate mixture by *Gordonia* sp. in a continuous stirred tank bioreactor system. *Environmental Technology & Innovation* 26
66. Kanehisa M, Sato Y, Kawashima M, Furumichi M, Tanabe M. 2015. KEGG as a reference resource for gene and protein annotation. *Nucleic Acids Research* 44: D457-D62
67. Kang D, Jacquioud S, Herschend J, Wei S, Nesme J, Sorensen SJ. 2019. Construction of Simplified Microbial Consortia to Degrade Recalcitrant

- Materials Based on Enrichment and Dilution-to-Extinction Cultures. *Front Microbiol* 10: 3010
68. Kasana RC, Pandey CB. 2018. Exiguobacterium: an overview of a versatile genus with potential in industry and agriculture. *Crit Rev Biotechnol* 38: 141-56
 69. Kastner J, Cooper DG, Maric M, Dodd P, Yargeau V. 2012. Aqueous leaching of di-2-ethylhexyl phthalate and "green" plasticizers from poly(vinyl chloride). *Sci Total Environ* 432: 357-64
 70. Khondee N, Tathong S, Pinyakong O, Muller R, Soonglerdsongpha S, et al. 2015. Lipopeptide biosurfactant production by chitosan-immobilized *Bacillus* sp. GY19 and their recovery by foam fractionation. *Biochem Eng J* 93: 47-54
 71. Kim S, Lee YS, Moon HB. 2020. Occurrence, distribution, and sources of phthalates and non-phthalate plasticizers in sediment from semi-enclosed bays of Korea. *Mar Pollut Bull* 151
 72. Kögel T, Bjørøy Ø, Toto B, Bienfait AM, Sanden M. 2020. Micro- and nanoplastic toxicity on aquatic life: Determining factors. *Sci Total Environ* 709: 136050
 73. Lempp M, Lubrano P, Bange G, Link H. 2020. Metabolism of non-growing bacteria. *Biol Chem* 401: 1479-85
 74. Li D, Yan J, Wang L, Zhang Y, Liu D, et al. 2016. Characterization of the phthalate acid catabolic gene cluster in phthalate acid esters transforming bacterium-*Gordonia* sp. strain HS-NH1. *Int Biodeter Biodegr* 106: 34-40
 75. Li FF, Liu YD, Wang DW, Zhang CS, Yang ZH, et al. 2018. Biodegradation of di-(2-ethylhexyl) phthalate by a halotolerant consortium LF. *Plos One* 13
 76. Li JL, Zhang JF, Yadav MP, Li X. 2019. Biodegradability and biodegradation pathway of di-(2-ethylhexyl) phthalate by *Burkholderia pyrrocinia* B1213. *Chemosphere* 225: 443-50
 77. Liu LH, Yuan T, Zhang JY, Tang GX, Lu HX, et al. 2022. Diversity of endophytic bacteria in wild rice (*Oryza meridionalis*) and potential for promoting plant growth and degrading phthalates. *Sci Total Environ* 806

78. Lo Brutto S, Iacofano D, Lo Turco V, Potorti AG, Rando R, et al. 2021. First Assessment of Plasticizers in Marine Coastal Litter-Feeder Fauna in the Mediterranean Sea. *Toxics* 9
79. Lu MY, Jiang WK, Gao QQ, Zhang ML, Hong Q. 2020. Degradation of dibutyl phthalate (DBP) by a bacterial consortium and characterization of two novel esterases capable of hydrolyzing PAEs sequentially. *Ecotox Environ Safe* 195
80. Lu Y, Tang F, Wang Y, Zhao JH, Zeng X, et al. 2009. Biodegradation of dimethyl phthalate, diethyl phthalate and di-n-butyl phthalate by *Rhodococcus* sp. L4 isolated from activated sludge. *J Hazard Mater* 168: 938-43
81. Lv HX, Mo CH, Zhao HM, Xiang L, Katsoyiannis A, et al. 2018. Soil contamination and sources of phthalates and its health risk in China: A review. *Environ Res* 164: 417-29
82. MacDonald DD, Carr RS, Calder FD, Long ER, Ingersoll CG. 1996. Development and evaluation of sediment quality guidelines for Florida coastal waters. *Ecotoxicology* 5: 253-78
83. Madhuri RJ, Saraswathi M, Gowthami K, Bhargavi M, Divya Y, Deepika V. 2019. Recent Approaches in the Production of Novel Enzymes From Environmental Samples by Enrichment Culture and Metagenomic Approach In *Recent Developments in Applied Microbiology and Biochemistry*, ed. V Buddolla, pp. 251-62: Elsevier BV
84. Magdouli S, Daghbir R, Brar SK, Drogui P, Tyagi RD. 2013. Di 2-ethylhexylphthalate in the aquatic and terrestrial environment: A critical review. *J Environ Manage* 127: 36-49
85. Malem F, Soonthondecha P, Khawmodjod P, Chunchakorn V, Whitlow HJ, Chienthavorn O. 2019. Occurrence of phthalate esters in the eastern coast of Thailand. *Environ Monit Assess* 191
86. Mansouri L, Tizaoui C, Geissen S-U, Bousselmi L. 2019. A comparative study on ozone, hydrogen peroxide and UV based advanced oxidation processes for efficient removal of diethyl phthalate in water. *J Hazard Mater* 363: 401-11

87. Matchado MS, Lauber M, Reitmeier S, Kacprowski T, Baumbach J, et al. 2021. Network analysis methods for studying microbial communities: A mini review. *Comput Struct Biotec* 19: 2687-98
88. Mecha AC, Chollom MN. 2020. Photocatalytic ozonation of wastewater: a review. *Environmental Chemistry Letters* 18: 1491-507
89. Mendes IV, Garcia MB, Bitencourt ACAj, Santana RH, Lins PdC, et al. 2021. Bacterial diversity dynamics in microbial consortia selected for lignin utilization. *Plos One* 16: e0255083
90. Meng L, Xu C, Wu F, Huhe. 2022. Microbial co-occurrence networks driven by low-abundance microbial taxa during composting dominate lignocellulose degradation. *Sci Total Environ* 845: 157197
91. Mi LJ, Xie ZY, Zhao Z, Zhong MY, Mi WY, et al. 2019. Occurrence and spatial distribution of phthalate esters in sediments of the Bohai and Yellow seas. *Sci Total Environ* 653: 792-800
92. Muangchinda C, Rungsihiranrut A, Prombutara P, Soonglerdsongpha S, Pinyakong O. 2018. 16S metagenomic analysis reveals adaptability of a mixed-PAH-degrading consortium isolated from crude oil-contaminated seawater to changing environmental conditions. *J Hazard Mater* 357: 119-27
93. Nahurira R, Ren L, Song JL, Jia Y, Wang JH, et al. 2017. Degradation of Di(2-Ethylhexyl) Phthalate by a Novel *Gordonia alkanivorans* Strain YC-RL2. *Curr Microbiol* 74: 309-19
94. Net S, Sempere R, Delmont A, Paluselli A, Ouddane B. 2015. Occurrence, Fate, Behavior and Ecotoxicological State of Phthalates in Different Environmental Matrices. *Environ Sci Technol* 49: 4019-35
95. Nshimiyimana JB, Khadka S, Zou P, Adhikari S, Proshad R, et al. 2020. Study on biodegradation kinetics of di-2-ethylhexyl phthalate by newly isolated halotolerant *Ochrobactrum anthropi* strain L1-W. *Bmc Res Notes* 13
96. Paluselli A, Fauvelle V, Galgani F, Sempere R. 2019. Phthalate Release from Plastic Fragments and Degradation in Seawater. *Environ Sci Technol* 53: 166-75

97. Paluselli A, Kim SK. 2020. Horizontal and vertical distribution of phthalates acid ester (PAEs) in seawater and sediment of East China Sea and Korean South Sea: Traces of plastic debris? *Mar Pollut Bull* 151
98. Qian XJ, Chen L, Sui Y, Chen C, Zhang WM, et al. 2020. Biotechnological potential and applications of microbial consortia. *Biotechnol Adv* 40
99. Quast C, Pruesse E, Yilmaz P, Gerken J, Schweer T, et al. 2013. The SILVA ribosomal RNA gene database project: improved data processing and web-based tools. *Nucleic Acids Res* 41: D590-6
100. Rani M, Weadge JT, Jabaji S. 2020. Isolation and Characterization of Biosurfactant-Producing Bacteria From Oil Well Batteries With Antimicrobial Activities Against Food-Borne and Plant Pathogens. *Front Microbiol* 11
101. Rapp KM, Jenkins JP, Betenbaugh MJ. 2020. Partners for life: building microbial consortia for the future. *Curr Opin Biotech* 66: 292-300
102. Ren L, Jia Y, Ruth N, Qiao C, Wang J, et al. 2016. Biodegradation of phthalic acid esters by a newly isolated Mycobacterium sp. YC-RL4 and the bioprocess with environmental samples. *Environ Sci Pollut R* 23: 16609-19
103. Ren L, Lin Z, Liu HM, Hu HQ. 2018a. Bacteria-mediated phthalic acid esters degradation and related molecular mechanisms. *Appl Microbiol Biot* 102: 1085-96
104. Ren L, Wang G, Huang YX, Guo JF, Li CY, et al. 2021. Phthalic acid esters degradation by a novel marine bacterial strain Mycolicibacterium phocaicum RL-HY01: Characterization, metabolic pathway and bioaugmentation. *Sci Total Environ* 791
105. Ren XY, Zeng GM, Tang L, Wang JJ, Wan J, et al. 2018b. Sorption, transport and biodegradation - An insight into bioavailability of persistent organic pollutants in soil. *Sci Total Environ* 610: 1154-63
106. Richter M, Rosselló-Móra R, Oliver Glöckner F, Peplies Jr. 2015. JSpeciesWS: a web server for prokaryotic species circumscription based on pairwise genome comparison. *Bioinformatics* 32: 929-31

107. Rios-Fuster B, Alomar C, Capo X, Paniagua Gonzalez G, Garcinuno Martinez RM, et al. 2022. Assessment of the impact of aquaculture facilities on transplanted mussels (*Mytilus galloprovincialis*): Integrating plasticizers and physiological analyses as a biomonitoring strategy. *J Hazard Mater* 424: 127264
108. Rodríguez Amor D, Dal Bello M. 2019. Bottom-Up Approaches to Synthetic Cooperation in Microbial Communities. *Life (Basel)* 9
109. Schwager E, Weingart G, Bielski C, Huttenhower C. 2020. CCREPE: Compositionality Corrected by PERmutation and RENormalization. *Bioconductor.org*
110. Sekiguchi T, Saika A, Nomura K, Watanabe T, Watanabe T, et al. 2011. Biodegradation of aliphatic polyesters soaked in deep seawaters and isolation of poly(epsilon-caprolactone)-degrading bacteria. *Polym Degrad Stabil* 96: 1397-403
111. Shannon P, Markiel A, Ozier O, Baliga NS, Wang JT, et al. 2003. Cytoscape: A software environment for integrated models of biomolecular interaction networks. *Genome Res* 13: 2498-504
112. Song MK, Wang YJ, Jiang LF, Peng K, Wei ZK, et al. 2019. The complex interactions between novel DEHP-metabolising bacteria and the microbes in agricultural soils. *Sci Total Environ* 660: 733-40
113. Song X, Zhang Z, Dai Y, Cun D, Cui B, et al. 2022. Biodegradation of phthalate acid esters by a versatile PAE-degrading strain *Rhodococcus* sp. LW-XY12 and associated genomic analysis. *Int Biodeter Biodegr* 170
114. Stingley RL, Brezna B, Khan AA, Cerniglia CE. 2004. Novel organization of genes in a phthalate degradation operon of *Mycobacterium vanbaalenii* PYR-1. *Microbiology* 150: 3749-61
115. Sun JQ, Wu XQ, Gan J. 2015. Uptake and Metabolism of Phthalate Esters by Edible Plants. *Environ Sci Technol* 49: 8471-78
116. Sun Y, Li X, Cao N, Duan C, Ding C, et al. 2022. Biodegradable microplastics enhance soil microbial network complexity and ecological stochasticity. *J Hazard Mater* 439: 129610

117. Uribe-Flores MM, Cerqueda-Garcia D, Hernandez-Nunez E, Cadena S, Garcia-Cruz NU, et al. 2019. Bacterial succession and co-occurrence patterns of an enriched marine microbial community during light crude oil degradation in a batch reactor. *J Appl Microbiol* 127: 495-507
118. Wang C, Zeng T, Gu C, Zhu S, Zhang Q, Luo X. 2019a. Photodegradation Pathways of Typical Phthalic Acid Esters Under UV, UV/TiO₂, and UV-Vis/Bi₂WO₆ Systems. *Front Chem* 7: 852
119. Wang L, Gan D, Gong L, Zhang Y, Wang J, et al. 2022. Analysis of the performance of the efficient di-(2-ethylhexyl) phthalate-degrading bacterium *Rhodococcus pyridinovorans* DNHP-S2 and associated catabolic pathways. *Chemosphere* 306: 135610
120. Wang LY, Gu YY, Zhang ZM, Sun AL, Shi XZ, et al. 2021a. Contaminant occurrence, mobility and ecological risk assessment of phthalate esters in the sediment-water system of the Hangzhou Bay. *Sci Total Environ* 770
121. Wang P, Gao JJ, Zhao Y, Zhang M, Zhou SJ. 2021b. Biodegradability of di-(2-ethylhexyl) phthalate by a newly isolated bacterium *Achromobacter* sp. RX. *Sci Total Environ* 755
122. Wang S, Cao Y, Wang S, Cai J, Zhang Z. 2020. DEHP induces immunosuppression through disturbing inflammatory factors and CYPs system homeostasis in common carp neutrophils. *Fish Shellfish Immunol* 96: 26-31
123. Wang X, Wu H, Wang X, Wang H, Zhao K, et al. 2021c. Network-directed isolation of the cooperator *Pseudomonas aeruginosa* ZM03 enhanced the dibutyl phthalate degradation capacity of *Arthrobacter nicotianae* ZM05 under pH stress. *J Hazard Mater* 410: 124667
124. Wang XJ, Shen S, Wu H, Wang HX, Wang LJ, Lu ZM. 2021d. *Acinetobacter tandoii* ZM06 Assists *Glutamicibacter nicotianae* ZM05 in Resisting Cadmium Pressure to Preserve Dipropyl Phthalate Biodegradation. *Microorganisms* 9
125. Wang Y, Qian H. 2021. Phthalates and Their Impacts on Human Health. *Healthcare (Basel)* 9

126. Wang YX, Zeng Q, Sun Y, Yang P, Wang P, et al. 2016. Semen phthalate metabolites, semen quality parameters and serum reproductive hormones: A cross-sectional study in China. *Environ Pollut* 211: 173-82
127. Wang YY, Zhan WH, Ren Q, Cheng SS, Wang JN, et al. 2019b. Biodegradation of di-(2-ethylhexyl) phthalate by a newly isolated *Gordonia* sp. and its application in the remediation of contaminated soils. *Sci Total Environ* 689: 645-51
128. Wei STS, Chen YL, Wu YW, Wu TY, Lai YL, et al. 2021. Integrated Multi-omics Investigations Reveal the Key Role of Synergistic Microbial Networks in Removing Plasticizer Di-(2-Ethylhexyl) Phthalate from Estuarine Sediments. *Msystems* 6
129. Wemheuer F, Taylor JA, Daniel R, Johnston E, Meinicke P, et al. 2020. Tax4Fun2: prediction of habitat-specific functional profiles and functional redundancy based on 16S rRNA gene sequences. *Environ Microbiome* 15
130. Wilhelm RC, Pepe-Ranney C, Weisenhorn P, Lipton M, Buckley DH. 2021. Competitive Exclusion and Metabolic Dependency among Microorganisms Structure the Cellulose Economy of an Agricultural Soil. *Mbio* 12
131. Wright RJ, Bosch R, Gibson MI, Christie-Oleza JA. 2020. Plasticizer Degradation by Marine Bacterial Isolates: A Proteogenomic and Metabolomic Characterization. *Environ Sci Technol* 54: 2244-56
132. Wu M, Tang J, Zhou X, Lei D, Zeng C, et al. 2022. Isolation of Dibutyl Phthalate-Degrading Bacteria and Its Coculture with *Citrobacter freundii* CD-9 to Degrade Fenvalerate. *J Microbiol Biotechnol* 32: 176-86
133. Wu XL, Wang YY, Liang RX, Dai QY, Chao WL. 2010. Degradation of Di-n-butyl Phthalate by Newly Isolated *Ochrobactrum* sp. *B Environ Contam Tox* 85: 235-37
134. Wyatt JM, Cain RB, Higgins IJ. 1987. Formation from synthetic two-stroke lubricants and degradation of 2-ethylhexanol by lakewater bacteria. *Appl Microbiol Biot* 25: 558-67

135. Xiaoyan T, Suyu W, Yang Y, Ran T, Yunv D, et al. 2015. Removal of six phthalic acid esters (PAEs) from domestic sewage by constructed wetlands. *Chem Eng J* 275: 198-205
136. Xu G, Li FH, Wang QH. 2008. Occurrence and degradation characteristics of dibutyl phthalate (DBP) and di-(2-ethylhexyl) phthalate (DEHP) in typical agricultural soils of China. *Sci Total Environ* 393: 333-40
137. Xu JM, Lu QH, de Toledo RA, Shim HJ. 2017. Degradation of di-2-ethylhexyl phthalate (DEHP) by an indigenous isolate *Acinetobacter* sp SN13. *Int Biodeter Biodegr* 117: 205-14
138. Xu YQ, Liu X, Zhao JR, Huang HQ, Wu MQ, et al. 2021. An efficient phthalate ester-degrading *Bacillus subtilis*: Degradation kinetics, metabolic pathway, and catalytic mechanism of the key enzyme. *Environ Pollut* 273
139. Yan Z, Hao Z, Wu H, Jiang H, Yang M, Wang C. 2019. Co-occurrence patterns of the microbial community in polycyclic aromatic hydrocarbon-contaminated riverine sediments. *J Hazard Mater* 367: 99-108
140. Yang CW, Chao WL, Hsieh CY, Chang BV. 2019. Biodegradation of Malachite Green in Milkfish Pond Sediments. *Sustainability-Basel* 11
141. Yang T, Ren L, Jia Y, Fan S, Wang J, et al. 2018a. Biodegradation of Di-(2-ethylhexyl) Phthalate by *Rhodococcus ruber* YC-YT1 in Contaminated Water and Soil. *Int J Environ Res Public Health* 15
142. Yang T, Ren L, Jia Y, Fan SH, Wang JH, et al. 2018b. Biodegradation of Di-(2-ethylhexyl) Phthalate by *Rhodococcus ruber* YC-YT1 in Contaminated Water and Soil. *Int J Env Res Pub He* 15
143. Yang WK, Chiang LF, Tan SW, Chen PJ. 2018c. Environmentally relevant concentrations of di(2-ethylhexyl)phthalate exposure alter larval growth and locomotion in medaka fish via multiple pathways. *Sci Total Environ* 640-641: 512-22
144. Yastrebova OV, Pyankova AA, Plotnikova EG. 2019. Phthalate-Degrading Bacteria Isolated from an Industrial Mining Area and the Processing of Potassium and Magnesium Salts. *Appl Biochem Micro+* 55: 397-404

145. Yuan SY, Huang IC, Chang BV. 2010. Biodegradation of dibutyl phthalate and di-(2-ethylhexyl) phthalate and microbial community changes in mangrove sediment. *J Hazard Mater* 184: 826-31
146. Zhang H, Yang L, Li Y, Wang C, Zhang W, et al. 2022. Pollution gradients shape the co-occurrence networks and interactions of sedimentary bacterial communities in Taihu Lake, a shallow eutrophic lake. *J Environ Manage* 305: 114380
147. Zhang HY, Lin Z, Liu B, Wang G, Weng LY, et al. 2020. Bioremediation of di-(2-ethylhexyl) phthalate contaminated red soil by *Gordonia terrae* RL-JC02: Characterization, metabolic pathway and kinetics. *Sci Total Environ* 733
148. Zhang JF, Zhang CN, Zhu YP, Li JL, Li XT. 2018. Biodegradation of seven phthalate esters by *Bacillus mojavensis* B1811. *Int Biodeter Biodegr* 132: 200-07
149. Zhang XY, Fan X, Qiu YJ, Li CY, Xing S, et al. 2014. Newly identified thermostable esterase from *Sulfobacillus acidophilus*: properties and performance in phthalate ester degradation. *Appl Environ Microb*
150. Zhang ZM, Wang LY, Gu YY, Sun AL, You JJ, et al. 2021. Probing the contamination characteristics, mobility, and risk assessments of typical plastic additive-phthalate esters from a typical coastal aquaculture area, China. *J Hazard Mater* 416: 125931
151. Zhao HM, Du H, Lin J, Chen XB, Li YW, et al. 2016. Complete degradation of the endocrine disruptor di-(2-ethylhexyl) phthalate by a novel *Agromyces* sp MT-O strain and its application to bioremediation of contaminated soil. *Sci Total Environ* 562: 170-78
152. Zhao HM, Hu RW, Chen XX, Chen XB, Lu H, et al. 2018a. Biodegradation pathway of di-(2-ethylhexyl) phthalate by a novel *Rhodococcus pyridinivorans* XB and its bioaugmentation for remediation of DEHP contaminated soil. *Sci Total Environ* 640: 1121-31
153. Zhao HM, Hu RW, Du H, Xin XP, Li YW, et al. 2018b. Functional genomic analysis of phthalate acid ester (PAE) catabolism genes in the

- versatile PAE-mineralising bacterium *Rhodococcus* sp. 2G. *Sci Total Environ* 640-641: 646-52
154. Zhao HM, Hu RW, Huang HB, Wen HF, Du H, et al. 2017. Enhanced dissipation of DEHP in soil and simultaneously reduced bioaccumulation of DEHP in vegetable using bioaugmentation with exogenous bacteria. *Biol Fert Soils* 53: 663-75
155. Zhao Z, Liu C, Xu Q, Ahmad S, Zhang H, et al. 2021. Characterization and genomic analysis of an efficient dibutyl phthalate degrading bacterium *Microbacterium* sp. USTB-Y. *World J Microbiol Biotechnol* 37: 212
156. Zhu FX, Doyle E, Zhu CY, Zhou DM, Gu C, Gao J. 2020. Metagenomic analysis exploring microbial assemblages and functional genes potentially involved in di (2-ethylhexyl) phthalate degradation in soil. *Sci Total Environ* 715
157. Zhu FX, Zhu CY, Doyle E, Liu HL, Zhou DM, Gao J. 2018. Fate of di (2 ethylhexyl) phthalate in different soils and associated bacterial community changes. *Sci Total Environ* 637: 460-69
158. Zhu FX, Zhu CY, Zhou DM, Gao J. 2019a. Fate of di (2-ethylhexyl) phthalate and its impact on soil bacterial community under aerobic and anaerobic conditions. *Chemosphere* 216: 84-93
159. Zhu QQ, Jia JB, Zhang KG, Zhang H, Liao CY. 2019b. Spatial distribution and mass loading of phthalate esters in wastewater treatment plants in China: An assessment of human exposure. *Sci Total Environ* 656: 862-69

APPENDIX

Appendix A: Media composition

Table A1 Compositions of the agar media used for bacterial isolation from enriched consortium C10.

ATCC Medium 159 (Atlas 2010)

Agar (25.0 g/L), Glucose (20.0 g/L), CaCO₃ (20.0 g/L), and Yeast extract (10.0 g/L)

Sporosarcina halophila Agar (Atlas 2010)

NaCl (30.0 g/L), Agar (20.0 g/L), MgCl₂·6H₂O (5.0 g/L), Peptone (5.0 g/L), NaCl (5.0 g/L), Yeast extract (2.0 g/L), and Beef extract (1.0 g/L)

ATCC Medium 589 (Atlas 2010)

Agar (20.0 g/L), K₂HPO₄ (7.0 g/L), Methionine (5.0 g/L), KH₂PO₄ (2.0 g/L), (NH₄)₂SO₄ (1.0 g/L), Sodium citrate (0.4 g/L), and MgSO₄·7H₂O (0.1 g/L)

Bacillus Medium (Atlas 2010)

Agar (25.0 g/L), Peptone (6.0 g/L), Pancreatic digest of casein (3.0 g/L), Yeast extract (3.0 g/L), Beef extract (1.5 g/L), and MnSO₄·4H₂O (1.0 µg/L)

Sea-water yeast extract agar (modified from Coombs and Franco (2003))

Yeast extract (0.25 g), K₂HPO₄ (0.5 g), and Agar (18 g) in 1000 mL of filtered seawater (using cellulose acetate filter, 0.45 µm)

Nutrient seawater agar with DEHP (50 mg/L)

NH₄NO₃ (1 g), K₂HPO₄ (0.02 g), C₆H₅FeO₇ (0.02 g), and Yeast extract (0.5 g) in 1000 mL of filtered seawater (using cellulose acetate filter, 0.45 µm)

0.25X Zobell Marine Agar

0.25X Tryptic soy agar supplemented with 4% NaCl (Betts 2006)

Appendix B: Standard curves

Table B1 GC peak areas of different concentrations (25 – 400 mg/L) of dimethyl phthalate (DMP).

DMP concentration	Peak area	Average peak area	Standard deviation
25 mg/L	16.6	16	15.7
50 mg/L	25.5	24.3	24.2
100 mg/L	70.2	79.1	72.3
200 mg/L	172.2	175.3	179.7
400 mg/L	365.8	368.6	354

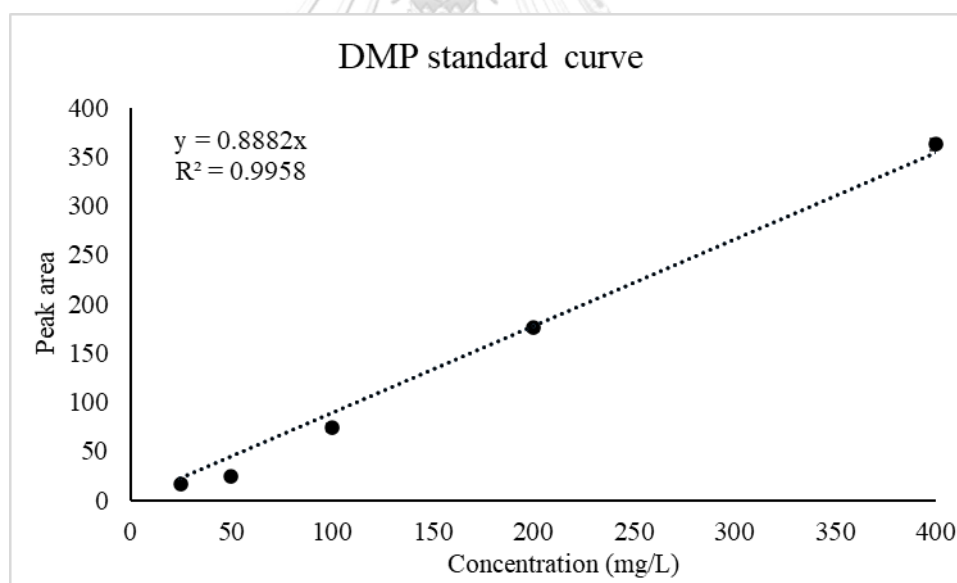


Figure B1 Standard curve for dimethyl phthalate (DMP).

Table B2 GC peak areas of different concentrations (25 – 400 mg/L) of diethyl phthalate (DEP).

DEP concentration	Peak area			Average	Standard
				peak area	deviation
25 mg/L	22.1	21.3	21.2	21.5	0.4
50 mg/L	35.2	34.9	34.1	34.7	0.5
100 mg/L	93.3	93.2	97.8	94.8	2.1
200 mg/L	212.8	213.2	214	213.3	0.5
400 mg/L	403	417.6	412.3	411.0	6.0

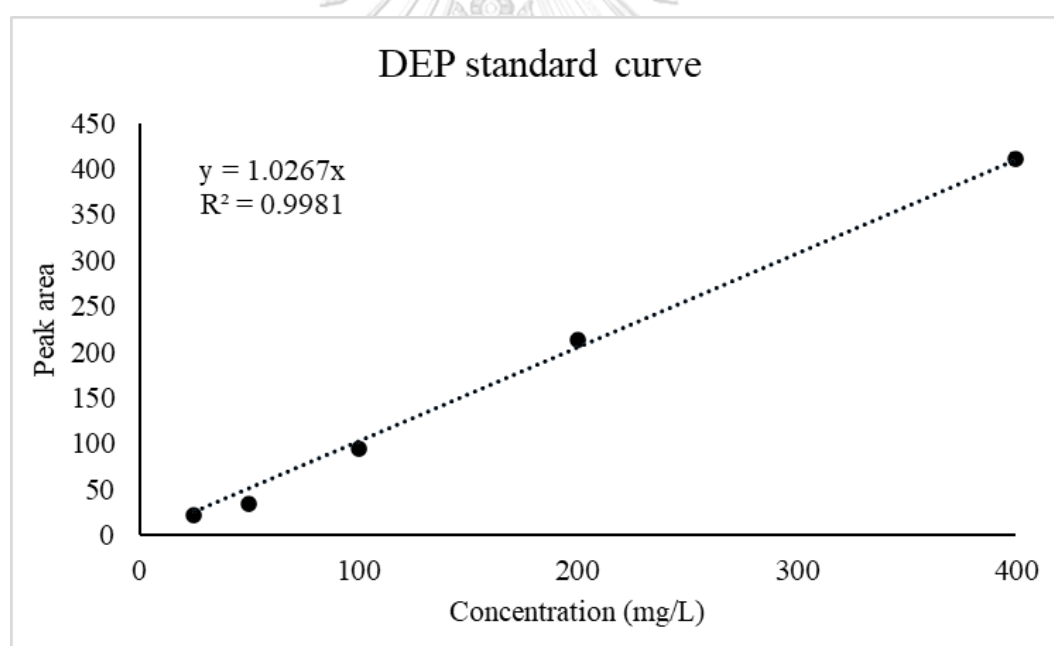


Figure B2 Standard curve for diethyl phthalate (DEP).

Table B3 GC peak areas of different concentrations (25 – 400 mg/L) of dibutyl phthalate (DBP).

DBP concentration	Peak area			Average	Standard
				peak area	deviation
25 mg/L	88.6	62.8	55.6	69.0	14.2
50 mg/L	85.4	77.4	76.4	79.7	4.0
100 mg/L	170.4	162.5	162.7	165.2	3.7
200 mg/L	362.5	366.6	367.9	365.7	2.3
400 mg/L	711	696	733	713.3	15.2

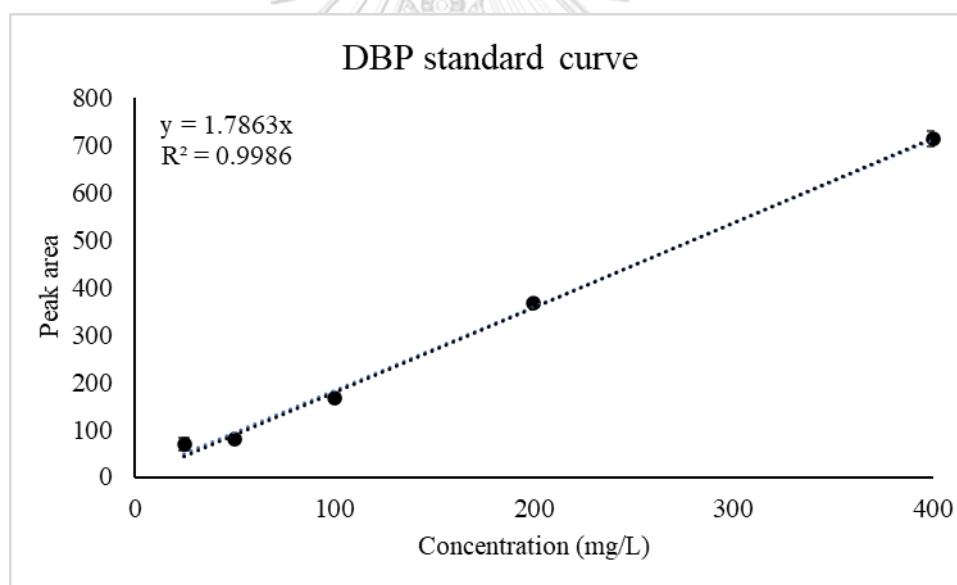


Figure B3 Standard curve for dibutyl phthalate (DBP).

Table B4 GC peak areas of different concentrations (25 – 400 mg/L) of di-(2-ethylhexyl) phthalate (DEHP).

DEHP concentration	Peak area			Average peak area	Standard deviation
50 mg/L	56.2	56.2	56.8	56.4	0.3
100 mg/L	109.9	110.7	111.6	110.7	0.7
200 mg/L	256.8	231.5	239.8	242.7	10.5
400 mg/L	452.9	459.8	459.8	457.5	3.3
800 mg/L	968.5	1041.9	947.4	985.9	40.5

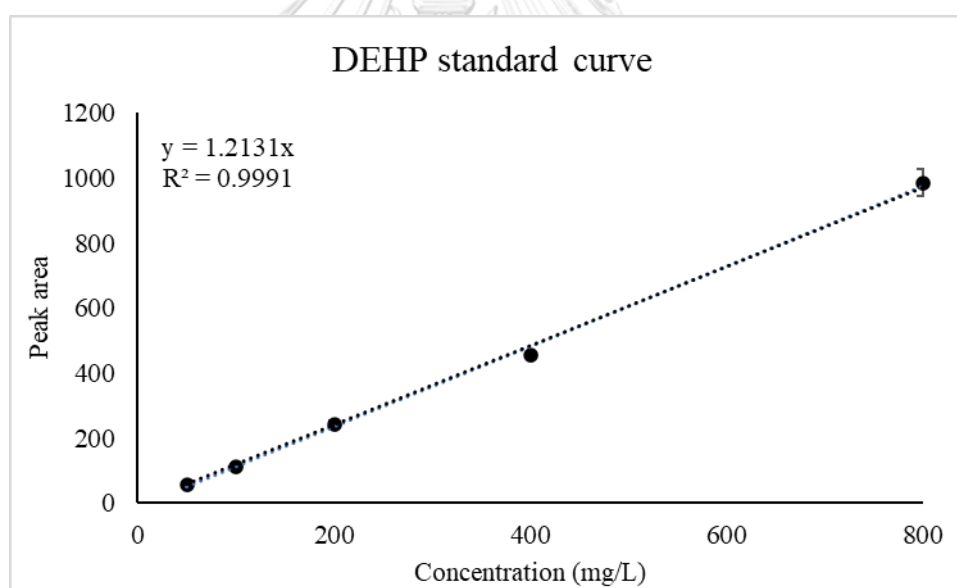


Figure B4 Standard curve for di-(2-ethylhexyl) phthalate (DEHP).

Table B5 GC peak areas of different concentrations (50 – 800 mg/L) of monoethylhexyl phthalate (MEHP).

MEHP concentration (mg/L)	Peak area			Average	SD
50	15.10	14.70	13.80	14.53	0.54
100	32.30	33.90	32.50	32.90	0.71
200	115.20	119.70	120.40	118.43	2.30
400	258.20	275.90	260.30	264.80	7.90
800	529.00	520.00	536.70	528.57	6.82

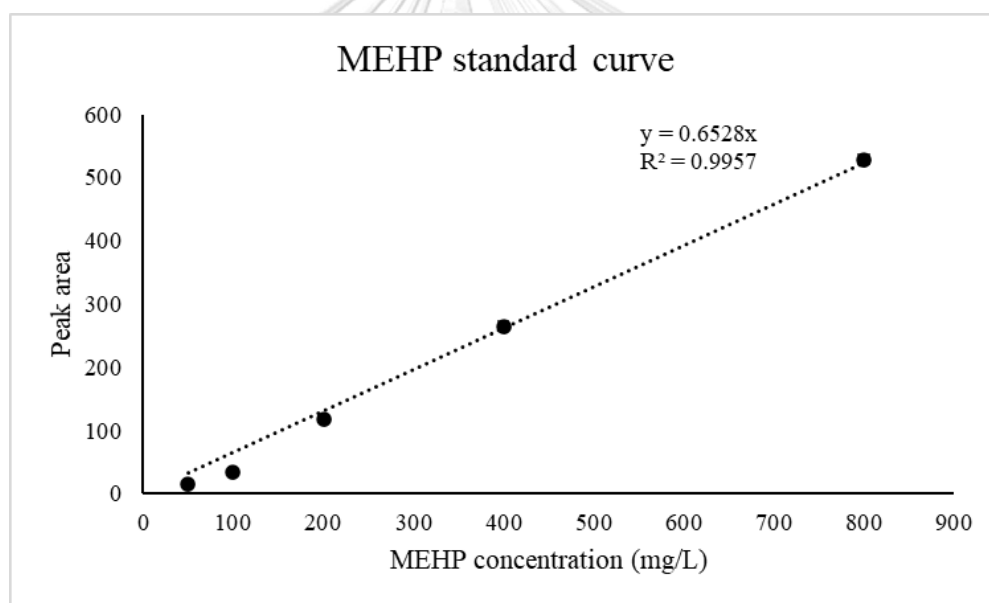


Figure B5 Standard curve of monoethylhexyl phthalate (MEHP).

Table B6 GC peak areas of different concentrations (25 – 400 mg/L) of 2-ethylhexanol (2-EHA).

2-EHA concentration (mg/L)	Peak area			Average	SD
25	45.8	44	43	44.27	1.16
50	85.2	80.4	77.5	81.03	3.18
100	167.3	164.1	165.3	165.57	1.32
200	368.4	366.6	383.2	372.73	7.44
400	796.8	775.2	775.9	782.63	10.02

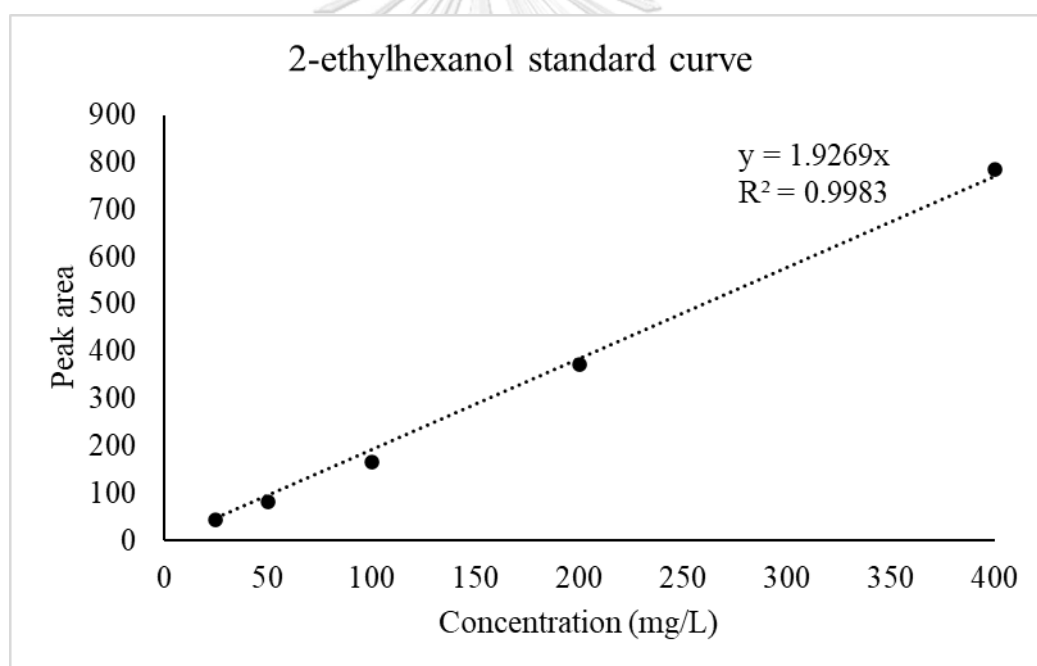


Figure B6 Standard curve of 2-ethylhexanol (2-EHA).

Table B7 Optical densities at 273 nm of different concentrations (25 – 200 mg/L) of phthalic acid.

Phthalic acid concentration (mg/L)	Optical density at 273 nm			Average	SD
25	0.216	0.223	0.217	0.22	0.00
50	0.42	0.423	0.41	0.42	0.01
100	0.825	0.838	0.822	0.83	0.01
150	1.272	1.264	1.264	1.27	0.00
200	1.642	1.617	1.696	1.65	0.03

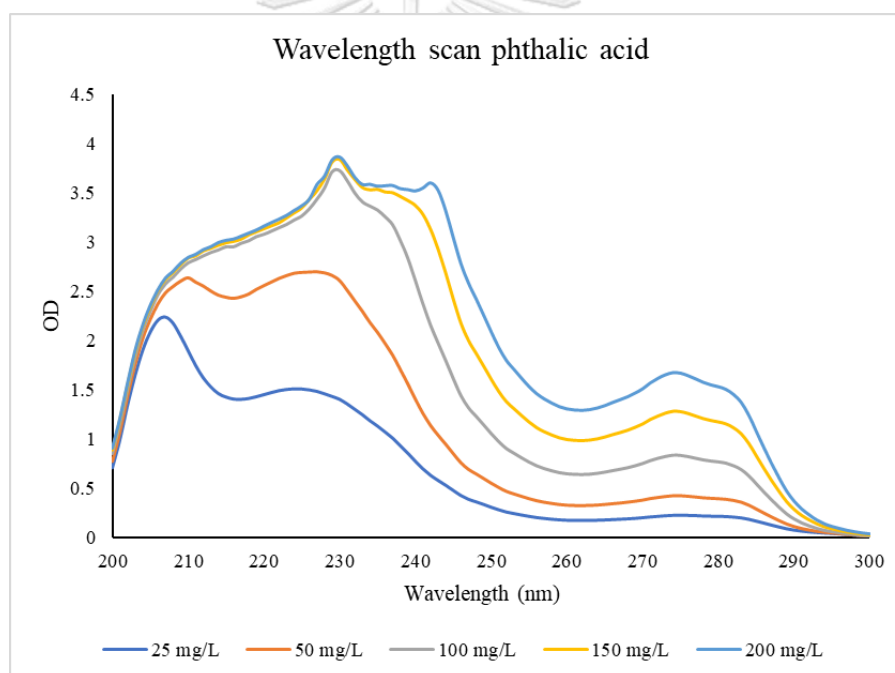


Figure B7 Wavelength scan of different concentrations (25 – 200 mg/L) of phthalic acid.

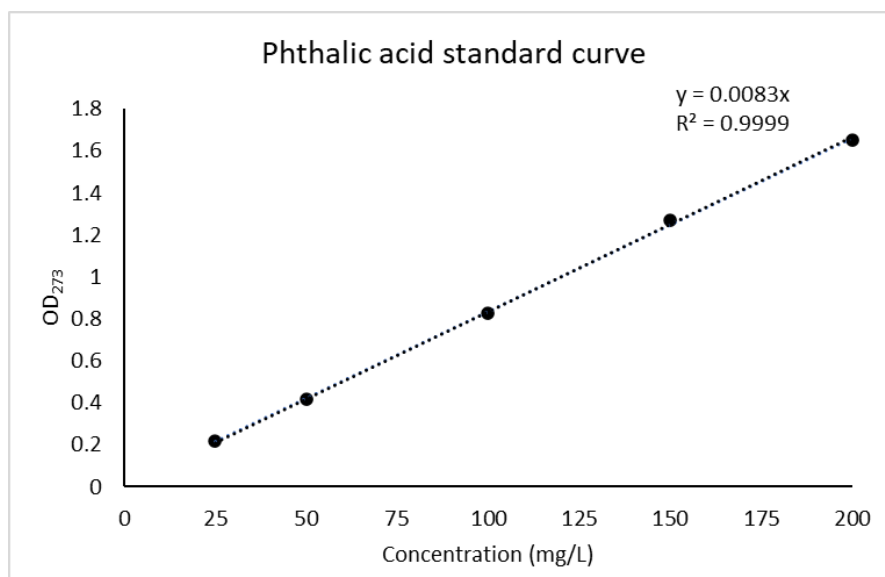


Figure B8 Standard curve of phthalic acid.

Table B8 Optical densities at 236 nm of different concentrations (25 – 200 mg/L) of protocatechuic acid.

Protocatechuic acid concentration (mg/L)	Optical density at 236 nm			Average	SD
25	0.553	0.604	0.605	0.59	0.02
50	1.14	1.127	1.137	1.13	0.01
100	2.237	2.248	2.259	2.25	0.01
150	3.147	3.148	3.15	3.15	0.00
200	3.431	3.454	3.35	3.41	0.04

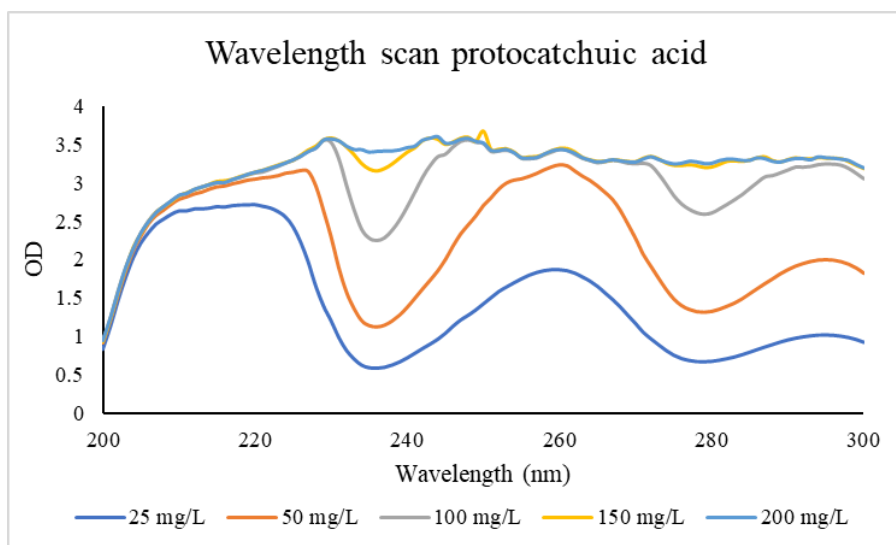


Figure B9 Wavelength scan of different concentrations (25 – 200 mg/L) of protocatchuic acid.

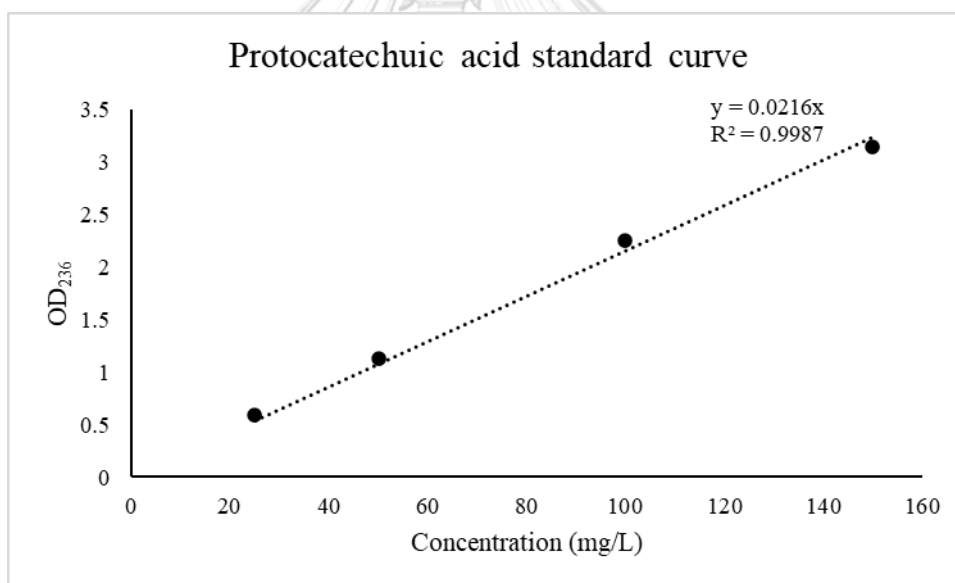


Figure B10 Standard curve of protocatchuic acid.

Table B9 Recovery of substrates from liquid medium and recovery of DEHP from sediment.

	Recovery percent			Average	Standard Deviation	Extraction solvent	Detection method
DEHP	107.23	95.21	96.47	99.64	5.39	Dichloromethane	GC-FID
DBP	96.20	103.68	99.13	99.67	3.08	Dichloromethane	GC-FID
DEP	108.90	106.55	97.67	104.37	4.78	Dichloromethane	GC-FID
DMP	99.41	90.76	102.03	97.40	4.82	Dichloromethane	GC-FID
MEHP	98.83	93.77	106.04	99.55	5.03	Dichloromethane	GC-FID
Phthalic acid	108.55	113.13	109.90	110.53	1.92	Ethyl acetate	UV spectrophotometry
Protocatechuic acid	121.00	123.75	123.52	122.76	1.25	Ethyl acetate	UV spectrophotometry
DEHP from sediment	97.64	104.32	90.43	97.46	5.67	Dichloromethane	GC-FID

Appendix C: Marine sediment properties

Table C1 Physical and chemical properties of marine sediment samples used for enrichment (Result provided by Assistant Professor Dr. Penjai Sompongchaiyakul and Dr. Sujaree Bureekul).

Sample	CaCO₃ (%w/w)	Fine grain size (%w/w)	Readily oxidizable organic carbon (%w/w)	Total nitrogen (%w/w)
S3	25 – 30	20 – 30	1 – 1.2	0.12 – 0.14
S8	15 – 20	90 – 100	2.2 – 2.4	0.26 – 0.28
S10	10 – 15	30 – 40	0.6 – 0.8	0.1 – 0.08
S13	10 – 15	70 – 90	1.2 – 1	0.12 – 0.14
S14	10 – 15	60 – 70	1 – 1.2	0.14 – 0.16
S22	5 – 10	90 – 100	1.8 – 2	0.24 – 0.26
S27	5 – 10	90 – 100	1.8 – 2	0.22 – 0.24
S32	10 – 15	90 – 100	1 – 1.2	0.2 – 0.22
S33	5 – 10	90 – 100	1 – 1.2	0.14 – 0.16

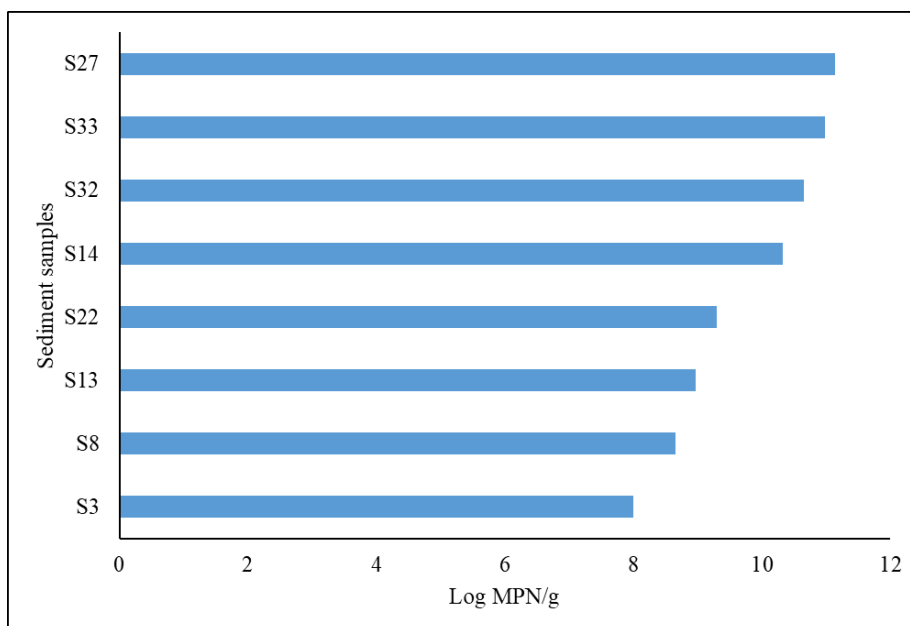


Figure C1 Total heterotrophic bacteria (log MPN/g) in the sediment samples S3, S8, S13, S14, S22, S27, S32, and S33.

Appendix D: Phase I Results

Table D1 Total heterotrophic bacterial count in the sediment samples used for enrichment in this study based on the most probable number (MPN) method.

Sediment	log MPN/g
C3	8.00
C8	8.66
C13	8.97
C22	9.29
C14	10.32
C32	10.65
C33	10.98
C27	11.15

Table D2 Percent degradation of DEHP (100 mg/L) by the nine enriched bacterial consortia.

Day 4					
	Percent degradation			Average	SD
C3	28.40	35.52	35.01	32.97	3.24
C8	2.73	-4.81	2.73	0.22	3.55
C10	91.29	100.00	95.62	95.63	3.56
C13	7.71	17.95	4.66	10.11	5.68
C14	45.95	34.57	55.20	45.24	8.44
C22	37.53	30.11	31.36	33.00	3.24
C27	30.15	40.25	31.05	33.41	4.56
C32	13.02	13.22	13.40	13.21	0.15
C33	26.80	33.40	30.75	30.31	2.71
Abiotic control	-1.97	6.48	1.08	1.87	3.49
Day 6					
	Percent degradation			Average	SD
C3	43.01	48.08	39.63	43.57	3.47
C8	40.52	48.92	40.88	43.44	3.88
C10	100.00	100.00	100.00	100.00	0.00
C13	49.19	51.13	39.67	46.66	5.01
C14	50.72	46.83	54.03	50.53	2.94
C22	74.00	93.08	78.63	81.90	8.13
C27	62.92	47.21	41.31	50.48	9.12

C32	29.03	38.36	43.66	37.02	6.05
C33	80.56	90.19	77.43	82.72	5.43
Abiotic control	-5.24	5.97	13.87	4.87	7.84

Table D3 Viable cell counts (Log CFU/mL) of the nine enriched bacterial consortia on days 0, 4, and 6 during DEHP degradation and in the biological control.

Day 0 (DEHP)					
	Log CFU/mL			Average	SD
C3	7.50	7.42	7.56	7.49	0.06
C8	7.41	7.40	7.42	7.41	0.01
C10	7.38	7.45	7.52	7.45	0.06
C13	7.46	7.28	7.52	7.42	0.10
C14	7.21	7.23	7.19	7.21	0.02
C22	7.14	7.04	7.09	7.09	0.04
C27	7.50	7.47	7.50	7.49	0.01
C32	7.30	7.45	7.18	7.31	0.11
C33	7.30	7.36	7.26	7.31	0.04
Day 0 (Biological control)					
	Log CFU/mL			Average	SD
C3	7.56	7.53	7.43	7.51	0.05
C8	7.64	7.64	7.59	7.63	0.03
C10	7.80	7.77	7.76	7.78	0.02
C13	7.46	7.43	7.46	7.45	0.02

C14	7.43	7.40	7.40	7.41	0.02
C22	7.74	7.70	7.72	7.72	0.02
C27	7.12	7.13	7.12	7.12	0.01
C32	7.63	7.62	7.59	7.62	0.02
C33	7.65	7.64	7.58	7.63	0.03

Day 4 (DEHP)

	Log CFU/mL			Average	SD
C3	8.75	8.81	8.79	8.78	0.02
C8	7.61	7.60	7.60	7.60	0.00
C10	8.08	7.85	7.59	7.84	0.20
C13	8.72	8.69	8.65	8.69	0.03
C14	9.25	9.10	8.91	9.09	0.14
C22	8.40	8.41	8.19	8.33	0.10
C27	8.61	8.76	8.88	8.75	0.11
C32	8.50	8.30	8.79	8.53	0.20
C33	8.57	8.78	8.50	8.62	0.12

Day 4 (Biological control)

	Log CFU/mL			Average	SD
C3	7.70	7.72	6.70	7.37	0.48
C8	7.70	6.77	6.77	7.08	0.44
C10	7.28	7.18	7.30	7.25	0.05
C13	7.04	7.86	7.08	7.33	0.38
C14	6.90	6.93	6.95	6.93	0.02

C22	7.20	7.79	7.32	7.44	0.25
C27	7.78	7.79	7.79	7.79	0.01
C32	7.60	6.91	6.91	7.14	0.33
C33	6.78	6.11	6.78	6.56	0.31

Day 6 (DEHP)

	Log CFU/mL			Average	SD
C3	8.77	8.65	8.55	8.66	0.09
C8	7.91	7.79	7.90	7.87	0.05
C10	7.70	7.69	7.78	7.72	0.04
C13	8.65	8.60	8.68	8.64	0.03
C14	8.30	8.59	8.41	8.43	0.12
C22	8.80	8.79	8.91	8.83	0.05
C27	9.29	9.10	9.18	9.19	0.08
C32	8.80	8.81	8.83	8.81	0.01
C33	8.05	8.17	8.11	8.11	0.05

Day 6 (Biological control)

	Log CFU/mL			Average	SD
C3	5.85	5.78	5.85	5.82	0.03
C8	6.45	6.30	6.46	6.40	0.07
C10	6.94	6.94	6.90	6.93	0.02
C13	6.61	6.60	6.62	6.61	0.01
C14	6.66	6.70	6.67	6.68	0.02
C22	6.36	6.38	6.36	6.37	0.01

C27	6.38	6.34	6.40	6.37	0.02
C32	6.54	6.57	6.54	6.55	0.01
C33	5.95	5.90	5.90	5.92	0.02

Table D4 Percent degradation of dibutyl phthalate (DBP), diethyl phthalate (DEP), and dimethyl phthalate (DMP) on day 4 by C10, C22, and C33.

DBP						
	Percent degradation (Day 4)			Average	SD	
C10	65.13	100.00	100.00	88.38	16.44	
C22	100	100	100	100	0	
C33	93.83	68.53	89.98	84.11	11.13	
Abiotic control	2.37	-0.21	3.81	1.99	1.66	
DEP						
	Percent degradation (Day 4)			Average	SD	
C10	100	100	100	100	0	
C22	100	100	100	100	0	
C33	100	100	100	100	0	
Abiotic control	3.71	-0.67	0.86	1.3	1.81	
DMP						
	Percent degradation (Day 4)			Average	SD	

C10	100	100	100	100	0
C22	100	100	100	100	0
C33	100	100	100	100	0
Abiotic control	-0.78	-2.05	0.21	-0.87	0.92

Table D5 Viable cell counts of C10, C22, and C33 on days 0 and 4 of the degradation of dibutyl phthalate (DBP), diethyl phthalate (DEP), and dimethyl phthalate (DMP).

Day 0					
	Log CFU/mL			Average	SD
C10	7.51	7.49	7.61	7.54	0.05
C22	7.1	7	7.2	7.10	0.08
C33	7.31	7.3	7.3	7.30	0.00
Day 4 (DBP)					
	Log CFU/mL			Average	SD
C10	9.39	9.26	9.24	9.30	0.07
C22	8.6	8.7	8.6	8.63	0.05
C33	8.59	8.61	8.67	8.62	0.03
Day 4 (DEP)					
	Log CFU/mL			Average	SD
C10	9.2	9.23	9.3	9.24	0.04
C22	8.7	8.65	8.75	8.70	0.04
C33	8.9	8.21	7.89	8.33	0.42
Day 4 (DMP)					
	Log CFU/mL			Average	SD

C10	9	8.86	8.9	8.92	0.06
C22	8.9	8.9	8.9	8.90	0.00
C33	8.51	8.39	8.41	8.44	0.05

Table D6 Phthalate ester (PAE) concentration remaining and percent degradation during degradation of the PAE mixture (DEHP, DBP, DEP, and DMP) by C10.

C10 (Day 2)										
	Concentration (mg/L)			Averag e	SD	Percent degradation			Averag e	SD
DMP	55.6	42.31	61.03	52.99	7.87	44.3	57.6	38.9	47.01	7.8
	4					6	9	7		7
DEP	59.3	50.99	57.03	55.80	3.54	40.6	49.0	42.9	44.20	3.5
	9					1	1	7		4
DBP	64.1	62.81	51.11	59.36	5.86	35.8	37.1	48.8	40.64	5.8
	5					5	9	9		6
DEH P	84.2	67.68	86.08	79.33	8.27	15.7	32.3	13.9	20.67	8.2
	3					7	2	2		7
C10 (Day 4)										
	Concentration (mg/L)			Averag e	SD	Percent degradation			Averag e	SD
DMP	0	0	0	0	0	100	100	100	100	0
DEP	0	0	0	0	0	100	100	100	100	0
DBP	15.5	35.11	24.62	25.09	8.00	84.4	64.8	75.3	74.91	8.0

	4					6	9	8		0
DEH	40.2	47.35	53.65	47.08	5.47	59.7	52.6	46.3	52.92	5.4
P	5					5	5	5		7

C10 (Day 6)

	Concentration (mg/L)			Average	SD	Percent degradation			Average	SD
DMP	0	0	0	0	0	100	100	100	100	0
DEP	0	0	0	0	0	100	100	100	100	0
DBP	9.14	0	0	3.05	4.31	90.8	100	100	96.95	4.3
						6				1
DEH	28.31	9.38	0	12.56	11.7	71.6	90.6	100	87.44	11.
P					7	9	2			77

Table D7 PAE concentration remaining and percent degradation during degradation of the PAE mixture (DEHP, DBP, DEP, and DMP) by C22.

C22 (Day 2)

	Concentration (mg/L)			Average	SD	Percent degradation			Average	SD
DMP	41.79	47.44	53.85	47.69	4.92	58.2	52.5	46.1	52.31	4.92
						1	6	5		
DEP	45.00	48.31	51.43	48.25	2.63	55.0	51.6	48.5	51.75	2.63
						0	9	7		
DBP	53.07	56.21	64.99	58.09	5.05	46.9	43.7	35.0	41.91	5.05
						3	9	1		

DEH	104.1	112.1	125.4	113.92	8.79	-	-	-	-13.92	8.79
P	3	8	5			4.13	12.1	25.4		
							8	5		

C22 (Day 4)

	Concentration (mg/L)			Average	SD	Percent degradation			Average	SD
DMP	0	0	0	0	0	100	100	100	100	0
DEP	0	0	0	0	0	100	100	100	100	0
DBP	0	6.33	26.54	10.95	11.3	100	93.6	73.4	89.05	11.3
					2		7	6		2
DEH	25.75	40.52	80.69	48.98	23.2	74.2	59.4	19.3	51.02	23.2
P					1	5	8	1		1

C22 (Day 6)

	Concentration (mg/L)			Average	SD	Percent degradation			Average	SD
DMP	0	0	0	0	0	100	100	100	100	0
DEP	0	0	0	0	0	100	100	100	100	0
DBP	0	0	38.57	12.86	18.1	100	100	61.4	87.14	18.1
					8			3		8
DEH	41.76	24.86	92.10	52.91	28.5	58.2	75.1	7.90	47.09	28.5
P					6	4	4			6

C22 (Day 8)

	Concentration			Average	SD	Percent			Average	SD
--	---------------	--	--	---------	----	---------	--	--	---------	----

	(mg/L)					degradation				
DMP	0	0	0	0	0	100	100	100	100	0
DEP	0	0	0	0	0	100	100	100	100	0
DBP	0	0	0	0	0	100	100	100	100	0
DEH	16.01	26.63	21.32	21.32	4.33	83.9	73.3	78.6	78.68	4.33
P						9	7	8		

Table D8 PAE concentration remaining and percent degradation during degradation of the PAE mixture (DEHP, DBP, DEP, and DMP) by C33.

C33 (Day 2)											
	Concentration					Percent			Average		SD
	(mg/L)					degradation					
DMP	0	0	0	0	0	100	100	100	100	0	
DEP	18.6	31.7	21.9	24.12	5.57	81.3	68.2	78.0	75.88	5.57	
	5	6	6			5	4	4			
DBP	37.8	49.5	39.5	42.30	5.17	62.1	50.4	60.4	57.70	5.17	
	4	4	2			6	6	8			
DEH	75.8	97.5	80.6	84.64	9.30	24.1	2.50	19.4	15.36	9.30	
P	2	0	0			8		0			
C33 (Day 4)											
	Concentration					Percent			Average		SD
	(mg/L)					degradation					
DMP	0	0	0	0	0	100	100	100	100	0	
DEP	0	0	0	0	0	100	100	100	100	0	

DBP	10.4	36.7	25.6	24.28	10.8	89.5	63.2	74.3	75.72	10.8
	1	8	4		1	9	2	6		1
DEH	75.5	91.6	78.0	81.75	7.08	24.4	8.34	21.9	18.25	7.08
P	6	6	3			4		7		

C33 (Day 6)

	Concentration (mg/L)			Average e	SD	Percent degradation			Average e	SD
DMP	0	0	0	0	0	100	100	100	100	0
DEP	0	0	0	0	0	100	100	100	100	0
DBP	0	0	0	0	0	100	100	100	100	0
DEH	54.3	65.1	60.6	60.04	4.43	45.6	34.8	39.3	39.96	4.43
P	2	2	9			8	8	1		

C33 (Day 8)

	Concentration (mg/L)			Average e	SD	Percent degradation			Average e	SD
DMP	0	0	0	0	0	100	100	100	100	0
DEP	0	0	0	0	0	100	100	100	100	0
DBP	0	0	0	0	0	100	100	100	100	0
DEH	30.4	38.9	49.1	39.52	7.67	69.5	61.0	50.8	60.48	7.67
P	3	3	9			7	7	1		

Table D9 PAE concentration remaining and percent degradation during degradation of the PAE mixture (DEHP, DBP, DEP, and DMP) in the abiotic control.

Abiotic control (Day 2)

	Concentration (mg/L)			Average	SD	Percent degradation			Average	SD
				e					e	
DMP	91.94	94.37	88.19	91.50	2.5	8.06	5.63	11.8	8.50	2.5
					4			1		4
DEP	88.47	93.45	90.01	90.64	2.0	11.53	6.55	9.99	9.36	2.0
					8					8
DBP	106.6	102.2	109.7	106.22	3.1	-6.65	-2.23	-	-6.22	3.1
	5	3	8		0			9.78		0
DEH	110.1	105.4	101.4	105.67	3.5	-	-5.45	-	-5.67	3.5
P	2	5	5		4	10.12		1.45		4
Abiotic control (Day 4)										
	Concentration (mg/L)			Average	SD	Percent degradation			Average	SD
				e					e	
DMP	90.71	94.87	90.87	92.15	1.9	9.29	5.13	9.13	7.85	1.9
					2					2
DEP	88.78	93.02	91.45	91.08	1.7	11.22	6.98	8.55	8.92	1.7
					5					5
DBP	104.0	109.5	106.0	106.54	2.2	-4.02	-9.51	-	-6.54	2.2
	2	1	8		6			6.08		6
DEH	106.9	103.4	100.0	103.48	2.8	-6.98	-3.45	-	-3.48	2.8
P	8	5	2		4			0.02		4
Abiotic control (Day 6)										
	Concentration			Average	SD	Percent			Average	SD

	(mg/L)			e	degradation			e		
DMP	83.26	93.81	90.76	89.28	4.4	16.74	6.19	9.24	10.72	4.4
					3					3
DEP	83.44	94.42	87.07	88.31	4.5	16.56	5.58	12.9	11.69	4.5
					7			3		7
DBP	99.45	120.8	107.7	109.36	8.8	0.55	-	-	-9.36	8.8
		7	6		2		20.87	7.76		2
DEH	108.8	101.6	95.50	102.02	5.4	-8.89	-1.67	4.50	-2.02	5.4
P	9	7			7					7
Abiotic control (Day 8)										
	Concentration			Averag	SD	Percent			Averag	SD
	(mg/L)			e		degradation			e	
DMP	83.05	94.65	86.87	88.19	4.8	16.95	5.35	13.1	11.81	4.8
					3			3		3
DEP	83.96	92.76	82.23	86.32	4.6	16.04	7.24	17.7	13.68	4.6
					1			7		1
DBP	118.0	110.6	102.3	110.34	6.4	-	-	-	-10.34	6.4
	1	7	4		0	18.01	10.67	2.34		0
DEH	103.7	97.30	101.5	100.85	2.6	-3.70	2.70	-	-0.85	2.6
P	0		6		6			1.56		6

Table D10 Viable cell counts of C10, C22, and C33 during degradation of the PAE mixture.

PAE Mixture C10

	Log CFU/mL			Average	SD
Day 0	6.56	6.65	6.99	6.73	0.19
Day 2	9.15	9.13	9.15	9.14	0.01
Day 4	9.45	9.41	9.50	9.45	0.04
Day 6	9.90	9.96	9.93	9.93	0.02
PAE Mixture C22					
	Log CFU/mL			Average	SD
Day 0	6.85	6.85	6.65	6.78	0.09
Day 2	7.77	7.78	7.79	7.78	0.01
Day 4	8.68	8.77	8.88	8.78	0.08
Day 6	8.93	8.95	8.94	8.94	0.01
Day 8	9.21	9	8.82	9.01	0.16
PAE Mixture C33					
	Log CFU/mL			Average	SD
Day 0	6.30	6.99	6.45	6.58	0.30
Day 2	8.01	8.12	8.28	8.14	0.11
Day 4	7.95	8.22	8.20	8.12	0.12
Day 6	8.49	8.36	8.42	8.42	0.05
Day 8	8.24	8.24	8.24	8.24	0.00

Table D11 DEHP concentrations remaining during degradation of different initial concentrations of DEHP by C10.

Initial DEHP concentration (50 mg/L)			
Day	Remaining concentration	Average	SD

(mg/L)					
0	48.13	50.00	50.57	49.57	1.04
1	35.65	37.69	26.90	33.41	4.68
2	15.48	29.11	23.71	22.77	5.60
3	15.22	22.47	15.22	17.64	3.42
4	13.01	0.00	15.22	9.41	6.71
5	0.00	0.00	0.00	0.00	0.00
6	0.00	0.00	0.00	0.00	0.00
7	0.00	0.00	0.00	0.00	0.00
8	0.00	0.00	0.00	0.00	0.00
Initial DEHP concentration (100 mg/L)					
Day	Remaining concentration			Average	SD
	(mg/L)				
0	116.34	105.72	101.57	107.88	6.22
1	76.00	97.94	97.94	90.62	10.34
2	55.21	65.12	64.05	61.46	4.44
3	38.49	32.38	34.86	35.24	2.51
4	38.22	29.28	29.28	32.26	4.21
5	0.00	16.46	12.12	9.53	6.96
6	11.50	0.00	0.00	3.83	5.42
7	0.00	0.00	0.00	0.00	0.00
8	0.00	0.00	0.00	0.00	0.00
Initial DEHP concentration (200 mg/L)					

Day	Remaining concentration			Average	SD
	(mg/L)				
0	250.64	229.94	178.27	219.62	30.43
1	191.37	217.29	193.84	200.83	11.68
2	163.67	157.75	141.73	154.38	9.27
3	123.60	127.31	104.66	118.52	9.92
4	81.75	62.28	93.07	79.04	12.71
5	25.39	28.84	25.21	26.48	1.67
6	43.88	19.46	0.00	21.12	17.95
7	0.00	0.00	0.00	0.00	0.00
8	0.00	0.00	0.00	0.00	0.00
Initial DEHP concentration (500 mg/L)					
Day	Remaining concentration			Average	SD
	(mg/L)				
0	505.71	496.24	489.60	497.18	6.61
1	499.78	499.78	496.59	498.72	1.50
2	446.43	480.93	435.64	454.33	19.32
3	252.41	197.29	307.79	252.50	45.11
4	143.32	167.92	257.28	189.51	48.96
5	379.37	38.49	231.71	216.52	139.58
6	15.04	77.15	41.23	44.47	25.46
7	114.22	73.70	17.43	68.45	39.69
8	15.05	42.00	18.00	25.02	12.07

Initial DEHP concentration (800 mg/L)					
Day	Remaining concentration			Average	SD
	(mg/L)				
0	965.85	710.25	806.69	827.60	105.39
1	410.16	545.00	641.42	532.19	94.85
2	405.82	468.99	603.73	492.85	82.54
3	271.34	329.03	250.29	283.55	33.28
4	280.37	230.03	350.44	286.94	49.38
5	175.26	215.25	193.40	194.64	16.35
6	241.09	412.28	326.64	326.67	69.89
7	190.83	300.01	190.83	227.23	51.47
8	70.69	128.64	128.64	109.32	27.32

Table D12 Viable cell counts of C10 cultured with DEHP intermediates as sole source of carbon and in the biological control (no carbon source added).

Biological control (C10)					
	Log CFU/mL			Average	SD
Day 0	7.14	6.88	7.00	7.01	0.11
Day 1	7.81	7.88	7.89	7.86	0.04
Day 2	7.78	8.05	7.92	7.92	0.11
Day 3	7.98	8.01	8.04	8.01	0.02
Day 4	7.8	7.88	7.96	7.88	0.07
Day 5	7.62	7.71	7.79	7.71	0.07

MEHP (C10)					
	Log CFU/mL			Average	SD
Day 0	7.05	7.00	7.18	7.08	0.08
Day 1	7.35	7.50	7.41	7.42	0.06
Day 2	8.42	8.55	8.75	8.57	0.14
Day 3	8.18	8.59	8.34	8.37	0.17
Day 4	8.65	8.3	8.17	8.37	0.20
Day 5	8.27	8.13	8.51	8.30	0.16
2-ethylhexanol (C10)					
	Log CFU/mL			Average	SD
Day 0	7.05	7.00	7.18	7.08	0.08
Day 1	6.70	6.84	7.17	6.90	0.20
Day 2	6.28	7.39	6.80	6.82	0.45
Day 3	8.75	8.28	7.60	8.21	0.47
Day 4	7.22	7.79	8.38	7.80	0.47
Day 5	7.62	7.42	8.35	7.80	0.40
Phthalic acid					
	Log CFU/mL			Average	SD
Day 0	7.05	7.00	7.18	7.08	0.08
Day 1	8.08	8.26	8.39	8.24	0.13
Day 2	8.23	8.30	8.58	8.37	0.15
Day 3	8.29	8.42	8.58	8.43	0.12
Day 4	8.25	8.32	8.49	8.35	0.10

Day 5	8.11	8.2	8.28	8.20	0.07
Protocatechuic acid					
	Log CFU/mL			Average	SD
Day 0	7.05	7.00	7.18	7.08	0.08
Day 1	8.43	8.12	7.89	8.15	0.22
Day 2	8.24	8.41	8.79	8.48	0.23
Day 3	8.40	8.84	8.69	8.64	0.18
Day 4	8.51	8.77	8.31	8.53	0.19
Day 5	8.27	8.36	7.91	8.18	0.19

Appendix E: Phase II Results

Table E1 Percent DEHP degradation by the twenty-one isolates from C10 on day 8.

	Percent DEHP degradation (Day 8)			Average	SD
OR01	15.09	15.62	16.86	15.86	0.74
OR02	12.56	4.33	8.62	8.51	3.36
OR03	-7.43	8.80	15.97	5.78	9.79
OR04	7.45	11.09	20.74	13.09	5.61
OR05	0.98	6.57	9.21	5.59	3.43
OR06	1.86	-3.43	8.09	2.18	4.71
OR07	18.68	4.27	7.80	10.25	6.13
OR08	15.74	12.86	8.27	12.29	3.08
OR09	29.21	20.13	25.73	25.02	3.74
OR10	10.27	10.20	12.45	10.97	1.04

OR11	37.97	44.64	25.14	35.92	8.09
OR12	12.06	4.59	13.59	10.08	3.93
OR13	86.72	81.27	80.05	82.68	2.90
OR14	17.93	28.76	39.05	28.58	8.62
OR15	19.22	6.67	6.43	10.77	5.97
OR16	59.30	64.87	53.12	59.10	4.80
OR17	23.98	31.66	25.46	27.03	3.33
OR18	39.61	39.61	37.10	38.77	1.18
OR19	48.94	39.86	41.41	43.41	3.97
OR20	42.38	40.89	38.45	40.57	1.62
OR21	76.83	84.69	92.09	84.54	6.46

Table E2 Viable cell counts of the twenty-one isolates on Day 0 and Day 8 of DEHP degradation.

	Log CFU/mL (Day 0)			Average	SD
OR01	6.62	6.69	6.76	6.69	0.06
OR02	6.69	6.77	6.61	6.69	0.07
OR03	7.70	7.79	7.59	7.69	0.08
OR04	7.70	7.79	7.59	7.69	0.08
OR05	7.03	7.21	7.38	7.21	0.14
OR06	7.96	7.54	7.85	7.78	0.18
OR07	7.57	7.41	6.96	7.31	0.26
OR08	7.70	7.66	7.76	7.71	0.04
OR09	7.56	7.70	7.91	7.72	0.14

OR10	7.15	7.09	6.96	7.07	0.08
OR11	7.29	7.68	7.97	7.65	0.28
OR12	7.68	7.27	7.52	7.49	0.17
OR13	7.59	7.70	7.81	7.70	0.09
OR14	7.59	7.40	7.51	7.50	0.08
OR15	7.19	7.33	7.45	7.32	0.11
OR16	7.28	7.21	7.10	7.20	0.07
OR17	7.68	7.62	7.53	7.61	0.06
OR18	7.08	7.14	7.36	7.19	0.12
OR19	6.92	7.02	7.10	7.01	0.07
OR20	6.81	6.92	7.03	6.92	0.09
OR21	6.95	6.83	7.07	6.95	0.10
Log CFU/mL (Day 8) Average SD					
OR01	6.98	7.32	7.59	7.30	0.25
OR02	6.41	6.32	6.52	6.42	0.08
OR03	7.49	7.41	7.30	7.40	0.08
OR04	8.27	8.33	8.11	8.24	0.09
OR05	6.30	6.31	6.30	6.30	0.00
OR06	8.77	8.72	8.76	8.75	0.02
OR07	8.10	7.99	7.85	7.98	0.10
OR08	7.89	8.21	8.21	8.10	0.15
OR09	8.71	8.67	8.32	8.57	0.18
OR10	6.22	6.73	6.13	6.36	0.26

OR11	8.57	8.44	8.56	8.52	0.06
OR12	8.44	8.50	8.70	8.55	0.11
OR13	8.75	9.12	8.89	8.92	0.15
OR14	8.60	8.70	8.97	8.76	0.16
OR15	7.66	7.55	7.68	7.63	0.06
OR16	8.69	8.80	8.84	8.78	0.06
OR17	8.50	8.70	8.26	8.49	0.18
OR18	8.07	8.26	8.48	8.27	0.17
OR19	6.65	6.81	6.52	6.66	0.12
OR20	6.80	6.69	6.83	6.77	0.06
OR21	9.60	9.41	9.91	9.64	0.21

Table E3 Viable cell counts of the twenty-one isolates of C10 on DEHP intermediates.

	OR01 (Log CFU/mL)			Average	SD	Day 5- Day 0
Day 0	6.60	6.70	6.78	6.69	0.07	
BC	6.85	6.48	6.70	6.67	0.15	-0.02
EHA-2	6.85	6.30	6.78	6.64	0.24	-0.05
EHA-1	6.78	7.08	6.85	6.90	0.13	0.21
DEHP	7.30	7.60	7.00	7.30	0.25	0.61
PA	6.95	6.95	7.00	6.97	0.02	0.28
PCA	6.85	6.95	6.95	6.92	0.05	0.23
MEHP	7.00	7.30	7.48	7.26	0.20	0.57

MBP	6.95	7.04	6.95	6.98	0.04	0.29
<hr/>						
<hr/>						
	OR02 (Log CFU/mL)			Average	SD	Day 5- Day 0
Day 0	6.60	6.70	6.78	6.69	0.07	
BC	6.00	6.70	6.60	6.43	0.31	-0.26
EHA-2	6.60	6.78	6.70	6.69	0.07	0.00
EHA-1	6.48	6.48	6.48	6.48	0.00	-0.21
DEHP	6.48	6.48	6.30	6.42	0.08	-0.27
PA	6.48	6.78	6.70	6.65	0.13	-0.04
PCA	6.70	6.78	6.70	6.73	0.04	0.04
MEHP	6.60	6.48	6.30	6.46	0.12	-0.23
MBP	6.30	6.78	6.85	6.64	0.24	-0.05
<hr/>						
	OR03 (Log CFU/mL)			Average	SD	Day 5- Day 0
Day 0	6.60	6.85	6.48	6.64	0.15	
BC	6.52	6.34	6.41	6.43	0.07	-0.21
EHA-2	6.04	6.18	6.00	6.07	0.08	-0.57
EHA-1	6.30	6.30	6.41	6.34	0.05	-0.30
DEHP	6.52	6.36	6.34	6.41	0.08	-0.23
PA	6.43	6.45	6.40	6.43	0.02	-0.21
PCA	6.85	6.70	6.60	6.72	0.10	0.08

MEHP	6.40	6.41	6.34	6.39	0.03	-0.25
MBP	6.78	6.70	6.30	6.59	0.21	-0.05
<hr/>						
	OR04 (Log CFU/mL)			Average	SD	Day 5- Day 0
Day 0	6.78	6.60	6.78	6.72	0.08	
BC	6.08	6.15	6.48	6.23	0.17	-0.49
EHA-2	6.00	6.04	6.26	6.10	0.11	-0.62
EHA-1	5.95	6.15	6.23	6.11	0.12	-0.61
DEHP	6.36	6.30	6.15	6.27	0.09	-0.45
PA	6.70	6.30	6.70	6.57	0.19	-0.15
PCA	6.48	6.43	6.28	6.40	0.08	-0.32
MEHP	5.48	5.60	5.48	5.52	0.06	-1.20
MBP	6.48	6.34	6.26	6.36	0.09	-0.36
<hr/>						
	OR05 (Log CFU/mL)			Average	SD	Day 5- Day 0
Day 0	6.32	6.48	6.41	6.40	0.07	
BC	6.70	6.48	6.85	6.67	0.15	0.30
EHA-2	7.40	7.32	7.30	7.34	0.04	1.00
EHA-1	6.00	6.30	6.30	6.20	0.14	-0.40
DEHP	6.30	6.30	6.30	6.30	0.00	-0.10
PA	6.78	6.78	6.60	6.72	0.08	0.38
PCA	6.30	6.15	6.08	6.18	0.09	-0.10

MEHP	6.60	6.30	6.00	6.30	0.25	0.20
MBP	6.48	6.48	6.78	6.58	0.14	0.08
<hr/>						
	OR06 (Log CFU/mL)			Average	SD	Day 5- Day 0
Day 0	6.70	7.08	6.70	6.83	0.18	
BC	6.95	7.11	7.11	7.06	0.08	0.23
EHA-2	7.04	7.18	7.08	7.10	0.06	0.27
EHA-1	6.78	6.60	6.85	6.74	0.10	-0.09
DEHP	6.95	6.85	6.48	6.76	0.20	-0.07
PA	6.90	7.08	7.11	7.03	0.09	0.20
PCA	7.08	7.20	7.23	7.17	0.07	0.34
MEHP	7.11	7.20	6.85	7.05	0.15	0.22
MBP	6.90	6.90	6.95	6.92	0.02	0.09
<hr/>						
	OR07 (Log CFU/mL)			Average	SD	Day 5- Day 0
Day 0	7.00	7.48	7.60	7.36	0.26	
BC	6.90	7.08	7.18	7.05	0.11	-0.31
EHA-2	6.70	6.85	6.90	6.82	0.09	-0.54
EHA-1	7.04	6.78	6.95	6.92	0.11	-0.44
DEHP	7.08	7.04	6.85	6.99	0.10	-0.37
PA	6.70	7.08	6.48	6.75	0.25	-0.61
PCA	7.30	7.00	7.00	7.10	0.14	-0.26

MEHP	7.00	7.00	7.48	7.16	0.22	-0.20
MBP	7.60	7.00	7.30	7.30	0.25	-0.06
<hr/>						
	OR08 (Log CFU/mL)			Average	SD	Day 5- Day 0
Day 0	6.78	6.70	6.70	6.73	0.04	
BC	6.00	6.85	6.90	6.58	0.41	-0.15
EHA-2	6.15	6.32	6.36	6.28	0.09	-0.45
EHA-1	6.30	6.48	6.00	6.26	0.20	-0.47
DEHP	6.30	6.00	6.00	6.10	0.14	-0.63
PA	6.95	6.30	6.00	6.42	0.40	-0.31
PCA	6.30	6.30	6.60	6.40	0.14	-0.33
MEHP	6.70	6.00	6.30	6.33	0.29	-0.40
MBP	6.60	6.30	6.30	6.40	0.14	-0.33
<hr/>						
	OR09 (Log CFU/mL)			Average	SD	Day 5- Day 0
Day 0	7.08	6.90	6.70	6.89	0.16	
BC	7.00	7.11	6.48	6.86	0.28	-0.03
EHA-2	6.48	6.60	6.85	6.64	0.15	-0.25
EHA-1	7.18	6.60	6.78	6.85	0.24	-0.04
DEHP	6.70	6.70	6.30	6.57	0.19	-0.32
PA	6.70	6.70	6.95	6.78	0.12	-0.11
PCA	6.48	6.85	7.00	6.77	0.22	-0.12

MEHP	6.90	6.70	6.60	6.73	0.13	-0.16
MBP	6.90	6.90	6.70	6.84	0.10	-0.05
<hr/>						
	OR10 (Log CFU/mL)			Average	SD	Day 5- Day 0
Day 0	6.15	5.95	6.08	6.06	0.08	
BC	6.38	6.23	6.28	6.30	0.06	0.24
EHA-2	6.15	6.15	6.08	6.12	0.03	0.06
EHA-1	6.48	6.00	6.48	6.32	0.22	0.26
DEHP	6.48	6.60	6.00	6.36	0.26	0.30
PA	6.04	5.78	5.70	5.84	0.15	-0.22
PCA	5.48	6.04	5.70	5.74	0.23	-0.32
MEHP	6.04	5.78	5.60	5.81	0.18	-0.25
MBP	6.30	6.00	6.00	6.10	0.14	0.04
<hr/>						
	OR11 (Log CFU/mL)			Average	SD	Day 5- Day 0
Day 0	7.30	7.95	7.85	7.70	0.29	
BC	7.70	7.70	7.30	7.57	0.19	-0.13
EHA-2	7.18	7.26	7.26	7.23	0.04	-0.47
EHA-1	7.34	7.23	7.11	7.23	0.09	-0.47
DEHP	7.60	7.48	7.48	7.52	0.06	-0.18
PA	7.48	7.48	7.70	7.55	0.10	-0.15
PCA	7.60	7.00	7.00	7.20	0.28	-0.50

MEHP	7.20	7.20	7.23	7.21	0.01	-0.49
MBP	7.78	7.70	7.70	7.73	0.04	0.03
<hr/>						
	OR12 (Log CFU/mL)			Average	SD	Day 5- Day 0
Day 0	6.70	6.60	6.30	6.53	0.17	
BC	6.00	6.60	6.60	6.40	0.28	-0.13
EHA-2	6.78	7.08	6.85	6.90	0.13	0.37
EHA-1	6.60	6.85	6.30	6.58	0.22	0.05
DEHP	6.70	6.48	6.48	6.55	0.10	0.02
PA	6.96	6.70	6.72	6.79	0.12	0.26
PCA	6.70	6.70	7.08	6.83	0.18	0.30
MEHP	6.60	6.60	6.48	6.56	0.06	0.03
MBP	6.85	6.95	5.78	6.53	0.53	0.00
<hr/>						
	OR13 (Log CFU/mL)			Average	SD	Day 5- Day 0
Day 0	6.95	6.78	7.00	6.91	0.10	
BC	7.04	7.20	7.00	7.08	0.09	0.17
EHA-2	6.95	6.90	6.90	6.92	0.02	0.01
EHA-1	7.11	7.04	7.15	7.10	0.04	0.19
DEHP	7.11	6.85	6.78	6.91	0.15	0.00
PA	7.30	7.48	7.00	7.26	0.20	0.35
PCA	7.30	7.30	7.00	7.20	0.14	0.29

MEHP	7.00	7.15	7.11	7.09	0.06	0.18
MBP	7.26	7.26	7.20	7.24	0.02	0.33
	OR14 (Log CFU/mL)			Average	SD	Day 5- Day 0
Day 0	6.78	6.78	6.60	6.72	0.08	
BC	7.00	7.04	6.85	6.96	0.08	0.24
EHA-2	6.85	6.48	6.70	6.67	0.15	-0.05
EHA-1	6.78	6.78	6.30	6.62	0.22	-0.10
DEHP	6.48	6.78	6.85	6.70	0.16	-0.02
PA	6.78	6.78	6.85	6.80	0.03	0.08
PCA	6.48	6.48	6.60	6.52	0.06	-0.20
MEHP	6.48	6.48	6.85	6.60	0.17	-0.12
MBP	6.85	6.70	6.60	6.72	0.10	0.00
	OR15 (Log CFU/mL)			Average	SD	Day 5- Day 0
Day 0	6.95	6.78	6.70	6.81	0.11	
BC	6.85	7.00	6.70	6.85	0.12	0.04
EHA-2	6.78	7.08	6.85	6.90	0.13	0.09
EHA-1	7.23	6.95	6.90	7.03	0.14	0.22
DEHP	6.60	6.70	6.60	6.63	0.05	-0.18
PA	6.85	7.04	6.90	6.93	0.08	0.12
PCA	6.95	6.95	6.70	6.87	0.12	0.06
MEHP	6.70	6.90	6.60	6.73	0.13	-0.08

MBP	7.60	7.60	7.48	7.56	0.06	0.75
<hr/>						
	OR16 (Log CFU/mL)			Average	SD	Day 5- Day 0
Day 0	7.08	6.90	7.00	6.99	0.07	
BC	6.85	6.95	6.95	6.92	0.05	-0.07
EHA-2	6.78	6.78	6.85	6.80	0.03	-0.19
EHA-1	6.85	7.04	7.00	6.96	0.08	-0.03
DEHP	6.78	6.85	6.70	6.77	0.06	-0.22
PA	7.30	7.48	7.00	7.26	0.20	0.27
PCA	6.90	6.70	7.04	6.88	0.14	-0.11
MEHP	7.00	7.48	7.30	7.26	0.20	0.27
MBP	7.00	6.85	6.00	6.62	0.44	-0.37
<hr/>						
	OR17 (Log CFU/mL)			Average	SD	Day 5- Day 0
Day 0	6.90	6.95	7.04	6.97	0.06	
BC	6.70	6.48	6.60	6.59	0.09	-0.38
EHA-2	6.90	6.00	6.60	6.50	0.38	-0.47
EHA-1	6.30	6.00	6.48	6.26	0.20	-0.71
DEHP	6.30	6.48	6.70	6.49	0.16	-0.48
PA	6.70	6.60	6.30	6.53	0.17	-0.44
PCA	6.85	6.00	6.60	6.48	0.36	-0.49
MEHP	6.00	6.30	6.70	6.33	0.29	-0.64

MBP	6.78	6.85	6.95	6.86	0.07	-0.11
	OR18 (Log CFU/mL)			Average	SD	Day 5- Day 0
Day 0	7.26	7.04	7.32	7.21	0.12	
BC	7.90	8.32	8.20	8.14	0.18	0.93
EHA-2	8.00	8.30	7.90	8.07	0.17	0.86
EHA-1	8.00	7.60	8.04	7.88	0.20	0.67
DEHP	8.00	8.30	8.48	8.26	0.20	1.05
PA	7.60	7.60	8.20	7.80	0.28	0.59
PCA	8.30	8.00	8.00	8.10	0.14	0.89
MEHP	8.48	8.48	8.00	8.32	0.22	1.11
MBP	8.15	7.90	7.85	7.96	0.13	0.75
	OR19 (Log CFU/mL)			Average	SD	Day 5- Day 0
Day 0	6.60	6.78	6.70	6.69	0.07	
BC	7.15	7.08	7.04	7.09	0.04	0.40
EHA-2	6.00	6.60	6.48	6.36	0.26	-0.33
EHA-1	6.00	6.60	6.78	6.46	0.33	-0.23
DEHP	6.60	6.78	6.48	6.62	0.12	-0.07
PA	6.30	6.48	6.60	6.46	0.12	-0.23
PCA	7.00	7.00	7.00	7.00	0.00	0.31
MEHP	7.30	7.00	7.00	7.10	0.14	0.41
MBP	6.85	6.95	6.48	6.76	0.20	0.07

	OR20 (Log CFU/mL)			Average	SD	Day 5- Day 0
Day 0	6.48	6.60	6.70	6.59	0.09	
BC	7.85	7.30	7.70	7.62	0.23	1.03
EHA-2	7.00	7.04	7.08	7.04	0.03	0.45
EHA-1	6.85	6.90	6.60	6.78	0.13	0.19
DEHP	6.85	6.70	6.78	6.77	0.06	0.18
PA	7.78	7.85	7.85	7.82	0.03	1.23
PCA	7.15	7.15	7.08	7.12	0.03	0.53
MEHP	7.48	7.00	7.00	7.16	0.22	0.57
MBP	7.70	7.85	7.95	7.83	0.10	1.24
	OR21 (Log CFU/mL)			Average	SD	Day 5- Day 0
Day 0	6.98	6.75	6.81	6.85	0.10	
BC	6.60	6.95	6.30	6.62	0.27	-0.23
EHA-2	6.60	6.70	6.60	6.63	0.05	-0.22
EHA-1	6.60	6.60	6.78	6.66	0.08	-0.19
DEHP	7.60	7.85	7.78	7.74	0.10	0.89
PA	5.95	5.65	5.85	5.82	0.12	-1.03
PCA	7.85	7.70	7.30	7.62	0.23	0.77
MEHP	7.48	7.95	7.78	7.74	0.20	0.89
MBP	6.30	6.30	6.70	6.43	0.19	-0.42

Table E4 Crude oil displacement activities of the twenty-one isolates from C10.

Isolates	Oil displacement zone (cm)			Average	SD
OR01	ND	ND	ND		
OR02	ND	ND	ND		
OR03	ND	ND	ND		
OR04	ND	ND	ND		
OR05	2	2.2	2.3	2.2	0.1
OR06	4.1	4	4	4.0	0.0
OR07	2.6	2.5	2.5	2.5	0.0
OR08	4	4.2	3.9	4.0	0.1
OR09	ND	ND	ND		
OR10	1.6	1.3	1.5	1.5	0.1
OR11	1.5	1.3	1.7	1.5	0.2
OR12	1.9	2	2.3	2.1	0.2
OR13	2.4	3	2	2.5	0.4
OR14	1.2	1.7	1.9	1.6	0.3
OR15	5.4	4.7	5	5.0	0.3
OR16	ND	ND	ND		
OR17	ND	ND	ND		
OR18	ND	ND	ND		
OR19	2.7	2.7	2.6	2.7	0.0
OR20	ND	ND	ND		
OR21	1.4	1.3	2	1.6	0.3
ND: Not detected					

Appendix F: Phase III Results

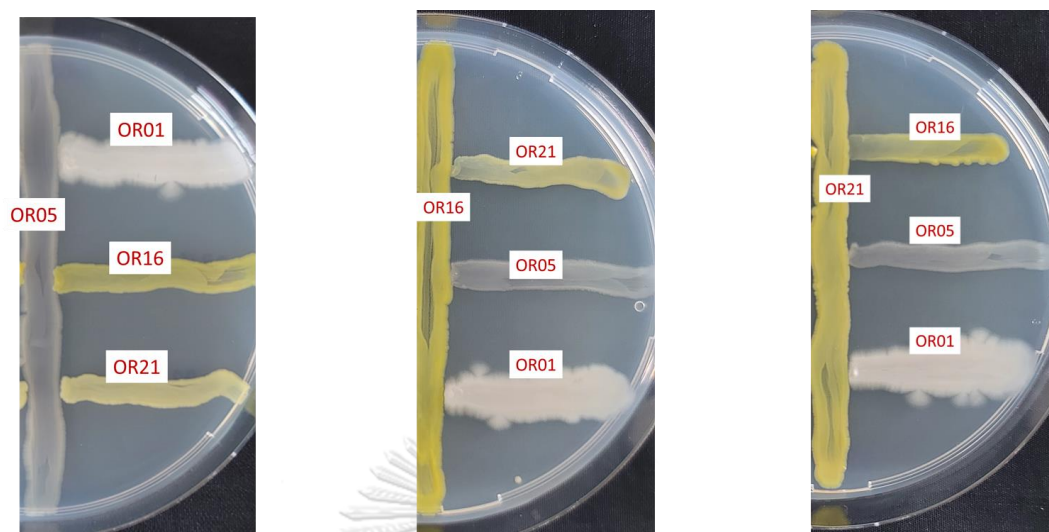


Figure F1 Antagonism test of OR01, OR05, OR16, and OR21 via the cross-streak method.

Table F1 Percent degradation of DEHP, DBP, DEP, and DMP by OR01, OR05, OR16, OR21, OR05 + OR21, Consortium A01 (OR01 + OR05 + OR16 + OR21), and Consortium A02 (OR05 + OR16 + OR21) on Day 4.

	Percent DEHP degradation (Day 4)			Average	SD
OR01	13.62	2.29	5.21	7.04	4.80
OR05	7.21	2.63	8.07	5.97	3.83
OR16	24.90	20.43	23.01	22.78	8.67
OR21	47.49	38.81	32.92	40	9.57
OR05 + OR21	79.24	78.51	62.30	73.35	18.19
A01	62.87	56.13	61.33	60.11	8.86
A02	80.41	70.35	88.00	79.59	7.23

Percent DBP degradation (Day			Average	SD	
4)					
OR01	6.02	4.18	0.00	3.40	2.52
OR05	21.74	13.59	15.19	16.84	7.39
OR16	10.49	5.74	10.13	8.79	4.98
OR21	100	100	100	100	45.63
OR05 +	100	100	100	100	0
OR21					
A01	94.61	100	95.46	96.69	2.35
A02	100	100	100	100	2.35
Percent DEP degradation (Day			Average	SD	
4)					
OR01	25.24	24.37	23.31	24.31	0.79
OR05	16.12	7.24	10.90	11.42	3.64
OR16	15.30	12.59	11.92	13.27	2.93
OR21	100	100	100	100	43.38
OR05 +	100	100	100	100	0.00
OR21					
A01	100	100	100	100	0.00
A02	100	100	100	100	0.00
Percent DMP degradation (Day			Average	SD	
4)					

OR01	20.41	16.32	19.18	18.64	1.71
OR05	27.56	28.46	29.10	28.38	0.63
OR16	26.14	20.70	24.60	23.81	2.83
OR21	100	100	100	100	38.13
OR05 + OR21	100	100	100	100	0
A01	100	100	100	100	0
A02	100	100	100	100	0

Table F2 Percent degradation of DEHP by OR21, OR05 + OR21, Consortium A01 (OR01 + OR05 + OR16 + OR21), and Consortium A02 (OR05 + OR16 + OR21) on days 2, 4, 6, and 8.

Sample	Percent degradation			Average	SD
A01 Day 2	33.56	39.10	34.76	35.81	2.38
A01 Day 4	62.87	56.13	61.33	60.11	2.88
A01 Day 6	57.16	64.52	78.75	66.81	8.96
A01 Day 8	75.49	73.49	74.58	74.52	0.82
Sample	Percent degradation			Average	SD
A02 Day 2	64.92	54.36	75.15	64.81	8.49
A02 Day 4	80.41	70.35	88.00	79.59	7.23
A02 Day 6	75.49	83.95	90.06	83.17	5.97
A02 Day 8	100.00	93.43	80.41	91.28	8.14

Sample	Percent degradation			Average	SD
OR21 Day 2	24.79	22.36	27.64	24.93	2.16
OR21 Day 4	47.49	38.81	32.92	39.74	5.98
OR21 Day 6	78.39	70.38	72.08	73.61	3.45
OR21 Day 8	75.48	90.04	88.10	84.54	6.46

Sample	Percent degradation			Average	SD
OR05 + OR21 Day 2	50.71	50.41	49.01	50.04	0.74
OR05 + OR21 Day 4	79.24	78.51	62.30	73.35	7.82
OR05 + OR21 Day 6	74.14	69.89	71.47	71.83	1.75
OR05 + OR21 Day 8	93.50	87.74	91.02	90.75	2.36

Table F3 Degradation of mixture of DEHP, DBP, DEP, and DMP by OR21, OR05 + OR21, Consortium A01 (OR01 + OR05 + OR16 + OR21), and Consortium A02 (OR05 + OR16 + OR21) on days 2, 4, 6, and 8.

Consortium A01 (Day 2)												
	Concentration			Average		SD		Percent		Average		SD
	(mg/L)			e				degradation		e		
DMP	0	0	0	0	0	100	100	100	100	100	0	
DEP	0	0	0	0	0	100	100	100	100	100	0	
DBP	0	14.9	22.2	12.39	9.26	100	85.2	78.0	87.76	9.15		
		2	6				7	2				
DEH	72.9	77.8	85.9	78.92	5.37	31.0	26.4	18.7	25.42	5.08		
P	5	2	8			6	6	5				

Consortium A01 (Day 4)

	Concentration			Average	SD	Percent			Average	SD
	(mg/L)			e		degradation			e	
DMP	0	0	0	0	0	100	100	100	100	0
DEP	0	0	0	0	0	100	100	100	100	0
DBP	0	0	0	0	0	100	100	100	100	0
DEH	42.1	27.0	43.6	37.59	7.49	60.1	74.4	58.7	64.48	7.07
P	2	4	1			9	5	9		

Consortium A01 (Day 6)

	Concentration			Average	SD	Percent			Average	SD
	(mg/L)			e		degradation			e	
DMP	0	0	0	0	0	100	100	100	100	0
DEP	0	0	0	0	0	100	100	100	100	0
DBP	0	0	0	0	0	100	100	100	100	0
DEH	19.9	28.8	55.0	34.62	14.9	81.1	72.7	47.9	67.28	14.0
P	5	5	7		1	5	4	6		9

Consortium A01 (Day 8)

	Concentration			Average	SD	Percent			Average	SD
	(mg/L)			e		degradation			e	
DMP	0	0	0	0	0	100	100	100	100	0
DEP	0	0	0	0	0	100	100	100	100	0

DBP	0	0	0	0	0	100	100	100	100	0
DEH	15.7	27.2	28.1	23.74	5.67	85.1	74.2	73.3	77.56	5.35
P	4	9	9			2	2	6		

Consortium A02 (Day 2)

	Concentration (mg/L)			Averag e	SD	Percent degradation			Averag e	SD
DMP	0	0	0	0	0	100	100	100	100	0
DEP	0	0	0	0	0	100	100	100	100	0
DBP	0	0	0	0	0	100	100	100	100	0
DEH	81.77	64.88	75.67	74.11	6.9	22.7	38.6	28.4	29.97	6.6
P					9	2	9	9		0

Consortium A02 (Day 4)

	Concentration (mg/L)			Averag e	SD	Percent degradation			Averag e	SD
DMP	0	0	0	0	0	100	100	100	100	0
DEP	0	0	0	0	0	100	100	100	100	0
DBP	0	0	0	0	0	100	100	100	100	0
DEH	44.43	37.26	28.77	36.82	6.4	58.0	64.7	72.8	65.20	6.0
P					0	1	9	1		5

Consortium A02 (Day 6)

	Concentration (mg/L)			Averag e	SD	Percent degradation			Averag e	SD
--	-------------------------	--	--	-------------	----	------------------------	--	--	-------------	----

DMP	0	0	0	0	0	100	100	100	100	0
DEP	0	0	0	0	0	100	100	100	100	0
DBP	0	0	0	0	0	100	100	100	100	0
DEH	30.91	28.44	33.55	30.97	2.0	70.7	73.1	68.2	70.74	1.9
P					9	9	2	9		7

Consortium A02 (Day 8)

	Concentration (mg/L)			Average	SD	Percent degradation			Average	SD
				e					e	
DMP	0	0	0	0	0	100	100	100	100	0
DEP	0	0	0	0	0	100	100	100	100	0
DBP	0	0	0	0	0	100	100	100	100	0
DEH	29.68	7.58	18.96	18.74	9.0	71.9	92.8	82.0	82.29	8.5
P					2	6	3	8		2

OR05 + OR21 (Day 2)

	Concentration (mg/L)			Average	SD	Percent degradation			Average	SD
				e					e	
DMP	0	0	0	0	0	100	100	100	100	0
DEP	0	0	0	0	0	100	100	100	100	0
DBP	4.70	9.74	9.46	7.97	2.3	95.3	90.3	90.6	92.13	2.2
					1	6	8	6		8
DEH	86.5	101.8	95.5	94.63	6.2	18.2	3.79	9.71	10.57	5.9
P	6	1	4		6	1				1

OR05 + OR21 (Day 4)

	Concentration			Averag	SD	Percent			Averag	SD
	(mg/L)			e		degradation			e	
DMP	0	0	0	0	0	100	100	100	100	0
DEP	0	0	0	0	0	100	100	100	100	0
DBP	0	0	0	0	0	100	100	100	100	0
DEH	69.4	76.42	71.8	72.57	2.9	34.4	27.7	32.0	31.42	2.7
P	1		8		0	1	9	7		4

OR05 + OR21 (Day 6)

	Concentration			Averag	SD	Percent			Averag	SD
	(mg/L)			e		degradation			e	
DMP	0	0	0	0	0	100	100	100	100	0
DEP	0	0	0	0	0	100	100	100	100	0
DBP	0	0	0	0	0	100	100	100	100	0
DEH	38.0	35.45	16.3	29.92	9.6	64.0	66.5	84.5	71.72	9.1
P	0		2		7	9	0	8		4

OR05 + OR21 (Day 8)

	Concentration			Averag	SD	Percent			Averag	SD
	(mg/L)			e		degradation			e	
DMP	0	0	0	0	0	100	100	100	100	0
DEP	0	0	0	0	0	100	100	100	100	0
DBP	0	0	0	0	0	100	100	100	100	0
DEH	9.97	7.83	16.8	11.54	3.8	90.5	92.6	84.1	89.09	3.6

P	2	3	7	0	1	2
----------	---	---	---	---	---	---

OR21 (Day 2)

	Concentration (mg/L)			Average	SD	Percent degradation			Average	SD
				e					e	
DMP	0	0	0	0.00	0.00	100	100	100	100	0
DEP	0	0	0	0.00	0.00	100	100	100	100	0
DBP	0	0	0	0.00	0.00	100	100	100	100	0
DEH	95.8	95.8	95.1	95.62	0.35	9.40	9.40	10.1	9.64	0.33
P	7	7	3					0		

OR21 (Day 4)

	Concentration (mg/L)			Average	SD	Percent degradation			Average	SD
				e					e	
DMP	0	0	0	0	0	100	100	100	100	0
DEP	0	0	0	0	0	100	100	100	100	0
DBP	0	0	0	0	0	100	100	100	100	0
DEH	70.0	80.8	82.4	77.79	5.50	33.7	23.5	22.1	26.49	5.19
P	7	7	3			9	8	0		

OR21 (Day 6)

	Concentration (mg/L)			Average	SD	Percent degradation			Average	SD
				e					e	
DMP	0	0	0	0	0	100	100	100	100	0

DEP	0	0	0	0	0	100	100	100	100	0
DBP	0	0	0	0	0	100	100	100	100	0
DEH	71.1	39.4	44.1	51.58	13.9	32.7	62.6	58.3	51.26	13.1
P	4	9	0		6	7	9	2		9

OR21 (Day 8)

	Concentration (mg/L)			Average	SD	Percent degradation			Average	SD
DMP	0	0	0	0	0	100	100	100	100	0
DEP	0	0	0	0	0	100	100	100	100	0
DBP	0	0	0	0	0	100	100	100	100	0
DEH	39.9	45.6	47.3	44.32	3.14	62.2	56.8	55.2	58.12	2.97
P	8	7	2			2	4	9		

Table F4 Viable cell counts of OR05 + OR21, Consortium A01 (OR01 + OR05 + OR16 + OR21), and Consortium A02 (OR05 + OR16 + OR21) on days 0, 2, 4, 6, and 8 of DEHP degradation.

A01 DEHP degradation (Day 0)						
	Log CFU/mL			Average	SD	
OR01	7.18	7.24	7.30	7.24	0.05	
OR05	7.10	7.35	7.44	7.30	0.15	
OR16	7.18	7.35	7.24	7.26	0.07	
OR21	7.24	7.30	7.24	7.26	0.03	
Total	7.78	7.92	7.92	7.87	0.07	

A01 DEHP degradation (Day 2)

	Log CFU/mL			Average	SD
OR01	7.60	7.48	7.30	7.46	0.12
OR05	7.95	7.90	7.95	7.94	0.02
OR16	8.67	8.67	7.70	8.35	0.46
OR21	8.66	8.70	7.71	8.36	0.46
Total	8.78	8.76	8.20	8.58	0.27

A01 DEHP degradation (Day 4)

	Log CFU/mL			Average	SD
OR01	7.60	8.00	7.00	7.53	0.41
OR05	7.85	7.78	7.00	7.54	0.38
OR16	8.79	8.71	8.70	8.73	0.04
OR21	9.65	8.69	8.67	9.01	0.46
Total	9.72	9.06	9.00	9.26	0.33

A01 DEHP degradation (Day 6)

	Log CFU/mL			Average	SD
OR01	6.48	6.30	6.00	6.26	0.20
OR05	7.60	7.48	7.78	7.62	0.12
OR16	8.85	8.84	8.79	8.83	0.02
OR21	8.70	8.71	8.85	8.75	0.07
Total	9.09	9.09	9.14	9.11	0.02

A01 DEHP degradation (Day 8)

	Log CFU/mL			Average	SD
OR01	6.48	6.00	6.30	6.26	0.20
OR05	7.60	7.70	7.60	7.63	0.05
OR16	8.96	8.89	8.90	8.92	0.03
OR21	8.95	8.96	8.95	8.95	0.00
Total	9.27	9.24	9.24	9.25	0.01

A02 DEHP degradation (Day 0)

	Log CFU/mL			Average	SD
OR05	7.22	7.48	7.56	7.42	0.15
OR16	7.30	7.48	7.37	7.38	0.07
OR21	7.37	7.43	7.37	7.39	0.03
Total	7.78	7.94	7.92	7.88	0.07

A02 DEHP degradation (Day 2)

	Log CFU/mL			Average	SD
OR05	7.95	8.00	8.04	8.00	0.04
OR16	8.86	8.84	8.85	8.85	0.01
OR21	8.67	8.70	8.70	8.69	0.01
Total	9.11	9.11	9.12	9.11	0.00

A02 DEHP degradation (Day 4)

	Log CFU/mL			Average	SD
--	------------	--	--	---------	----

OR05	7.78	7.85	7.95	7.86	0.07
OR16	9.01	8.95	8.95	8.97	0.03
OR21	9.00	8.95	9.00	8.98	0.02
Total	9.32	9.27	9.29	9.30	0.02

A02 DEHP degradation (Day 6)

	Log CFU/mL			Average	SD
OR05	7.60	7.78	7.70	7.69	0.07
OR16	8.79	8.77	8.78	8.78	0.01
OR21	8.65	8.70	8.59	8.65	0.04
Total	9.04	9.06	9.02	9.04	0.02

A02 DEHP degradation (Day 8)

	Log CFU/mL			Average	SD
OR05	7.00	7.30	7.00	7.10	0.14
OR16	8.00	8.04	8.20	8.08	0.09
OR21	8.48	8.30	8.48	8.42	0.08
Total	8.61	8.52	8.67	8.60	0.06

OR05 + OR21 DEHP degradation (Day 0)

	Log CFU/mL			Average	SD
OR05	7.30	7.37	7.43	7.36	0.05
OR21	7.67	7.73	7.67	7.69	0.03
Total	7.82	7.88	7.87	7.86	0.03

OR05 + OR21 DEHP degradation (Day 2)

	Log CFU/mL			Average	SD
OR05	8.04	8.48	8.46	8.33	0.20
OR21	9.30	9.48	9.40	9.39	0.07
Total	9.32	9.52	9.45	9.43	0.08

OR05 + OR21 DEHP degradation (Day 4)

	Log CFU/mL			Average	SD
OR05	8.00	8.00	8.04	8.01	0.02
OR21	9.15	9.28	9.30	9.24	0.07
Total	9.18	9.30	9.32	9.27	0.06

OR05 + OR21 DEHP degradation (Day 6)

	Log CFU/mL			Average	SD
OR05	7.48	7.30	7.00	7.26	0.20
OR21	9.19	9.36	9.20	9.25	0.08
Total	9.20	9.37	9.21	9.26	0.08

OR05 + OR21 DEHP degradation (Day 8)

	Log CFU/mL			Average	SD
OR05	7.48	8.11	8.30	7.96	0.35
OR21	9.00	9.20	9.05	9.08	0.09
Total	9.01	9.24	9.12	9.12	0.09

Table F5 Viable cell counts of OR05 + OR21, Consortium A01 (OR01 + OR05 + OR16 + OR21), and Consortium A02 (OR05 + OR16 + OR21) on days 0, 2, 4, 6, and 8 of the degradation of a mixture of DEHP, DBP, DEP, and DMP.

A01 Mix PAE degradation (Day 0)					
	Log CFU/mL			Average	SD
OR01	7.18	7.24	7.30	7.24	0.05
OR05	7.10	7.35	7.44	7.30	0.15
OR16	7.18	7.35	7.24	7.26	0.07
OR21	7.24	7.30	7.24	7.26	0.03
Total	7.78	7.92	7.92	7.87	0.07
A01 Mix PAE degradation (Day 2)					
	Log CFU/mL			Average	SD
OR01	7.48	7.30	7.00	7.26	0.20
OR05	7.95	7.90	7.78	7.88	0.07
OR16	7.70	7.60	7.48	7.59	0.09
OR21	8.80	8.71	8.79	8.76	0.04
Total	8.90	8.81	8.85	8.86	0.04
A01 Mix PAE degradation (Day 4)					
	Log CFU/mL			Average	SD
OR01	7.70	7.70	7.78	7.73	0.04
OR05	7.48	7.60	7.48	7.52	0.06
OR16	8.18	8.18	8.20	8.19	0.01

OR21	8.15	8.11	8.20	8.15	0.04
Total	8.57	8.57	8.61	8.58	0.02

A01 Mix PAE degradation (Day 6)

	Log CFU/mL			Average	SD
OR01	6.85	6.78	6.70	6.77	0.06
OR05	7.85	7.90	7.95	7.90	0.04
OR16	8.30	8.28	8.30	8.29	0.01
OR21	8.20	8.26	8.23	8.23	0.02
Total	8.64	8.66	8.67	8.66	0.01

A01 Mix PAE degradation (Day 8)

	Log CFU/mL			Average	SD
OR01	6.48	6.00	6.00	6.16	0.22
OR05	7.60	7.48	7.00	7.36	0.26
OR16	8.28	8.32	8.26	8.29	0.03
OR21	8.34	8.32	8.26	8.31	0.04
Total	8.66	8.65	8.57	8.63	0.04

A02 Mix PAE degradation (Day 0)

	Log CFU/mL			Average	SD
OR05	7.22	7.48	7.56	7.42	0.15
OR16	7.30	7.48	7.37	7.38	0.07
OR21	7.37	7.43	7.37	7.39	0.03

Total	7.78	7.94	7.92	7.88	0.07
--------------	------	------	------	------	------

A02 Mix PAE degradation (Day 2)

	Log CFU/mL			Average	SD
OR05	8.60	8.60	8.61	8.61	0.01
OR16	8.80	8.79	8.78	8.79	0.01
OR21	8.49	8.46	8.48	8.48	0.01
Total	9.13	9.11	9.12	9.12	0.01

A02 Mix PAE degradation (Day 4)

	Log CFU/mL			Average	SD
OR05	7.78	7.85	7.90	7.84	0.05
OR16	9.15	9.00	9.11	9.09	0.06
OR21	9.00	9.08	8.95	9.01	0.05
Total	9.39	9.36	9.36	9.37	0.02

A02 Mix PAE degradation (Day 6)

	Log CFU/mL			Average	SD
OR05	8.23	8.26	8.32	8.27	0.04
OR16	9.36	9.32	9.26	9.31	0.04
OR21	9.00	9.48	9.30	9.26	0.20
Total	9.54	9.72	9.60	9.62	0.08

A02 Mix PAE degradation (Day 8)

	Log CFU/mL			Average	SD
--	------------	--	--	---------	----

OR05	7.30	7.48	7.60	7.46	0.12
OR16	7.95	7.90	7.85	7.90	0.04
OR21	8.30	8.70	8.78	8.59	0.21
Total	8.49	8.79	8.85	8.71	0.16

OR05 + OR21 Mix PAE degradation (Day 0)

	Log CFU/mL			Average	SD
OR05	7.30	7.37	7.43	7.36	0.05
OR21	7.67	7.73	7.67	7.69	0.03
Total	7.82	7.88	7.87	7.86	0.03

OR05 + OR21 Mix PAE degradation (Day 2)

	Log CFU/mL			Average	SD
OR05	8.46	8.30	8.45	8.40	0.07
OR21	9.48	9.30	9.32	9.37	0.08
Total	9.52	9.34	9.38	9.41	0.08

OR05 + OR21 Mix PAE degradation (Day 4)

	Log CFU/mL			Average	SD
OR05	8.04	8.08	8.15	8.09	0.04
OR21	9.30	9.67	9.48	9.48	0.15
Total	9.32	9.68	9.50	9.50	0.15

OR05 + OR21 Mix PAE degradation (Day 6)

	Log CFU/mL			Average	SD
OR05	7.48	7.48	7.60	7.52	0.06
OR21	9.43	9.30	9.30	9.34	0.06
Total	9.44	9.31	9.31	9.35	0.06
OR05 + OR21 Mix PAE degradation (Day 8)					
	Log CFU/mL			Average	SD
OR05	7.30	7.48	7.00	7.26	0.20
OR21	9.27	9.30	9.23	9.27	0.03
Total	9.27	9.31	9.23	9.27	0.03

Table F6 Percent degradation of MEHP on day 8 by OR05, OR16, OR21, OR05 + OR16, OR05 + OR21, and Consortium A02.

MEHP degradation (Day 8)						
	Percent degradation			Average	SD	
Abiotic control	5.56	12.30	9.82	9.23	2.78	
OR05	17.83	29.29	21.10	22.74	4.82	
OR16	18.11	19.60	53.37	30.36	16.28	
OR21	88.66	95.11	92.22	92.00	2.64	
OR05 + OR16	27.83	28.91	31.07	29.27	1.35	
OR05 + OR21	93.74	97.05	93.11	94.63	1.73	
Consortium A02	93.49	98.19	88.98	94.09	3.76	

Table F7 Percent degradation of phthalic acid on day 4 by OR05, OR16, OR21, OR05 + OR16, OR05 + OR21, and Consortium A02.

Phthalic acid degradation (Day 4)					
	Percent degradation			Average	SD
Abiotic control	3.27	5.34	0.85	3.15	1.84
OR05	4.88	1.19	-2.27	1.27	2.92
OR16	8.11	4.31	3.61	5.34	1.98
OR21	0.73	1.77	4.42	2.31	1.55
OR05 + OR16	8.11	4.31	3.61	5.34	1.98
OR05 + OR21	6.04	4.19	2.92	4.38	1.28
Consortium A02	8.57	8.57	15.03	7.55	3.04

Table F8 Percent degradation of protocatechuic acid on day 4 by OR05, OR16, OR21, OR05 + OR16, OR05 + OR21, and Consortium A02.

Protocatechuic acid degradation (Day 4)					
	Percent degradation			Average	SD
Abiotic control	-3.63	-2.88	-1.33	-2.61	0.96
OR05	1.60	1.50	1.61	1.57	0.05
OR16	12.23	21.80	17.39	17.14	3.91
OR21	18.97	21.19	23.42	21.19	1.81
OR05 + OR16	18.18	14.90	21.04	18.04	2.51
OR05 + OR21	26.13	27.11	26.09	26.44	0.47
Consortium A02	29.67	28.80	29.29	27.85	0.35

Table F9 Average nucleotide identity (ANI) values of the genomes of OR05, OR16, and OR21 with publicly available genomes of closely related type strains. ANIb refers to ANI values calculated using BLAST+.

<i>Sporosarcina</i> sp. OR05				
Genome	ANIb (%)	Aligned (%)	Aligned (bp)	Total (bp)
<i>Sporosarcina luteola</i> NBRC 105378 [T]	74.37	55.84	2025385	3626936
<i>Sporosarcina limicola</i> DSM 13886 [T]	70.77	43.07	1561970	3626936
<i>Sporosarcina pasteurii</i> NCTC4822 [T]	69.79	39.01	1414861	3626936
<i>Sporosarcina ureae</i> DSM 2281 [T]	69.31	38.22	1386170	3626936
<i>Sporosarcina globispora</i> DSM 4 [T]	66.18	24.61	892669	3626936
<i>Microbacterium</i> sp. OR16				
Genome	ANIb (%)	Aligned (%)	Aligned (bp)	Total (bp)
<i>Microbacterium</i> sp. OR21	86.9	76.42	2128435	2785191
<i>Microbacterium esteraromaticum</i> DSM 8609 [T]	84.91	70.63	1967263	2785191
<i>Microbacterium paraoxydans</i> NBRC 103076 [T]	77.3	56.84	1583187	2785191
<i>Microbacterium hydrocarbonoxydans</i>	77.21	56.66	1578040	2785191

NBRC 103074 [T]				
<i>Microbacterium hydrocarbonoxydans</i>	77.18	56.95	1586179	2785191
DSM 16089 [T]				
<i>Microbacterium oxydans</i> DSM 20578	76.79	57.74	1608200	2785191
[T]				
<i>Microbacterium oxydans</i> NBRC	76.78	57.7	1607087	2785191
15586 [T]				
<i>Microbacterium laevaniformans</i>	74.08	43.2	1203273	2785191
DSM 20140 [T]				
<i>Microbacterium marinum</i> DSM	73.93	46.49	1294942	2785191
24947 [T]				
<i>Microbacterium halotolerans</i> YIM	73.33	38.46	1071259	2785191
70130 [T]				
<i>Microbacterium</i> sp. OR21				
Genome	ANIb	Aligned	Aligned	Total
	(%)	(%)	(bp)	(bp)
<i>Microbacterium esteraromaticum</i>	85.77	70.61	2148341	3042717
DSM 8609 [T]				
<i>Microbacterium paraoxydans</i> NBRC	77.60	53.96	1641913	3042717
103076 [T]				
<i>Microbacterium hydrocarbonoxydans</i>	77.21	54.29	1651902	3042717
NBRC 103074 [T]				
<i>Microbacterium hydrocarbonoxydans</i>	77.18	54.62	1661915	3042717

DSM 16089 [T]					
<i>Microbacterium oxydans</i> DSM 20578	76.69	55.42	1686294	3042717	
[T]					
<i>Microbacterium oxydans</i> NBRC 15586	76.68	55.44	1686874	3042717	
[T]					
<i>Microbacterium marinum</i> DSM 24947	74.97	44.13	1342676	3042717	
[T]					
<i>Microbacterium laevaniformans</i> DSM 20140	74.04	40.93	1245500	3042717	
[T]					
<i>Microbacterium halotolerans</i> YIM 70130	73.21	34.49	1049302	3042717	
[T]					

Table F10 DEHP concentrations remaining (mg/L) in the sediment fractions of the abiotic, natural attenuation and A02 bioaugmented microcosms.

Abiotic sediment					
	Concentration remaining (mg/kg)			Average	SD
Day 0	103.22	113.48	98.10	104.93	6.40
Day 5	104.42	91.03	104.42	99.95	6.31
Day 8	97.64	104.32	90.43	97.46	5.67
Day 11	103.56	107.63	95.39	102.19	5.09
Day 16	94.21	103.77	100.48	99.49	3.97
Day 21	92.51	90.40	108.90	97.27	8.27

Day 26	96.45	115.51	89.65	100.53	10.95
---------------	-------	--------	-------	--------	-------

Non-sterile sediment

	Concentration remaining (mg/kg)			Average	SD
Day 0	103.59	129.28	87.52	106.80	17.20
Day 5	68.01	78.04	79.69	75.24	5.16
Day 8	63.20	79.55	78.86	73.87	7.55
Day 11	56.05	53.44	77.08	62.19	10.58
Day 16	49.22	59.59	57.00	55.27	4.40
Day 21	63.14	46.16	48.14	52.48	7.58
Day 26	56.67	42.21	48.50	49.13	5.92

Non-sterile sediment + Consortium A02

	Concentration remaining (mg/kg)			Average	SD
Day 0	92.05	114.58	105.10	103.91	9.24
Day 5	89.58	97.13	68.01	84.91	12.34
Day 8	44.51	66.08	68.97	59.86	10.91
Day 11	45.48	52.21	53.44	50.38	3.50
Day 16	30.23	39.84	50.10	40.06	8.12
Day 21	20.20	29.40	26.38	25.33	3.83
Day 26	30.23	16.62	16.62	21.16	6.41

Table F11 Percent DEHP degradation in the sediment fractions of the abiotic, natural attenuation and A02 bioaugmented microcosms.

Abiotic sediment					
	Percent degradation			Average	SD
Day 5	0.46	13.22	0.46	4.72	6.02
Day 8	6.92	0.55	13.79	7.09	5.41
Day 11	1.28	-2.61	9.07	2.58	4.85
Day 16	10.19	1.07	4.22	5.16	3.78
Day 21	11.81	13.82	-3.82	7.27	7.88
Day 26	8.06	-10.11	14.54	4.16	10.44
Non-sterile sediment					
	Percent degradation			Average	SD
Day 5	35.17	25.61	24.04	28.27	4.92
Day 8	39.75	24.17	24.82	29.58	7.20
Day 11	46.56	49.05	26.53	40.71	10.08
Day 16	53.07	43.20	45.67	47.31	4.20
Day 21	39.81	55.99	54.11	49.97	7.23
Day 26	45.97	59.77	53.77	53.17	5.65
Non-sterile sediment + Consortium A02					
	Percent degradation			Average	SD
Day 5	14.61	7.40	35.17	19.06	11.76
Day 8	57.57	37.00	34.25	42.94	10.40

Day 11	56.65	50.23	49.05	51.98	3.34
Day 16	71.19	62.02	52.24	61.81	7.74
Day 21	80.75	71.97	74.85	75.86	3.65
Day 26	71.19	84.15	84.15	79.83	6.11

Table F12 DEHP concentrations (mg/L) in the seawater fraction of the abiotic sediment microcosm.

Seawater (Abiotic)					
	Concentration (mg/L)			Average	SD
Day 0	0.00	0.00	0.00	0.00	0.00
Day 5	4.58	0.00	0.00	1.53	2.16
Day 8	2.78	1.24	1.55	1.85	0.67
Day 11	0.00	1.15	2.04	1.06	0.84
Day 16	1.46	2.14	3.19	2.27	0.71
Day 21	1.46	1.44	2.72	1.88	0.60
Day 26	0.00	0.00	1.85	0.62	0.87

Table F13 Total heterotrophic viable bacterial count (MPN/g) in the sediment fraction of the sediment microcosms.

Sediment sample	Log CFU/g
Original sediment	6.95
Natural attenuation Day 0	6.79
A02 bioaugmented Day 0	7.91
Natural attenuation Day 5	6.78

A02 bioaugmented Day 5	8.48
Natural attenuation Day 8	6.98
A02 bioaugmented Day 8	7.11
Natural attenuation Day 11	6.78
A02 bioaugmented Day 11	6.78
Natural attenuation Day 16	7.63
A02 bioaugmented Day 16	6.91
Natural attenuation Day 21	6.36
A02 bioaugmented Day 21	6.45
Natural attenuation Day 26	7.41
A02 bioaugmented Day 26	7.09

VITA

NAME Ritu Ningthoujam

DATE OF BIRTH 13 October 1992

PLACE OF BIRTH Manipur, India

INSTITUTIONS ATTENDED National Institute of Technology, Durgapur, India
Sharda University, Greater Noida, India

PUBLICATION Ningthoujam R, Satiraphan M, Sompongchaiyakul P, Bureekul S, Luadnakrob P, Pinyakong O. 2023. Bacterial community shifts in a di-(2-ethylhexyl) phthalate-degrading enriched consortium and the isolation and characterization of degraders predicted through network analyses. *Chemosphere* 310, 136730. <https://doi.org/10.1016/j.chemosphere.2022.136730>

Dechsakulwatana C, Rungsahiranrut A, Muangchinda C, Ningthoujam R, Klankeo P, Pinyakong O. 2022. Biodegradation of petroleum oil using a constructed nonpathogenic and heavy metal-tolerant bacterial consortium isolated from marine sponges. *Journal of Environmental Chemical Engineering*: 108752. <https://doi.org/10.1016/j.jece.2022.108752>

Sahoo B, Ningthoujam R & Chaudhuri S. 2019. Isolation and characterization of a lindane degrading bacteria *Paracoccus* sp. NITDBR1 and evaluation of its plant growth promoting traits. *International Microbiology* 22, 155–167. <https://doi.org/10.1007/s10123-018-00037-1>